The role of membrane lipid remodelling in the antimicrobial resistance arsenal of *Pseudomonas aeruginosa*

Rebekah Alison Jones

A thesis submitted to Warwick Medical School in fulfilment of the requirements for the degree of Doctor of Philosophy

April 2020

University of Warwick
Coventry, UK.

Table of Contents

Table of Figures

List of Tables

Acknowledgments

I firstly give great thanks to my supervisor, Professor Yin Chen, for taking a chance on me after appearing out of the blue, and providing excellent guidance and generous support. I extend my thanks to Professor David Scanlan, for continued insightful discussions. Thank you to the MRC DTP in Interdisciplinary Biomedical Research for providing the opportunity. I thank all Chen lab members, past and present, for all help and problem solving. Special thanks go to Dr Alastair Smith for methodology development and training, to Julie Scanlan for showing me the lab ropes, to Holly Shropshire, for being my patholipid teammate and to Dr Eleanor Townsend, for generous sharing of her expertise.

I thank my fiancé Richard Drydale, for always telling me that I can do it, and I thank my Dad, for always telling me that it's ok if I can't do it. Thank you to my sister Jemimah, for giving everything a lighter perspective. I also thank Dr Tom Rawlings for his unwavering support and understanding, without which I definitely would not have reached the end. Thank you to my office friends Dr Hannah Bridgewater and Sophie Kirşen, for sharing in my problems.

To Mum and Mike, if you could see me now.

Declaration

I declare that the work presented in this thesis was carried out by myself under the direct supervision of Professor Yin Chen, and co-supervised by Professor David Scanlan, with two exceptions. 1) *Pseudomonas* phage RJGB18 was isolated by Georgia Beard, under my direct supervision, and 2) exoproteome precipitates were processed by Andrew Murphy for MS analysis. None of the work presented has been previously submitted for any other degree. No data is currently published.

Rebekah Jones

Abbreviations

A-PG	Alanyl-PG
aa-PGs	Amino acid modified phosphatidylglycerol
AACs	Aminoglycoside acetyltransferases
ABC	Ammonium bicarbonate
Agt	Glycosyltransferase
ALP	Alkaline phosphatase
AMPs	Antimicrobial peptides
AMR	Antimicrobial resistance
CAA	2-chloroacetamide
CAMPs	Cyclic antimicrobial peptides
CDP	Cytidine diphosphate
CF	Cystic fibrosis
CFF	Cystic fibrosis foundation
CFU	Colony forming units
CL	Cardiolipin
DAG	Diacylglycerol
DGDG	di-galactosyldiacylglycerol
DOC	Sodium deoxycholate
EDTA	Ethylenediaminetetraacetic acid
ESBLs	Extended-spectrum β-lactamases
ESI	Electrospray ionisation
FDR	False detection rate
G3P	sn-glycerol-3-phosphate
GADG	Glucuronic acid diacylglycerol
GP	Glycerophospholipid
HILIC	Hydrophilic interaction chromatography
HPLC	High performance liquid chromatography
IM	Inner membrane
IPTG	Isopropyl β-d-1-thiogalactopyranoside
L-PG	Lysyl-PG
LB	Lysogeny broth
LDS	Lithium dodecyl sulfate
LPS	Lipopolysaccharide
m/z	Mass to charge ratio
MAG	Monoacylglycerol
MDO	Membrane-derived oligosaccharides
MDR	Multi-drug resistant
MGDG	Monoglycosyl diacylglycerol
MHB	Mueller-Hinton broth
MIC	Minimum inhibitory concentrations
MOI	Multiplicity of infection

MS	Mass spectrometry
MS/MS	Tandem mass spectrometry
NGM	Nematode growth medium
NMR	Nuclear magnetic resonance
OD600	Optical density at 600 nm
OL	Ornithine lipid
OM	Outer membrane
Omp	Outer membrane porin
P	Phosphorus
PA	Phosphatidic acid
PAGE	Polyacrylamide gel electrophoresis
PAP	Phosphatidic acid phosphatases
PBS	Phosphate buffered saline
PC	Phosphatidylcholine
PCR	Polymerase chain reaction
PE	Phosphatidylethanolamine
PFU	Plaque forming units
PG	Phosphatidylglycerol
PGP	Phosphatidylglycerol phosphate
Pi	Inorganic phosphate
PlcP	Phospholipase C enzyme
pNP	*para*-nitrophenol
pNPP	*para*-nitrophenol phosphate
PS	Phosphatidylserine
PTFE	Polytetrafluoroethylene
QS	Quorum sensing
RND	Resistance-nodulation-cell division
RT	Room temperature
SOC	Super optimal broth with catabolite repression
TCA	Trichloroacetic acid
TEM	Transmission electron microscopy
Tn	Transposon
UGL	Unknown glycolipid
WT	Wild type

Abstract

Pseudomonas aeruginosa is a common cause of hospital-acquired infections, with prevalence in immunocompromised individuals and multi-drug resistance capabilities. Phosphate stress triggers a cascade of virulence factors in *P. aeruginosa*, with phosphorus scarcity known to occur in several infection models. Here I show that *P. aeruginosa* is able to modify its membrane lipid composition in adaptation to low phosphorus availability, termed lipid remodelling, in a process that substitutes membrane phospholipids for non-phosphate lipid classes. High performance liquid chromatography coupled to mass spectrometry (HPLC/MS) confirmed the production of glycolipids in response to phosphate stress in *P. aeruginosa*. An intracellular phospholipase C, PlcP (PA3219), removes phospholipid head groups, liberating diacylglycerol to become the base for glycolipid synthesis. Heterologous expression in *Escherichia coli* confirmed two glycosyltransferases, PA3218 (Agt1) and PA0842 (Agt2), catalyse the production of monoglycosyl diacylglycerol (MGDG) and glucuronic acid diacylglycerol (GADG) glycolipids, respectively. When grown under low phosphate conditions, *P. aeruginosa* has significantly decreased sensitivity to antimicrobial peptide polymyxin B, compared to growth with sufficient phosphate. Here, I show that mutants defective for glycolipid synthesis are less able to survive when challenged with polymyxin B under low phosphate conditions, compared to wild type. Proteomic analyses also revealed potential changes in carbapenem sensitivity and virulence factor expression as a result of lipid remodelling. Critically, this study emphasises a role for glycolipids beyond simple phosphate conservation, in proposing antimicrobial resistance trade-offs as a result of this phenotypic adaptation to phosphorus stress in *P. aeruginosa*.

Chapter 1 Introduction

1.1 Importance of opportunistic pathogen *Pseudomonas aeruginosa*

Pseudomonas aeruginosa (*P. aeruginosa*) is a Gram-negative opportunistic pathogen with a large genome between 5.5 and 7 Mb (Ciofu & Bjarnsholt, 2010). The large genome lends itself to *P. aeruginosa* survival and adaptation in many different complex growth environments, owing to a diverse array of metabolic pathways, regulatory genes, transport proteins and efflux pumps (Stover et al., 2000). *P. aeruginosa* has become one of the most prevalent hospital-acquired infections, often presenting in immunosuppressed patients, or in those with cystic fibrosis or significant burns. Importantly, *P. aeruginosa* infections have proved difficult to eradicate due to its intrinsic resistance to many classes of antimicrobials, alongside acquired resistance mechanisms and its ability to form biofilms. A recent systematic review alludes to 131 *P. aeruginosa* outbreaks across 22 countries worldwide in a 15-year period, with 49 of these described as multi-drug resistant (MDR) (Wieland et al., 2018). Carbapenem-resistant *P. aeruginosa* has been named by the World Health Organisation (WHO) as a critical priority pathogen for the urgent development of new antibiotics (Tacconelli et al., 2018), with carbapenems often considered a last line of defence in MDR infections. Overall, antimicrobial resistance (AMR) is an increasingly serious worldwide threat to public health and, in conjunction with a lack of development of new antimicrobials, is estimated to pose risk to 10 million lives by 2050 (Rechel et al., 2018).

A recent systematic review reports that nosocomial outbreaks of *P. aeruginosa* can be found equally in both intensive care units and in peripheral wards (Wieland et al., 2018). In summarising the mortality of these outbreaks, where reported, in 55 outbreaks affecting 619 individuals the mortality rate is reported as 23.3% (Wieland et al., 2018). A high mortality rate is also reported elsewhere in burns patients and those in intensive care (Lambert et al., 2011; Mahar et al., 2010). Medical equipment and water sources were identified as key reservoirs of *P. aeruginosa* hospital outbreaks (Kizny Gordon et al., 2017), with suppressed immunity and the use of

medical implements in ventilation, invasive procedures and catheterisation being key risk factors for patients in acquiring the infection (Corne et al., 2005; DiazGranados et al., 2009; Robertson et al., 2015; Wieland et al., 2018). The major presentations of *P. aeruginosa* infection are in the bloodstream, lungs (pneumonia), urinary tract and surgical wounds (Mittal et al., 2009; Wieland et al., 2018). Ventilator-associated pneumonia is also particularly problematic in the paediatric intensive care setting, linked to considerable patient morbidity, with *P. aeruginosa* again reported as a common culprit (Venkatachalam et al., 2011). In addition, *P. aeruginosa* can persist for months on dry surfaces and can therefore lead to a constant source of infection without rigorous disinfectant procedures (Kramer et al., 2006). Systematic studies of hospital-associated acquisition of *P. aeruginosa* infection serve to highlight the ubiquitous danger of this highly adaptable opportunistic pathogen.

For patients with cystic fibrosis (CF), *P. aeruginosa* is a particularly devastating infection contributing to a progressive decline in lung function and decreased life span (Emerson et al., 2002; Kosorok et al., 2001). CF is the result of a mutated CF transmembrane conductance regulator gene (CFTR), leading to defective chloride ion transport across mucosal surfaces, including the lungs, thereby reducing the ability to clear airborne pathogens (Folkesson et al., 2012). *P. aeruginosa* is the second most common pathogen found in CF patient lungs, behind *Staphylococcus aureus* (*S. aureus*), with positive news being that since 2003 *P. aeruginosa* prevalence has declined from 57.5% of all US-based CF Foundation (CFF) registry patients to 44.4% in 2018 (CFF, 2018; Koch, 2002). During 2018, around 20% of children with CF, up to the age of 10 years old, harboured a *P. aeruginosa* infection (CFF, 2018). Owing to the overall decline likely due to more aggressive antibiotic treatment in early life, a high proportion of CF adolescents will enter adult life without an active *P. aeruginosa* infection. However, in adult age groups the prevalence increases dramatically; between 50-70% of adult CF patients are positive for *P. aeruginosa* infection (CFF, 2018; Folkesson et al., 2012). *P. aeruginosa* infections are considered to be initially intermittent that go on to use an arsenal of adaptive mechanisms to survive in the challenging CF airway environment (Folkesson et al., 2012). During this adaptation, *P. aeruginosa* transitions to a mucoid state; the notorious and difficult to treat biofilm

(Hoo et al., 2018; Johansen & Hoiby, 1992). In this chronic state of infection significant irreversible damage to lung tissue is caused by both the bacterial infection itself and the constant inflammatory response induced by its presence (Nichols et al., 2008).

1.2 Antimicrobial resistance in *Pseudomonas aeruginosa*

Given the clinical importance of difficult to treat *P. aeruginosa* infections, a significant amount of research has been conducted into the antimicrobial resistance mechanisms of this bacterium. As such, the methods of resistance employed by *P. aeruginosa* have been classified into four major groups: reduced uptake of the antibiotic, enhanced removal of the antibiotic through efflux, cellular inactivation of antibiotics and finally, a reduced affinity of antibiotics to their cellular targets (Figure 1.1; Wardell et al., 2019). Alongside intrinsic resistance mechanisms, *P. aeruginosa* gains resistance to antimicrobials through both mutations to endogenous genes and the acquisition of exogenous resistance genes through horizontal gene transfer (Poole, 2011).

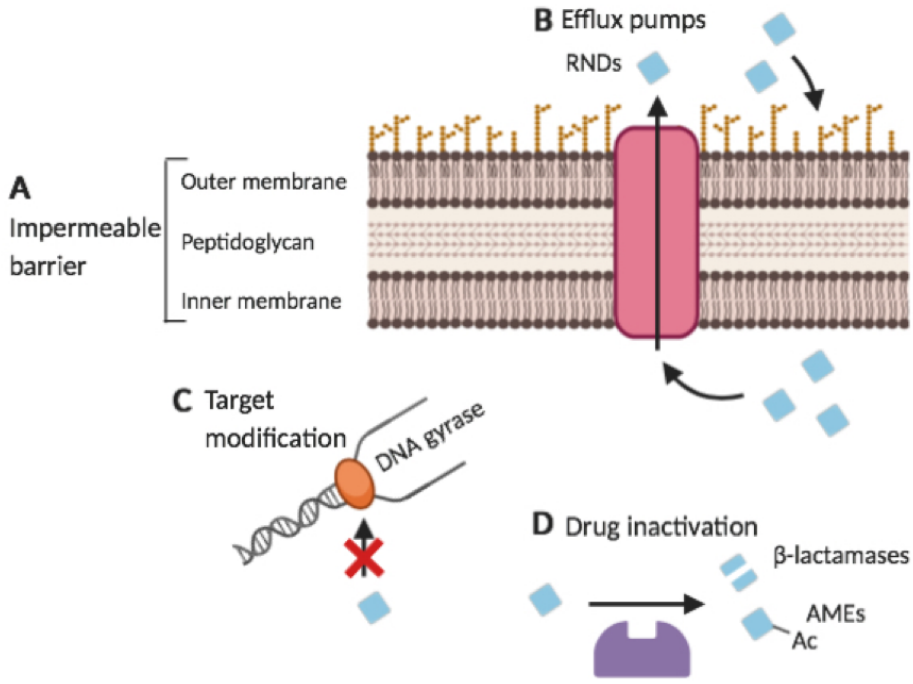

Figure 1.1. Schematic of antibiotic resistance mechanisms in Gram-negative bacteria, with specific examples for *Pseudomonas aeruginosa*. A) Intrinsic resistance due to impermeability of the cell membrane. B) Efflux pumps remove drugs from the cell, and can accommodate several classes of antibiotics. Members of the resistance-nodulation-cell division (RND) family are a common example in *P. aeruginosa*. C) Mutations in proteins that prevent drug binding but still allow protein activity, e.g. the *gyrA* subunit of DNA gyrase in *P. aeruginosa*. D) Inactivation of the drug through modification, e.g. aminoglycoside modifying enzymes (AMEs), or through degradation e.g. β-lactamases. Figure adapted from (Allen et al., 2010).

1.2.1 Resistance to β-lactam antibiotics

β-lactams are bactericidal antibiotics that act to inhibit penicillin binding proteins (PBPs), thereby preventing cross-linking of the peptidoglycan layer of the bacterial cell wall. This class encompasses antibiotics that contain a β-lactam ring in their structure: penicillins and penicillin derivatives, carbapenems, cephalosporins, monobactams and some β-lactam inhibitors (Bush & Bradford, 2016). As a well-characterised example of the intrinsic resistance of this bacterium, *P. aeruginosa* chromosomally encodes β-lactamases AmpC and PoxB (Alvarez-Ortega et al., 2011; Kong et al., 2005; Lodge et al., 1990) that will inactivate β-lactam antibiotics by disrupting the amide bond of the β-lactam ring. Cephalosporinase AmpC is more widely reported in clinical isolates of *P. aeruginosa*, with mutations that lead to its overexpression conferring resistance to broad spectrum cephalosporins (Jacoby, 2009; Tam et al., 2007).

Although carbapenems also induce AmpC expression, their fast-acting potency and stability to hydrolysis still allows their success against AmpC positive *P. aeruginosa* infections (Jacoby, 2009; Poole, 2011). However, it would appear that derepression of AmpC can occur concomitantly with other mechanisms to contribute to resistance against carbapenems. Outer membrane porin OprD is the key route of entry for carbapenems (Trias & Nikaido, 1990), and thus mutations resulting in decreased expression of OprD confer resistance to anti-pseudomonal imipenem and meropenem (Quale et al., 2006; Rodríguez-Martínez et al., 2009). A variety of mutations in OprD lead to decreased expression, including point mutations resulting in premature stop codons and frameshifting caused by insertions or deletions, ranging from 1 bp to larger fragment insertions or deletions (Quale et al., 2006). Efflux pumps are further described to be involved in the interplay of AmpC-OprD based carbapenem resistance (Quale et al., 2006). Although efflux appears to have a minor role in overall carbapenem resistance, three key resistance nodule division (RND) efflux pumps, MexAB-OprM, MexCD-OprJ, and MexXY-OprM (Poole, 2004), are linked to overall β-lactam resistance, with the former characterised as a key exporter of meropenem, but not imipenem (Köhler et al., 1999), in clinical isolates of *P. aeruginosa* (Pournaras et al., 2005). Overall, it is the mutational deactivation of outer membrane porin OprD that is most common in carbapenem-resistant *P. aeruginosa* isolates (Naenna et al., 2010), but resistance becomes more potent when present in conjunction with other mechanisms (Li et al., 2012; Rodríguez-Martínez et al., 2009; Wang et al., 2010).

In addition to chromosomally encoded β-lactamases AmpC and PoxB, *P. aeruginosa* can acquire increasingly extended-spectrum β-lactamases (ESBLs) and carbapenemases through plasmids or transposable elements (Poirel & Nordmann, 2005). This has significantly broadened the anti-β-lactam arsenal of *P. aeruginosa*, that originally only encompassed penicillins and early generation, narrow spectrum cephalosporins (Poole, 2011). The more recently described ESBLs are able to hydrolyse nearly all β-lactams, including third generation broad spectrum cephalosporin ceftazidime as well as carbapenems, sparing only monobactams (Poole, 2011; Walsh et al., 2005). ESBL VEB-1, harboured on a class 1 integron, confers resistance to

ceftazimide and was originally described in *Escherichia coli* (*E. coli*) (Poirel et al., 1999), but is further widespread in other Gram-negative pathogens, including *P. aeruginosa* (Aubert et al., 2012; Maurya et al., 2014; Strateva et al., 2007). Indeed, of over 800 β-lactamases described in Gram-negative rods, over 120 have been identified in *P. aeruginosa* (Zhao & Hu, 2010). A key group of these occurring in a significant proportion of *P. aeruginosa* isolates are oxicillinases, the OXA group; a very diverse class of β-lactamases able to hydrolyse an expansive range of β-lactam antibiotics (Hocquet et al., 2010; Poirel et al., 2010). Indeed, some of the OXA group of β-lactamases found in *P. aeruginosa* are also able to hydrolyse carbapenems, and are further grouped as class D carbapenemases (Figure 1.2; Rouhi & Ramazanzadeh, 2018; Walsh, 2010). Class B carbapenemases are metallo-β-lactamases (MBLs), encompassing the IMP, VIM, SPM, GIM, SIM and AIM enzymes (Sedighi et al., 2014), that are a major cause of high resistance to carbapenems in *P. aeruginosa* (Poole, 2011; Walsh, 2010). Class A carbapenemases are more rare in *P. aeruginosa*, with thus far only KPC and GES enzymes from this class being described in this bacterium (Viedma et al., 2009; Villegas et al., 2007; Zhao & Hu, 2010). MBLs are often harboured by class 1 or class 3 integrons, with IMP and VIM having numerous variants and being the most widespread (Walsh, 2008), and often investigated in terms of imipenem resistance (Karlowsky et al., 2018; Sedighi et al., 2014; Tsakris et al., 2009; Zhao et al., 2009).

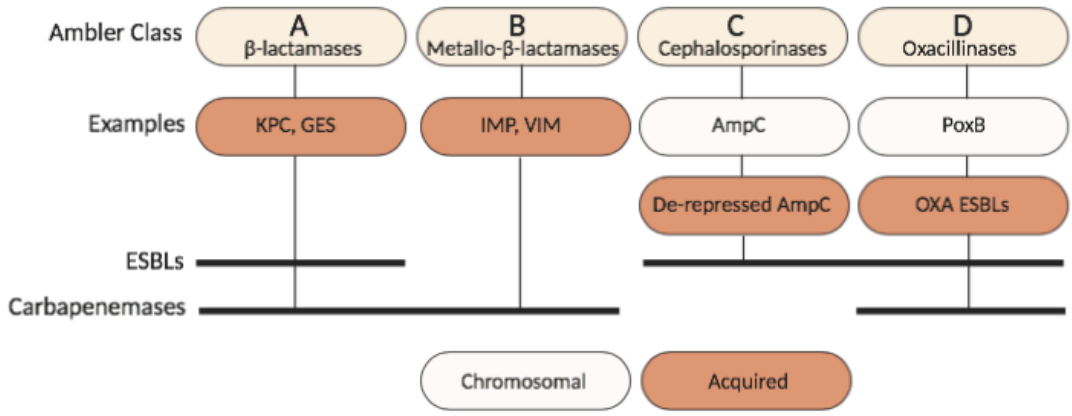

Figure 1.2. Ambler's classification of β-lactamases, with common examples of each class that can be found in *P. aeruginosa*, both intrinsic and acquired. ESBLs: extended-spectrum β-lactamases. Figure adapted from (Ruppé et al., 2015).

Importantly, alongside the other mechanisms of carbapenem resistance, the acquisition of ESBLs and carbapenemases will invariably contribute to more broad spectrum resistance to the β-lactam class of antibiotics in *P. aeruginosa*. This is especially concerning as carbapenems are often considered a last line of defence in treating MDR *P. aeruginosa* infections. In addition, *P. aeruginosa* also represents a significant reservoir of mobile AMR genes facilitating the spread of ESBLs, including the spread of MBLs to pathogenic Enterobacteriaceae (Poole, 2011; Walsh, 2010). A further clinical issue is that often ESBLs, in particular MBLs, are not inhibited by commonly used β-lactam inhibitors, such as clavulanic acid (Poirel et al., 2010; Walsh, 2010).

1.2.2 Resistance to polymyxins

The rise of MDR bacteria has led to the resurgence of the cationic antimicrobial peptide class of antibiotics, namely polymyxins (Landman et al., 2008). Importantly, polymyxin B and colistin, also known as polymyxin E, exhibit antibacterial activity towards *P. aeruginosa*, with colistin often used in treatment of CF patients (Falagas et al., 2005; Langton Hewer & Smyth, 2017). These positively charged antimicrobial peptides (AMPs) enter the bacterial cell via self-promoted uptake, first binding to the anionic proportion of the lipopolysaccharide (LPS) layer, the phosphate groups of lipid A, creating a disruption that allows the polycation to cross the membrane (Molina et al., 2009). Resistance mechanisms employed by *P. aeruginosa* against antimicrobial peptides tend to be those that modify the outer membrane, thereby perturbing interaction with AMPs.

A well characterised AMP resistance method is the modification of phosphate groups in lipid A with the addition of 4-amino-4-deoxy-L-arabinose (Ara4N), reducing available negatively charged groups and therefore increasing resistance to CAMPs (Lee & Sousa, 2014; Needham & Trent, 2013). Gene loci in *P. aeruginosa* that are homologous to the genes responsible for lipid A-Ara4N modification in *Salmonella enterica* serovar Typhimurium have been characterised as *pmrHFIJKLME* (polymyxin

resistance) (Gunn et al., 2000; Moskowitz et al., 2004). This operon is now also known as *arnBCADTEF* (AraN synthesis) in *P. aeruginosa*, where AraA generates UDP-4-keto-pentose by oxidative decarboxylation of UDP-GlcA, followed by AraB pyridoxal-phosphate dependent transaminase activity generating UDP-Ara4N (Lee & Sousa, 2014). AraT glycosyltransferase catalyses the addition of Ara4N to either phosphate group of lipid A. The *arn* operon in *P. aeruginosa* has been shown to be induced by the presence of cationic peptides, including clinically used polymyxins, regulated by two-component systems ParRS, CprRS and PmrAB (Fernández et al., 2010, 2012), or in Mg^{2+}-limiting conditions (McPhee et al., 2003), orchestrated by the two component regulatory systems PmrAB and PhoPQ (Macfarlene et al., 2000; McPhee et al., 2006). Intriguingly, the CF lung environment appears to induce the lipid A-Ara4N modification, with 33% of *P. aeruginosa* isolates from CF patients found to be displaying the modification (Ernst et al., 2007). The myriad of two-component systems and the variety of conditions that influence their activity reveals a complex regulation in defence against antimicrobial peptides in *P. aeruginosa*, likely developed due to continual exposure to host defence peptides from both competing bacterial species and the human host.

A further polymyxin resistance mechanism characterised in *P. aeruginosa* is the addition of phosphoethanolamine (PEtN) to lipid A, carried out by PetN transferase EptA (Nowicki et al., 2015). EptA, as for AraT, modifies a phosphate group on lipid A. A further two-component system, ColRS, is involved in the regulation of PetN-lipid A modification, and is activated in response to the presence of zinc (Gutu et al., 2013). In addition to well characterised chromosomally-encoded polymyxin resistance, plasmid-mediated colistin resistance genes have been more recently described (Moradali et al., 2017). *Mcr-1* (mobilised colistin resistance) encodes for a PetN transferase for the modification of lipid A with PEtN (Liu et al., 2016). Although first described in *E. coli*, the *mcr-1* gene was also found to have transferred to *P. aeruginosa* via conjugation (Liu et al., 2016). The prospect of acquired polymyxin resistance alongside successful chromosomally-encoded mechanisms is a worrying prospect for these critical antimicrobials.

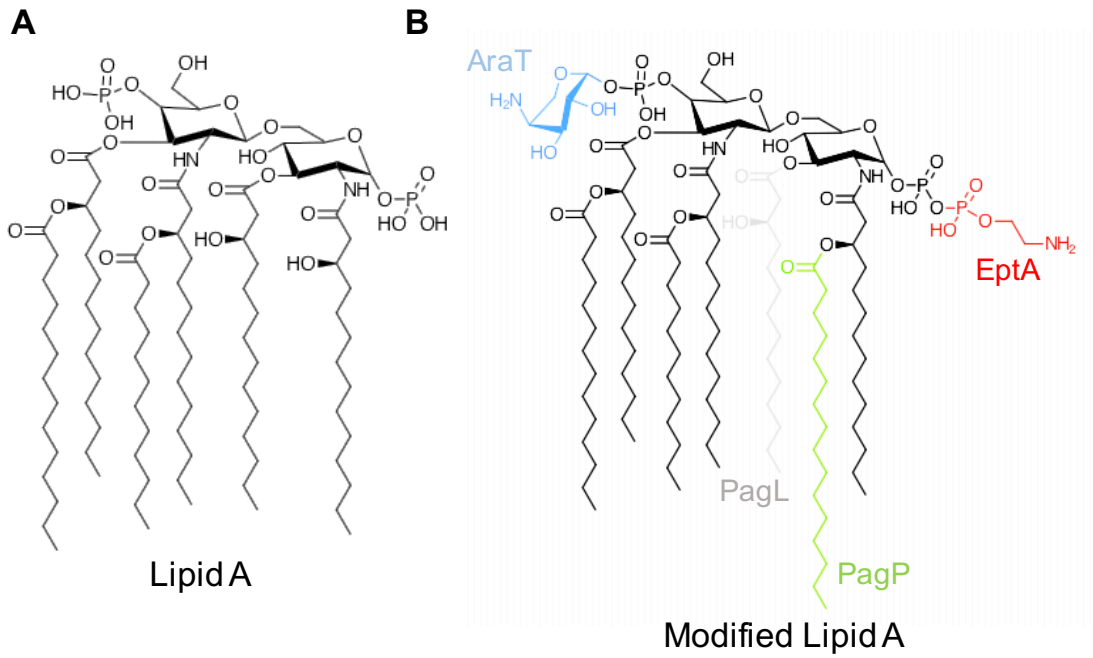

Figure 1.3. A) Unmodified lipid A is composed of a β-1',6-linked disaccharide of glucosamine that is phosphorylated and hexa-acylated. B) Possible modifications to lipid A including addition of phosphoethanolamine by EptA (red), addition of aminoarabinose by AraT (blue), addition of a fatty acyl chain (PagP) and removal of a fatty acyl chain by PagL (grey). Figure adapted from (Needham & Trent, 2013).

1.2.3 Resistance to aminoglycosides

Aminoglycosides are another key component of anti-pseudomonal treatment, characterised by the presence of an aminocyclitol ring attached to amino sugars by glycosidic linkages (Germovsek et al., 2017; Ramirez & Tolmasky, 2010). These polycationic molecules will first bind anionic charges on bacterial cell membranes, for example in the LPS layer, thereby disrupting divalent cation cross-links in the LPS structure creating an increase in permeability that allows the aminoglycoside compound to enter the periplasmic space (Ramirez & Tolmasky, 2010). On reaching the cytosol via the hijacking of aerobic bacterial electron transport system (Bryan & Van Den Elzen, 1977), aminoglycosides bind to the 30S subunit of bacterial ribosomes, thereby inhibiting translation of proteins and causing cell death (Davis, 1987; Jana & Deb, 2006). Aminoglycosides are more successfully used in combination treatments (Karaiskos et al., 2019), likely due to damage created by other antibiotics increasing the permeability of bacterial cells, thereby allowing easier access to the bactericidal target of aminoglycosides in the cytosol. In treating *P. aeruginosa* infections, amikacin,

gentamicin and tobramycin are employed (Poole, 2005), with the latter particularly used in treating CF patients (Prayle & Smyth, 2010; Ratjen et al., 2009).

Incidences of aminoglycoside resistance in *P. aeruginosa*, as with many classes of antibiotics, is on the rise across all areas of the world in isolates from a wide array of infection sites (Poole, 2005). As for acquired β-lactamases, genes conferring resistance to aminoglycosides are often encoded on mobile elements, such as transposons and integrons (Poole, 2005). Dauntingly, these mobile elements often also harbour additional resistance genes (Figure 1.4; Mugnier et al., 1996). Most resistance to gentamicin and tobramycin is from aminoglycoside modifying enzymes (AMEs) present in *P. aeruginosa* leading to their inactivation (Jana & Deb, 2006). However, the structure of amikacin is different enough to escape activity of some AMEs, therefore mechanisms conferring resistance to gentamicin and tobramycin do not necessarily also translate to resistance to amikacin (Jana & Deb, 2006). Several types of AMEs are described in *P. aeruginosa*: those that phosphorylate aminoglycosides, those that acetylate, and those that adenylate (Poole, 2005; Ramirez & Tolmasky, 2010).

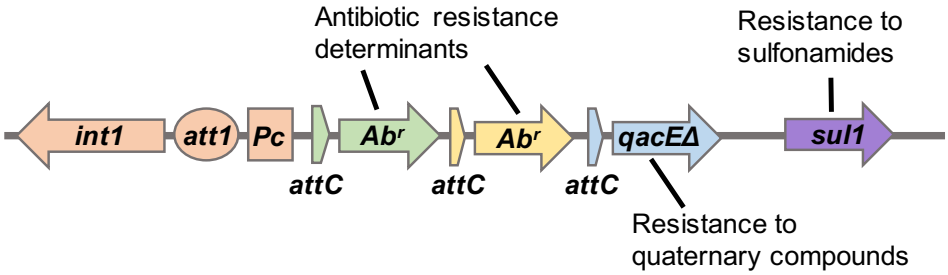

Figure 1.4. Mobile genetic elements often harbour multiple antimicrobial resistance cassettes. Figure shows the organisation of a typical class 1 integron containing an integrase (*int1*), primary recombination site (*att1*) and integrase substrate sites (*attC*). A common promoter (Pc) drives high expression of antibiotic resistance genes (Ab^r), including resistance to aminoglycosides. Genes *qacEΔ* and *sul1* provide additional resistance. Figure adapted from (Alekshun & Levy, 2007).

Aminoglycoside acetyltransferases (AACs) that modify the 3-amino group of gentamicin are common in *P. aeruginosa* (Alvarez & Mendoza, 1993; Phillips et al., 1986). Further, there are two AACs able to acetylate at the 6' position of aminoglycosides, AAC(6')-I and AAC(6')-II (Poole, 2005). Indeed, AAC(6')-II is the most

common AAC in *P. aeruginosa*, and leads to resistance to both gentamicin and tobramycin, but not amikacin (Ramirez & Tolmasky, 2010). Though less common, AAC(6')-I is an important player in resistance to amikacin, as well as tobramycin (Falkiner et al., 1982; Poirel et al., 2001). To inactivate aminoglycosides through adenylation, *P. aeruginosa* uses aminoglycoside nucleotidyltransferases (ANTs), with the most prevalent being ANT(2')-I, able to inactivate both tobramycin and gentamicin, but again, not amikacin (Poole, 2005). The final group of AMEs are aminoglycoside phosphotransferases (APHs). In general, APHs provide resistance to kanamycin, neomycin and streptomycin, aminoglycosides that are invariably not used in treating *P. aeruginosa* infections as inherent insensitivity has been long established (Griffith, 1966; Poole, 2005). However, a more recent variant is linked to amikacin resistance (Vaziri et al., 2011).

In an AME-independent mechanism for aminoglycoside resistance, *P. aeruginosa* can display 'impermeability resistance' to all aminoglycosides, an attribute that is thought to be due to reduced outer membrane permeability (MacLeod et al., 2000). Impermeability resistance currently lacks a specific biochemical mechanism, but it is particularly important in tobramycin resistance in *P. aeruginosa* isolates from CF patients (Strateva & Yordanov, 2009). The overexpression of multi-drug efflux pump MexXY is linked to this phenomenon (Bolard et al., 2019; Feng et al., 2019; Islam et al., 2004; Kawalek et al., 2019). A further, more recently described AME-independent mechanism is the ability of *P. aeruginosa* to modify the 16S rRNA binding target of aminoglycosides through methylation (MacLeod et al., 2000). Methylases RmtA and RmtD give *P. aeruginosa* high level pan-resistance to all clinically used aminoglycosides (Doi et al., 2007; Yokoyama et al., 2003). Interestingly, *P. aeruginosa* can accrue mutations, for example during long term evolution in CF patients, that together lead to increased resistance to aminoglycosides (El'Garch et al., 2007).

1.2.4 Resistance to fluoroquinolones

Bactericidal quinolone-based compounds target bacterial DNA gyrase and topoisomerase IV, thereby interfering with processes to repair DNA, carry out

transcription and to replicate (Bolon, 2009). Most clinically used quinolone antibiotics are those with an added fluorine atom, termed fluoroquinolones, that were found to have both improved pharmacokinetic properties and a broader spectrum of activity (Pham et al., 2019). Ciprofloxacin is a commonly used fluoroquinolone in treating *P. aeruginosa* infections, benefitting from a piperazine ring addition that improves potency against Gram-negative bacteria (Van Caekenberghe & Pattyn, 1984). Indeed, ciprofloxacin is still one of the most commonly prescribed antibiotics overall (Correia et al., 2017). Aerosolised levofloxacin is also used in treatment of CF patients (Smith et al., 2017). Perhaps unsurprisingly, resistance to fluoroquinolones in *P. aeruginosa* can arise from mutations to the drug targets: DNA gyrase and topoisomerase IV (Poole, 2011). In addition, efflux has a larger role in resistance to this class of antibiotic, with the two mechanisms often found together in fluoroquinolone-resistant phenotypes (Réjiba et al., 2008).

Bacterial DNA gyrase and topoisomerase IV are both comprised of two subunits, encoded by *gyrA* and *gyrB* for DNA gyrase and *parC* and *parE* for topoisomerase IV (Bolon, 2009). In *P. aeruginosa*, the most common mutations conferring resistance to fluoroquinolones occur in GyrA and/or ParC, at sites known as quinolone resistance determining regions (QRDR) (Drlica et al., 2009; Nakano et al., 1997). Clinical isolates of *P. aeruginosa* carrying several mutations in *gyrA* and *parC* are characterised as highly resistant (Higgins et al., 2003; Muramatsu et al., 2005). Mutations found in *gyrB* and *parE* are less common in this bacterium (Lee et al., 2005; Poole, 2011).

P. aeruginosa further defends itself from fluoroquinolones by reducing intracellular accumulation of the drug through reducing membrane permeability (Correia et al., 2017). In preventing fluoroquinolone entry to the cell, the reduced or loss of expression of several different outer membrane porins (Omp) has been implicated in the fluoroquinolone resistance of *P. aeruginosa* (Delcour, 2009; Fernández & Hancock, 2012). Mutations in Omp regulatory genes have been characterised to decrease the permeability of this bacterium to fluoroquinolones (Correia et al., 2017). Alongside reducing entry through the cell membrane, *P. aeruginosa* further expels fluoroquinolones using efflux pumps. Of the many efflux pumps *P. aeruginosa* is

known to encode, four RND family multi-drug efflux pumps have been shown to also accommodate fluoroquinolones: MexAB-OprM, MexCD-OprJ, MexEF-OprN, and MexXY-OprM (Poole, 2011). Mutations in the regulatory genes of efflux pumps leading to increased expression is implicated in fluoroquinolone resistance (Henrichfreise et al., 2007; Hocquet et al., 2008; Sobel et al., 2005). On rare occasions, *P. aeruginosa* has been found to acquire quinolone resistance proteins (Qnr) encoded on plasmids that will protect DNA gyrase from fluoroquinolone attack (Ogbolu et al., 2011; Tran et al., 2005). However, this mechanism is much more prevalent in pathogenic Enterobacteriaceae (Jacoby, 2017).

1.2.5 The role of bacterial cell membranes in antimicrobial resistance

Aside from the important antibiotic inactivating enzymes, the bacterial cell membrane clearly has a significant role in antimicrobial resistance in *P. aeruginosa*. This impermeability resistance can be attributed to outer membrane porins (OMPs), with *P. aeruginosa* having several smaller role-specific porins as opposed to larger general diffusion porins found in other bacterial species (Chevalier et al., 2017; Hancock & Brinkman, 2002), thereby making entry for antimicrobial compounds more difficult. A major example of the role of porins in AMR is the derepression of OprD in carbapenem resistance (section 1.2.1). In addition, multi-drug efflux pumps span the membrane and are shown to be able to accommodate numerous antimicrobial compounds, including β-lactams, fluoroquinolones and, to a lesser extent, aminoglycosides.

Together this begs the question of the role of the phospholipid bilayer in this phenomenon, with it being previously shown that the lipid environment is linked to the structure and function of membrane proteins (Laganowsky et al., 2014). The bilayer is no longer considered a homogenous distribution of lipids and proteins, but as a collection of microdomains differing in their composition (Contreras et al., 2011). Phospholipid-protein interaction occurs via lipid head group interaction with the protein, often at areas that contain charged amino acids (Liko et al., 2018; Ulmschneider & Sansom, 2001). Indeed, the lipid composition surrounding *E. coli* lactose permease LacY required the native phospholipid composition found in this

organism to orientate itself correctly (Vitrac et al., 2019). In addition, the stability and function of outer membrane protein OmpF was linked to its lipid environment, in that binding to anionic phospholipids and LPS is thought to lead to an open protein conformation, thereby increasing access of antibiotics accommodated by OmpF by organisms that possess it, such as *E. coli* (Ionescu et al., 2017; Liko et al., 2018). For *P. aeruginosa*, binding between OprH and the LPS layer provides structural stability to the outer membrane, directly contributing to the intrinsic low permeability of this bacterium (Edrington et al., 2011; Kucharska et al., 2016). Together this suggests that any changes to the membrane lipid composition of bacteria, including pathogens like *P. aeruginosa*, could alter the stability or function of outer membrane proteins, including those involved in AMR.

1.3 Phosphorus starvation in bacteria

1.3.1 Cellular responses to phosphorus starvation in *P. aeruginosa*

The PhoBR (phosphate-starvation-inducible) two-component system is considered a master regulator for orchestrating the response to available phosphorus in bacterial cells. PhoB represents the activator, and its activity is promoted by PhoR under phosphorus stress, and repressed otherwise (Carmany et al., 2003; Filloux et al., 1988; Siehnel et al., 1988). Under phosphorus stress the histidine kinase PhoR will phosphorylate PhoB, thereby activating its transcription regulation function. Genes that are under the control of PhoB each have a conserved Pho box sequence in their promoter region, together forming the *pho* regulon (Anba et al., 1990; Filloux et al., 1988). The Pho box is defined as two 11-nucleotide direct repeats, each containing 7 well conserved bases and 4 less well conserved bases (Santos-Beneit, 2015). A total of 73 Pho-boxes have been predicted in *P. aeruginosa* strain PAO1 (Yuan et al., 2006). However, the genes influenced by phosphorus stress may be considerably more than this figure. The most common genes activated by the PhoBR system in response to phosphorus scarcity are those that enhance acquisition of the nutrient, its transport and its storage (Santos-Beneit, 2015).

Inorganic phosphate (Pi) is required for important cellular processes such as DNA and RNA synthesis, membrane phospholipid synthesis and intracellular signalling, therefore it is understandable that bacteria have several Pi-acquisition systems. An important high-affinity Pi-specific transporter is the Pst operon: *pstS*, *pstC*, *pstA*, *pstB*, under the control of PhoBR, and present in *P. aeruginosa*. PstS encodes a Pi-binding protein that localises to the periplasm, donating Pi molecules to membrane-spanning operon members PstC and PstA, that form a channel in the cytoplasmic membrane (de Almeida et al., 2015). PstB is an ATPase that provides the energy for this transport (Chan & Torriani, 1996). Some Pseudomonads also encode for a low affinity Pi transporter, known as PitA (Lidbury et al., 2016). *PstSCAB* is further controlled by *phoU*, a regulator located downstream from the operon. When *phoU* is mutated, PhoR continually phosphorylates PhoB, leading to high expression of the *pho* regulon (Rice et al., 2009; Santos-Beneit, 2015). It is suggested that PhoU is required for PhoB dephosphorylation under Pi-replete conditions (Santos-Beneit, 2015). PhoU acts to avoid uncontrolled Pi uptake that could be toxic to the cell by acting as a negative regulator in the Pi-stress response (Gardner et al., 2014; Surin et al., 1986).

Pseudomonads are known to secrete several protein classes involved in acquiring Pi, including enzymes alkaline phosphatases (ALP), phospholipases, phosphonatases and phosphodiesterases (Lidbury et al., 2017). Major phosphate acquisition mechanisms upregulated in response to phosphate stress in *P. aeruginosa* are summarised in Table 1.1. ALPs have the ability to hydrolyse many monophosphate esters, with the goal of releasing Pi for cellular use (Sharma et al., 2014). Glycerolphosphodiester phosphodiesterases extend the bacterium's ability to acquire Pi from more complex compounds, such as the glycerol phospho-choline head of phosphatidylcholine, and can be secreted (GlpQ) or cytoplasmic (UgpQ) (Lidbury et al., 2017), with the final Pi-release step then catalysed by ALPs. An array of proteins linked to phosphonate acquisition are described in *P. aeruginosa*, denoted *phn*. However, numerous genes are yet to be fully characterised (Bains et al., 2012). When DNA is presented as the source of phosphate to *P. aeruginosa*, the production of an extracellular deoxyribonuclease (DNase) is elicited, representing another mechanism utilised for phosphate acquisition in this bacterium (Mulcahy et al., 2010). Phosphate-specific

porin OprP and polyphosphate-specific porin OprO are also upregulated in response to phosphate stress in *P. aeruginosa* (Siehnel et al., 1992). *P. aeruginosa* also secretes phospholipases that are categorised as haemolytic, PlcH, or non-haemolytic, PlcN and PlcB, that are upregulated in response to phosphate stress (Barker et al., 2004; Shoriridge et al., 1992). These phospholipases can cleave phospholipids present in eukaryotic membranes, thereby representing an important mechanism of potential phosphate acquisition in the host environment.

Table 1.1. Phosphate-acquisition related genes with confirmed functions that are upregulated under phosphate stress in *Pseudomonas aeruginosa* (Bains et al., 2012).

Locus tag	Gene name	Description
PA3279	*oprP*	Phosphate-specific outer membrane porin
PA3280	*oprO*	Pyrophosphate-specific outer membrane porin
PA0347	*glpQ*	Glycerophosphoryl diester phosphodiesterase
PA3296	*phoA*	Alkaline phosphatase
PA3909	*eddB*	Extracellular DNA degradation protein
PA3382	*phnE*	Phosphonate transporter protein E
PA3319	*plcN*	Non-haemolytic phospholipase C precursor
PA0844	*plcH*	Haemolytic phospholipase C precursor
PA0026	*plcB*	Phospholipase C

P. aeruginosa is well known to exhibit Pi-chemotaxis, in that it is attracted to Pi when under phosphorus stress (Kato et al., 1992). The Pst complex in conjunction with PhoU act as negative regulators of Pi-chemotaxis, with mutants exhibiting a Pi-chemotactic response regardless of the Pi-status of the bacterium (Kato et al., 1994; Nikata et al., 1996). *P. aeruginosa* has been shown to possess two chemoreceptors responsible for Pi-taxis, named CtpH and CtpL, serving as chemoreceptors to high and low Pi conditions, respectively (Rico-Jiménez et al., 2016; Wu et al., 2000). Pi-starvation also induces hyper-swarming motility in *P. aeruginosa* (Blus-Kadosh et al., 2013). The Pi-chemotactic response is strongly linked to virulence in *P. aeruginosa*.

1.3.2 Phosphate-mediated virulence in *Pseudomonas aeruginosa*

A role for the Pho regulon has been stipulated in several aspects of *P. aeruginosa* virulence, including quorum sensing, biofilm formation, the type III secretion system and in interaction with hosts. PhoB elicits production of many proteins, one such being a phosphodiesterase, which in turn has been shown to decrease cyclic-di-GMP levels in *P. fluorescens* (Monds et al., 2007). An increase in cyclic-di-GMP based signalling is linked to biofilm formation, therefore suggesting that in the interplay between PhoB and biofilm formation, PhoB is a negative regulator. Indeed, this has been confirmed in several Pseudomonads, including *P. aeruginosa*, where PhoB modulates several downstream effectors to both negatively regulate biofilm formation, and to repress expression of the type three secretion system (Haddad et al., 2009; Monds et al., 2007; Monds et al., 2001). In a similar vein, phosphate starvation has been shown to promote hyper-swarming in *P. aeruginosa*; a phenotype that would not be conducive to biofilm formation (Bains et al., 2012).

Several incidences link the PhoBR phosphate-response system to quorum sensing (QS) in *P. aeruginosa*. Bacterial QS is a change in gene regulation based on environmental cues and social surroundings, and is also considered a cell-density-dependent response (Fuqua et al., 2001; Mekalanos, 1992). *P. aeruginosa* is known to release several communicator molecules; two are acyl-homoserine lactones (AHLs) and a third is a quinolone based molecule (Pesci et al., 1999; Pesci et al., 1997). The two AHL QS systems are known as *las* and *rhl*, and are well characterised in terms of virulence in *P. aeruginosa*, and interact with the third QS system, *Pseudomonas* quinolone signal (PQS) (McKnight et al., 2000). Overall, the *las* and *rhl* systems exert influence over 6% of the *P. aeruginosa* genome, including multiple virulence factors (Schuster et al., 2003; Smith & Iglewski, 2003). Putative Pho boxes have been identified preceding *rhlR*, *rhlI*, *lasR* and *pqsR* genes, suggesting that phosphate availability has an influence on all three QS systems (Jensen et al., 2006). In a complex system, PQS has been shown to modulate *rhlR* expression in a PhoB-dependent manner (Jensen et al., 2006). A fourth QS system has been recently identified in *P. aeruginosa*, IQS (integrating QS), and is important in orchestrating the QS response in clinical isolates that often exhibit

loss-of-function mutations in the *las* system (Lee et al., 2013; Lee & Zhang, 2014). Importantly, IQS production is activated by phosphate limitation (Lee et al., 2013). Virulence regulator σVreI, encoded by the vreAIR operon, is further involved in the control of *P. aeruginosa* virulence factors, and its expression occurs when phosphate is limiting in a PhoB-dependent manner (Quesada et al., 2016). The link between phosphate depletion and its subsequent effect on the QS response should not be understated, given the clinical relevance of phosphate-depletion and the myriad of important virulence genes expressed under QS control in *P. aeruginosa* (Lee & Zhang, 2014).

In host-pathogen interaction, phosphorus scarcity as a trigger of virulence has been shown in several models, for example in mice, *Caenorhabditis elegans* (*C. elegans*), epithelial cells and in zebrafish. Following intestinal surgery in mice, phosphorus levels were rapidly depleted to those that facilitated *P. aeruginosa* virulence, with the dramatic effects being mitigated by the introduction of an oral phosphate solution (Long et al., 2008). Indeed, hypophosphatemia following major surgery can be a predictor of patients developing fatal sepsis (Shor et al., 2006). Phosphate depletion in a *C. elegans* infection model facilitated a lethal phenotype in *P. aeruginosa* in a PhoB and PQS dependent manner (Zaborin et al., 2009). MDR *P. aeruginosa* strains were found to express PstS, the high affinity Pi-transporter, in a concentrated manner on protruding appendages in an epithelial cell model (Zaborina et al., 2008). The PstS-rich appendages contribute to the bacterium's ability to adhere to intestinal epithelial cells and also disrupt the integrity of the cell barrier (Zaborina et al., 2008).

1.3.3 Membrane phospholipids as a source of phosphate

Phospholipids can be considered a reservoir of phosphate to *P. aeruginosa*, extracellularly in terms of host phospholipids, but they also represent 15-20% of bacterial cellular phosphorus content (Karl & Björkman, 2015). Indeed, the replacement of membrane phospholipids with phosphorus-free lipids has been known for some time in two *Pseudomonas* species: *Pseudomonas fluorescens* and *Pseudomonas diminuta* (Minnikin & Abdolrahimzadeh, 1974; Minnikin et al., 1974).

Under phosphorus stress, environmental organism *Sinorhizobium meliloti* expresses an intracellular phospholipase C that removes the head groups of its native phospholipids, from which inorganic phosphate can be liberated for use in the cell (Zavaleta-Pastor et al., 2010). Finally, marine environments are inherently phosphorus-scarce, leading to organisms such as phytoplankton synthesising substitute lipid classes in place of phospholipids (Van Mooy et al., 2009).

1.4 Bacterial lipid membranes

1.4.1 Phospholipid biosynthesis

Gram negative bacterial cell walls are composed of an inner phospholipid bilayer (inner membrane – IM), followed by a layer of peptidoglycan, and surrounded by the outer phospholipid bilayer (outer membrane – OM). Initial studies of bacterial cell membranes used *Escherichia coli* (*E. coli*) as a model, leading to the more simplistic view that bacterial membranes are composed of two major phospholipids classes, phosphatidylethanolamine (PE) and phosphatidylglycerol (PG), alongside a smaller proportion of cardiolipin (CL) (Zhang & Rock, 2008). This composition allows a balance in electrostatic charges between zwitterionic phospholipid PE and negatively charged PG and CL, which is important for maintaining the steric conformation of many integral membrane proteins (Kondakova et al., 2015).

In terms of *Pseudomonas* spp., the lipid composition in different strains does not vary significantly. For *P. aeruginosa*, alongside PE, PG and CL as for *E. coli*, the lipidome can also contain a small proportion of phosphatidylcholine (PC), owing to an additional PC synthesis pathway (Kondakova et al., 2015). In these four major glycerophospholipid (GP) species, PE and PG account for 95% of *Pseudomonas* spp. membrane; 75% PE and 20% PG (Kondakova et al., 2015). The synthesis of GPs in bacteria stems from the addition of any one of a variety of polar head groups to phosphatidic acid (PA).

Bacteria can source PA through different pathways, with the initial step being the generation of sn-glycerol-3-phosphate (G3P; Figure 1.5). Precursor dihydroxyacetone phosphate is converted to G3P by GpsA in bacteria, or alternatively G3P is directly

obtained through GlpT organophosphate: phosphate antiporter (Kondakova et al., 2015; López-Lara & Geiger, 2017). G3P can also be obtained through phosphorylation of available glycerol by GlpK (Yao & Rock, 2013). G3P then undergoes two acylation steps to form PA. The first acylation occurs at the sn-1 position, carried out by either PlsB or PlsY distinct acyltransferase families. PlsC family acyltransferases then carry out the second acylation at the sn-2 position, resulting in the formation of PA. PA is further converted into the major bacterial glycerophospholipid precursor CDP-diacylglycerol (CDP-DAG) by CDP-DAG synthase CdsA (Icho et al., 1985; López-Lara & Geiger, 2017; Yao & Rock, 2013).

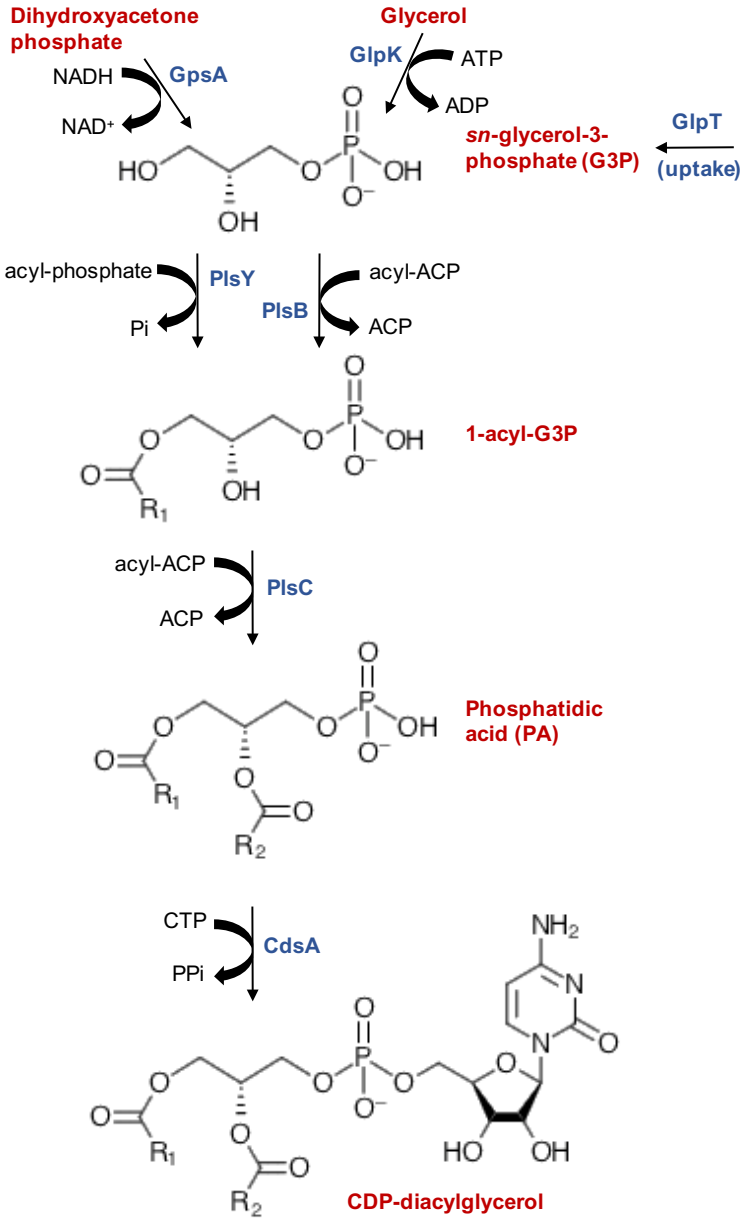

Figure 1.5. Various pathways through which bacteria access phosphatidic acid to generate CDP-diacylglycerol; the base for phospholipid synthesis. Figure adapted from (López-Lara & Geiger, 2017).

CDP-DAG is the common precursor for the biosynthesis of glycerophospholipid classes in bacteria, including abundant PE, and PG, CL and PC present in *Pseudomonas* spp. membranes (Figure 1.6). Condensation of CDP-DAG with L-serine to form phosphatidylserine (PS), carried out by PS synthase (PssA), is the first step in the generation of PE (Kondakova et al., 2015; López-Lara & Geiger, 2017). This is followed by the decarboxylation of PS by PS decarboxylase (Psd) to complete the formation of abundant, zwitterionic PE (López-Lara & Geiger, 2017). CDP-DAG can also follow an

alternative pathway to form PG and CL. PG phosphate synthase (PgsA) condenses G3P with CDP-DAG to form PG phosphate (PGP), with PGP then dephosphorylated by a PGP-specific phosphatase (PgpA in *Pseudomonads*) to form PG (Kondakova et al., 2015). PG can then be further utilised in the production of CL, through the condensation of two molecules of PG by a CL synthase (ClsA, ClsB, ClsC, where the latter synthesises CL from PE and PG), producing CL (Tan et al., 2012). Finally, many prokaryotes lack the capability to synthesise PC. However, those that do, including *P. aeruginosa*, encode the PC synthase (Pcs) pathway (Kondakova et al., 2015). Pcs uses choline to convert CDP-DAG into PC and CMP. Overall, the diversity of fatty acid chains present in the glycerophospholipid precursor CDP-DAG and a variety of head group moieties create wide diversity in phospholipid species in bacteria.

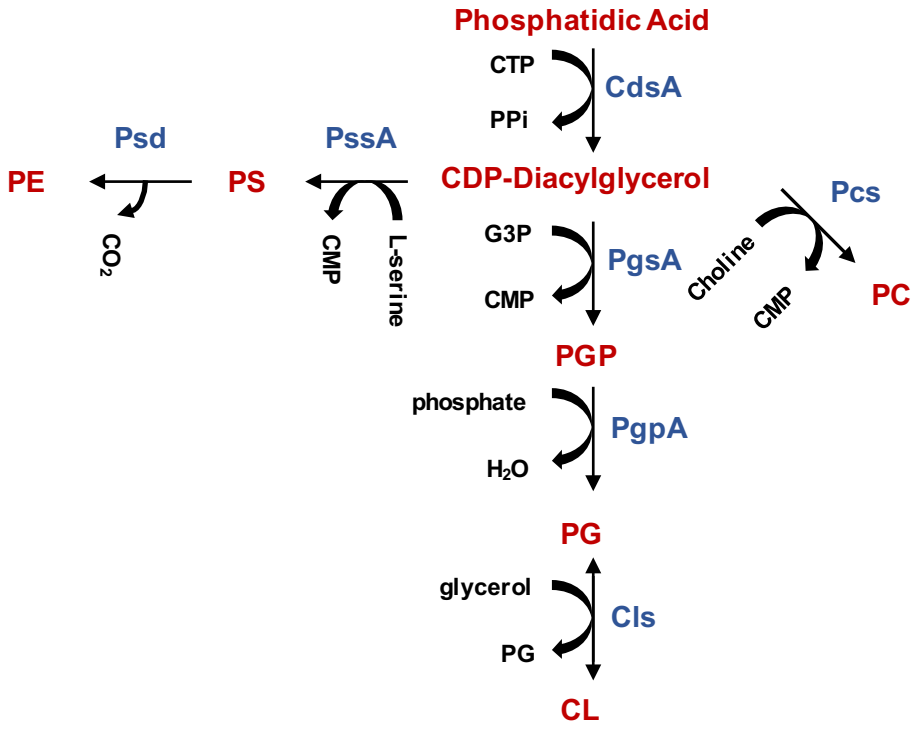

Figure 1.6. Synthesis of predominant *P. aeruginosa* membrane phospholipids phosphatidylethanolamine (PE) and phosphatidylglycerol (PG) proceeds through common precursor cytidine diphosphate diacylglycerol (CDP-DAG). For PE, a further phosphatidylserine (PS) step is required, whereas intermediate phosphatidylglycerol phosphate (PGP) is required for PG synthesis. Phospholipids and their precursors are in red, with synthesis enzymes in blue. CL: cardiolipin, PC: phosphatidylcholine.

1.4.2 Alternative glycerolipids in bacteria

The biosynthesis of glycerophospholipids in bacteria allows for the generation of great diversity in phospholipid structure, which is attributed to the diverse roles lipids can undertake within a cell (Dowhan, 1997). More recently, the synthesis and roles of non-phosphate (non-P) containing lipids has been investigated, particularly with respect to environmental microbiology. When low phosphate (P) conditions are present in the environment, bacteria will respond in a way to reduce the P requirements of the cell. Phospholipids represent a significant source of P in the cell, as much as 15-20% (Karl & Björkman, 2015). As such, many bacterial species are able to access this P source through lipid remodelling. Lipid remodelling is the process by which bacteria will selectively modify the lipid composition of the membrane in response to nutrient stresses.

Diacylglycerol (DAG) is the base molecule upon which non-P glycerolipid synthesis occurs, with several non-P lipid classes being recently described (López-Lara & Geiger, 2017). Glycoglycerolipids in plants and both photosynthetic and non-photosynthetic bacteria have been reviewed, where, in general, bacterial glycolipids have one or two sugar derivatives bound to DAG (Hölzl & Dörmann, 2007). A variety of glycolipids have been described in numerous bacterial phyla. In *Pseudomonas diminuta*, an intriguing bacterium that does not synthesise the normally major phospholipid species PE, several glycolipid classes are utilised in the membrane as the dominant components (Minnikin et al., 1974; Wilkinson, 1969).

Sulfur-containing lipids are also a non-P lipid, having first been described in plants and algae, namely sulfoquinovosyldiacylglycerol (SQDG). Elucidation of SQDG synthesis in *Rhodobacter sphaeroides* (*R. sphaeroides*) revealed the *sqdA* and operon *sqdBDC* synthesis pathway (Benning & Somerville, 1992). Under phosphate stress, some bacteria will also accumulate betaine lipids as non-P lipids in the membrane. Particularly, research focusing on diacylglycerol trimethylhomoserine (DGTS) found *btaA* and *btaB* genes to be essential in the biosynthesis of this alternate lipid in *R. sphaeroides* (Hofmann & Eichenberger, 1996; Riekhof et al., 2005).

As mentioned previously, DAG, as opposed to PA in glycerophospholipid synthesis, is the precursor molecule for non-P glycerolipids. Phospholipases are a diverse class of proteins that act on intact phospholipids at known cleavage sites, resulting in varying products. A recent discovery in *Sinorhizobium meliloti* (*S. meliloti*) found a novel intracellular phospholipase C, PlcP, that degrades phospholipids in response to P-stress, thereby producing DAG (Zavaleta-Pastor et al., 2010). This DAG is then the anchor on which non-P glycerolipid synthesis can occur, and likely the phosphoalcohol product is utilised as a source of phosphate for the cell (Figure 1.7). Indeed, further studies supported this finding in the marine bacterium *Phaeobacter* sp. MED193, confirming the lipid remodelling role for a PlcP with 57% sequence similarity to rhizobial PlcP (Sebastián et al., 2016). In addition, PlcP is often genomically located alongside a glycosyltransferase, Agt. The same study showed that expressing Agt from SAR11 clade marine bacterium *Pelagibacter ubique* in *E. coli* is sufficient for the accumulation of non-P glycolipids monoglycosyl diacylglycerol (MGDG) and glucuronic acid diacylglycerol (GADG) (Sebastián et al., 2016).

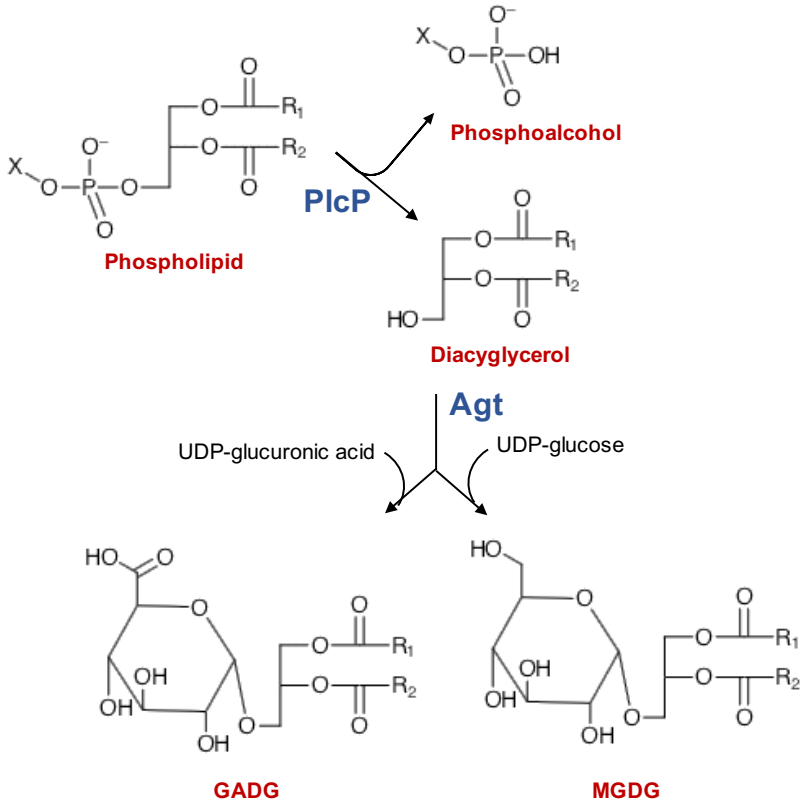

Figure 1.7. Glycolipid synthesis in marine bacterium *Phaeobacter* sp. MED193. Intracellular phospholipase C PlcP cleaves phospholipids, yielding diacylglycerol and phosphoalcohol. A glycosyltransferase (Agt) adds sugar moieties to DAG to form glucuronic acid diacylglycerol (GADG) or mono glycosyl diacylglycerol (MGDG). Figure adapted from (Sebastián et al., 2016).

1.4.2.1 Rhamnolipids

P. aeruginosa is able to produce a glycolipid composed of one or two rhamnose sugars linked to 3-hydroxy fatty acids, known as rhamnolipids (Soberón-Chávez et al., 2005). Rhamnolipids are produced by the *rhlAB* operon and are secreted by *P. aeruginosa*, acting as biosurfactants to access insoluble substrates and increase nutrient uptake (Caiazza et al., 2005). Under quorum sensing control, rhamnolipids have been stipulated as a virulence factor for *P. aeruginosa*. In interaction with epithelial cells, rhamnolipids are responsible for the disruption of the integrity of the epithelial layer, allowing paracellular invasion by the bacterial cells (Zulianello et al., 2006). Rhamnolipids also cause damage to tracheal cilia and have been found in the sputum of CF patients (Hastie et al., 1986; Kownatzki et al., 1987), and play a further role in the colonisation of lung tissue through solubilisation of phospholipids that are present

in lung surfactant, thereby enhancing the activity of secreted haemolytic phospholipase C (Liu, 1974). The biosurfactant capabilities of rhamnolipids are thought to facilitate the swarming motility of *P. aeruginosa* on semi-solid surfaces by decreasing surface tension (Kohler et al., 2000). Finally, rhamnolipids may act as a natural antimicrobial to enhance the competitiveness of *P. aeruginosa* (Haba et al., 2003).

1.4.3 Amino acid derived lipids in bacteria

As a further distinct lipid class that has been characterised in bacteria, amino acid based lipids (AA lipids) have a different mode of synthesis. AA lipids are glycerol-free intact polar lipids found in bacterial membranes. Arguably the most well characterised AA lipid is ornithine lipid (OL), produced in several bacterial species in response to phosphorus stress, including *Pseudomonads* (Minnikin & Abdolrahimzadeh, 1974; Wilkinson, 1970). The biosynthetic pathway for OL was first described in *S. meliloti*, where the processive activity of enzymes OlsB and OlsA was found to generate OL (Figure 1.8; Gao et al., 2004; Weissenmayer et al., 2002). N-acyltransferase OlsB links the carboxyl group of a 3-hydroxy fatty acid with the α-amino group of ornithine, in an amide linkage, generating biosynthetic intermediate lyso-OL (Weissenmayer et al., 2002). Esterification of lyso-OL by O-acyltransferase OlsA, through linkage between the carboxyl group of an incoming 3-hydroxy fatty acid and the 3-hydroxyl group on the present fatty acid, is the second and final step in OL production (Weissenmayer et al., 2002). In *Pseudomonas* species, a commonly found OL structure is 3-hydroxyoctadecanoic acid amide-linked to ornithine and further esterified to hexadecanoic acid (Kaawai et al., 1988). The OL synthesis pathway has also been characterised in *P. aeruginosa*, where two-gene operon PA4350–PA4351 (now termed *olsBA*) was found to be upregulated in response to phosphorus stress and subsequently responsible for OL production in this bacterium (Lewenza et al., 2011).

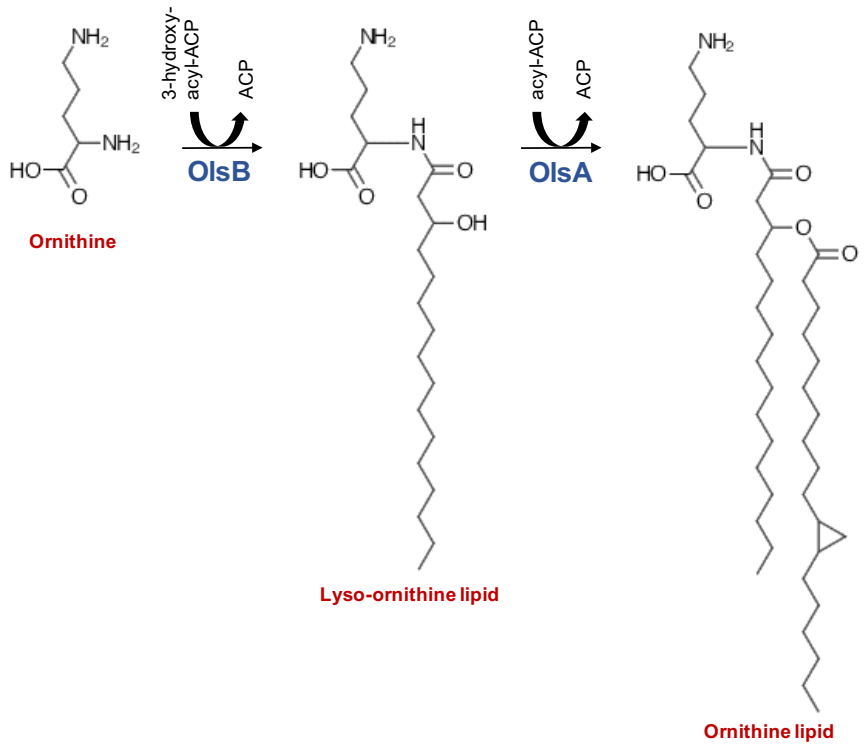

Figure 1.8. Ornithine lipid biosynthesis is catalysed by acyltransferases OlsBA. ACP: acyl carrier protein. Figure adapted from (Vences-Guzmán et al., 2012).

Further examples of amino acid derived lipids can be found in a wide range of bacterial species. Glutamine lipid (QL) has been demonstrated in several species, such as *Ruegeria pomeroyi* DSS-3 (Smith et al., 2019). In a similar vein to OL, glutamine lipid (QL) is synthesised through an amide linkage of a fatty acid to glutamine by N-acyltransferase GlsB, and, in this bacterium, the second esterification step is carried out by O-acyltransferase OlsA, the same enzyme used for OL synthesis (Smith et al., 2019). QL production has also been characterised in *R. sphaeroides* (Moore et al., 2016; Zhang et al., 2009), along with a further amino acid derived lipid, lysine lipid (Moore et al., 2016). Indeed, a multitude of glycerol-free AA lipids have been described across numerous bacterial species, including glycine lipid, serine-glycine lipid, ornithine-taurine lipid and modified methyl-ornithine lipid variations (Batrakov et al., 1999; Moore et al., 2013; Shiozaki et al., 1998). Glycerol-free AA lipids are an interesting and diverse class of lipid, with roles in bacterial response to stress conditions (Vences-Guzmán et al., 2011), their production can be critical to survival in some organisms (Smith et al., 2019).

1.4.3.1 Lipid A

Lipid A is a well-studied molecule that also lacks a glycerol backbone. Lipid A forms the membrane anchor of the LPS layer in the asymmetrical outer membrane of many Gram-negative bacteria. The synthesis of lipid A is a multistep process that begins with the formation of UDP-2,3-diacyl-glucosamine, through two acylations of UDP-GlcNAc (Xiao et al., 2017). Subsequent steps create a glycosidic link to form a disaccharide of glucosamine, that is phosphorylated at the 1-position and 4'-position, denoted lipid IV_A (Xiao et al., 2017). Two successive glycosyl transfer reactions decorate lipid IV_A with sugars, and the two final acylation steps of this tetra-acyl tetra-saccharide results in the hexa-acylated lipid A molecule (Xiao et al., 2017). Lipid A is glycosylated with a core oligosaccharide, which together play a critical role in the integrity of the outer membrane as a permeability barrier (Whitfield & Trent, 2014). The final component of LPS is the structurally diverse O-antigen sugars (Whitfield & Trent, 2014).

Lipid A is considered an endotoxin as it elicits a strong immunogenic response, and as such bacteria have developed modification methods in attempt to dampen this recognition (Needham & Trent, 2013; Raetz & Whitfield, 2002). In *P. aeruginosa*, PagP is a palmitoyl transferase localised in the outer membrane that will add palmitate from a membrane phospholipid to lipid A, resulting in hepta-acylated lipid A that confers increased resistance to CAMPs and a reduced immune response (Bishop et al., 2000; Rutten et al., 2006). PagL has been described as lipid A 3-O-deacylase, hydrolysing the ester bond at the 3-position of lipid A thereby releasing the fatty acid and leaving a penta-acylated lipid A, which again decreases the host immune response (Ernst et al., 2006; Kawasaki et al., 2004). More recently, PagL deacylation of lipid A in *P. aeruginosa* was shown to significantly perturb polymyxin B activity (Han et al., 2018). PagP and PagL have been stipulated in *P. aeruginosa* colonisation of CF patients as important for adaptation and survival in the CF lung (Ernst et al., 2006; Thaipisuttikul et al., 2014). Additional lipid A modification mechanisms confer resistance to antimicrobial peptides (section 1.2.2).

1.4.4 Amino acid decoration of phospholipids

The bacterial membrane is an important protective barrier against defence molecules produced by other organisms present in the surrounding environment. Potent broad spectrum host defence peptides (HDPs) are produced by all classes of life. As such, many bacterial species are able to undergo rapid membrane modifications to alter biochemical properties and therefore perturb unwanted interactions. The decoration of phospholipids with amino acids is a widespread bacterial membrane modification, such as the addition of lysine or alanine to PG (amino acid-PGs; aa-PGs) (Roy, 2009). Lysl-PG (L-PG) is the only phospholipid to possess an overall net positive charge, whereas alanyl-PG (A-PG) is zwitterionic. The use of aa-PG species over native membrane phospholipids serves to decrease the net negative charge of the bacterial membrane (Arendt et al., 2013; Roy, 2009). This confers protection against charged antimicrobial peptides, alongside some other classes of antibiotic that have been shown to interact with the bacterial cell membrane, such as daptomycin in treating Gram-positive *Staphylococcus aureus* (*S. aureus*) (Muraih et al., 2011; Pogliano et al., 2012).

In elucidating the pathway for bacterial synthesis of L-PG, multiple peptide resistance factor (MprF) is well characterised in *S. aureus* as essential for L-PG production (Nesbitt & Lennarz, 1968; Peschel et al., 2001). MprF is an L-PG synthase; a membrane bound protein that competes for Lys-tRNA to generate L-PG in the inner membrane (Staubitz et al., 2004). The phospholipid flippase domain of MprF delivers L-PG to the outer membrane (Slavetinsky et al., 2012). *S. aureus* mutant in MprF was identified to be more susceptible to lantibiotic gallidermin (a polycyclic peptide), human defensins and other cyclic antimicrobial peptides (CAMPs) than its WT counterpart (Kristian et al., 2003; Peschel et al., 2001), highlighting the key role of modified membrane charge through aa-PGs in interaction with a wide variety of charged molecules. For *S. aureus*, the importance of L-PG production extends to other antimicrobials, with L-PG defect mutants more susceptible to positively charged antibiotic gentamicin, with moenomycin and vancomycin displaying increased binding affinity to L-PG negative cells (Nishi et al., 2004). L-PG production has been described in other Gram-positive

pathogens, including *Listeria monocytogenes* (*L. monocytogenes*) (Fischer & Leopold, 1999). An MprF homolog has been characterised as an L-PG synthase, with the *L. monocytogenes* mutant in *mprF* also conferring increased susceptibility to CAMPs, from both bacterial and human sources (Thedieck et al., 2006). Important pathogen *Mycobacterium tuberculosis* (*M. tuberculosis*) encodes two domain protein LysX, having both the function of lysyl transferase MprF and lysyl-tRNA synthase, to produce L-PG (Maloney et al., 2009). Equally in this bacterium, a lack of L-PG confers sensitivity to CAMPs including defensins, and is thereby linked to the intracellular survival of *M. tuberculosis* in phagocytic cells (Fol et al., 2013; Maloney et al., 2009).

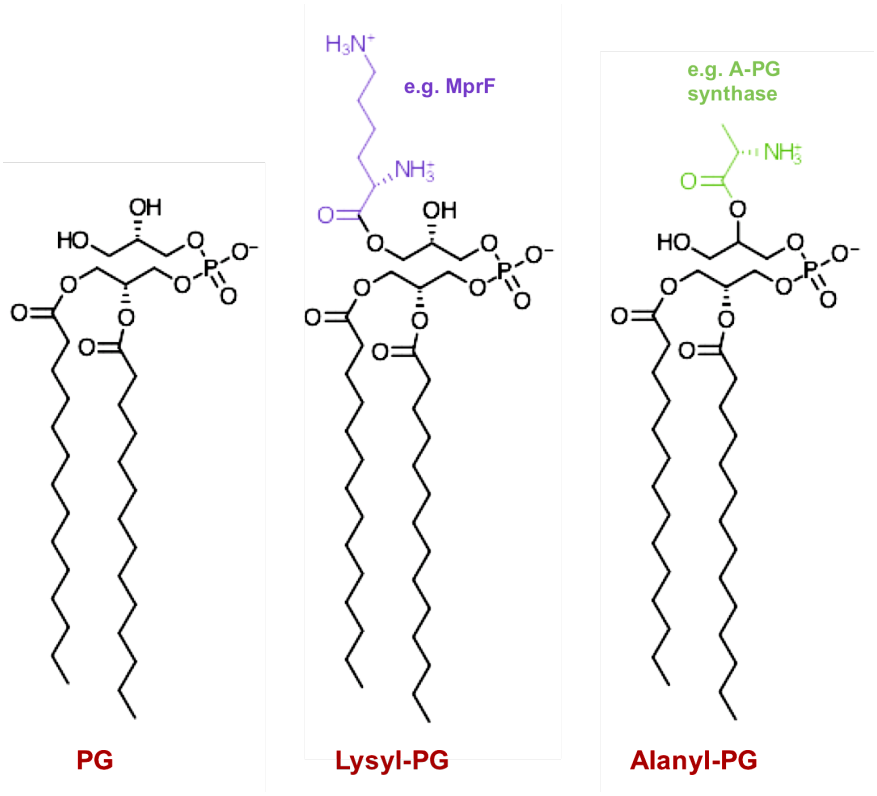

Figure 1.9. Amino acid modifications of phosphatidylglycerol (PG). MprF catalyses the addition of lysine to generate lysyl-PG in some bacterial species (purple). In *P. aeruginosa*, MprF homolog alanyl-PG synthase (A-PG) catalyses the biosynthesis of alanyl-PG (green). Figure adapted from (Slavetinsky et al., 2017).

Other members of the MprF protein family can produce A-PG through the addition of alanyl from Ala-tRNA onto PG. Generally, MprF proteins have a restricted specificity for their aminoacyl tRNA substrate. For example, food poisoning pathogen *Clostridium perfringens* has two homologs of *S. aureus* MprF, one necessary for L-PG and the

second for A-PG (Slavetinsky et al., 2012). For *P. aeruginosa*, only one orthologous *mprF* gene has been described, encoding a transmembrane protein strictly synthesising A-PG only, thereby denoted A-PG synthase (Arendt et al., 2013; Klein et al., 2009). The production of A-PG in *P. aeruginosa* is the result of a stress response, under acidic pH conditions (pH 5.3, applicable to cystic fibrosis lung conditions (Coakley et al., 2003)) as much as 6% of the lipidome is A-PG (Klein et al., 2009). Intriguingly, even though A-PG is zwitterionic and therefore does not alter net membrane charge to the same extent as L-PG with its positive overall net charge, a *P. aeruginosa* mutant unable to synthesise A-PG exhibited significantly increased sensitivity to the cationic peptide protamine (Klein et al., 2009). This suggests other mechanisms to be involved in this phenomenon. For example, a decreased ability of the peptide to reach the membrane, or altered membrane permeability. This is supported by further findings that the presence of A-PG in the *P. aeruginosa* membrane increases resistance to the β-lactam cefsulodin, which has a different mode of action to CAMPs (Arendt et al., 2012; Roy et al., 2009). As the ability to produce A-PG conferred better survival in the presence of lactate due to lower internal accumulation of the osmolyte, it is suggested that membrane permeability is reduced due to the presence of A-PG in *P. aeruginosa* (Roy et al., 2009). A more recent PG variant reported in *P. aeruginosa* is glucosaminyl-PG, where glucosamine, a product of metabolism in this bacterium, is esterified to PG (Abbes et al., 2018). Any impact of glucosaminyl-PG on antimicrobial resistance or host-pathogen interaction is yet to be determined.

Overall, changes to the *P. aeruginosa* lipid membrane encompass amino acid modifications of phospholipids and a variety of lipid A modifications. In terms of introducing alternative lipids into the membrane, only ornithine lipid production has been characterised as a surrogate membrane lipid in *P. aeruginosa*. The synthesis of glycolipids in *P. aeruginosa* has not been characterised. Thus, this project aimed to investigate the synthesis pathway and phenotypic effects of glycolipids in *P. aeruginosa*.

1.5 PhD project aims

The aims of this project were to:

1. Investigate whether *Pseudomonas aeruginosa* is able to produce the glycolipids monoglycosyl diacylglycerol (MGDG) and glucuronic diacylglycerol (GADG) in response to phosphorus stress.
2. Identify the genes responsible for the production of these glycolipids in *Pseudomonas aeruginosa.*
3. Characterise proteomic changes in *Pseudomonas aeruginosa* in response to phosphate stress, including any alterations when unable to produce glycolipids through mutant analysis.
4. Investigate antimicrobial resistance trade-offs as a result of the membrane modifications to relieve phosphorus stress.
5. Determine any role for membrane lipid remodelling in host-pathogen interactions.

Chapter 2 Materials and Methods

2.1 Cultivation of bacteria for lipid analysis

2.1.1 Maintenance of *P. aeruginosa* strains

P. aeruginosa strains PAO1 and PA14 were obtained from the DSMZ microorganism collection (Germany). A freeze-dried ampoule was resuspended in 1 mL lysogeny broth (LB), plated onto LB agar plates and incubated at 37°C overnight. Single colonies were resuspended in 3 mL LB, and grown at 37°C, 150 rpm shaking overnight before addition of 50% glycerol (w/v) (autoclaved) in a 50:50 (v/v) ratio and stored at -80°C. Routinely, wild type PAO1 was plated onto LB and stored for use for 2 weeks at 4°C.

A defined medium previously outlined for *Pseudomonas fluorescens* to control phosphate levels was used; modified minimal media A (Lidbury et al., 2016), comprising: Na-succinate 20 mM, NaCl 200 mg L^{-1}, NH_4Cl 450 mg L^{-1}, $CaCl_2$ 200 mg L^{-1}, KCl 200 mg L^{-1}, $MgCl_2$ 450 mg L^{-1}, with trace metals $FeCl_2$ 10 mg L^{-1} and $MnCl_2$ 10 mg L^{-1}, and 10 mM 4-(2-hydroxyethyl)-1-piperazineethanesulfonic acid (HEPES) buffer used at pH 7. Phosphate source Na_2HPO_4 was added to a final concentration of 100 µM (low P) or 1 mM (high P). An intermediate phosphate source of 600 µM Na_2HPO_4 was used for overnight cultures in some experiments to prevent any excess storage of phosphate that could hamper results. All components were filter sterilised using 0.22 µM pore size filters, and made up using ddH_2O.

2.1.2 Confirmation of *P. aeruginosa* mutants

P. aeruginosa PAO1 mutants in lipid remodelling gene loci PA3218, PA3219, PA0842, PA4350 and PA4351 were obtained from the University of Washington transposon mutant library collection (strain annotation outlined in table 2.1). Mutants were maintained as above, with the addition of tetracycline at 5 µg mL^{-1} final concentration where necessary. Mutants were verified using polymerase chain reaction (PCR). To do so, *P. aeruginosa* DNA was extracted using a freeze-boil method: a single colony resuspended in 100 µL PCR grade water was subjected to -80°C for 10 minutes, followed by 80°C water bath for 10 minutes, repeating for two cycles. PCR was carried

out using KAPA-Taq reagents (Sigma). PCR reaction was carried out in a total volume of 50 µL: 29.5 µL PCR grade water, 10 µL 10X Taq buffer, 0.5 µL KAPA-Taq DNA polymerase, 2 µL appropriate forward and reverse primers (10 mM; table 2.1), 1 µL dNTPs and 5 µL extracted DNA template. The PCR cycle was as follows: 95°C initial denaturation for 5 minutes, followed by 30 cycles of: denaturation 95°C for 30 sec, annealing at 55-60°C for 30 sec (primer dependent) and extension at 72°C for 1 min per kb, with a final extension at 72°C for 1 min per kb. PCR products were run on a 1% agarose gel in 1x TBE, using a 1 kb ladder (NEB) to confirm the expected size for transposon insertion mutation.

Table 2.1. Primers used for the confirmation of correct transposon sequence insertion in *P. aeruginosa* mutants (strains obtained from the University of Washington transposon mutant library). PA0842 is *agt2*, PA3218 is *agt1* and PA3219 is *plcP*.

Strain	Gene locus	Primer name	Sequence 5' to 3'
PW2532	PA0842-D03::ISlacZ/hah	PW2532_F	AAGCCTTTGCCTGAGAGCTA
		PW2532_R	GCAGTACAGCGAGCACTACG
PW2533	PA0842-A05::ISphoA/hah	PW2533_F	GGATGGAAGAGTTGGCTGTC
		PW2533_R	AGAGTCGGACAAGGTGATCG
PW6388	PA3218-F06::ISphoA/hah	PW6388_F	CAAGATCCTCGTGCATGACC
		PW6388_R	GGCATGAGGCTATTGATCGT
PW6389	PA3219-H02::ISphoA/hah	PW6389_F	ACGCAGGTATTCGGGAAAG
		PW6389_R	CAAGATCGGAAAAACACCGT
PW6390	PA3219-G05::ISlacZ/hah	PW6390_F	ACGATCAATAGCCTCATGCC
		PW6390_R	CAAGATCGGAAAAACACCGT
PW8345	*olsB*-F01::ISlacZ/hah	PW8345_F	CAGTCTTCCAGGGAGCCTTC
		PW8345_R	TTGAGCAGGATGAACACGTC
PW8346	*olsB*-D06::ISlacZ/hah	PW8346_F	CTGAGCTTGCACAACAAAGC
		PW8346_R	ACATGGTTGGCTACCCACAG
PW8347	*olsA*-F06::ISphoA/hah	PW8347_F	GACGTGTTCATCCTGCTCAA
		PW8347_R	GTGGTACGCAATGCGAAGAT
PW8348	*olsA*-F07::ISphoA/hah	PW8348_F	ACCTGTGCACCGACTACCTG
		PW8348_R	CGAGGTGGCTGAGCAAGT
-	Tn specific (ISphoA/hah)	Hah-138	CGGGTGCAGTAATATCGCCCT
-	Tn specific (ISlacZ/hah)	Lac-148	GGGTAACGCCAGGGTTTTCC

PlcP and *agt2* each had two strains with a Tn insertion available, and *agt1* had one strain (Table 2.2). Oligonucleotide primers specific to flanking regions of each gene were first tested for gene specificity in WT *P. aeruginosa* strain PAO1 (Figure 2.1). Within this process, I changed from using direct colony PCR to first using the freeze/boil protocol to release DNA from the bacterial cells before using for PCR, resulting in a much better PCR product yield.

Table 2.2. Orientation of transposon insertions in lipid remodelling mutant strains and expected PCR product sizes of gene-specific primer sets in WT *P. aeruginosa* PAO1, and the Tn-specific with flanking primer combination in mutant strains.

Strain	Gene (locus)	Transposon orientation	Expected product in WT (bp)	Expected product in mutant (bp)
PW6390	*plcP* (PA3219)	Reverse	858	297
PW6389	*plcP* (PA3219)	Forward	1174	599
PW6388	*agt1* (PA3218)	Forward	882	523
PW2532	*agt2* (PA0842)	Forward	860	551
PW2533	*agt2* (PA0842)	Reverse	788	243

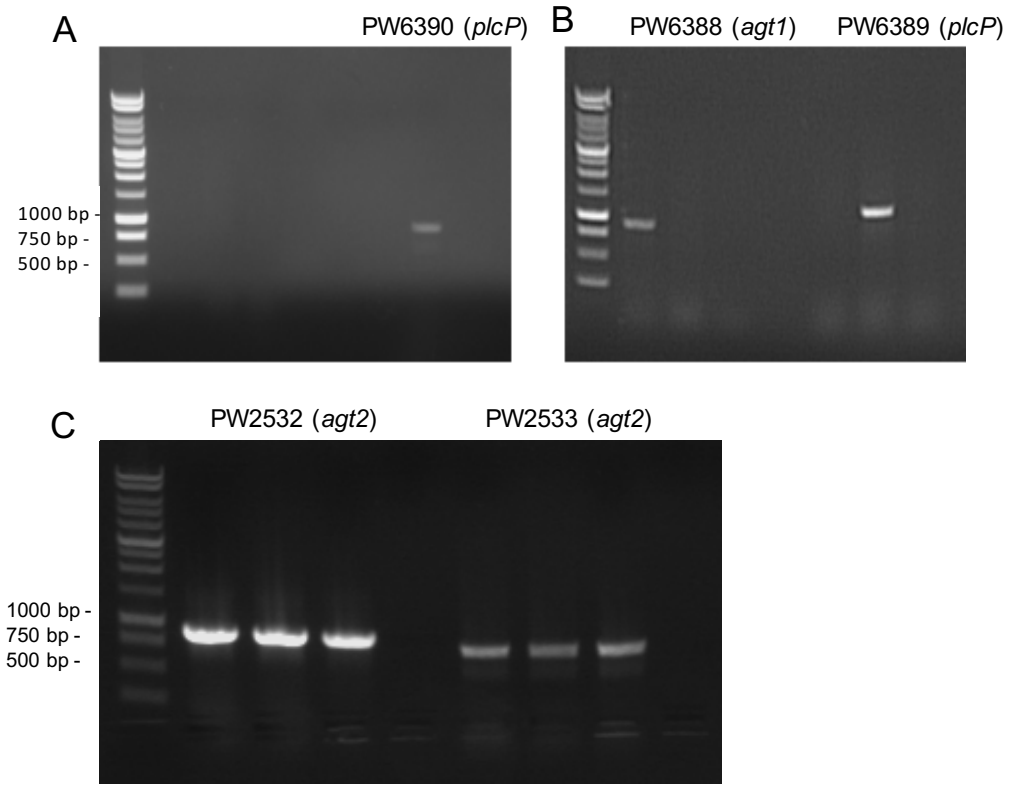

Figure 2.1. Confirmation that flanking primers were gene-specific in WT *P. aeruginosa* strain PAO1. A) and B) Confirmation of gene-specific primers for *plcP* and *agt1* genes using direct colony PCR. C) Confirmation of gene-specific primer sets for the *agt2* gene using *P. aeruginosa* WT PAO1 DNA extracted through a freeze/boil series.

Tn insertion into the correct location in the glycolipid remodelling mutant strains was confirmed using a Tn-specific primer in combination with a forward or reverse flanking primer, depending on the orientation of the transposon insertion. All mutant strains were confirmed through production of the expected PCR product sizes (Figure 2.2, Table 2.2), and the confirmed colonies were then used to create glycerol stocks for future use.

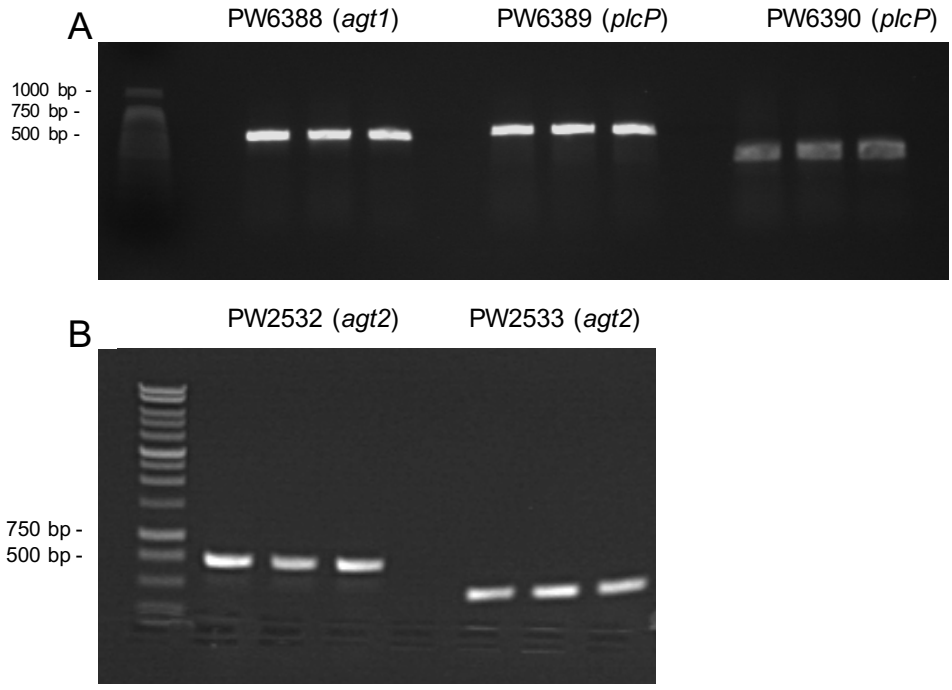

Figure 2.2. Pairs of transposon-specific and gene-specific PCR primers confirmed the correct location of transposon insertion in lipid remodelling mutant strains (*plcP*, *agt1* and *agt2* genes) of *P. aeruginosa* PAO1.

2.1.3 Alkaline phosphatase assay

Alkaline phosphatase (ALP) activity was monitored as a measure of phosphate stress, and can be detected easily as it is secreted by *P. aeruginosa*. The assay utilises the cleavage of *para*-nitrophenol phosphate (pNPP) by ALP to yield yellow-coloured *para*-nitrophenol (pNP). Liquid *P. aeruginosa* culture samples were incubated with 10 mM pNPP (made up using 100 mM pH 8 Tris buffer) to a final concentration of 1 mM pNPP, for 1 hour in the dark. Samples were centrifuged at 14,000 x *g* for 10 minutes, and the yellow-pNP supernatant measured in 150 µl triplicates at 407 nm (BioRad iMark microplate reader). Readings were normalised using both a Tris-only incubation

control and further by bacterial density (optical density reading at 600 nm (OD600)). Production of pNP was quantified using a calibration curve of pNP standards (Figure 2.3).

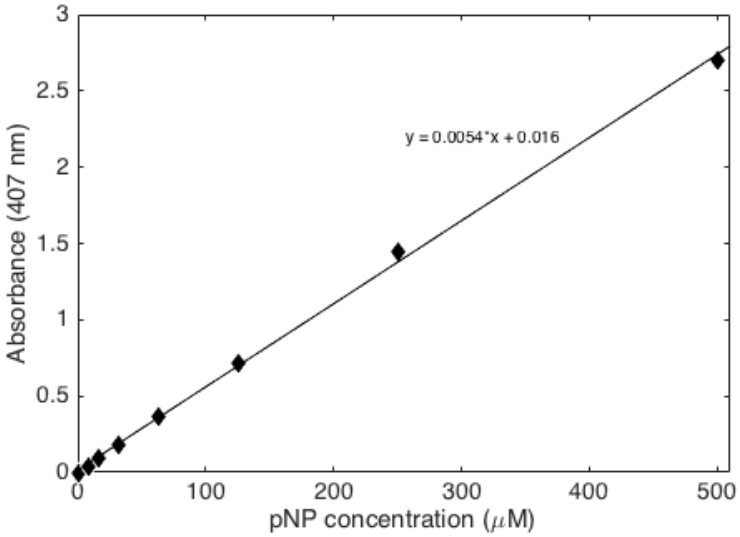

Figure 2.3. Standard curve of *para*-nitrophenol (pNP) from 0-500 µM measured at an absorbance wavelength of 407 nm. Each was blank corrected using buffer only.

2.1.4 Transformation of BLR(DE3)pLysS *E. coli*

P. aeruginosa genes PA3218 (Agt1) and PA0842 (Agt2) were codon optimised for *E. coli* and chemically synthesised (GenScript) into plasmid pET-28a(+). *E. coli* BLR(DE3) competent cells were thawed for 5 minutes before incubation with 10 ng pET-28a_Agt plasmid, and placed on ice for 5 minutes. Cells were then subjected to heat shock at 42°C for 30 seconds, placed back on ice for 2 minutes. Recovery super optimal broth with catabolite repression (SOC) was added, with samples incubated at 37°C shaking, for 1 hour. Transformed cells were then plated onto kanamycin-LB agar (50 µg mL^{-1}), grown overnight at 37°C. Single colonies were picked to grow in small volume LB-Kan (50 µg mL^{-1}) to 0.6 OD_{600} before induction with 0.4 mM isopropyl β-d-1-thiogalactopyranoside (IPTG) overnight at 25°C. 1 mL samples were then pelleted at 10,000 x *g* for 5 minutes. Pellets were stored at -80°C until lipid extraction and subsequent analysis on HPLC-MS.

2.1.5 Iron-restricted growth

Succinate medium was used to create iron (Fe) limited conditions for *P. aeruginosa*: K_2HPO_4 6 g L^{-1}, KH_2PO_4 3 g L^{-1}, $(NH_4)_2PO_4$ 1 g L^{-1}, $MgSO_4$ 0.2 g L^{-1}, succinic acid 4 g L^{-1} and NaOH 1.1 g L^{-1}, adjusted to pH 7.0 and filter sterilised. 10 mL of LB medium was inoculated with a single colony of *P. aeruginosa* PAO1 WT and grown overnight at 37°C, 180 rpm. The overnight culture was diluted 1:10 in 50 mL final culture volume of succinate Fe-restricted medium, and incubated for 24 hrs at 37°C, 180 rpm. After the 24 hrs, this step was repeated. After the final 24 hrs, samples were taken for HPLC-MS analysis of the lipidome.

2.1.6 Extraction of membrane lipids

Intact polar membrane lipids were extracted using a modified version of the typically used Folch extraction method (Folch et al., 1957; Sebastián et al., 2016). Liquid *P. aeruginosa* cultures growing in +/-phosphate modified minimal medium A were sampled after 8 hrs, collecting the equivalent to OD_{600} 0.5 into a 2 mL glass chromacol vial (Thermo Scientific), pelleted at 4°C, 4,000 rpm for 15 minutes. If required, pellets were then stored at -80°C for <1 month, using a PTFE-lined lid (Thermo Scientific). For lipid extraction, 500 µL ice-cold methanol (LC-MS grade) was added to the pellet and vortexed to resuspend, followed by the addition of 300 µL dH_2O and 1 mL chloroform (HPLC grade) and further vortexing for 30 seconds. Centrifuging at 3000 rpm for 5 minutes at 4°C, with the brake off, gives separation of the lipid fraction as the lower phase, which is collected using a glass Pasteur pipette and transferred into a fresh 2 mL glass chromacol vial. This chloroform extract was then dried under a stream of nitrogen (Techne sample concentrator) and resuspended in 1 mL acetonitrile (HPLC grade) for analysis.

2.1.7 Lipidome analysis using HPLC-MS

Extracted lipid samples were analysed using an UltiMate 3000 HPLC (Thermo Scientific) system coupled to AmazonSL quadrupole ion trap (Bruker) mass spectrometer (MS), using electrospray ionisation. Hydrophilic interaction chromatography (HILIC) using a BEH amide XP column (Waters) was utilised to

separate lipid classes based on head group properties. The column chamber was maintained at 30°C and the samples passed through at a 150 µL min^{-1} flow rate. The mobile phase of acetonitrile:ammonium acetate (pH 9.2) was used to elute the sample in a 15 minute per sample gradient, from 95% to 28% (w/v) ammonium acetate. Tandem MS (or MS^n) was used to fragment the intact lipids for identification. Resulting fragments have characteristic masses (m/z values) associated to lipid classes, in positive ion and/or negative ion mode. Characteristic masses can be losses of particular size charged fragments, or as a neutral loss. The data were analysed using Bruker Compass software package (DataAnalysis and QuantAnalysis).

2.2 Host-pathogen interaction

2.2.1 Maintenance of *Caenorhabditis elegans*

Caenorhabditis elegans (*C. elegans*) strain N2 was routinely maintained on *E. coli* OP50 lawns grown on standard nematode growth medium (NGM), as shown in Table 2.3 as "NGM +P" to indicate this as the phosphate-containing medium. NGM was modified to low phosphate ("NGM –P", Table 2.3) as previously described (Zaborin et al., 2009), through removing the potassium phosphate (K-Ph) buffer component (1 M K-Ph buffer: 9.5 g KH_2PO_4 and 5.25 g K_2HPO_4 in 100 mL ddH_2O), and instead adjusting to pH6 using HCl. To compensate for the lack of iron resulting from K-Ph removal, as phosphate will introduce some iron contamination through chelation of Fe^{3+} (Rasmussen & Toftlund, 1986), NGM –P was further supplemented with 0.5 µM $FeSO_4$.

Table 2.3. Components of nematode growth media (NGM) as classical NGM (NGM +P) or modified to restrict available phosphorus (NGM –P).

Component	NGM +P (to 400 mL)	NGM –P (to 400 mL)
NaCl	1.2 g	1.2 g
Peptone	1 g	1 g
Agar	6.8 g	6.8 g
1 M $MgSO_4$	400 µL	400 µL
1 M $CaCl_2$	400 µL	400 µL
Cholesterol (5 mg mL^{-1} in ethanol)	400 µL	400 µL
1 M K-Ph buffer, pH6	10 mL	-
0.5 mM $FeSO_4$	-	400 µL
HCl	-	to pH6

For NGM +P, NaCl, peptone and agar were autoclaved together in 400 mL dH_2O, followed by cooling to 55°C in a water bath. For NGM –P, the pH was adjusted to pH6 using HCl before autoclaving. All other components were sterilised separately and added on cooling. 10 mL of NGM was used in each 60 mm plate. *E. coli* OP50 was routinely maintained on LB agar plates. Colonies were then suspended in 5 mL LB media and grown overnight at 37°C, and kept at 4°C for up to 2 months. 50 µL *E. coli* OP50 culture was added to the centre of each NGM plate, and grown to lawn overnight at 37°C. The seeded plates were then stored at 4°C, for up to three weeks. *C. elegans* living on *E. coli* OP50 were kept largely at 20°C, but the temperature was adjusted to 16°C or 25°C when necessary. *C. elegans* were passaged through "chunking"; the aseptic transfer of a small portion of agar containing tens-hundreds of nematodes onto a fresh seeded *E. coli* OP50 plate.

2.2.2 X-phosphate assay

To ensure *P. aeruginosa* was phosphate stressed on NGM –P plates, and therefore also undergoing lipid remodelling, alkaline phosphatase (ALP) production was examined using ALP substrate X-phosphate (also known as 5-bromo-4-chloro-3-

indolyl phosphate disodium salt, BCIP) as an indicator of phosphate stress. X-phosphate was dissolved in dH_2O at a concentration of 40 mg mL^{-1} and stored in the dark at -20°C. 25 µL 40 mg mL^{-1} X-phosphate suspension was spread onto NGM ±P plates and allowed to dry before streaking *P. aeruginosa* WT onto each plate. Plates were then incubated overnight at 37°C in the dark before observing colour changes.

2.2.3 *C. elegans* age synchronisation

C. elegans strain N2 were kept at 25°C for 36-48 hours to allow the laying of tens-hundreds of eggs. Eggs and worms were collected in 5 mL of M9 buffer (M9 buffer: KH_2PO_4 3 g L^{-1}, Na_2HPO_4 6 g L^{-1}, NaCl 5 g L^{-1}, to 1 L with dH_2O and autoclaved, cooled before adding 1 mL of sterile 1M $MgSO_4$ and stored at RT). The egg and worm suspension was centrifuged for 2 minutes at 400 x *g*, the supernatant discarded, and the pellet washed three times using 10 mL M9 buffer until bacterial turbidity was no longer present. Next, the pellet was subject to a bleaching solution to dissolve adult tissue, and leave the protected eggs behind. Bleaching solution is made fresh as 1 mL dH_2O, 5 mL 1 M NaOH and 2 mL ~4% NaClO as a 2X stock, diluting to working volume through addition of equal volume of M9 buffer. The pellet was shaken in bleaching solution for 3-5 minutes until adult tissue is mostly dissolved, and then immediately centrifuged for 1 minute at 400 x *g*, supernatant discarded and 15 mL M9 buffer added to neutralise the bleach. A further three washes in 15 mL M9 buffer were carried out, followed by gentle resuspension of eggs in 7 mL M9 buffer. Eggs were allowed to hatch over a 24 hour period placed at gentle agitation at room temperature. Worms arrested at L1 stage due to a lack of food source, thereby becoming age synchronised. L1 worms were pelleted by centrifuging at 400 x *g* for 2 minutes, supernatant discarded, and the egg pellet added dropwise to a seeded NGM *E. coli* OP50 plate, allowed to dry and placed at 20°C to grow to L4 or adult stage for use in *P. aeruginosa* infection model.

2.2.4 *C. elegans* infection model

The base method to investigate virulence of *P. aeruginosa* in *C. elegans* comparing high and low phosphate conditions is one previously published (Zaborin et al., 2009).

P. aeruginosa strain PAO1 was grown overnight on LB agar plates, before resuspending bacteria to an OD_{600} of 1 in either phosphate buffered saline solution (PBS) or 10% (w/v) glycerol, for high and low phosphate conditions, respectively. 100 µL of these suspensions were added in a dropwise manner to NGM +P or NGM –P plates, and incubated for 24 hrs at 37°C and a further 20 hrs at 20°C. 10 age synchronised adult worms were added per *P. aeruginosa* NGM ±P plate, in 5 replicates, having been previously starved of *E. coli* OP50 for at least 24 hrs. Survival was monitored for up to 7 days. This method required optimisation, with several components being altered in attempt to replicate the original findings for wild type (WT) *P. aeruginosa* PAO1 by Zaborin *et al*. Therefore, this method became the subject of the method development section 5.2.1.

2.2.5 *C. elegans* feeding preference assay

C. elegans will preferentially avoid strains that are sensed to be more virulent than other food sources present. *P. aeruginosa* PAO1 WT strain and Δ*agt1* (PA3218), Δ*agt2* (PA0842), and Δ*plcP* (PA3219) mutants were used to inoculate 5 mL minimal media A with 600 µM Na_2HPO_4 as an intermediate level of phosphate source, incubated overnight at 37°C, 180 rpm. Cultures were then diluted 1:10 in low phosphate minimal medium A (100 µM), and incubated at 37°C, 180 rpm shaking until each reached OD_{600} 0.5. Using only NGM –P plates, to maintain lipid remodelled states, 5 µL of culture was dropped onto each plate, equidistant apart from other strains. Strains compared for palatability were WT vs *Δagt1* vs *Δagt2* and WT vs *ΔplcP*. 20 L4 stage age synchronised *C. elegans* were added to the middle of each plate (not directly into any bacteria), with 4 replicate plates per test. Nematodes present on a bacterial spot at times of counting (6 hrs, 24 hrs and 48 hrs) was recorded as an indicator of feeding preference.

2.2.6 *Galleria mellonella* host-pathogen infection model

LB media was inoculated with a single colony of *P. aeruginosa* WT or Δ*plcP* strain and incubated overnight at 37°C, 180 rpm. Overnight cultures were diluted using LB to an OD_{600} of 0.1 and further incubated until reaching 0.6 OD_{600} (approximately 3 hours). Cultures were then diluted 1 in 300 in 10 mM $MgSO_4$ to an OD_{600} of 0.002, and further

serially diluted to 10^{-4}. This final dilution gave a CFU count of ~200 cells mL^{-1}, therefore the infection inoculum of 10 µL should contain very few bacterial cells. A low infection load is required for *P. aeruginosa* as it is highly virulent in this model (Jander et al., 2000). 10 µL of 10^{-4} dilution was injected into each *G. mellonella* larvae using a Hamilton syringe multi-step dispenser with a 30G needle, with 10 larvae used per biological replicate. Larvae injected with 10 µL of 10 mM $MgSO_4$ were used as controls. Larvae were scored as dead or alive based on reaction to touch, and on a health index scale based on the degree of melanisation (Champion et al., 2018).

2.3 Antimicrobial assays

2.3.1 Determining minimum inhibitory concentration

The broth microdilution method was used to determine the minimum inhibitory concentrations (MIC) of antimicrobial peptides polymyxin B and colistin (polymyxin E) (Wiegand et al., 2008). Using a polypropylene 96-well microtiter plate (Corning 3879), freshly prepared antimicrobial peptides were diluted across the first 10 columns in two-fold steps, from 128 mg L^{-1} down to 0.25 mg L^{-1} in minimal medium A, in 50 µL final volumes. A sterility control of 100 µL minimal medium A only was placed in column 12. Single colonies of *P. aeruginosa* PAO1 WT or lipid remodelling mutants were grown in 5 mL minimal medium A containing 600 µM Na_2HPO_4 overnight at 37°C, 180 rpm shaking. The subsequent culture was split into high (1 mM) and low (100 µM) phosphate minimal medium A (~0.05-0.1 OD_{600}), and grown to ~0.5-0.6 OD_{600}; long enough for lipid remodelling to occur in low phosphate conditions. Cultures were then adjusted to 1×10^8 colony forming units (CFU) mL^{-1}, and 50 µL added to each drug-containing well, therefore a 1:2 dilution giving a final bacterial load of 5×10^5 CFU mL^{-1}. A final growth control well in column 11 using 50 µL blank minimal medium A and 50 µL 1×10^8 CFU mL^{-1} bacterial suspension was used. From the growth control, 10 µL was taken and added to 990 µL minimal medium A, further diluted 1:10, and 100 µL of each dilution spread plated onto LB agar plates and incubated overnight at 37°C. The 96-well microtiter plate was incubated at 37°C for 24 hours before visual inspection of growth. MIC is defined as the lowest concentration of antimicrobial

peptide that inhibited growth of *P. aeruginosa*. Colonies were counted on the growth control plates to ensure the desired bacterial inoculum had been achieved.

2.3.2 Antibiotic kill curve assay

Single colonies of *P. aeruginosa* PAO1 WT and lipid remodelling mutant strains (PW2532, PW6388, PW6390) were suspended in 5 mL minimal medium A containing 600 μM Na_2HPO_4 as an intermediate concentration of phosphate source. After overnight growth at 37°C, 180 rpm shaking, the cultures were split into high (1 mM) and low (100 μM) phosphate to 0.1 OD_{600} and grown to a final OD_{600} of 0.6. Cultures were then diluted 1:100 in prewarmed minimal media A containing twice the MIC of the drug; 4 μg mL^{-1} polymyxin B sulfate (Sigma). Cultures containing antimicrobial peptides were incubated at 37°C, 180 rpm shaking, and assayed for survivors at 0, 2, 5, 10 and 20 minutes by serial dilution plating onto LB agar plates.

2.3.3 Antibiotic disc sensitivity

The standard Kirby-Bauer antimicrobial disc method was utilised to test *P. aeruginosa* sensitivity against several classes of antibiotics (Barry & Badal, 1982). *P. aeruginosa* PAO1 WT and lipid remodelling mutant cultures were procured in high (1 mM) and low (100 μM) phosphate minimal medium A, as before. The cultures were then streaked onto minimal medium A ±P agarose plates (1.5% agarose added to ±P minimal medium A recipe), and incubated at 37°C overnight. A sterile loop was touched to 4/5 individual plate colonies and suspended in 2 mL sterile 0.9% saline solution. The turbidity was adjusted to match 0.5 McFarland standard by comparing to the Wickerham card. A sterile swap was dipped into the adjusted bacterial suspension, squeezed of excess, and spread plated across minimal medium A agarose ±P plates in a tight zig-zag pattern. The plates were allowed to dry for 5 minutes before adding desired antimicrobial discs, and then incubated at 37°C for 18 hours, after which zones of clearance were measured. Concentrations of antibiotic discs (Thermo Scientific) used were: ciprofloxacin 1 μg, meropenem 10 μg, ceftazimide 30 μg, gentamicin 10 μg, ertapenem 10 μg, imipenem 10 μg and doripenem 10 μg.

2.3.4 Sub-inhibitory antimicrobial peptide assay

5 mL cation-adjusted Mueller-Hinton broth (MHB) was inoculated with a single colony of *P. aeruginosa* PAO1 WT and incubated overnight at 37°C at 180 rpm. Cultures were then diluted 1/20 to give an initial OD_{600} of ~0.1, and grown with or without the addition of antimicrobial peptide at a final concentration of 0.2 μg mL^{-1}, added from fresh stocks of polymyxin B sulfate or colistin (Sigma). At incubation time points 8 hrs and 24 hrs, samples were taken for lipid analysis (sections 2.1.6-2.1.7).

2.4 Bacteriophage assays

2.4.1 Bacteriophage isolation and propagation

50 mL LB media was inoculated with *P. aeruginosa* PAO1 WT and incubated at 37°C, 180 rpm shaking until mid-exponential phase (0.4-0.5 OD_{600}). 5 mL sewage water (from Warwickshire sewage treatment works) was passed through a 0.22 μM pore size filter and added to the culture, and continued to grow overnight at 37°C, 180 rpm shaking. The phage lysate culture was filtered through 0.22 μM pore size filters and stored at 4°C. The overlay agar method was then used to isolate bacteriophages that may be present. Using a serial dilution from 10^{-1} to 10^{-8}, 50 μL of each filtered phage lysate dilution was mixed with 200 μL of an exponential phase *P. aeruginosa* PAO1 WT culture and allowed to bind at RT for 15 minutes. 3 mL of top agar (LB media with 0.7% agar) was added, pre-warmed to 55°C, and poured onto a 10 cm LB agar plate. After setting for 30 minutes at RT, plates were inverted and incubated overnight at 37°C. Observed plaques were picked using a filter micropipette tip and resuspended in 1 mL LB media and allowed to dissolve overnight at 4°C. Three further repeats of the propagation and overlay agar methods were used for purification of specific phage isolates. To remove the possibility of introducing additional phosphate in future phosphate-controlled experiments, the LB medium was exchanged for minimal medium A using a 100 kDa buffer exchange column (Sartorius Vivaspin). Phage titre was enumerated using the overlay agar method for a serial dilution series.

2.4.2 Transmission electron microscopy (TEM)

A Formvar coated grid (Agar Scientific) was ionised using high-voltage glow discharge to a pressure of 5 x 10^{-1} for 1 minute. A 5 µL drop of purified phage lysate (undiluted) was added to the grid and allowed to sit for 2 minutes before blotting. A drop of uranyl acetate was added, left for 1 minute, before blotting again. The grid was then placed into the TEM sample holder, which was kept at 36 mA in the specimen chamber. The TEM beam current was set to 7 µA to image the bacteriophage. Focus was adjusted and images were taken digitally.

2.4.3 Bacteriophage adsorption assay

P. aeruginosa WT and lipid remodelling mutants Δ*plcP*, Δ*agt1*, Δ*agt2* and Δ*olsA* were cultured as before (section 2.3.2), allowing lipid remodelling to occur after 8 hrs under phosphate stress (100 µM phosphate source), and diluted to 0.6 OD_{600} giving 2 x 10^8 CFU mL^{-1} on average. 100 µL of phage at 2 x 10^7 PFU mL^{-1} (plaque forming units) was added per 5 mL of culture, giving a multiplicity of infection (MOI) of 0.001. Culture and phage mixtures were incubated at 37°C for 3 minutes before passing 1 mL through a 0.22 µM pore size spin filter column at 13,000 rpm for 1 minute, to remove phage bound to bacterial cells. Free phage in filtered supernatants were enumerated using the agar overlay method, and a percentage of bound phage was calculated compared to phage titre in a control with no bacterial cells present.

2.4.4 Bacteriophage DNA extraction and sequencing

Phage samples were first concentrated using a 100 kDa centrifugal filter (Amicon column), centrifuging at 3000 x *g* until the volume had reduced to ~1 mL remaining. 750 µL of phage concentrate was placed into 1.5 mL Eppendorf tube, along with 15 µL DNAse I and 80 µL DNAse buffer (NEB) and placed in a hot block at 37°C for 20 minutes. An equal volume of phenol (pH 8) was added, the tube inverted to mix, and centrifuged at 13,000 x *g* for 10 minutes at 4°C. The top aqueous layer was retained into a fresh Eppendorf tube and an equal volume of phenol:chloroform (1:1) was added and centrifuged at 13,000 x *g* for 10 minutes at 4°C. The aqueous layer was again retained into a fresh Eppendorf tube and an equal volume of

phenol:chloroform:isoamylalcohol (25:24:1) was added and centrifuged at 13,000 x *g* for 10 minutes at 4°C. The aqueous layer was retained and 1/10x volume of ammonium acetate and 2x volume of ice cold ethanol were added before incubating overnight at -20°C. DNA was then pelleted by centrifugation at 16,000 x *g* for 10 minutes at RT. The supernatant was discarded and the pellet was washed twice with 2 mL 70% ethanol (RT), centrifuging at 16,000 x *g* for 10 minutes at RT each time. The final supernatant was discarded and the sample tube was left open for residual ethanol to evaporate. The DNA pellet was resuspended in 50 µL nuclease-free water and the concentration measured on a Nanodrop spectrophotometer (Thermo Scientific). Phage DNA was sent to MicrobesNG (Birmingham) for genome sequencing and initial sequence assembly. Assembled contigs were annotated using PROKKA with a custom database of proteins extracted specifically from bacteriophage genomes (Seemann, 2014). Other phage genome analyses used BLAST and MEGA7 (Kumar et al, 2016).

2.5 Phenotypic characterisation methods

2.5.1 Membrane sensitivity assays

Chelator ethylenediaminetetraacetic acid (EDTA) was used to assess bacterial membrane sensitivity. Minimal medium A plates, supplemented with either 1 mM or 100 µM phosphate source, were made through the addition of 1.5% (w/v) agarose, autoclaving and cooling to 55°C. After pouring several blank plates (20 mL per 100 mm plate), EDTA was added to a final concentration of 0.5 mM before pouring the rest of the plates. *P. aeruginosa* PAO1 WT and lipid remodelling mutants were cultured as before (section 2.3.2), and serially diluted before 5 µL spots were plated in a grid onto control and EDTA plates, containing high or low phosphate as appropriate. Spots were allowed to dry before plate incubation at 37°C for 24 hrs. In some experiments, plates were incubated for a longer period, either at 37°C or at RT.

2.5.2 Swarming motility assay

P. aeruginosa PAO1 WT and lipid remodelling mutants were cultured in minimal medium A with high (1 mM) or low (100 µM) phosphate, as before (section 2.5.1), to

ensure logarithmic phase growth and time for lipid remodelling to occur. Swarming plates were made fresh as described previously (Blus-Kadosh et al., 2013), for high phosphate plates: 100 mL per litre 5X M9 salts (5X M9: $Na_2HPO_4 \bullet 7H_2O$ 35 g L^{-1}, KH_2PO_4 15 g L^{-1}, NaCl 2.5 g L^{-1}, autoclaved), 0.5% casamino acids, 50 µM $FeCl_3$, 0.4% Na-succinate, 1 mM $MgSO_4$ and 0.5% agar. The single modification for low phosphate swarming plates was 0.5 mL 5X M9 salts per litre, giving 36 mM P for high P and 0.18 mM P for low P. 25 mL M9 swarming agar was used per 100 mm plate and allowed to dry for several hours at RT before use. A single 2.5 µL spot of each *P. aeruginosa* culture per plate was incubated upright at 37°C for 24 hrs, using damp paper towels to maintain humidity.

2.6 Proteomic analysis

2.6.1 Proteomic sample preparation

P. aeruginosa PAO1 WT and Δ*plcP* mutant (gene PA3219, strain PW6390) were streak plated onto LB agar from glycerol stocks on three different occasions, and single colonies were resuspended in 50 mL minimal medium A with intermediate phosphate concentration (600 µM), and incubated at 37°C, 180 rpm shaking for 16 hrs. Cultures were pelleted at 4000 rpm, RT for 5 minutes before washing twice in prewarmed minimal medium A. The cultures were then diluted to an OD_{600} of 0.05 in 50 mL prewarmed minimal medium A containing high P (1 mM) or low P (100 µM), and incubated for 8 hours at 37°C, 180 rpm shaking, to allow lipid remodelling to occur. 1 mL culture samples were pelleted at 10,000 rpm for 10 minutes for cell proteome samples, at 0 hrs (before lipid remodelling) and between 6-8 hrs (after lipid remodelling, upon reaching OD_{600} 0.6-0.7). For exoproteome samples, 20 mL of culture was passed through 0.22 µm filter. All samples were stored at -20°C before analysis.

2.6.2 Exoproteome sample preparation

To investigate the secreted proteome of *P. aeruginosa*, using the same cultures as prepared previously (section 2.6.1), at 0 hrs 30 mL of culture was filtered through a 0.22 µM pore size filter, and at 8 hrs 15 mL of culture was filtered through a 0.22 µM

pore size filter. Proteins were precipitated by adding 0.025x volume 0.6% (w/v) sodium deoxycholate (DOC) and vortexing, incubating at RT for 10 minutes, before addition of 900 µL 50% (w/v) trichloroacetic acid (TCA), vortexing, and incubation on ice for 30 minutes. Precipitate was pelleted by centrifuging at 4000 rpm for 15 minutes at 4°C, before resuspending in 1 mL dH_2O and transferring to Eppendorf tubes. Precipitation was repeated using 37.5 µL 0.6% (w/v) DOC and 90 µL 50% (w/v) TCA, followed by incubation on ice for 30 minutes and centrifuging for 10 minutes, 8000 rpm at 4°C. Pellets were resuspended in 1 mL ethanol:ether (1:1, v/v), centrifuged for 15 minutes, 13 000 rpm at 4°C, before removing all supernatant and allowing to air dry. Samples were stored at -20°C before analysis.

2.6.3 Proteomic analysis

P. aeruginosa PAO1 WT and PlcP mutant pellet samples were resuspended in LDS (lithium dodecyl sulfate) sample buffer containing 1% β-mercaptoethanol before lysing at 95°C and vortexing. 30 µL of each sample was run on NuPAGE 10% Bis-Tris protein gel (Invitrogen) for a short time before staining with SafeStain (Thermo Fisher) and excising the whole protein band. In-gel proteins were de-stained using 50% ethanol 50 mM ammonium bicarbonate (ABC), before being reduced and alkylated for 5 min at 70°C using 10 mM TCEP (tris(2-carboxyethyl)phosphine) and 40 mM CAA (2-chloroacetamide), respectively. After washing with 50% ethanol 50 mM ABC, peptides were lysed overnight using trypsin. Finally, peptides were extracted by sonication in a water bath (10 min RT), concentrated using a Speed-Vac (50 mins) and resuspended in 2.5% acetonitrile 0.05% formic acid. Extracted peptides were analysed by nanoLC-ESI-MS/MS using the Ultimate 3000/Orbitrap Fusion instrumentation (Thermo Scientific). Cellular proteome samples were subject to a 2 hr run per sample, and exoproteomes for 1.5 hr per sample. The UniProt proteome for *P. aeruginosa* strain PAO1 was used for peptide analysis. Further data analysis was carried out using MaxQuant and Perseus software (Tyanova et al., 2016; Temu et al., 2016); proteins without triplicate measures were filtered out.

2.7 Statistical analyses and figure generation

Statistical analysis and graphical interpretation of most data was carried out using R or MatLab. Statistical tests used include Students *t*-test, Mantel-Cox log-rank test and one-way ANOVA. Images were created using BioRender and ChemDoodle. Proteomic datasets were analysed using MaxQuant and Perseus. Lipidomic datasets were analysed using DataAnalysis and QuantAnalysis (Bruker Software). QuantAnalysis was used to calculate the size of the area representing a lipid peak through integration, with the data then used to manually calculate relative abundancies. Phylogenetic analyses were generated using MEGA7. NCBI nucleotide BLAST was used to identify similar *Pseudomonas* bacteriophages, and protein BLAST used to determine phage proteins functions. A BLAST search for the presence of *agt1* and *agt2* glycosyltransferase genes was carried out using *P. aeruginosa* genomes in the IMG database.

Chapter 3 *P. aeruginosa* remodels phospholipid membrane in response to phosphorus deficiency

3.1 Introduction

Competition for many nutrients will occur naturally in environmental bacterial communities, with a major example being competition for available phosphorus. Soil- and water-dwelling *P. aeruginosa* will experience this natural competition for phosphorus. However, low phosphorus environments are also clinically relevant in establishing *P. aeruginosa* infection. Phospholipids represent a significant source of phosphate in a bacterial cell, making up 15-20% of the total cellular phosphate (Karl & Björkman, 2015). Thus, in phosphate-limiting environments, the liberation of this phosphate source for more important cellular processes can be carried out through lipid remodelling. Lipid remodelling is the process by which bacteria selectively modify their membrane lipid composition in response to nutrient stress, thereby replacing phospholipids with non-phosphate containing lipids. Previous studies have identified an intracellular phospholipase C, PlcP, in many different organisms that has a major role in lipid remodelling in response to phosphate stress (Zavaleta-Pastor et al., 2010). PlcP facilitates the production of non-phosphate lipid classes through cleavage of phospholipid head groups, liberating diacylglycerol (DAG) that becomes the building block of some non-phosphate lipid classes. Some bacterial species encode a glycosyltransferase alongside *plcP*, termed *agt*, that will add sugar moieties as head groups to DAG, thereby generating a further non-phosphate lipid class: glycolipids (Sebastián et al., 2016).

P. aeruginosa has been shown to modify its membrane components under different conditions, usually through addition of different moieties that result in a change to membrane properties (section 1.4). When cultured as a biofilm, *P. aeruginosa* was observed to utilise different chain length fatty acids within phospholipids, dependent upon biofilm age (Benamara et al., 2014). Under phosphate stress *P. aeruginosa* was found to upregulate the expression of a distinct operon containing OlsA and OlsB. Further, OlsBA was found to be responsible for the production of an alternative membrane lipid class in this organism, the amino acid lipid ornithine lipid (Lewenza et

al., 2011). Further lipid remodelling pathways to produce other lipid classes as alternatives to phospholipids have not been characterised in *P. aeruginosa*.

In this chapter I investigate the role of a PlcP homologue in *P. aeruginosa*, with 47% protein sequence similarity to PlcP from marine bacterium *Phaeobacter* sp. MED193 (Sebastian et al. 2016). Additionally, two glycosyltransferases, Agt1 and Agt2, are characterised for their role in production of glycolipids MGDG and GADG. I show that, unlike previous findings in other organisms with dual-role glycosyltransferases, Agt1 is responsible for MGDG production and Agt2 is responsible for GADG production in response to phosphate stress in *P. aeruginosa.*

3.2 Results

3.2.1 *P. aeruginosa* undergoes lipid remodelling in response to phosphate stress

In order to analyse any lipidome alterations *P. aeruginosa* makes in response to phosphate (Pi) stress, strain PAO1 was cultured in a defined minimal medium that either was Pi-sufficient (1 mM) or induced Pi stress (100 µM). The depletion of phosphorus resulted in a slower growth rate in *P. aeruginosa* (Figure 3.1A). Phosphorus stress was monitored through alkaline phosphatase activity, a secreted enzyme that is widely accepted as an indicator for bacterial Pi stress (Tabatabai & Bremner, 1969), with *P. aeruginosa* exhibiting significantly higher activity in Pi-deplete conditions (Figure 3.1B).

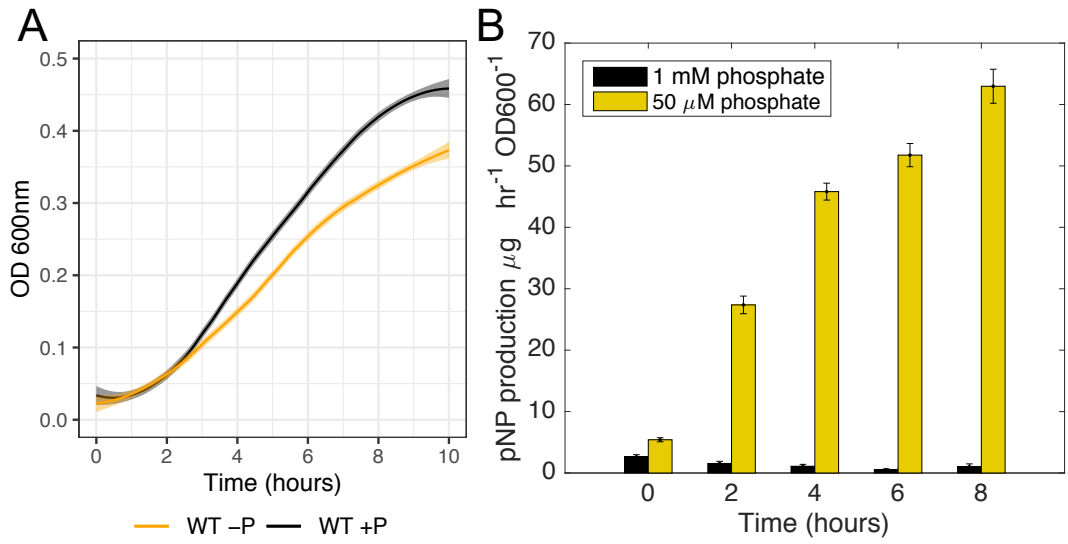

Figure 3.1. A) Growth of *P. aeruginosa* PAO1 WT in minimal medium A containing 1 mM phosphate (+P, black) or 100 µM Pi (-P, yellow) over 12 hours, measured in a plate reader using 1 mL culture per well in a 24 well plate. Shading indicates standard error (n = 3 biological replicates). B) Liberation of *para*-nitrophenol (pNP) from *para*-nitrophenol phosphate (pNPP) through alkaline phosphatase activity, under Pi-replete (1 mM, black) and Pi-deplete (100 µM, yellow) conditions. Error bars represent the standard deviation of three independent replicates.

To gain an understanding of the Pi-responsive proteome in *P. aeruginosa*, the WT strain was cultured in high and low phosphate for 8 hours and 1 mL culture samples were used to analyse the cellular proteome of *P. aeruginosa*. A total of 2844 proteins were detected using nanoLC-ESI-MS/MS instrumentation on a 2 hour run per sample, with 175 of those found to be differentially regulated by phosphorus availability when significance was considered at a false detection rate (FDR) of <0.05. Of these, 132 proteins were more highly expressed in phosphorus deplete conditions, and 43 were more highly expressed when phosphorus was sufficient (Figure 3.2). Protein functions, locus tags and the fold change difference between WT in high P (1 mM) and in low Pi (100 µM) are detailed in Appendix 1.

In line with previous transcriptomic studies of *P. aeruginosa* PAO1 under Pi stress (Bains et al., 2012), major Pi-acquisition mechanisms were more highly expressed under Pi stress. This included high-affinity Pi-specific transporter operon *pstSCAB*, master regulatory proteins PhoBR and its regulator PhoU, phosphodiesterase (PDase) GlpQ and phosphate-specific outer membrane porins OprO and OprP. Additional Pi-acquisition proteins were also upregulated including alkaline phosphatases (ALP),

phosphonate transporters and extracellular DNA degradation enzymes such as EddB and EddA, the latter of which possesses both ALP and PDase activity (Wilton et al., 2018). Pi-taxis chemoreceptor proteins CtpH and CtpL were also upregulated, consistent with previous reports on Pi stress driving swarming phenotypes in *P. aeruginosa* (Bains et al., 2012). Phospholipases PlcH, PlcN and PlcB were upregulated, with haemolytic PlcH having a strong link to virulence in *P. aeruginosa* (Haghi et al., 2018). Other virulence proteins were also upregulated under Pi stress, including important quorum sensing proteins LasI and LasA, alongside Pseudomonas Quinolone Signal proteins PqsA and PqsC. Several phenazine biosynthesis proteins were upregulated under Pi stress (PA1902, PA4209-PA4210, PA4214-PA4215), particularly linked to pyocyanin production; a further important virulence factor in *P. aeruginosa* (Cezairliyan et al., 2013). An interesting cluster of proteins responsible for the synthesis of antimetabolite l-2-Amino-4-Methoxy-trans-3-Butenoic Acid (AMB), PA2302-PA2305, were also upregulated under Pi stress, and may be involved in enhancing the competitiveness of *P. aeruginosa* against other bacterial species in phosphate-limited host environments (Murcia et al., 2015). The upregulation of virulence-linked sigma factor VreI, and its regulator VreB, was also found under Pi stress, consistent with previous reports (Faure et al., 2013; Llamas et al., 2009). Overall, as expected, a multitude of proteins involved in phosphate acquisition are upregulated under Pi stress, alongside previously characterised virulence factors in *P. aeruginosa*.

The majority of proteins that are more highly expressed when Pi is sufficient have uncharacterised functions. Those that are characterised are linked to iron acquisition, for example superoxide dismutase SodM, pyoverdine receptor FpvB and further proteins linked to iron transport and heme binding, for example HemO (Heinzl et al., 2018). This suggests that as the non-stressed culture headed towards stationary phase, available iron was becoming depleted. More notably, PA0141, involved in the storage of available phosphate as polyphosphate molecules, was highly upregulated in *P. aeruginosa* when phosphate was sufficient.

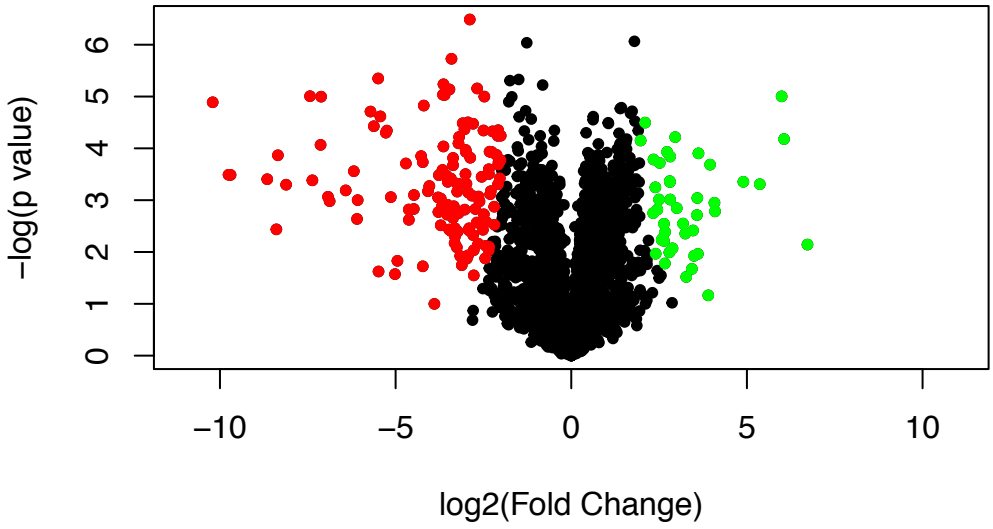

Figure 3.2. Volcano plot depicting differentially expressed proteins when comparing *P. aeruginosa* PAO1 WT in phosphate-deplete and phosphate-replete conditions. Significantly upregulated proteins when under phosphate stress are shown in red, and those that are significantly upregulated when phosphate is sufficient are in green (see Appendix 1 for full annotated list). Significance was accepted when the false discovery rate (FDR) was < 0.05, and a fold change ≥ 2.

Samples for lipidome analysis by HPLC/MS were taken from planktonic *P. aeruginosa* cultures grown in the minimal medium A supplemented with different concentrations of Pi (1 mM or 100 µM) for 8 hours. Major bacterial membrane phospholipids phosphatidylglycerol (PG) and phosphatidylethanolamine (PE) were found under both conditions, with PG being the most predominant species. Under Pi stress, several additional lipid species were present that were not found when Pi is sufficient (Figure 3.3A). At 13.2 minutes, non-P amino acid-derived ornithine lipid (OL) was found, consistent with previous reports that Pi stress induces production of OL in *P. aeruginosa* (Lewenza et al., 2011). *P. aeruginosa* PAO1 OL had a predominant intact mass of 651 m/z (mass to charge ratio) indicating fatty acid chain lengths of 3-hydroxy 18:1 and 16:0. MS fragmentation of 651 m/z in positive ionisation mode yielded a diagnostic fragment of 115 m/z, as described previously (Zhang et al. 2009), thereby confirming the identity as OL.

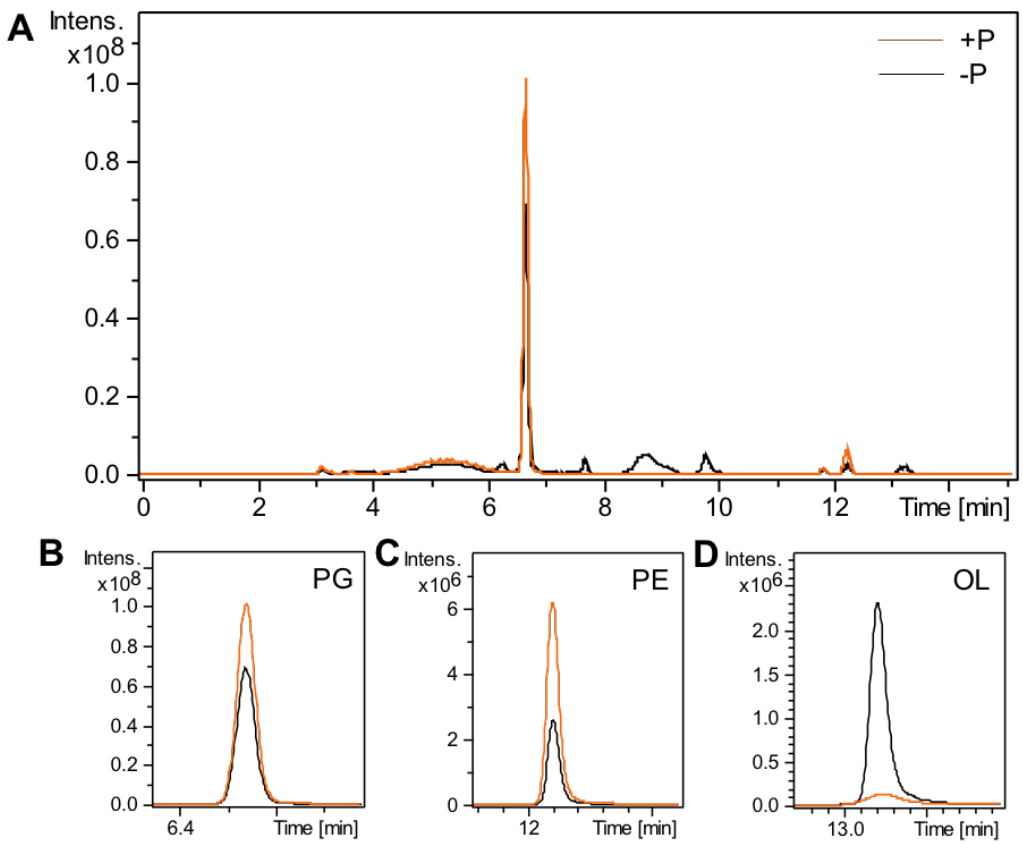

Figure 3.3. A) Representative chromatogram in negative ionisation mode of WT *P. aeruginosa* lipidome when grown under phosphorus stress (-P, black) compared to growth under phosphorus sufficient conditions (+P, orange). B-D) Extracted ion chromatograms depicting known lipid species phosphatidylglycerol (PG), phosphatidylethanolamine (PE) and ornithine lipid (OL), respectively.

Three lipid species spanning 7.7 – 9.8 minutes were only present when *P. aeruginosa* was under Pi stress, and together contributed a more significant proportion of the total lipidome than OL. The predominant intact masses of each species in negative ionisation mode were 755 m/z, 767 m/z and 769 m/z found at 7.7, 8.7 and 9.8 minutes, respectively. In positive ionisation mode, the lipids gained an ammonium adduct (19 m/z), typical of the HPLC/MS conditions used, to exhibit masses of 774 m/z, 786 m/z and 788 m/z, respectively. On analysing the MS fragmentation spectra for the three species, each appeared to be typical of a glycolipid (Figure 3.4A-C). Each intact lipid mass first lost a head group, yielding 595 m/z as the mass of diacylglycerol, the major building block of glycolipids. Further fragmentation caused a loss of either fatty acyl chain, leaving monoacylglycerols (MAGs) with a C16:0 (313 m/z) or C18:1 (339 m/z) fatty acid. To determine the identity of the sugar head group moieties, a search for neutral loss of the head group mass was required. Known glycolipids monoglycosyl

diacylglycerol (MGDG) and glucuronic acid diacylglycerol (GADG) exhibit neutral loss of hexosyl and hexuronic acid head groups, with masses of 179 m/z and 193 m/z, respectively (Sebastián et al., 2016). For *P. aeruginosa* PAO1, the lipid species identity at 7.8 minutes was found to be MGDG, and at 9.8 minutes was found to be GADG (Figure 3.4). The third predicted glycolipid peak at 8.7 minutes has a head group size of 191 m/z, and is currently an unknown glycolipid requiring further investigation.

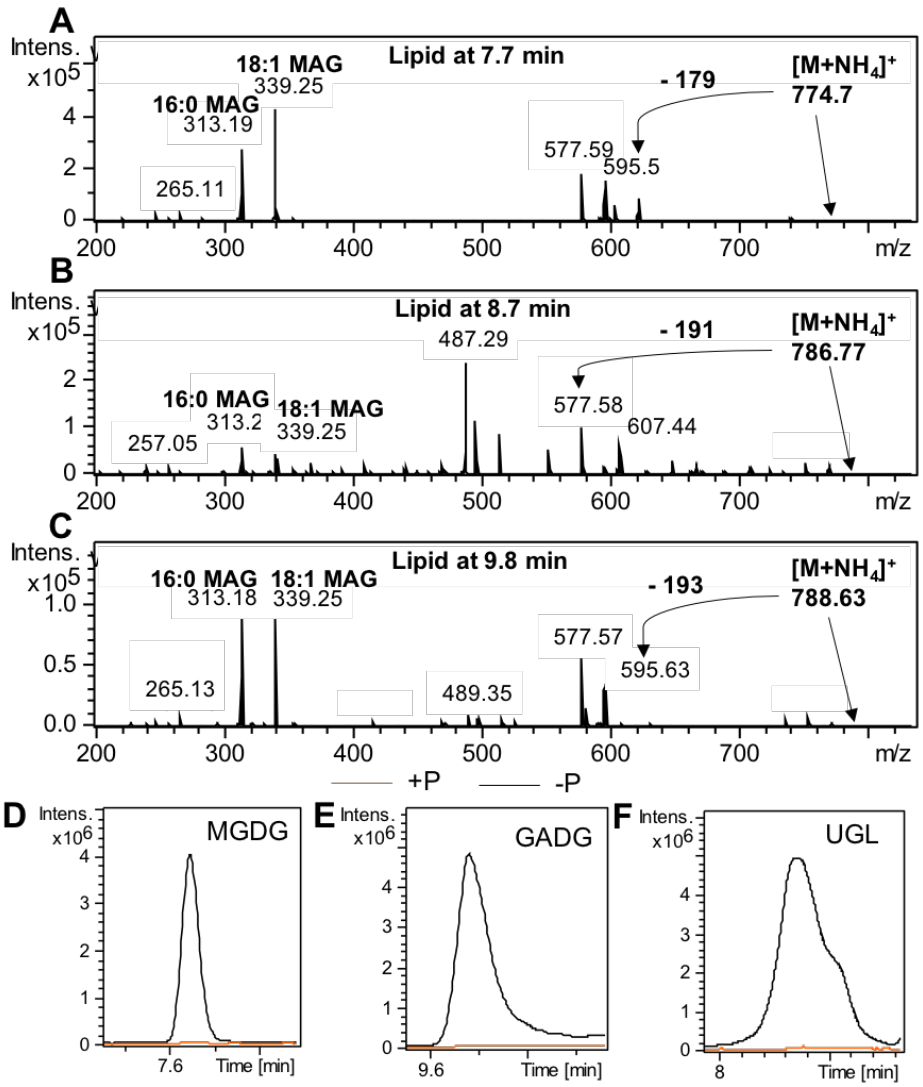

Figure 3.4. A-C) Mass spectrometry fragmentation spectra of unknown lipid species present under phosphorus stress in *P. aeruginosa*, at retention times of 7.7, 8.7 and 9.8 minutes, respectively. Each spectrum depicts an intact lipid mass with an ammonium adduct exhibiting neutral loss of a head group, yielding diacylglycerol (595 m/z). Further fragmentation yields monoacylglycerols (MAG) with C16:0 or C18:1 fatty acyl chains. D-F) Extracted ion chromatograms of suspected glycolipid species in *P. aeruginosa* (phosphate stress = black, phosphate sufficient = orange). MGDG: monoglycosyl diacylglycerol, GADG: glucuronic acid diacylglycerol and UGL: unconfirmed glycolipid.

3.2.2 The PlcP/Agt1 operon has a significant role in lipid remodelling in *P. aeruginosa*

After HPLC/MS confirmation that *P. aeruginosa* is capable of lipid remodelling under Pi stress and produced glycolipids that have not been previously described in this bacterium, the genes required for this process needed to be elucidated. Candidate

gene PA3219 was selected based on 47% protein sequence identity to the intracellular phospholipase gene *plcP* from marine organism *Phaeobacter* sp. MED193 (Sebastián et al., 2016). Further, PA3219 was found to be upregulated in response to phosphate stress on proteomic analysis (4.62 log fold change compared to high P; appendix 1). As is often the case in bacterial genomes, the putative *plcP* locus PA3219 is located in an operon with a probable glycosyltransferase gene (Figure 3.5A), PA3218, which exhibits 41% protein sequence identity to the characterised glycolipid synthesis glycosyltransferase, Agt, from the marine bacterium *Phaeobacter* sp. MED193 (Agt_{MED193}). Agt_{MED193} is a bifunctional enzyme that was found to be required for the synthesis of both MGDG and GADG glycolipids (Sebastián et al., 2016). Further, several additional putative glycosyltransferases in the *P. aeruginosa* PAO1 genome with varying protein sequence identity to Agt_{MED193} were identified through protein BLAST search. Of these, gene PA0842 was very highly upregulated in response to Pi stress in a previous transcriptomic study (Bains et al., 2012), further supported by proteomic analysis (4.08 log fold change compared to high P; appendix 1). PA0842 has 35% protein sequence identity to Agt_{MED193} and was chosen as a second candidate Agt in *P. aeruginosa*, denoted Agt2. In addition, Pho boxes can be clearly identified in the promoter region of both the *plcP*/*agt1* operon and gene *agt2* in *P. aeruginosa* (Figure 3.5B), suggesting their activity will be influenced by phosphate stress.

A

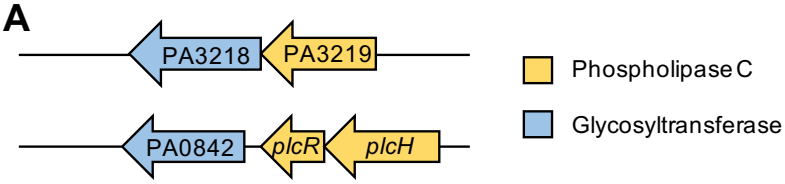

B

Consensus *P. aeruginosa* Pho box
CTGTCATNNNN**CTGTCAC**

***plcP/agt1* promoter region**
TCTGGTCGTGGCTGTAGTGGCGCAGGGAAAGGATCGAACCCATGGCGAAGC
TCCCGGAGGCAGGCGCCCAGTCTACCCGCTGGCGCCGGCGACAGACAGCCG
GGCCCTGTCACGCAACGGTCGCCGGC**CTGTCAC**AGTC**GTTTCAC**CGGCGCCG
GCCAAGATCGGAAAAACACCGTCGGAGACCCGCCG…

***agt2* promoter region**
GCGTCGACGACGAGGAGCAGCGTCACGCCGCCATCGACGAACGCCTCAAGGC
CCTGCGCAAGCAGATCTTCGGCGAGGAGAACCCACGCCTGCTGCAACGCTGA
AATCCACGGCGCCCCGACAGGGGCG**CCGTCAC**GCAA**GCGTCAC**CAAAACTTC
ACATCCGCTACACGGCGTCGGTCGACACTGACGTC…

Figure 3.5. A) Genomic organisation of predicted lipid remodelling genes in *P. aeruginosa*. Glycosyltransferases (blue) PA3218 and PA0842 are predicted to be involved in glycolipid synthesis, and are often located in operon with phospholipase C related genes (yellow). PA3219 is predicted to be PlcP in *P. aeruginosa*. PlcH: haemolytic phospholipase C; PlcR: phospholipase C accessory protein. B) Predicted Pho box sequences (orange) in the regulatory regions of each glycosyltransferase. Consensus sequence taken from (Blanco et al., 2002).

To investigate the role of PlcP/Agt1 and Agt2 in the production of MGDG and GADG in *P. aeruginosa*, mutants in predicted glycolipid synthesis genes PA3219 (*plcP*), PA3218 (*agt1*) and PA0842 (*agt2*) were obtained from a transposon mutant library collection (University of Washington; (Jacobs et al., 2003)) and confirmed using PCR (section 2.1). Planktonic cultures of Δ*plcP*, Δ*agt1* and Δ*agt2* were grown in minimal medium A under restricted phosphate conditions (100 µM), and samples were taken for lipidome analysis after 8 hours. Phosphorus stress was confirmed through ALP activity, with no significant differences found between the mutants and WT (Figure 3.6D). HPLC/MS analysis revealed that production of MGDG was ablated in Δ*agt1*, however GADG was still produced (Figure 3.7). In Δ*agt2*, GADG was no longer produced, and, intriguingly, MGDG production was significantly reduced but not abolished. For Δ*plcP*, it would be expected that neither glycolipid would be produced given the resultant lack of production of key building block DAG. However, a small amount of GADG could still be found, but no MGDG (Figure 3.7). Growth comparisons

under Pi-replete and Pi-deplete conditions suggest the activity of PlcP represents an energy drain in *P. aeruginosa*, as the slower growth rate seen in WT under P-stress is now comparable to P-sufficient conditions (Figure 3.6C).

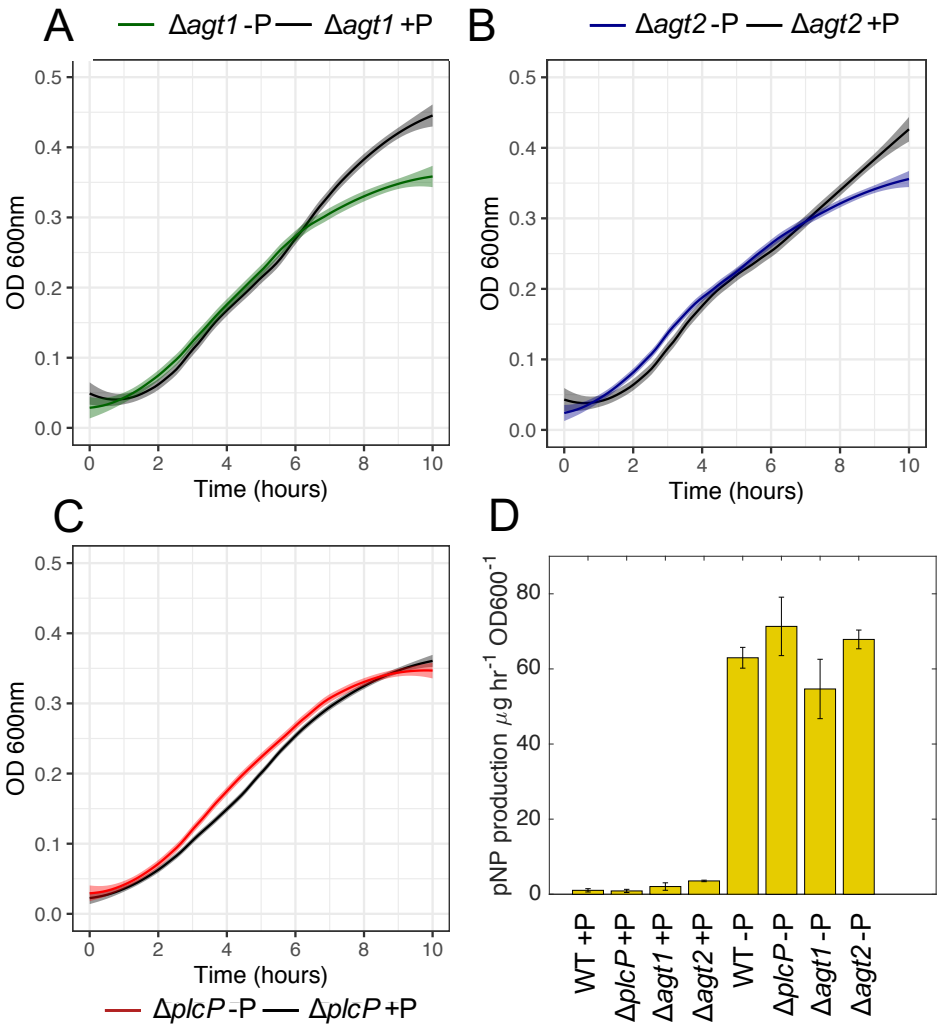

Figure 3.6. A-C) Growth in minimal medium A supplemented with sufficient phosphate (1 mM; +P) or low phosphate (100 µM; -P) for *P. aeruginosa* glycolipid remodelling mutants Δ*agt1*, Δ*agt2* and Δ*plcP*. Growth rate was monitored in a plate reader using 1 mL culture per well in a 24 well plate. Shading indicates standard error (n = 3). D) Alkaline phosphatase activity for glycolipid remodelling mutants after 8 hrs growth under Pi sufficient (+P) or Pi stress (-P) conditions, measured by liberation of *para*-nitrophenol from *para*-nitrophenol phosphate. Error bars represent standard deviation (n = 3).

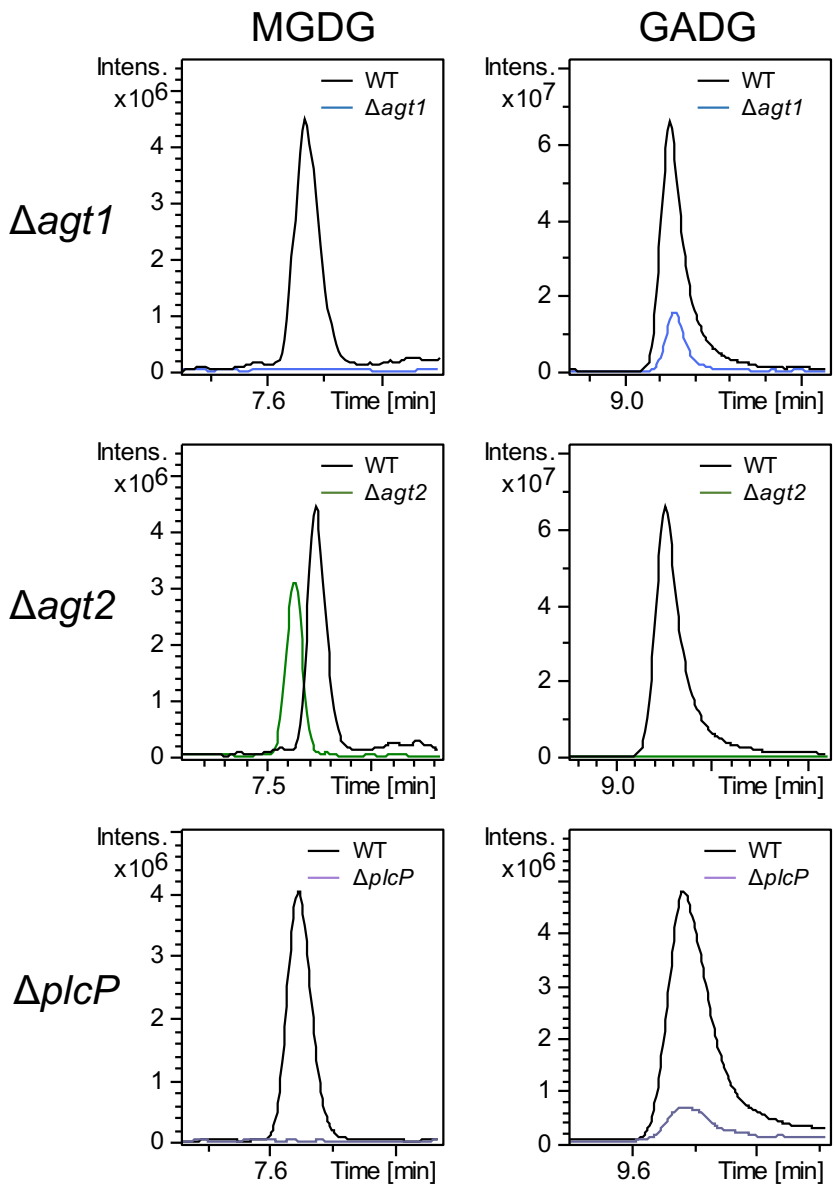

Figure 3.7. Production of glycolipids in *P. aeruginosa* mutants in predicted lipid remodelling genes *agt1* (top, blue), *agt2* (middle, green) and *plcP* (bottom, purple), under low phosphate conditions (100 µM). Monoglycosyl diacylglycerol (MGDG) glycolipid production is shown in the left panels, and glucuronic diacylglycerol (GADG) production is shown in the right panels. Each mutant is compared to WT *P. aeruginosa* glycolipid production (black).

To further confirm the distinct roles of *agt1* and *agt2* in the production of MGDG or GADG only, respectively, the genes from *P. aeruginosa* were heterologously expressed in *E. coli*. Expression of *agt1* was sufficient for the accumulation of MGDG in *E. coli*, not present in the empty vector control (Figure 3.8A). Equally, expression of *agt2* elicited production of GADG in *E. coli*, not present in the empty vector control (Figure 3.8B). Neither glycosyltransferase elicited production of both glycolipids when

expressed in *E. coli*, nor could the mass for the UGL be found, as can be seen in the overall lipid chromatograms. Further, the retention times for the glycolipids in *E. coli* matched those found for native *P. aeruginosa* glycolipids: MGDG was found at 7.7 minutes and GADG was found at 9.8 minutes. As a final confirmation step, MS fragmentation reveals loss of polar head groups to yield major product ion DAG (595 m/z), and further fragmentation yielding MAGs, in a pattern that is characteristic of these glycolipids (Figure 3.8C-D).

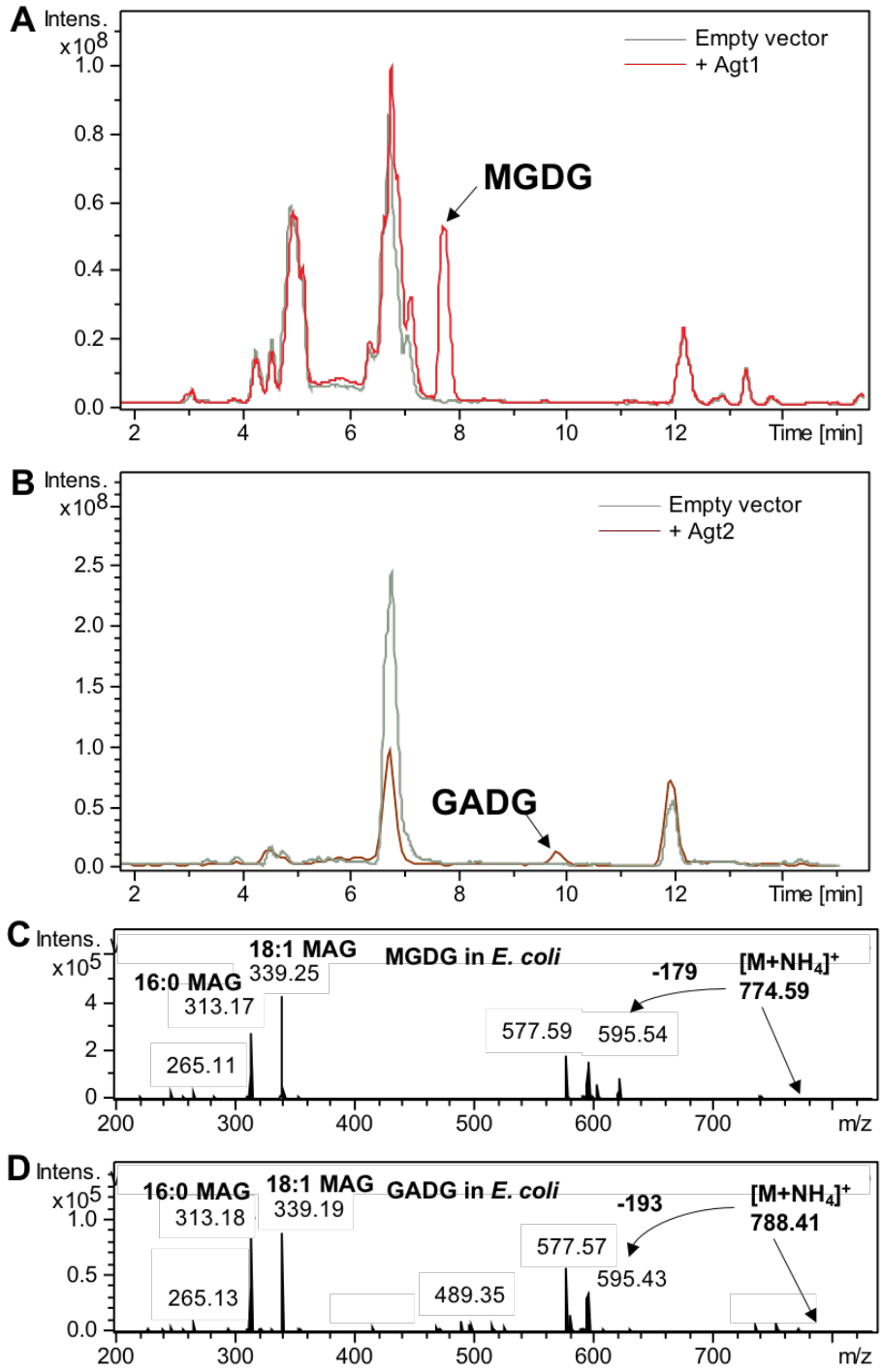

Figure 3.8. Heterologous expression of glycosyltransferases Agt1 and Agt2 from *P. aeruginosa* in *E. coli*. A) Representative *E. coli* lipid chromatogram highlighting only MGDG production when expressing Agt1. B) Representative *E. coli* lipid chromatogram highlighting only GADG production when expressing Agt2. C-D) Mass spectrometry fragmentation spectra of MGDG and GADG species in *E. coli*.

3.2.3 Overall lipidome composition of *P. aeruginosa* changes under phosphate stress

Using QuantAnalysis software (Bruker), the major species of each lipid class were quantified by integration of their peak area for *P. aeruginosa* WT and glycolipid mutants under Pi-replete and Pi-deplete conditions. Under Pi-replete conditions, WT and all glycolipid remodelling mutants exhibited a typical *Pseudomonas* lipidome, primarily composed of PG (93-97%), and a smaller percentage of PE (3-6%) (Table 3.1). When under P-stress, a replacement of native phospholipids with non-P containing lipids was observed, including the introduction of OL, MGDG and GADG (Figure 3.9). In terms of membrane properties, PG and GADG are negatively charged lipids, PE and OL are zwitterionic with a net neutral charge at neutral pH, and MGDG is neutral (Semeniuk et al., 2014). In this way, it appears that *P. aeruginosa* acts to try and maintain the overall charge composition of the lipid membrane, observed through different proportions of non-P lipids present in the membrane in glycolipid remodelling mutants (Table 3.1).

Table 3.1. Overall membrane lipid components (%) of *P. aeruginosa* WT and glycolipid synthesis mutants (Δ*plcP*, Δ*agt1* and Δ*agt2*) under high and low phosphate conditions (± P). (A) Symbols indicate statistical significance compared to WT –P using one-way ANOVA with Dunnett's post hoc test (* $p < 0.05$, ** $p < 0.01$, *** $p < 0.001$). B) Symbols indicate statistical significance compared to WT -P using Welch two-sample *t*-test ('.' $p < 0.1$, * $p < 0.05$).

A	**PG** (% ± SD)	**PE** (% ± SD)	**OL** (% ± SD)	**MGDG** (% ± SD)	**GADG** (% ± SD)
WT –P	79.4 (± 1.1)	2.8 (± 0.7)	2.5 (± 0.9)	5.1 (± 0.5)	10.2 (± 0.7)
WT +P	95.1 (± 1.8)***	4.9 (± 1.8)	0.0 ***	0.0 ***	0.0 ***
***ΔplcP* –P**	93.1 (± 0.9)***	4.8 (± 0.4)	1.5 (± 0.4)	0.0 ***	0.6 (± 0.1)***
***ΔplcP* +P**	94.4 (± 0.9)***	5.6 (± 0.9)	0.0 ***	0.0 ***	0.0 ***
***Δagt1* –P**	61.0 (± 1.7)***	4.5 (± 0.9)	2.8 (± 0.6)	0.0 ***	31.7 (± 1.6)***
***Δagt1* +P**	97.2 (± 0.1)***	2.8 (± 0.1)	0.0 ***	0.0 ***	0.0 ***
***Δagt2* –P**	93.3 (± 0.3)***	3.6 (± 0.4) *	1.3 (± 0.3) *	1.8 (± 0.2)***	0.0 ***
***Δagt2* +P**	93.7 (± 2.2)***	6.3 (± 2.2)	0.0 ***	0.0 ***	0.0 ***

B	**Negative charge** (%)	**Neutral charge** (%)
	89.63	10.37
	95.13 *	4.87 *
	93.68 .	6.32 .
	94.37 *	5.63 *
	92.73	7.27
	97.23 *	2.77 *
	93.29 .	6.71 .
	93.75 .	6.25 .

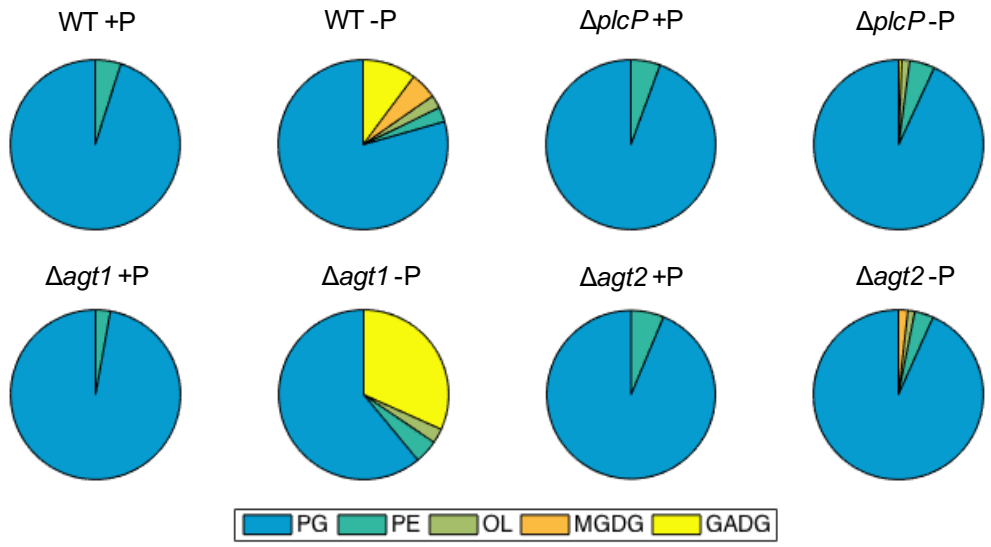

Figure 3.9. Overall proportions of phospholipids (PG and PE) and non-phosphate containing lipids (OL, MGDG and GADG) of *P. aeruginosa* under phosphorus stress (-P) or phosphorus sufficiency (+P). Lipids of WT and glycolipid remodelling mutants Δ*agt1*, Δ*agt2* and Δ*plcP* were quantified.

For Δ*agt1*, when PlcP is still actively cleaving phospholipids in the membrane, negatively charged GADG is allowed to accumulate to significantly higher levels than WT (31% compared to 10%, $p < 0.001$). Presumably, *P. aeruginosa* is able to maintain membrane stability through GADG replacing PG in the Δ*agt1* mutant (PG 79% in WT compared to 61% in Δ*agt1*, $p < 0.001$). For Δ*agt2*, the inclusion of neutral MGDG in the membrane is lower than that of WT, and appears to be concomitant with a decrease in OL accumulation. It is likely that the *P. aeruginosa* membrane is unable to sustain a comparable proportion of neutral MGDG to that of GADG found in Δ*agt1*. Indeed, in Δ*agt2* PG represents ~93% in both ±P conditions, suggesting that PE is being replaced for other neutral lipids in the Δ*agt2* mutant, though the difference was not found to be statistically significant (PE 6.3% in +P, compared to 3.6% in –P, $p = 0.15$). However, there was a significant difference for PE between WT and Δ*agt2* when both are under Pi stress ($p < 0.05$). For Δ*plcP*, the lipidome is very comparable to WT under P-stress, with the single difference being a very small proportion of GADG (0.6% ± 0.1%, $p < 0.001$). This is likely due to a lack of glycolipid building block DAG normally produced by PlcP activity, as in this mutant Agt2 would still be active, but *agt1* would be disrupted by the transposon insertion in *plcP*.

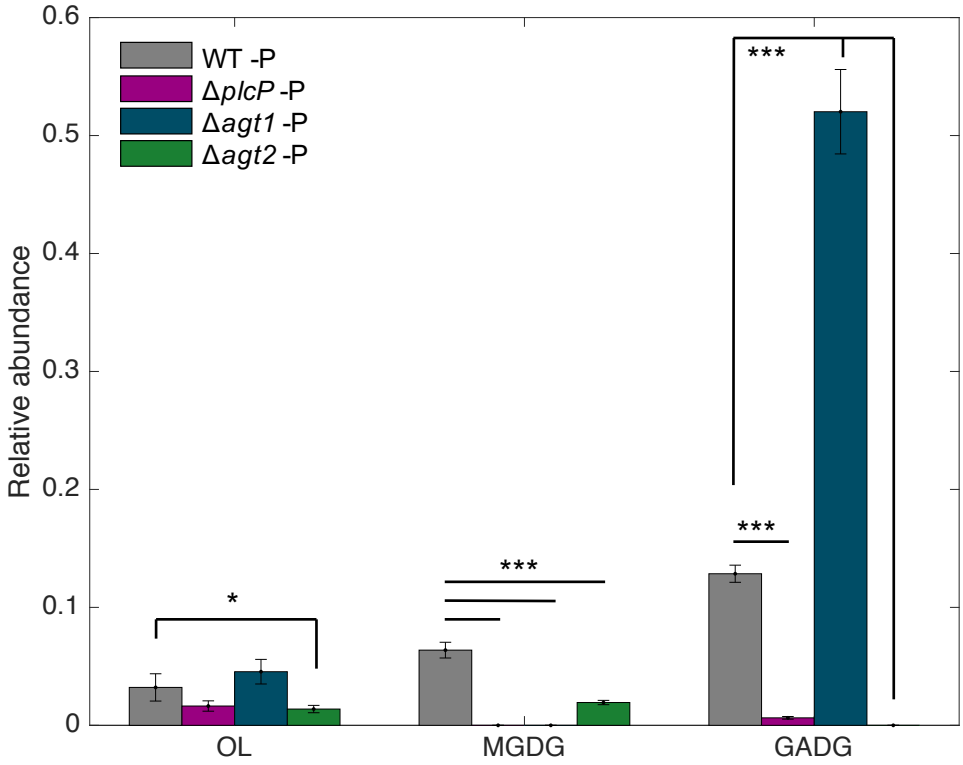

Figure 3.10. Relative abundance of alternative lipid classes produced in response to phosphorus stress in *P. aeruginosa*. OL, MGDG and GADG were quantified in WT and glycolipid remodelling mutants Δ*agt1*, Δ*agt2* and Δ*plcP* and their abundance calculated relative to PG.

3.2.4 Iron depletion does not elicit lipid remodelling in *P. aeruginosa*

During growth under Pi stress, *P. aeruginosa* PAO1 WT and glycolipid remodelling mutant strains consistently turned a blue-green colour after 6-8 hours of growth (Figure 3.11A). A colour change was not seen when P was sufficient. Additionally, proteomic analysis highlighted upregulation of phenazine synthesis proteins, which can include chromogenic pyochelin that manifests as a blue colour (Turner & Messenger, 1986). *P. aeruginosa* strains are well known to produce coloured siderophores, such as pyochelin and pyoverdine, when iron is limited (Cornelis & Dingemans, 2013). In order to determine if iron restriction played a role in lipid remodelling, specifically in the production of glycolipids, *P. aeruginosa* WT was grown under iron limiting conditions and the lipidome was analysed using HPLC/MS. Iron limitation was achieved through multiple sub-cultures of *P. aeruginosa*, grown overnight in LB medium, in a succinate-based medium with no additional iron, or supplemented with 100 µM $FeCl_3$ as an iron sufficient control. Fe-restriction was monitored through production of chromogenic pyoverdine, eliciting a yellow culture

only when *P. aeruginosa* was under iron stress (Figure 3.11B). No changes to the *P. aeruginosa* lipidome were observed as a result of iron restriction (Figure 3.11C) as only major species PG and PE were detected, with no indication of any lipid remodelling.

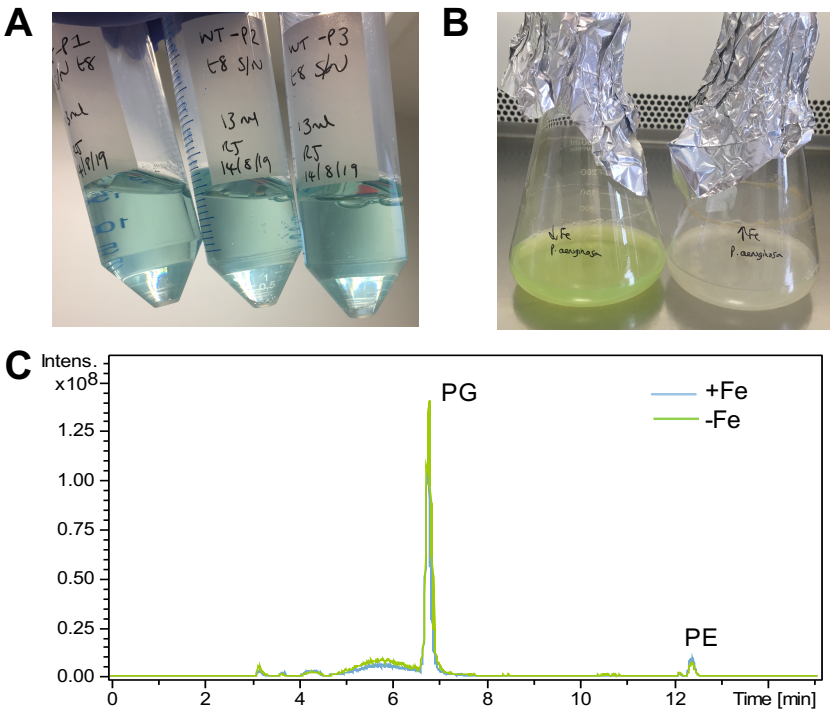

Figure 3.11. A) Blue-green coloured 0.22 µM filtered supernatant of *P. aeruginosa* WT grown under phosphate stress for 8 hours. B) Pyoverdine production in *P. aeruginosa* under Fe-restriction (yellow) compared to supplementation with 100 µM $FeCl_3$ (beige). C) Representative overall lipid chromatograms in negative ionisation mode of *P. aeruginosa* WT grown under iron restrictive (-Fe, green) or iron surplus (+Fe, blue) conditions. PG: phosphatidylglycerol and PE: phosphatidylethanolamine.

3.2.5 Glycolipid synthesis pathway is widespread in *P. aeruginosa* strains

In order to determine the prevalence of glycolipid production in *P. aeruginosa*, the completed genome sequences of 94 strains (Integrated Microbial Genomes database) were investigated for the presence of glycosyltransferases *agt1* and *agt2*. Amino acid sequences from *P. aeruginosa* PAO1 for PA3218 and PA0842 were used as query sequences for Agt1 and Agt2, respectively. Protein BLAST revealed PA0842 to be common across all *P. aeruginosa* species analysed, with protein hits exhibiting amino acid sequence identities of 97-100% (Table 3.2). In *P. aeruginosa* strain PAO1, PA0842 is located in an operon with a phospholipase C and a phospholipase C accessory

protein, commonly denoted as PlcH (haemolytic Plc) and PlcR, respectively. The gene neighbourhoods for PA0842 homologs were analysed for the presence of PlcH and PlcR, and it was found that this genomic context was retained throughout *P. aeruginosa* strains. In addition, Agt1 (PA3218) could be identified in all strains analysed, again with high protein sequence identity of 98.5-100% for the majority of species compared to Agt1 from *P. aeruginosa* PAO1, with two exceptions, sv. O12 PA7 and AR441, exhibiting 87% identity (Table 3.2). Investigation of gene neighbourhoods for Agt1 also confirmed the maintenance of the location in an operon with a phospholipase C, that we know to be PlcP with a key role in membrane lipid remodelling. Together these data show the glycolipid synthesis genes to be widespread across *P. aeruginosa* strains, including those isolated from many different clinical samples, and may be important for virulence in these organisms.

Table 3.2. Protein BLAST identification of locus tags homologous to *agt1* and *agt2* glycolipid synthesis genes in *P. aeruginosa* strains. Amino acid sequences of PA3218 (Agt1) and PA0842 (Agt2) from strain PAO1 were used as query sequences.

***P. aeruginosa* strain**	***agt2* locus tag**	***agt1* locus tag**
12-4-4(59)	Ga0123778_114449	Ga0123778_111868
14649	Ga0071081_1121156	Ga0071081_1151594
14650	Ga0071078_1011198	Ga0071078_112549
19BR	Ga0248322_11878	Ga0248322_113734
213BR	Ga0036904_11879	Ga0036904_113760
8380	Ga0123667_114557	Ga0123667_111892
AES-1R	Ga0105935_112216	Ga0105935_113158
AJ D 2	Ga0395468_854	Ga0395468_3353
AR_0354	Ga0272040_01_2807356_2808576	Ga0272040_01_6550596_6551651
AR_0360	Ga0272319_01_3455297_3456517	Ga0272319_01_679654_680709
AR_455	Ga0349608_01_6011993_6013213	Ga0349608_01_3448498_3449553
AR_458	Ga0350086_01_1364223_1365443	Ga0350086_01_5098419_5099474
AR441	Ga0349683_01_4672877_4674097	Ga0349683_01_1879124_1880179
ATCC 15692	Ga0174979_114286	Ga0174979_111794
ATCC 27853	Ga0133450_114562	Ga0133450_111789
B10W	Ga0174977_114731	Ga0174977_111880
B136-33	G655_21145	G655_08740
BA7823	Ga0399483_01_4564387_4564986	Ga0399483_01_1737804_1738859
BAMCPA07-48	Ga0133421_114930	Ga0133421_111958
c7447m	Ga0034254_00877	Ga0034254_03392
Carb01 63	Ga0123806_115199	Ga0123806_112201
Cu1510	Ga0125155_112051	Ga0125155_114535
DHS01	DPADHS01_04365	DPADHS01_19380
DK2	PADK2_21495	PADK2_08235
DSM 50071	Ga0081678_114289	Ga0081678_111769
F22031	Ga0133363_114486	Ga0133363_111866
F23197	Ga0123716_114372	Ga0123716_111775
F30658	Ga0123814_114858	Ga0123814_111922
F5677	Ga0272182_01_4774431_4775651	Ga0272182_01_2008248_2009303

F63912	Ga0125144_114612	Ga0125144_111815
F9670	Ga0123675_114554	Ga0123675_111797
F9676	Ga0081746_114350	Ga0081746_111812
H27930	Ga0123748_114400	Ga0123748_111813
H47921	Ga0123745_114788	Ga0123745_111916
H5708	Ga0125197_114357	Ga0125197_111787
IOMTU 133	Ga0125117_114705	Ga0125117_111964
LES400	T222_23200	T222_09615
LES431	T223_22870	T223_09285
LESB65	T224_22800	T224_09600
M1608	Ga0125123_111780	Ga0125123_114161
M18	PAM18_4198	PAM18_1753
M37351	Ga0123746_111779	Ga0123746_114606
MTB-1	U769_21605	U769_08820
N17-1	Ga0133283_114431	Ga0133283_111775
NCGM 1984	Ga0069487_114712	Ga0069487_111829
NCGM1900	Ga0069483_111893	Ga0069483_113106
NCGM2.S1	NCGM2_1616	NCGM2_4333
NCGM257	Ga0123816_114842	Ga0123816_111998
NCTC10332	Ga0111760_114317	Ga0111760_111779
NHmuc	Ga0174978_111296	Ga0174978_113770
PA_150577	Ga0258935_01_4647317_4648537	Ga0258935_01_1875598_1876653
PA_D1	Ga0175649_114525	Ga0175649_111883
PA_D16	Ga0175650_114559	Ga0175650_111883
PA_D2	Ga0175975_114523	Ga0175975_111883
PA_D21	Ga0174817_114522	Ga0174817_111884
PA_D22	Ga0175478_114563	Ga0175478_111883
PA_D25	Ga0175479_114572	Ga0175479_111886
PA_D5	Ga0175314_114558	Ga0175314_111883
PA_D9	Ga0175801_114530	Ga0175801_112426
PA1	PA1S_gp4364	PA1S_gp1049
PA1088	Ga0174816_114598	Ga0174816_111775
PA11803	Ga0175651_115032	Ga0175651_112016
PA121617	Ga0175312_114401	Ga0175312_111813
PA1R	PA1R_gp4364	PA1R_gp1049
PA1RG	Ga0113987_114499	Ga0113987_111869
PA7790	Ga0174976_124813	Ga0174976_121825
PA8281	Ga0175803_114734	Ga0175803_111816
PA83	Ga0226249_01_5016223_5017443	Ga0226249_01_1967397_1968452
PA96	PA96_4322	PA96_1712
PACS2	PaerPA_01001324	PaerPA_01003815
PAK	Y880_0122405	Y880_0104770
PAO1	**PA0842**	**Ga0097782_15205/PA3218**
PAO581	Ga0034253_00876	Ga0034253_03217
PSE305	Ga0098285_111610	Ga0098285_114354
RP73	M062_04095	M062_17180
S04 90	Ga0175152_124808	Ga0175152_121916
S86968	Ga0125010_114699	Ga0125010_111890
SCV20265	SCV20265_4686	SCV20265_1838
SCVFeb	Ga0175802_114242	Ga0175802_111766
SCVJan	Ga0175480_114242	Ga0175480_111766
SJTD-1	A214_02884	A214_05412
ST277	Ga0062142_101948	Ga0062142_101386
sv. O12 PA7	PSPA7_4678	PSPA7_1909
T38079	Ga0123648_114521	Ga0123648_111780
T52373	Ga0125064_114327	Ga0125064_111765
T63266	Ga0123787_114538	Ga0123787_111765

UCBPP-PA14	PA14_53380	PA14_22600
VA-134	Ga0133270_114297	Ga0133270_111758
W16407	Ga0125011_114694	Ga0125011_111935
W36662	Ga0125121_114683	Ga0125121_111960
W45909	Ga0125012_114687	Ga0125012_111860
W60856	Ga0123715_111730	Ga0123715_112390
X78812	Ga0123617_114291	Ga0123617_111776
YL84	AI22_11705	AI22_24595

Given that Agt1 and Agt2 have incredibly similar roles in *P. aeruginosa*, and that their substrates of UDP-glucose and UDP-glucuronic acid are chemically almost identical, it is interesting that these enzymes have comparatively low protein sequence similarity between themselves. On comparing protein sequences, a 35% amino acid identity was found between Agt1 and Agt2 from *P. aeruginosa* strain PAO1, rising to 50% when taking into account conservative amino acid substitutions (Figure 3.12).

```
Score          Expect  Method                          Identities      Positives       Gaps
154 bits(389)  8e-48   Compositional matrix adjust.    113/324(35%)    162/324(50%)    39/324(12%)

Query  5    LSIALISETYPPEVNGVANTLGRLHAGLQQLGHRVQVVRPRQPGDDGRRSDAELVLTRGW  64
            + + ++S+ + P+VNGV  +L  L   L+ LGH+V+V+ P                 R
Sbjct  1    MRLLIVSDAWLPQVNGVVTSLLALQRELELLGHQVRVLSPAD--------------FRCL  46

Query  65   PLPGYPG--LQWGMSSLHKLLRCWKRQRPDVLYIATEGPLGFSALRAARRLGIPAVSGFH  122
            P P YP   L W +  L  L+  +    PD +++ATEGPLG++A R   + G+   S  H
Sbjct  47   PCPSYPEIPLAWNLWRLGGLIEAFA---PDAVHLATEGPLGWAARRWLGKRGLDFTSAIH  103

Query  123  TNFQQYSEHYGFGPLTRLVTGY--LRWFHNRTQMTLVPSGSQRMELQRRGFERLNLLSRG  180
            T F +Y       P   L  GY  LR FH  ++  LV +   R E     F+ L L  +G
Sbjct  104  TRFPEYLRDRC--PWLPLSWGYAFLRTFHRPSRAVLVSTPRLRDEFCAWRFQHLRLWRKG  161

Query  181  VDSQLFHPSRRDPELRRRWGLGEQDIAVLHVGRLAAEKNLGLLGGTFRALCAAHPQLKLR  240
            VD++LFHP+   P          E+    L+VGRLA EKNL      F  L     +L
Sbjct  162  VDTELFHPAETPPA-------KERPPVFLYVGRLATEKNLE----AFLDL-----ELPGE  205

Query  241  LVLVGDGPERKHLERDLPEALFCGVQRGETLAAHYASGDLFLFPSLSETFGNVVLEAQAA  300
              LVGDGP+R  LE+  P+A F G + G  LA  Y +  + +FPSL++T+G V+LEA A
Sbjct  206  KWLVGDGPQRAALEQRYPQARFLGYRHGRALADAYRAASVLVFPSLTDTYGLVMLEALAC  265

Query  301  GLAVVAFDQAAAGQHIRHGHNGVL  324
            G+ V AF         ++ G  GV+
Sbjct  266  GVPVAAFAVPGPLDVLQQGVTGVM  289
```

Figure 3.12. NCBI BLAST (Altschul et al., 1990) output aligning the protein sequences of Agt1 (Sbjct sequence) and Agt2 (Query sequence) glycosyltransferases from *P. aeruginosa* strain PAO1.

To further investigate the apparent dissimilarity of Agt1 and Agt2 in terms of overall protein sequence in *P. aeruginosa*, a phylogenetic tree was constructed to place these proteins in the wider context of the glycosyltransferase protein family. Bacterial glycosyltransferases that are known to be involved in the production of glycolipids were used to construct evolutionary relationships. Loci from *Agrobacterium*

tumefaciens (atu2297) and *Pelagibacter* sp. HTCC7211 (PB7211_960) are bifunctional glycosyltransferases that elicit production of both MGDG and GADG (Sebastián et al., 2016; Semeniuk et al., 2014). Opportunistic pathogen *Enterococcus faecalis* uses BgsB to generate MGDG and BgsA to generate di-galactosyldiacylglycerol (DGDG) (Diederich et al., 2014). The Q3J3A9 locus in *R. sphaeroides* is the glycosyltransferase SqdB involved in sulfoquinovosyl diacylglycerol (SQDG) synthesis in this bacterium (Benning & Somerville, 1992). Protein sequences were aligned using MUSCLE software before construction of an evolutionary tree using the Neighbor-Joining method with a bootstrap value of 100 in MEGA7 (Figure 3.13).

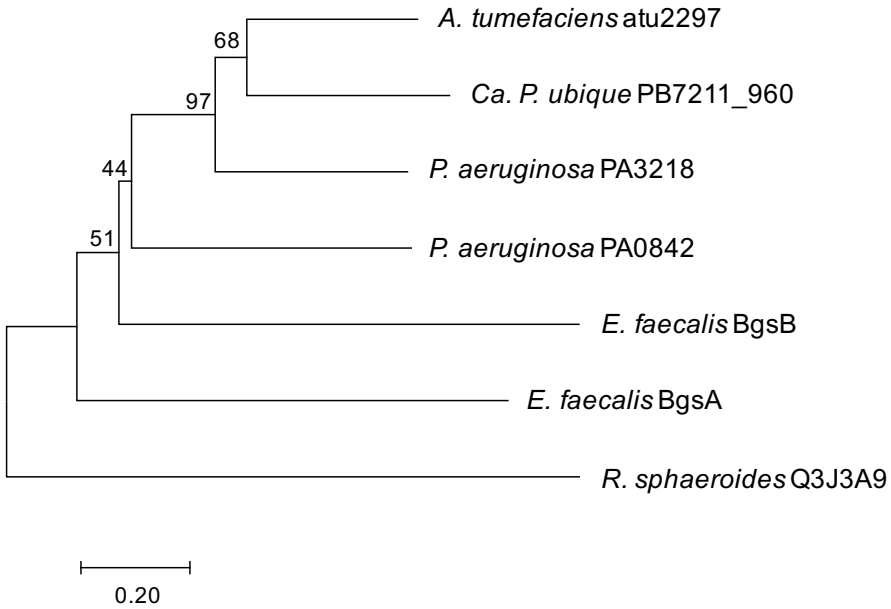

Figure 3.13. Evolutionary relationships of bacterial glycosyltransferases involved in glycolipid synthesis. The evolutionary history was inferred using the Neighbor-Joining method in the MEGA7 software (Kumar et al., 2016). The optimal tree with the sum of branch length = 4.67494048 is shown. The percentage of replicate trees in which the associated taxa clustered together in the bootstrap test (100 replicates) are shown next to the branches (Felsenstein, 1985). The tree is drawn to scale, with branch lengths in the same units as those of the evolutionary distances used to infer the phylogenetic tree.

3.3 Discussion

P. aeruginosa has been previously shown to produce ornithine lipid as a surrogate membrane lipid when under phosphate stress (Kim et al., 2018; Lewenza et al., 2011), indicating its ability to undergo membrane lipid remodelling. In addition to confirming OL production under Pi stress, three additional non-P lipids are produced under these

conditions: glycolipids MGDG and GADG, and a third glycolipid with an unknown head group. The production of non-P lipids occurs simultaneously with a marked reduction in phospholipid PG, and a slight reduction in PE (Table 3.1). Alongside previous findings in environmental heterotrophic bacteria and marine bacterial species (Sebastián et al., 2016), it appears the purpose of lipid remodelling is as a strategy to reduce the phosphate demands on the bacterial cell, given the concomitant reduction in membrane phospholipids. Additionally, this has been shown as a reduction in phospholipids per cell without documented changes in cell size or overall cell volume (Sebastián et al., 2016). For *P. aeruginosa*, it appears the activity of PlcP in removing phospholipids from the membrane represents a burden to the bacterial cell, as shown by comparable growth rates in high and low P for Δ*plcP* (Figure 3.5). This is corroborated in the Δ*agt1* and Δ*agt2* mutants, when PlcP will still be active, where the exponential growth phases are comparable in high and low P. In this way, lipid remodelling appears to become a balance between enabling sustained growth when a nutrient is highly limiting, and energy-costly processes in the removal of already synthesised phospholipids and the synthesis and introduction of surrogate membrane lipids.

Bacterial glycosyltransferases responsible for the synthesis of MGDG and GADG glycolipids require DAG as the precursor molecule (Diercks et al., 2015; Semeniuk et al., 2014). Phospholipid synthesis proceeds via the production of phosphatidic acid (PA), which can be considered a phosphorylated DAG molecule (López-Lara & Geiger, 2017). Therefore, the generation of DAG can occur through the de-phosphorylation of PA or through the activity of phospholipase C enzymes, that cleave the head group of phospholipids to generate DAG. Phosphatidic acid phosphatases (PAP) catalyse the dephosphorylation of PA, thereby yielding DAG and inorganic phosphate (Carman & Han, 2009), for example PgpB in *E. coli*. Overall, few PAPs have been identified in bacterial species. Therefore, the possibility for this pathway in generating additional DAG is inconclusive in *P. aeruginosa*. The specificity of PlcP, a phospholipase C, has been characterised, with the enzyme showing preferential cleavage of PG and PA species, followed by PE species (Wei et al., 2018). A significant reduction in PG was indeed found in *P. aeruginosa* WT undergoing lipid remodelling, in line with reports

on the activities of PlcP. However, the Δ*plcP* mutant is unable to produce DAG through the native lipid remodelling pathway, yet is still able to produce a small amount of GADG, suggesting an alternate source of DAG in *P. aeruginosa*. *E. coli* is able to synthesise membrane-derived oligosaccharides (MDO) as osmoprotectants, and during this process DAG is generated as a by-product through the activity of MdoB (Jackson et al., 1984; Parsons & Rock, 2013). An early study identifies the production of MDO in *P. aeruginosa* (Schulman & Kennedy, 1979). However, the biosynthetic pathway has not been determined. MDO biosynthesis gene MdoH is, however, identified in another Pseudomonad, *P. syringae* (Loubens et al., 1993). BLAST analysis identifies locus tag PA1689 as an MdoH homologue in *P. aeruginosa*, exhibiting 72.4% protein identity to MdoH from *P. syringae*. Together this suggests a strong likelihood of the presence of this pathway in *P. aeruginosa*, thereby representing an alternate source of DAG. In addition, the activity of MdoB in *E. coli* also explains the accumulation of glycolipids without the addition of exogenous DAG following over-expression of *agt1* and *agt2* from *P. aeruginosa,* as the *plcP* gene is not present in *E. coli*.

Unlike some organisms that have a bifunctional glycosyltransferase to generate both MGDG and GADG (Semeniuk et al., 2014), *P. aeruginosa* possesses two *agt* genes to carry out this role through encoding both *agt1* and *agt2*. The *plcP/agt1* operon is conserved throughout many *Pseudomonas* spp., and specifically can be highlighted widely in *P. aeruginosa* genomes in the Pseudomonas Genome Database (Winsor et al., 2009). *agt2* can also be found widely in *P. aeruginosa* genomes, consistently located alongside haemolytic phospholipase C *plcH* and its accessory protein *plcR*. It is intriguing that the glycosyltransferases are located alongside differing PLCs, in that PlcP is an intracellular enzyme, whereas PlcH is secreted and denoted a key virulence factor in *P. aeruginosa* (Vasil et al., 2009). The primary substrate for PlcH is phosphatidylcholine, a major component of lung surfactant, suggesting a key role for PlcH in acquiring essential nutrients including inorganic phosphate during infection (Ostroff et al., 1989). As hypothesised previously, PlcP also represents a method of phosphorus acquisition, though given the presence of multiple PLCs in *P. aeruginosa*, a more important role may simply be reducing the phosphate requirements of the cell

through phospholipid substitution. In addition to different roles for the phospholipase C enzymes, Agt1 and Agt2 have distinct roles in the production of MGDG and GADG glycolipids in *P. aeruginosa*, respectively. Given the similarity of their substrates, UDP-glucose and UDP-glucuronic acid, it is intriguing that there is no redundancy in their roles in glycolipid generation, as confirmed by their heterologous expression in *E. coli*. A further distinct glycosyltransferase must be responsible for the production of the unknown glycolipid, given its absence when *agt1* and *agt2* are expressed in *E. coli*. Structural characterisation or probing of active site residues to determine substrate specificities would be an interesting further step in this area of research. In addition, nuclear magnetic resonance (NMR) characterisation is necessary to elucidate the structure of the unknown glycolipid.

Despite carrying out lipid remodelling under phosphorus stress, phospholipids remain the major component of the *P. aeruginosa* cell membrane, suggesting a significant functional role. It appears that *P. aeruginosa* attempts to maintain overall membrane properties through substitution of lipids for those that possess the same properties, for example anionic PG for GADG, and zwitterionic PE for neutral MGDG and OL. This maintenance of membrane properties also occurs in other species capable of lipid remodelling, such as phytoplankton (Van Mooy et al., 2006). Indeed, in marine bacterial communities, residing in oceans that are inherently phosphorus scarce, phospholipids are introduced into the membrane when provided with excess phosphate (Sebastián et al., 2016). In this context, it could be argued that forming phospholipids actually represents the lipid remodelling phenomenon, as non-P lipids are likely to be the native membrane constituents, given that extremely low phosphorus availability is the norm for these bacterial species. On the other hand, the phospholipid-dominated membrane has been shown to be important for the structure and function of membrane-spanning proteins (Laganowsky et al., 2014). A lack of PG or PE in *E. coli* conditional mutants has been implicated in protein translocation, for example failure in the translocation of outer membrane porins PhoE and OmpA (Cronan, 2003). PE is also shown to be essential in the correct folding of LacY (Cronan, 2003). Together this implies that lipid remodelling may perturb the function of membrane proteins and may have resulted in an evolutionary pressure to

maintain phospholipids as the dominant component of bacterial cell membranes. *P. aeruginosa* maintains a balance between accessing stored phosphorus and reducing phosphate requirements through surrogate introduction of non-P lipids, whilst also maintaining membrane protein function in a phospholipid predominant environment.

Chapter 4 Phenotypic characterisation of lipid remodelling in *P. aeruginosa*

4.1 Introduction

Modifications to some components of the *P. aeruginosa* lipid membrane have been shown to confer resistance to some classes of antibiotic, in particular cationic antimicrobial peptides (CAMPs). Clinically used CAMPs, polymyxin B and colistin, first interact with anionic lipid A in the lipopolysaccharide layer of Gram-negative bacteria, before further puncturing the lipid membrane to cause cell death. *P. aeruginosa* employs two well-characterised mechanisms to modify the lipid A component of LPS, both are chemical additions to the phosphate groups in lipid A, thereby neutralising available negative charges on the membrane utilised by CAMPs for interaction. Using the *arn* operon, *P. aeruginosa* adds 4-amino-4-deoxy-L-arabinose (Ara4N) to lipid A (Lee & Sousa, 2014; Needham & Trent, 2013). *P. aeruginosa* can also add a phosphoethanolamine (PEtN) to lipid A, using PEtN transferase EptA (Nowicki et al., 2015). Both mechanisms serve to reduce available negative charges on the membrane, thereby increasing resistance to AMPs. Interestingly, these mechanisms have been shown to be induced in response to the presence of AMPs themselves (*arn* operon), in Mg^{2+}-limiting conditions (*arn* operon) or in the presence of zinc (EptA) (McPhee et al., 2003; Gutu et al., 2013), but, to my knowledge, these mechanisms have not been characterised as a response to phosphorus stress in *P. aeruginosa*. Through the elucidation of the ornithine lipid (OL) synthesis pathway in response to phosphate stress in *P. aeruginosa*, Lewenza et al. also show a 100-fold increase in resistance to polymyxin B under phosphate stress, alongside a significant decrease in membrane permeability (Lewenza et al., 2011). This phenomenon was not found to be OL-dependent, with the authors hypothesising that alternative membrane lipid changes related to the conservation of phosphate may be responsible for the impermeability. Given that I have shown the production of glycolipids to represent a greater proportion of the lipidome than OL, I hypothesised that the introduction of glycolipids into the outer membrane may be responsible for increased polymyxin resistance found under phosphate stress.

The addition of Ara4N to lipid A that confers resistance to colistin can be developed in *P. aeruginosa* under consistent exposure to colistin in an *arn*-independent manner (Chung et al., 2017). Further, the authors suggest the reappearance of colistin resistance in the *arnB* mutant may be due to other physiological changes likely to be associated with cell membrane changes. Given that lipid A modifications conferring AMP resistance are influenced by two-component systems that are themselves induced by the presence of AMPs, for example PhoPQ and PmrAB, I hypothesised that glycolipid production may be an alternative mechanism included in this response to AMPs. In addition, *P. aeruginosa* mutations in *pmrB* that lead to constitutive overexpression of the *arn* operon, and hence the Ara4N lipid A modification and subsequent AMP resistance, were found to exhibit differences in their lipid profiles compared to their WT counterpart (Han, et al., 2018). Glycerophospholipids were found to be significantly decreased in polymyxin resistant *pmrB* mutants, and I hypothesised that this may be due to the inclusion of alternative non-phosphate lipid classes in the membrane to contribute to decreased polymyxin sensitivity, such as the glycolipids.

The *P. aeruginosa* cell membrane is notorious in its intrinsic impermeability, contributed to by the presence of several smaller content-specific porins, in comparison to larger, more generalised membrane porins present in other bacterial species (Chevalier et al., 2017; Hancock & Brinkman, 2002). Membrane-spanning proteins play a significant role in both the entry and expulsion of antibiotics, through outer membrane porins (Omps) and efflux pumps, respectively. The phospholipid environment in the bacterial cell membrane has been stipulated in the stability and function of outer membrane proteins, particularly in charge interactions between phospholipids and proteins, and could include those linked to AMR. For example, OmpF in *E. coli* required its native phospholipid composition to fold correctly (Ionescu et al., 2017; Liko et al., 2018). Alterations to the lipid environment surrounding Omps and efflux pumps in *P. aeruginosa* may influence its resistance to other classes of antibiotics should membrane changes perturb their stability or activity.

In this chapter I investigate the survival of *P. aeruginosa* WT and lipid remodelling mutants (Δ*plcP*, Δ*agt1* and Δ*agt2*) when challenged with AMP polymyxin B. I also test the sensitivity of glycolipid remodelling mutants to other major classes of antibiotics that are typically used to treat *P. aeruginosa* infections. In addition, I analyse proteomic differences between WT and the Δ*plcP* mutant under phosphorus stress. The phenotypic response to phosphorus stress and the subsequent influence this may have on *P. aeruginosa* AMR could prove important in terms of choice of antimicrobial treatment of *P. aeruginosa* infections, given the clinical relevance of phosphate stress in this bacterium.

4.2 Results

4.2.1 Glycolipids provide protection against antimicrobial peptide polymyxin B

To investigate the role of glycolipids in altering membrane interaction with antimicrobial peptides, planktonic cultures of *P. aeruginosa* WT and lipid remodelling mutants (Δ*plcP*, Δ*agt1* and Δ*agt2*) were challenged with twice the reported minimum inhibitory concentration (MIC) of polymyxin B (4 μg mL^{-1}) (Hogardt et al., 2004). Using the broth microdilution method to determine the MIC for polymyxin B in high and low phosphate media, WT *P. aeruginosa* had an MIC of 1 μg mL^{-1} for both conditions (Figure 4.1A). However, when using twice this MIC (2 μg mL^{-1}) in subsequent survival assays, very little death was seen under low phosphate conditions. Therefore the concentration was increased to 4 μg mL^{-1} in line with previous MIC reports. In addition, *P. aeruginosa* under low phosphate conditions grew poorly in the 96-well microplate, reaching an average of 0.16 OD_{600} in the growth control, compared to 0.6 OD_{600} in the high phosphate growth control. Bacterial survival at 0, 2, 5, 10 and 20 minutes when challenged with 4 μg mL^{-1} polymyxin B under high and low phosphate (P) conditions was recorded through CFU counts. For WT *P. aeruginosa*, there was a significant increase (over 10-fold) in survival when challenged with polymyxin B under phosphate stress, compared to phosphate replete conditions (Figure 4.1B), consistent with previous reports (Lewenza et al., 2011). For all glycolipid remodelling mutants, Δ*plcP*, Δ*agt1* and Δ*agt2*, survival under Pi stress conditions when challenged with polymyxin

B was reduced (Figure 4.1D), with no differences found after 20 minutes between the strains when grown in Pi sufficient conditions (Figure 4.1C).

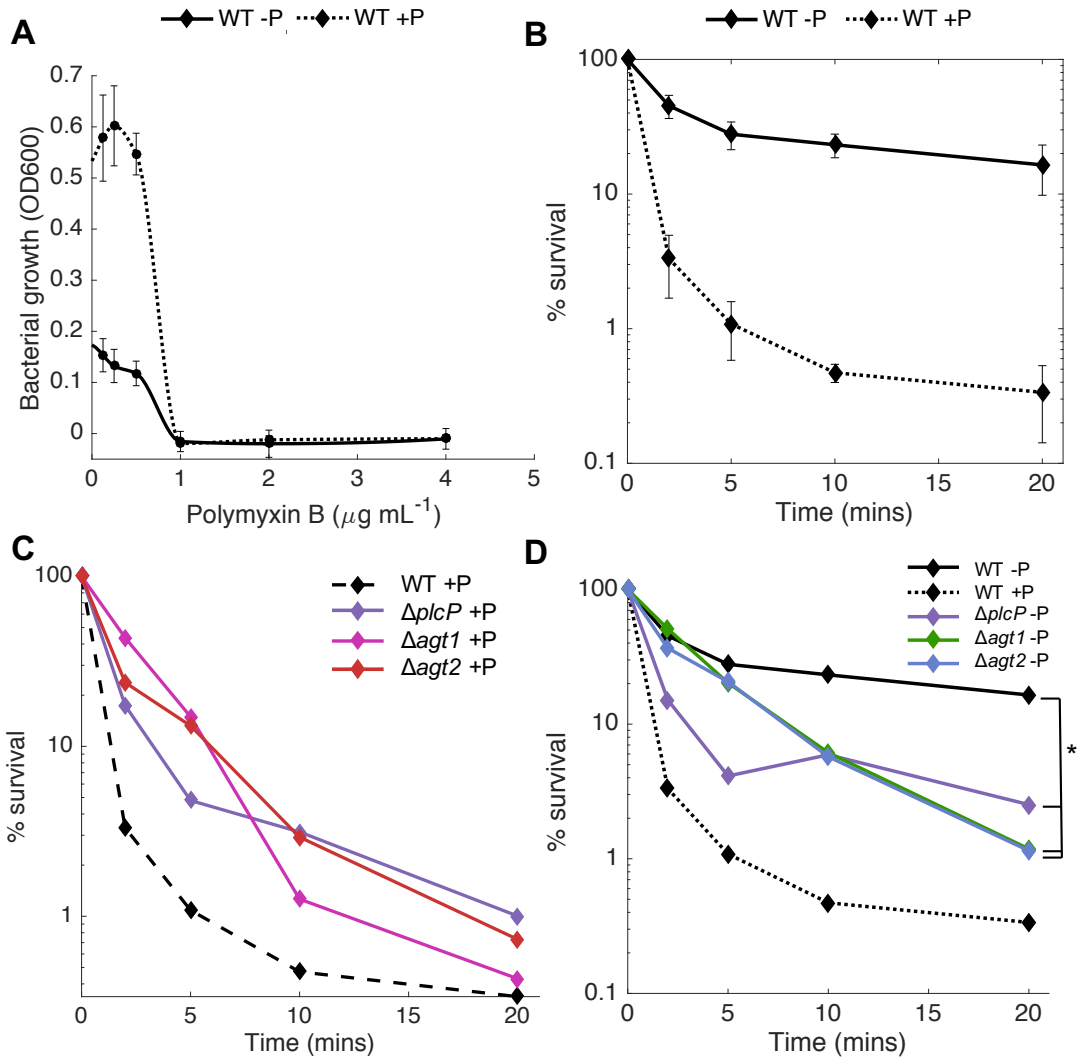

Figure 4.1. Survival of *P. aeruginosa* after treatment with polymyxin B (4 µg mL^{-1}) is linked to glycolipid production. A) Determining the minimum inhibitory concentration of polymyxin B in WT *P. aeruginosa* in high (dotted line) and low (solid line) phosphate conditions. B) Survival of WT *P. aeruginosa* when challenged with 4 µg mL^{-1} polymyxin B, under high and low phosphate conditions. C) Survival of WT and glycolipid remodelling mutants Δ*plcP* (purple), Δ*agt1* (pink) and Δ*agt2* (red) when challenged with 4 µg mL^{-1} polymyxin B under high phosphate conditions only. D) Survival of glycolipid remodelling mutants Δ*plcP* (dark purple), Δ*agt1* (green) and Δ*agt2* (blue) when challenged with 4 µg mL^{-1} polymyxin B under low phosphate conditions, compared to WT under Pi stress (solid black) and P sufficiency (dotted black). All experiments are the average of three biological replicates, error bars denote standard deviation. * $p < 0.05$.

In Δ*plcP*, where MGDG production is ablated and GADG production is significantly knocked down, survival at 20 minutes under Pi stress was found to be 2.5% (± 2.35%), compared to 16.5% (± 6.6%) in WT *P. aeruginosa* ($p < 0.05$, t-test). A comparable phenotype was found for Δ*agt1*, where survival at 20 minutes was found to be 1.2% (± 0.12%), with only MGDG production being lost in this mutant ($p < 0.05$, t-test). Δ*agt2* also exhibited decreased survival when challenged with polymyxin B, 1.1% (± 0.25%) compared to 16.5% (± 6.6%) in WT *P. aeruginosa* ($p < 0.05$, t-test). For Δ*agt2*, GADG production is ablated, but MGDG production is also affected, being significantly reduced compared to WT *P. aeruginosa* under Pi stress (section 3.2.3). As MGDG is a neutral lipid and GADG is negatively charged, and given that in all mutants the production of MGDG is either ablated or significantly reduced (Figure 3.10), I hypothesise that neutral MGDG glycolipid confers the protection from polymyxin B under WT conditions.

4.2.2 Glycolipid production is not induced by sub-inhibitory levels of antimicrobial peptides

The lipid A modification with Ara4N that confers resistance to AMPs has been shown to be controlled by the two component systems PhoPQ and PmrAB that are induced by AMPs themselves. As the presence of glycolipids in the *P. aeruginosa* membrane confers some protection to polymyxin B, I investigated whether regulation of the pathway is linked to other AMP resistance mechanisms and also induced due to the presence of AMPs. In addition, in a transcriptomic study some *P. aeruginosa* WT samples showed an increase in the expression of *plcP* in response to sub-inhibitory colistin (Cummins et al., 2009). The sub-inhibitory concentration of AMPs (0.15 μg mL^{-1}) used during *P. aeruginosa* WT growth in cation-adjusted Mueller Hinton broth (MHB) was not found to interfere with growth (Figure 4.2A-B). HPLC/MS lipid analysis of *P. aeruginosa* WT grown in the presence of AMPs for 24 hours did not reveal any changes to the lipidome as a result of AMP exposure (Figure 4.2C-D). In terms of alternative lipid classes, a small amount of ornithine lipid was found to be produced when *P. aeruginosa* was cultured in MHB, irrespective of the presence of AMPs. As such, I concluded that control of glycolipid synthesis genes is first as a response to

phosphorus stress, with increased resistance to polymyxin B representing a positive AMR trade-off in the phenotypic response to Pi stress in *P. aeruginosa*.

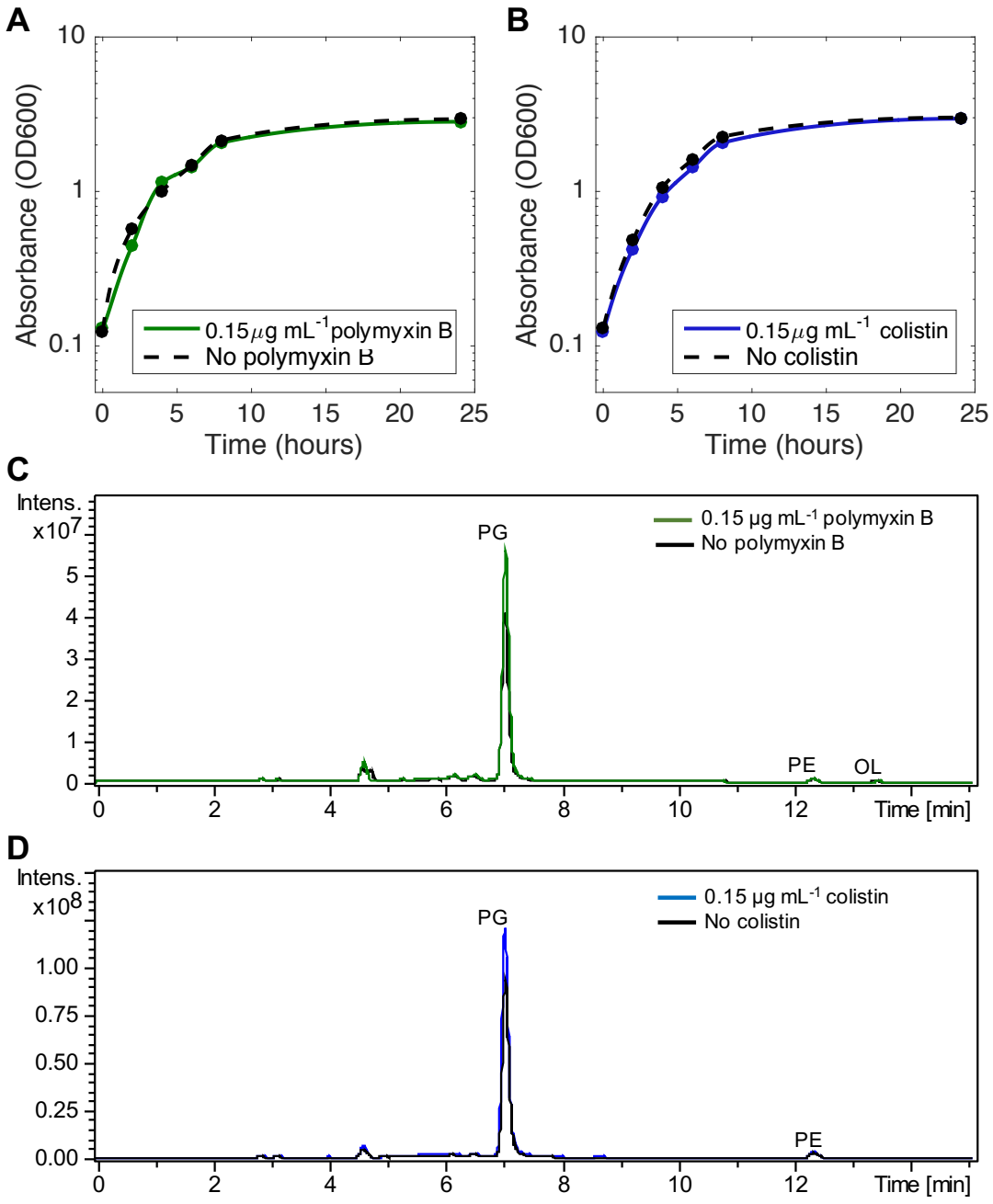

Figure 4.2. Subinhibitory antimicrobial peptides do not induce glycolipid production in *P. aeruginosa*. A-B) Growth curves of WT *P. aeruginosa* PAO1 in cation adjusted Mueller Hinton (MH) broth alone (black) or with 0.15 μg mL^{-1} polymyxin B (green) or colistin (blue). C-D) Representative HPLC chromatograms in negative ionisation mode showing the lipidome of *P. aeruginosa* in MH broth alone (black), or with added subinhibitory antimicrobial peptides. PG: phosphatidylglycerol, PE: phosphatidylethanolamine, OL: ornithine lipid.

4.2.3 The *P. aeruginosa* cellular proteome is influenced by glycolipid synthesis

To investigate whether any important proteins, or those linked to AMR, are affected by the production of glycolipids in response to Pi stress, the *P. aeruginosa* cellular proteome was analysed. On comparing WT and Δ*plcP* under Pi stress, 13 proteins were identified to be differentially expressed. Of these, 4 were more highly expressed in Δ*plcP*, and the remaining 9 were more highly expressed in WT *P. aeruginosa* (Figure 4.3). The most highly downregulated protein in Δ*plcP* compared to WT *P. aeruginosa* was locus tag PA2491 (6.1 fold change), which has been previously characterised as MexS (Sobel et al., 2005). Mutations in MexS were shown to exhibit increased expression of RND efflux pump MexEF-OprN, which leads to a concomitant decrease in outer membrane porin OprD (Sobel et al., 2005). Overexpression of MexEF-OprN confers resistance to quinolones, chloramphenicol, and trimethoprim (Jin et al., 2011). OprD is a key route of entry for carbapenem antibiotics, particularly imipenem (Masuda et al., 1995). Further, MexS represents a negative regulator of the type III secretion system (Jin et al., 2011). Thus, as MexS is downregulated in Δ*plcP* compared to WT *P. aeruginosa*, it is possible that Δ*plcP* may exhibit decreased sensitivity to antibiotics expelled by MexEF-OprN, and those that gain entry through OprD.

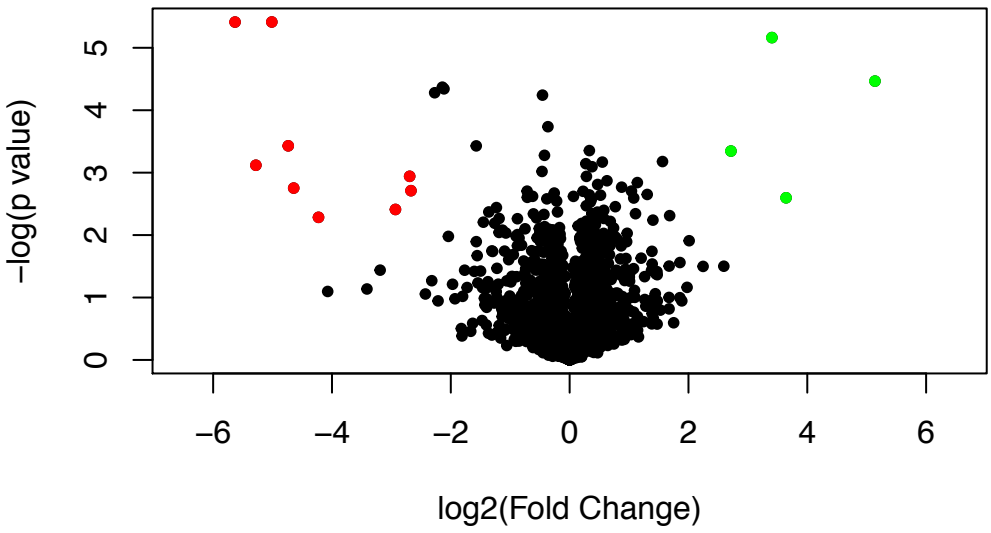

Figure 4.3. Volcano plot depicting differentially expressed proteins when comparing *P. aeruginosa* WT and glycolipid-deficient Δ*plcP* under phosphate stress conditions. More highly expressed proteins in WT are shown in red, and those that are more highly expressed when *P. aeruginosa* is unable to produce glycolipids (Δ*plcP*) are in green (see Table 4.1 for full annotated list). Significance was accepted when the false discovery rate (FDR) was < 0.05, and a fold change ≥ 2.

A further operon linked to carbapenem transport was more highly expressed in WT *P. aeruginosa* compared to Δ*plcP*, gene loci PA4500-4502 encoding for a dipeptide transporter (PA4501; OpdP) and related peptide binding proteins DppA3 and DppA4 (PA4500 and PA4502). OpdP (also known as OccD3) is an ortholog of known carbapenem transporter OprD, and its properties have been shown to favour the translocation of both meropenem and imipenem in *P. aeruginosa* (Isabella et al., 2015; Soundararajan et al., 2017). Thus, as OpdP porin expression is lower in Δ*plcP* compared to WT *P. aeruginosa*, the glycolipid-deficient mutant may exhibit decreased sensitivity to carbapenem antibiotics.

Other known proteins upregulated in WT *P. aeruginosa* compared to Δ*plcP* include the condensin MksF that forms part of the MksBEF operon linked to chromosome partitioning in *P. aeruginosa* (Petrushenko et al., 2011). However, neither of the other members of this operon are differentially regulated, and as MksF is a very large protein (948 amino acids), it could be that peptides were incorrectly attributed to belong to MksF. A thiol:disulfide interchange protein, DsbG, also has increased expression in WT *P. aeruginosa* compared to Δ*plcP*. Other differentially expressed

proteins are uncharacterised. Using PaperBLAST (Price & Arkin, 2017) to identify any potential interesting roles of homologous proteins revealed PA2493 to have 53% protein identity to YhbW from *E. coli*. YhbW is linked to maintaining cell envelope integrity in *E. coli* (Hayden & Ades, 2008), and thus a similar protein may be required due to membrane imbalances caused by lipid remodelling in WT *P. aeruginosa*.

Known proteins upregulated in glycolipid deficient Δ*plcP* compared to WT *P. aeruginosa* include inner membrane core protein in type IV pili PilC, superoxide dismutase SodM and Fe(III)-pyochelin outer membrane receptor FptA. However, other structural proteins related to type IV pili were not differentially expressed, suggesting a potential artefact, though it is plausible that the membrane alterations in WT *P. aeruginosa* leads to less pili. SodM and FptA are both linked to iron starvation (Hoegy et al., 2009; Sønderholm et al., 2017). However, a more global proteomic response to iron starvation would be expected if Δ*plcP* was truly iron stressed compared to WT *P. aeruginosa*. The final protein (PA5190) upregulated in Δ*plcP* is uncharacterised.

Table 4.1. Glycolipid responsive proteome in WT *P. aeruginosa* PAO1. Locus tags from the *Pseudomonas* genome reference database are listed alongside known or predicted protein functions. Log2 transformation of fold change values show the differences between WT *P. aeruginosa* and glycolipid deficient Δ*plcP,* and are the mean of 3 replicates. All glycolipid responsive proteins displayed have a log2(Fold Change) of ≥2 and all were considered significant with a false detection rate of <0.05 (FDR<0.05). Negative values indicate downregulation in Δ*plcP* compared to WT *P. aeruginosa* under phosphorus stress.

Gene locus	Log2(Fold Change)	FDR	Protein	Function
PA2491	-6.1	0.000	MexS	Negative regulator of type III secretion system
PA2483	-5.3	0.002	-	unknown
PA2462	-3.9	0.002	-	Contact-dependent toxin
PA4686	-3.6	0.006	MksF	Condensin
PA4582	-3.4	0.004	-	unknown
PA4500	-2.5	0.001	DppA3	Solute binding protein specific for dipeptides
PA4502	-2.3	0.000	DppA4	Solute binding protein specific for tripeptides
PA2476	-2.2	0.025	DsbG	Thiol:disulfide interchange protein
PA4501	-2.0	0.001	OpdP	Gly-glu dipeptide porin
PA2464	-1.9	0.013	-	unknown
PA5190	3.1	0.019	-	unknown
PA4527	4.2	0.000	PilC	Inner membrane core protein in type IV pili
PA4221	5.1	0.000	FptA	Fe(III)-pyochelin outer membrane receptor
PA4468	5.7	0.000	SodM	Superoxide dismutase

4.2.4 The role of *P. aeruginosa* glycolipids in sensitivity to other antibiotic classes

A wide variety of antibiotics are used to treat *P. aeruginosa* infections. Therefore, commonly used representatives from fluoroquinolones (ciprofloxacin), aminoglycosides (gentamicin), carbapenems (meropenem) and cephalosporins (ceftazimide) were used to test *P. aeruginosa* sensitivity in P-stress conditions. The standard sensitivity test using discs impregnated with antibiotics was modified to use agar plates controlling phosphate concentration. 1.5% (w/v) pure agarose was added to minimal medium A, to limit the introduction of additional phosphate. *P. aeruginosa* was able to grow on both Pi-replete and Pi-deplete minimal medium A plates. To ensure *P. aeruginosa* was starved of phosphate on minimal medium A "-P" plates, containing 100 µM phosphate source, the alkaline phosphatase substrate X-phosphate (XP; also known as BCIP) was utilised as a chromogenic indicator of Pi stress. Both spread plates from liquid culture and streak plates directly from *P. aeruginosa* WT glycerol stock resulted in a blue colour when XP was present, indicating Pi stress, where minimal medium A plates with a high concentration of phosphate remained beige (Figure 4.4).

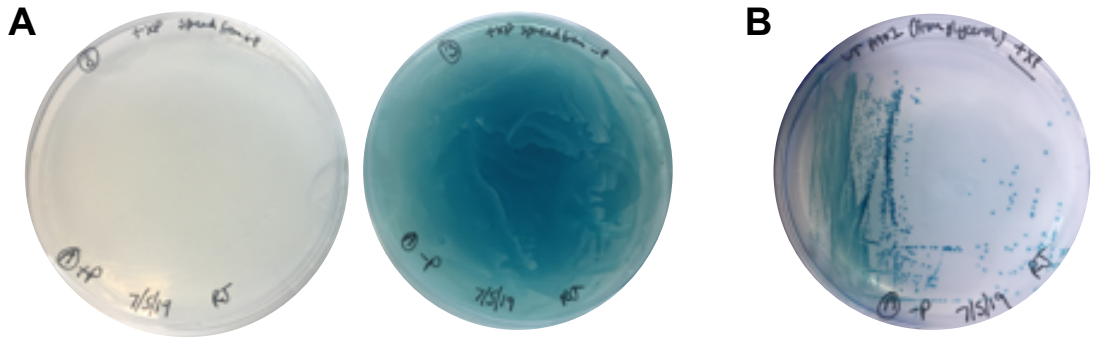

Figure 4.4. A) Agar plates made using modified minimal medium A with 1.5% (w/v) agarose, supplemented with 1 mM phosphate source (left) or 100 µM phosphate source (right). Chromogenic indicator of phosphate stress X-phosphate indicates *P. aeruginosa* is starved of phosphate at a concentration of 100 µM only (blue colour). B) *P. aeruginosa* is under phosphate stress on minimal medium A plates containing 100 µM phosphate source after streaking directly from glycerol stocks.

WT and glycolipid remodelling mutants were first cultured on minimal medium A plates supplemented with high (1 mM) or low (100 µM) concentrations of phosphate. A few colonies were picked and resuspended in saline solution, adjusted to 0.5 McFarland standard (Thermo Scientific), and used to make spread plates before the addition of antimicrobial sensitivity discs impregnated with either ciprofloxacin (1 µg), gentamicin (10 µg), meropenem (10 µg) or ceftazimide (30 µg). Plates were incubated at 37°C for 24 hrs before measuring zones of clearance. No significant differences for ciprofloxacin, gentamicin or ceftazimide were observed between WT with Pi stress or P sufficiency, nor between each of the glycolipid remodelling mutants compared to WT under Pi stress (Figure 4.5). For meropenem, there was no difference observed between WT with Pi stress or Pi sufficiency. However, for each glycolipid remodelling mutant, Δ*plcP*, Δ*agt1* and Δ*agt2*, under Pi stress there was a significant decrease in sensitivity to meropenem when compared to WT under Pi stress ($p < 0.05$, *t*-test; Figure 4.5D). Together this suggests a further trade-off between glycolipid production and AMR; the WT production of glycolipids in response to Pi stress results in relatively higher sensitivity to meropenem when compared to glycolipid-deficient strains.

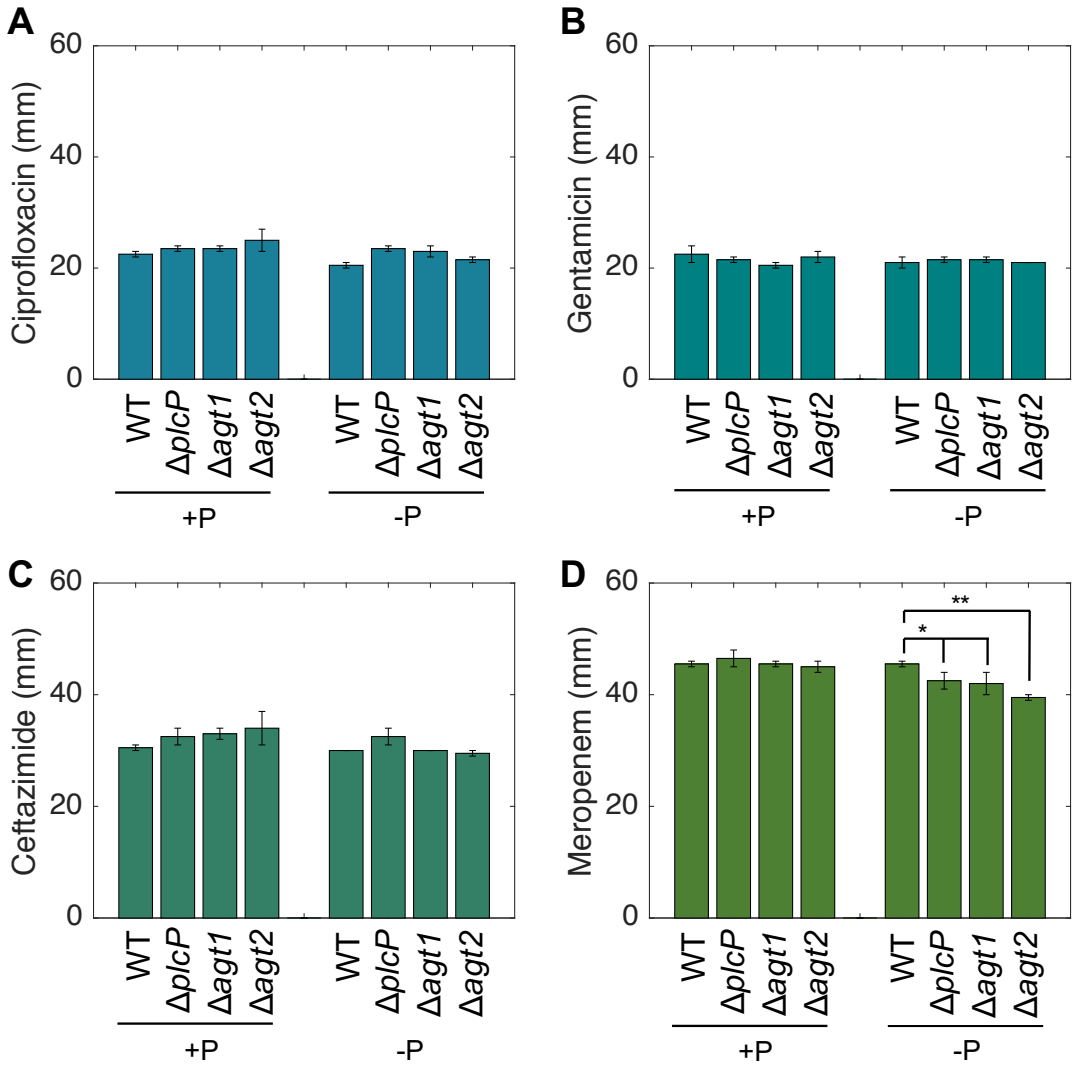

Figure 4.5. Zones of clearance when *P. aeruginosa* WT and glycolipid synthesis mutants Δ*plcP*, Δ*agt1* and Δ*agt2* were grown in the presence of ciprofloxacin (1 µg; A), gentamicin (10 µg; B), ceftazimide (30 µg; C) and meropenem (10 µg; D) discs. Antibiotics were tested under phosphate replete conditions (1 mM, "+P") and under phosphate stress (100 µM, "-P"). Data are the average of three independent replicates and error bars represent standard deviation. * $p < 0.05$, ** $p < 0.01$.

To further investigate the observed decrease in sensitivity to meropenem as a result of the inability to produce glycolipids under Pi stress, the sensitivity of *P. aeruginosa* to other members of the carbapenem class of antibiotics was tested as before. Disruption to regulator MexS, shown in my proteomic dataset to be downregulated when *P. aeruginosa* is unable to produce glycolipids (Δ*plcP*), is linked to an increase in the expression of efflux pump MexEF-OprN, which in turn leads to decreased expression of outer membrane porin OprD (Figure 4.6) (Sobel et al., 2005). OprD (PA0958) protein expression was slightly decreased in Δ*plcP*, however this was not a

significant decrease. OprD is the main entry route of carbapenems, particularly imipenem. Therefore, investigating sensitivity to imipenem was an essential next step. In addition, expression of carbapenem transporter OpdP was significantly lower in Δ*plcP*, and could contribute to the observed decrease in sensitivity to meropenem.

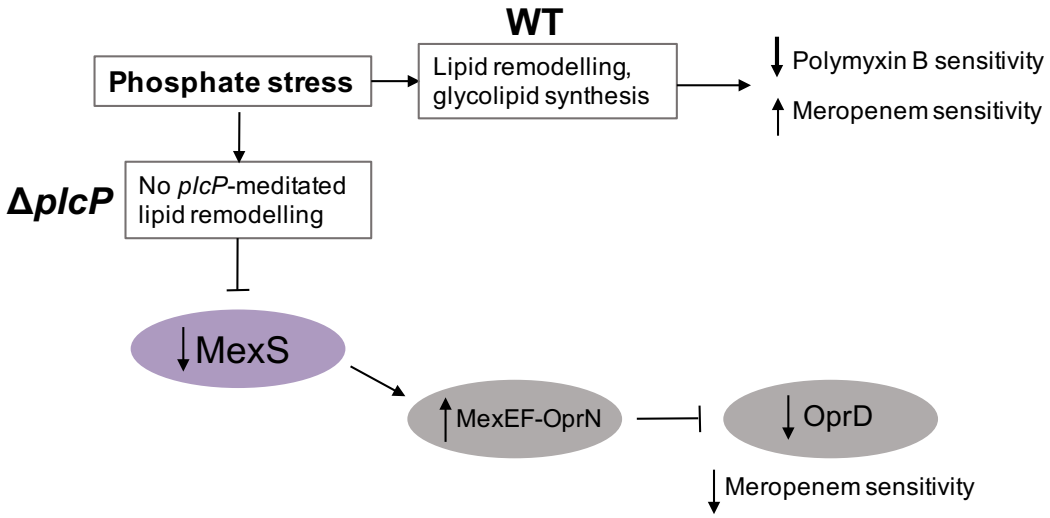

Figure 4.6. Proposed model of proteomic changes due to Δ*plcP*-mediated lipid remodelling that influence antibiotic resistance. Regulatory protein MexS is downregulated in Δ*plcP* compared to WT *P. aeruginosa*. Disruption of MexS regulation leads to an increase in efflux pump MexEF-OprN expression and a decrease in expression of carbapenem transporter OprD (Sobel et al., 2005).

However, for imipenem (10 µg), and also for doripenem (10 µg) and ertapenem (10 µg), there were no significant differences in sensitivity observed between WT *P. aeruginosa* and glycolipid remodelling mutants under Pi stress (Figure 4.7A-C). On testing a variety of concentrations of imipenem using the broth microdilution MIC method for WT and Δ*plcP* in Pi stress and Pi sufficient conditions, there was no difference in the MIC between the two strains, with each found to be 4 µg mL^{-1}, under Pi-replete or Pi-deplete conditions (Figure 4.7D).

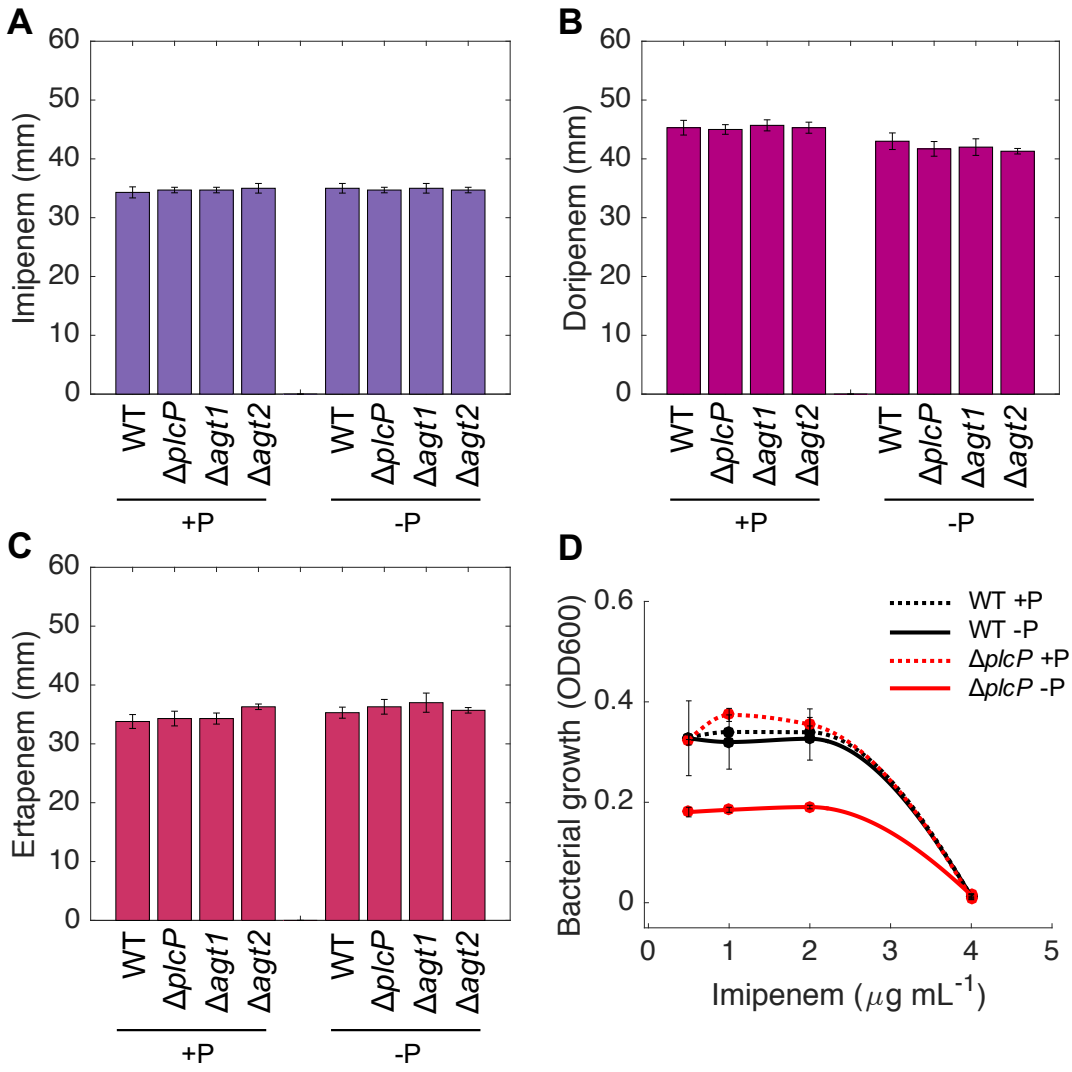

Figure 4.7. Zones of clearance when *P. aeruginosa* WT and glycolipid synthesis mutants Δ*plcP*, Δ*agt1* and Δ*agt2* were grown in the presence of carbapenems. A) Imipenem (10 µg), B) doripenem (10 µg), C) ertapenem (10 µg). Sensitivity was tested under phosphate replete (1 mM, "+P") and phosphate stress (100 µM, "-P") conditions. D) Determining the minimum inhibitory concentration of imipenem in WT *P. aeruginosa* and glycolipid-deficient Δ*plcP*, under phosphate replete (1 mM, "+P") and phosphate stress (100 µM, "-P") conditions. Data are the average of two technical replicates, error bars indicate standard deviation.

4.2.5 Characterisation of other phenotypic changes

To investigate overall membrane integrity in *P. aeruginosa*, WT and glycolipid remodelling mutant strains were challenged with EDTA. EDTA disrupts the outer membrane of gram negative bacteria by chelating divalent cations in the LPS layer, that are important for maintaining outer membrane integrity (Clifton et al., 2015). 0.5 mM EDTA was added to minimal medium A agarose plates, with serial dilutions of

bacterial cultures pre-grown under Pi-replete or Pi-deplete conditions then spotted across each plate. After incubation for 48 hrs, *P. aeruginosa* strains grown under Pi stress in the presence of EDTA survived ten-fold less than those grown when P is sufficient (Figure 4.8C-D). However, this was not glycolipid dependent as Δ*plcP* and Δ*agt1* survived at the same rate as WT *P. aeruginosa* under Pi stress. Intriguingly, growth of Δ*agt2* was absent under both Pi stress and Pi sufficiency at 48 hrs. Further incubation for 5 days revealed Δ*agt2* growth, surviving to a dilution ten-fold lower than WT, Δ*plcP* and Δ*agt1* in both concentrations of phosphate (Figure 4.8E-F).

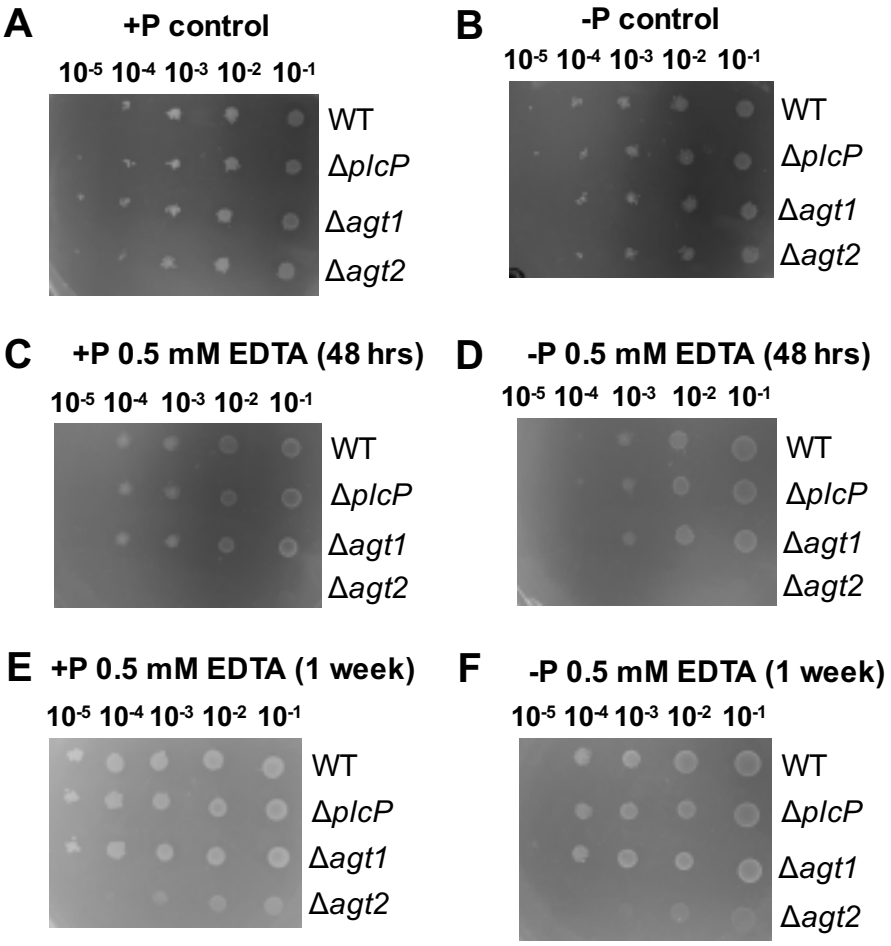

Figure 4.8. Survival of *P. aeruginosa* WT and glycolipid synthesis mutants when challenged with 0.5 mM EDTA, incubated for 48 hrs (C-D) and 1 week (E-F). High phosphate conditions are shown in left panels (1 mM, "+P") and low phosphate shown in right panels (100 µM, "-P"). Representative images taken from three biological replicates and growth controls under phosphate sufficiency (A) and phosphate stress (B) are shown.

During development of the EDTA assay, minimal medium A agarose plates were first used with a lower percentage of agarose (1%, w/v). *P. aeruginosa* exhibited slight swarming on some control plates with low phosphate concentration (Figure 4.9A), before the concentration of agarose was increased. This is consistent with previous reports of phosphate stress inducing swarming in *P. aeruginosa* (Bains et al., 2012). It was observed that WT *P. aeruginosa* appeared to be able to swarm to a greater degree than glycolipid synthesis mutants. Therefore, the role of glycolipids in affecting swarming ability of WT *P. aeruginosa* compared to Δ*plcP*, Δ*agt1* and Δ*agt2* was investigated. However, the ability of *P. aeruginosa* glycolipid synthesis mutants to swarm was not impaired, as all mutants displayed a clear bullseye swarming pattern under phosphate stress (Figure 4.9B). WT *P. aeruginosa* exhibited the same bullseye pattern. However, the growth was not as strong and did not come out well when photographed.

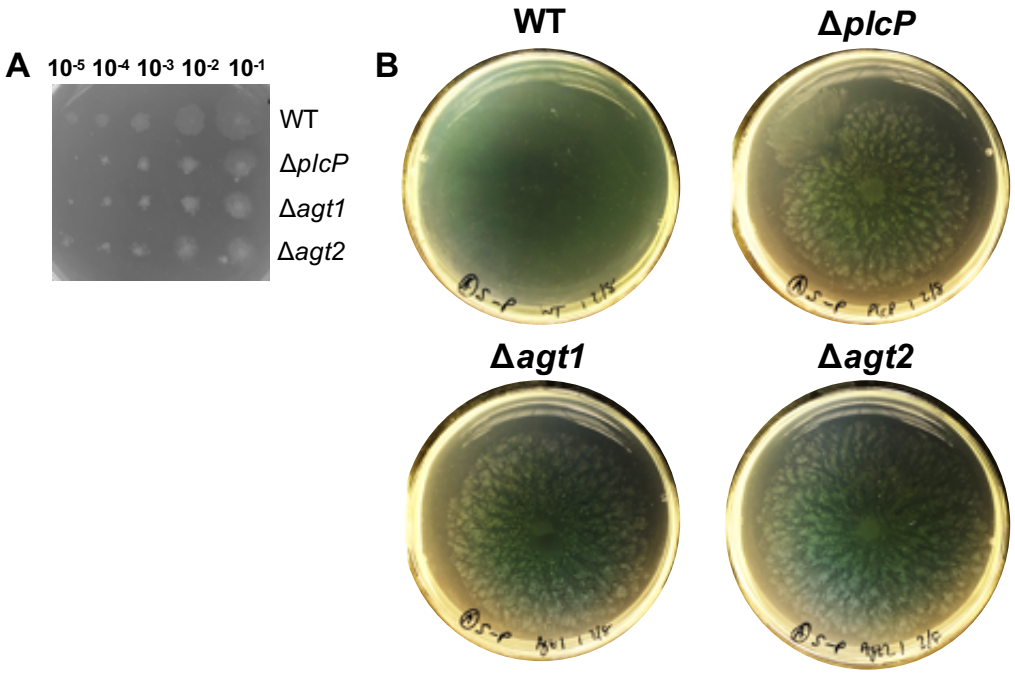

Figure 4.9. Swarming ability of *P. aeruginosa* WT and glycolipid synthesis mutants (Δ*plcP*, Δ*agt1* and Δ*agt2*). A) Slight swarming observed on control growth plates (minimal medium A with 1% agarose and 100 µM phosphate). B) Swarming patterns of WT *P. aeruginosa* and glycolipid synthesis mutants Δ*plcP*, Δ*agt1* and Δ*agt2*, achieved using minimal medium A plates containing 0.5% (w/v) agarose.

In developing the swarming assay, different published methods were tried before swarming was successfully achieved. One method did not supplement plates with an iron source, leading to production of bright yellow siderophore pyoverdine in WT, Δ*plcP* and Δ*agt1* strains (Figure 4.10), in response to iron stress. However for Δ*agt2*, this pyoverdine production was not observed. This apparent disruption of pyoverdine production could link to the lack of Δ*agt2* growth in the presence of EDTA, as EDTA is a known iron chelator.

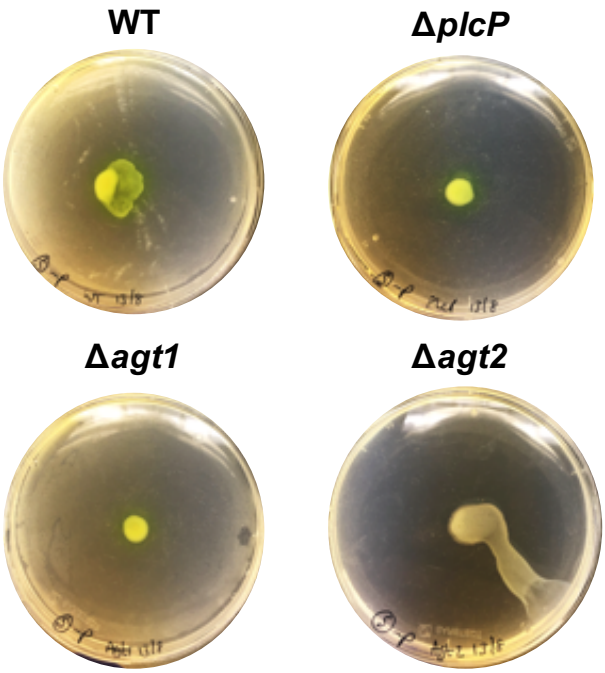

Figure 4.10. Pyoverdine production in *P. aeruginosa* WT and glycolipid synthesis strains (Δ*plcP*, Δ*agt1* and Δ*agt2*) on swarming plates with no supplemented iron source (medium described in 2.5.2, without the addition of 50 µM $FeCl_3$).

4.3 Discussion

Glycolipids are not widely characterised in pathogenic bacteria. Thus, there is limited research into phenotypic changes as a result of their presence in the membrane, including antimicrobial resistance. In *P. aeruginosa*, the production of ornithine lipid (OL) was not found to be responsible for the large decrease in sensitivity to polymyxin B under low phosphate conditions (Lewenza et al., 2001). A further study did show that overexpression of OL in *P. aeruginosa* conferred decreased sensitivity to cationic AMPs LL-37, magainin and defensin (Kim et al., 2018). The same study showed a

decrease in sensitivity to polymyxin B as a result of OL overexpression. However, a disc diffusion method was used, which is not recommended as AMPs such as polymyxin B and colistin do not diffuse consistently through agar plates (EUCAST, 2016). It is likely that overexpression of zwitterionic OL to levels above native OL production in *P. aeruginosa* altered membrane properties such as overall charge, thereby perturbing cationic AMP interaction. As I have shown that glycolipids MGDG and GADG form a greater proportion of the *P. aeruginosa* membrane, they are likely to have a greater effect on membrane properties after native membrane lipid remodelling in *P. aeruginosa*. When considering overall membrane charge in WT and glycolipid synthesis mutants Δ*plcP*, Δ*agt1* and Δ*agt2* under Pi stress (Table 3.1), WT exhibits the largest proportion of neutral membrane lipids at 10%. The glycolipid remodelling mutants range between 6-7%, compared to WT under P sufficiency at 4.8%. As these differences are largely dependent on the presence of neutral MGDG, of which production is ablated or significantly reduced in all glycolipid mutants, I hypothesise that MGDG confers a protective effect against cationic AMP insult through increasing net membrane charge. Importantly, the proteomic dataset confirms that previously described mechanisms that modify the LPS layer to result in polymyxin B resistance (Chung et al., 2017; Nowicki et al., 2015) are not differentially expressed between WT and glycolipid remodelling mutant *ΔplcP*. The glycolipid protection is a novel mechanism that occurs as a result of phenotypic adaptation to surrounding environmental phosphorus depletion.

OLs can be found in both inner and outer membranes of gram negative bacteria, but appear more likely to accumulate in the outer membrane (Dees & Shively, 1982; Geiger et al., 2010). In this way, OL will influence outer membrane properties. For glycolipids in gram negative bacteria, it is not clear to which membrane they would accumulate in. However, based on a loss of protection against polymyxin B in glycolipid-deficient mutants, it is likely that glycolipids accumulate in the outer membrane. However, this should be clarified with future experiments, through using sucrose isopycnic gradient ultracentrifugation to separate inner and outer membranes and analysing the lipid content using HPLC/MS. In addition, the effect of the presence of glycolipids, likely in the outer membrane, on the LPS layer should be

investigated. LPS analysis, for example overall abundance and the number of positive charges, or perhaps alternative modifications due to phosphate stress, will be key in elucidating the mechanism for glycolipid protection from AMPs under phosphate stress. However, mutants in genes that compromised LPS integrity, leading to increased outer membrane permeability, were shown to have increased sensitivity to polymyxin B (Fernández et al., 2013). Therefore, the protective effect of glycolipids is likely due to changes in membrane charge. The effects of glycolipids on membrane permeability were investigated using both 1-N-phenylnaphthylamine and nitrocefin, however the data were poor. Optimising these experiments would be beneficial in determining whether polymyxin B sensitivity is decreased due to decreased membrane permeability.

The majority of cellular proteomic differences between WT and Δ*plcP* under Pi stress were either uncharacterised proteins, or belonged to a protein subset that it is difficult to fathom a reason for the difference. For example, where only one of an operon is differentially expressed, it is difficult to believe this is a real change. Equally, for those expressed only under iron stress, I would expect a broader iron stress response that would include fundamental iron stress response proteins, such as the master regulator Fur. A key future direction for proteomic analysis is to separate the cell membrane protein fraction for analysis. One of the differentially expressed proteins was interesting in that the expression of MexS was reduced in Δ*plcP* compared to WT. Disruption of MexS is linked to the upregulation of efflux pump MexEF-OprN, which in turn reduces the presence of outer membrane porin OprD (Llanes et al., 2011). The concomitant reduction of carbapenem entry porin OprD linked well to the decreased sensitivity to meropenem observed in each glycolipid remodelling mutant. However, an increase in MexEF-OprN should also confer increased resistance to ciprofloxacin, as this efflux pump is known to accommodate quinolones (Livermore, 2001), and this was not observed in the data. Additionally, loss of OprD results in a larger increase in the MIC of imipenem than meropenem (Livermore, 2001), and no difference in imipenem sensitivity was observed between WT and glycolipid-deficient mutants to support the difference in sensitivity to meropenem. In addition, MexEF-OprN is actually considered to be quiescent in lab strains, and thus may not be relevant in this

system in *P. aeruginosa* PAO1 (Sobel et al., 2005). Finally, proteomic analysis did not reveal differences in the expression of MexT (PA2492) or its subsequent protein targets, which would be expected given that MexS and MexT have been shown to interact in a complex regulatory system (Jin et al., 2011). Overall, the significant difference in sensitivity to meropenem is likely due to another mechanism that is influenced by the presence of glycolipids, and it is intriguing that it does not also hold true for imipenem. Indeed, the significant reduction in expression of dipeptide porin OpdP in Δ*plcP* may explain the inconsistencies in changes in sensitivity to meropenem and imipenem. OpdP is known to transport carbapenems in *P. aeruginosa*, with structural analysis revealing a more favourable interaction between meropenem and OpdP (Soundararajan et al., 2017). Thus, a lower expression of OpdP in Δ*plcP* compared to WT may have resulted in the relative decrease in sensitivity to meropenem alone.

EDTA is a chelator that disrupts outer membrane integrity by removing divalent cations, such as Mg^{2+} and Ca^{2+}, that normally bridge negative charges in the LPS layer, and thus are critical for maintaining outer membrane integrity (Vaara, 1992). It appears that *P. aeruginosa* is more sensitive to EDTA treatment after lipid remodelling. However, this was not glycolipid-dependent, suggesting additional membrane changes as a result of phosphate stress. As the lipid A component of the LPS layer represents a consumer of phosphate, there may be mechanisms in *P. aeruginosa* that alter the LPS layer in response to phosphate stress. This is a further reason to investigate LPS structure under phosphate stress conditions. For Δ*agt2*, EDTA treatment and swarming analysis revealed an interesting phenotype in that it does not appear to produce the siderophore pyoverdine in response to iron stress, and thus grew poorly when chelator EDTA was present. Mutants obtained from the University of Washington transposon mutant library are confirmed through Sanger sequencing and Tn-seq. However, it is worth whole genome sequencing Δ*agt2* in future to eliminate potential off-target effects. This observation is unlikely to be related to GADG glycolipid production, as lack of growth in the presence of EDTA occurred under both phosphate replete and phosphate deplete conditions. In

addition, the *agt2* gene is not chromosomally located near to pyoverdine synthesis genes, ruling out transposon insertion affecting expression of neighbouring genes.

Overall, the production of glycolipids as a phenotypic adaptation to phosphorus stress appears to result in fitness trade-offs in terms of AMR for *P. aeruginosa*. The presence of glycolipids in the membrane confers protection against the cationic activity of polymyxin B, yet slightly negatively impacts the ability of *P. aeruginosa* to resist treatment with meropenem. The precise mechanisms remain elusive.

Chapter 5 The role of lipid remodelling in host-pathogen interaction

5.1 Introduction

5.1.1 The role of phosphate stress in virulence

The PhoBR system has been shown to control expression of many virulence factors in *P. aeruginosa*, including those linked to quorum sensing and swarming, alongside other virulence regulatory genes (section 1.3.2). In terms of the effects of phosphate depletion on host-pathogen interaction, after intestinal surgery in mice, inorganic phosphate was shown to be depleted to levels that facilitated activation of virulence in *P. aeruginosa* (Long et al., 2008). Indeed, in sepsis patients severe depletion of phosphate can become a predictor of mortality (Shor et al., 2006). Further, *P. aeruginosa* strain PAO1 is normally attenuated for killing in a *C. elegans* infection model, but low phosphate conditions seemingly activated virulence resulting in significant death in *C. elegans* (Zaborin et al., 2009). Equally, in a *Danio rerio* (zebrafish) infection model, pre-growing *P. aeruginosa* under phosphate stress dramatically increased the virulence of the bacterium compared to phosphate sufficient conditions (Díaz-Pascual et al., 2017). Additionally, phosphate acquisition genes in cystic fibrosis isolate *P. aeruginosa* PASS1 were found to be upregulated in the zebrafish infection model (Kumar et al., 2018). Finally, after *P. aeruginosa* interaction with human primary airway epithelial cells, transcriptomic analysis revealed the upregulation of several phosphate-acquisition genes (Frisk et al., 2004), likely to extend to the expression of the cascade of Pi-influenced virulence genes and could be important in understanding the establishment of *P. aeruginosa* infections in CF patients.

Given that glycolipid synthesis genes *plcP*, *agt1* and *agt2* are also upregulated in several of the above models, and my proteomic data confirmed their upregulation in response to phosphate stress, this chapter aimed to elucidate any role for lipid remodelling in the success of *P. aeruginosa* establishing infection in the host.

5.1.2 *C. elegans* and *G. mellonella* as model organisms for host-pathogen interaction

Insects are now widely used as model organisms, including the use of the greater wax moth *Galleria mellonella* (*G. mellonella*), which has become popular due to cost effectiveness and the ability to obtain results within 48 hrs (Browne et al., 2013). The bacterial load used to inoculate *G. mellonella* larvae can be accurately quantified, and the larvae are incubated at 37°C, reflective of human body temperature (Browne et al., 2013). Hemocytes in *G. mellonella* form the cellular immune response and phagocytose pathogens, and are characterised as similar to human neutrophils in their pathogen recognition and killing properties (Altincicek et al., 2008; Lavine & Strand, 2002). The similarities between the innate immune systems of mammals and *G. mellonella* are well characterised (Browne et al., 2013). Importantly, for *P. aeruginosa* there is a positive correlation between pathogenicity in *G. mellonella* and in mammals, where mutants less virulent in *G. mellonella* also showed reduced virulence in a burn wound mouse model (Jander et al., 2000).

C. elegans is a free living nematode that initially became a model for studying developmental and behavioural biology, but has since become a common model for studying host-pathogen interaction. The nematodes are self-fertilising and lay eggs to produce progeny. After hatching, *C. elegans* proceed through four larval stages (L1, L2, L3 and L4) before becoming adult worms (Lee et al., 2016). Under nutrient or temperature stress, *C. elegans* can enter a Dauer stage until more favourable conditions return (Lee et al., 2016). Unlike *G. mellonella*, *C. elegans* does not have cellular based immunity, but instead possesses physical barriers to pathogen colonisation, alongside systemic immunity comprised of numerous antimicrobial molecules (Marsh & May, 2012). *C. elegans* is also temperature sensitive and infection assays are carried out between 15-25°C. Therefore, the model may not be as good for revealing mammalian virulence factors.

For *P. aeruginosa*, pathogenicity in *C. elegans* is dependent upon growth medium. For example, strain PA14 exhibits a “slow-killing” phenotype over several days on minimal

medium, yet hypervirulent “fast” killing can occur on rich medium (Mahajan-Miklos et al., 1999). PA14 has been shown to lead to *C. elegans* death through accumulation in the intestine (“slow”) or production of secreted phenazines as virulence factors (“fast”) (Mahajan-Miklos et al., 1999; Tan et al., 1999). *P. aeruginosa* strain PAO1 is less virulent in *C. elegans*, but has been shown to cause paralytic death through cyanide poisoning (Gallagher & Manoil, 2001). Importantly, as mentioned previously, phosphate stress was shown to trigger a lethal phenotype in *P. aeruginosa* PAO1, with a complex interplay between quorum sensing, iron and phosphate acquisition systems thought to be responsible (Zaborin et al., 2009). Given the characterised phosphate-restricted phenotype in *C. elegans*, this system was utilised as a platform for investigating the role of glycolipid production in the virulence seen under phosphate stress.

5.1.3 Bacteriophage therapy

Given the rise of MDR and extensively drug resistant pathogens found in clinical settings and the lack of development of novel antimicrobials, bacteriophage (phage) therapy has gained traction as an alternative strategy for tackling AMR. Phages can have a lysogenic life cycle, where injected genetic material integrates into the host cell genome, forming a prophage. Phages can also have a lytic life cycle, where host replication machinery is utilised to immediately reproduce within the host cell, causing lysis and viral particle release. Lytic phage cocktails are utilised in phage therapy, and have been tested against several critical pathogens that have the highest associated risk of mortality in the healthcare setting, which includes *P. aeruginosa* (Mulani et al., 2019). Phage therapy has proved successful in reducing or eradicating *P. aeruginosa* presence in murine models, *G. mellonella* models and in human patients with sepsis (Mulani et al., 2019). In addition, phage therapy as a combination treatment with antibiotics proved successful in creating a synergistic effect in treating biofilms, murine infection models and in human patients with an aortic graft infection and a bladder infection (Tagliaferri et al., 2019). Phage therapy in treating CF patients is a more complex challenge, given the necessity to nebulise phage for introduction into the lung and the challenge of penetrating thick CF sputum. Some studies reported

positive results in CF patients. However, these often lacked appropriate controls and had small sample sizes (Trend et al., 2017). Overall, phage therapeutic treatment is a promising alternative to tackle AMR and requires additional research to determine therapeutic efficacy and safety.

During bacterial adaptation to host environments often essential nutrients are scarce, and this can include phosphorus limitation. I have shown that membrane lipid alterations under Pi stress, specifically the surrogate introduction of glycolipids MGDG and GADG, can affect the interaction of AMPs with the membrane. Phage binding sites include an array of membrane structures, including membrane spanning proteins and the LPS layer (Chaturongakul & Ounjai, 2014), which may be altered after membrane lipid remodelling in *P. aeruginosa*. In this chapter I investigate whether production of glycolipids in response to Pi stress interferes with the interaction of bacteriophage.

5.2 Results

5.2.1 The *P. aeruginosa* exoproteome is influenced by lipid remodelling

As the bacterial membrane represents the barrier for secreting proteins, the *P. aeruginosa* exoproteome was analysed to investigate the role of membrane lipid remodelling in affecting protein secretion. To gain an understanding of the Pi-responsive exoproteome in *P. aeruginosa*, first the WT strain was cultured in high and low phosphate for 8 hours and 15 mL 0.22 µM pore size filtered supernatant was used to analyse the secreted proteins in *P. aeruginosa* cultures. 264 proteins were detected using nanoLC-ESI-MS/MS instrumentation on a 1.5 hour run per sample, with 103 of those found to be differentially regulated by phosphorus availability when significance was considered at a false detection rate (FDR) of <0.05. Of these, 50 proteins were more highly expressed when *P. aeruginosa* was under phosphate stress, and 53 were more highly expressed when phosphorus was sufficient (Figure 5.1). Protein functions, locus tags and the fold change difference between WT in high P (1 mM) and in low P (100 µM) are detailed in Appendix 2.

As expected, proteins associated with phosphate acquisition were more highly expressed when *P. aeruginosa* was under phosphate stress. This included phosphate binding protein PstS, glycerophosphoryl diester phosphodiesterases (e.g. GlpQ), secreted alkaline phosphatases, secreted phospholipases (PlcH, PlcN and PlcB) and extracellular DNA degradation enzymes EddA and EddB. Some phosphate transporter proteins were also upregulated, including pyrophosphate-specific transporter OprO and a phosphonate transporter binding protein (PA3383). Some virulence factors were also detected in the exoproteome and more highly upregulated in response to phosphate stress, including a protease (LasA), an elastase (LasB), the exotoxin A precursor ToxA and an immunomodulating metalloprotease (ImpA) (Tian et al., 2019). LasA and LasB expression is related to the upregulation of the *las*-dependent QS system.

Several outer membrane proteins were more highly expressed in WT *P. aeruginosa* when phosphate was sufficient, suggesting that changes due to phosphate stress are influencing their presence in the membrane. Outer membrane porins OprD, OprF, OprC and OprG and probable outer membrane proteins PA2760, PA4837 and PA1288, were all more highly expressed under phosphate sufficient conditions. As for the cellular proteome (section 3.2.1), some receptors for the acquisition of iron were more highly expressed under phosphate replete conditions, including a ferripyoverdine receptor (PA2398) and a probable outer membrane receptor for iron transport (PA4514). Interestingly, LPS assembly proteins LptD and LptE (Botos et al., 2016) were also more highly upregulated under phosphate replete conditions, suggesting that the LPS layer may indeed be influenced as a result of membrane changes under phosphate stress.

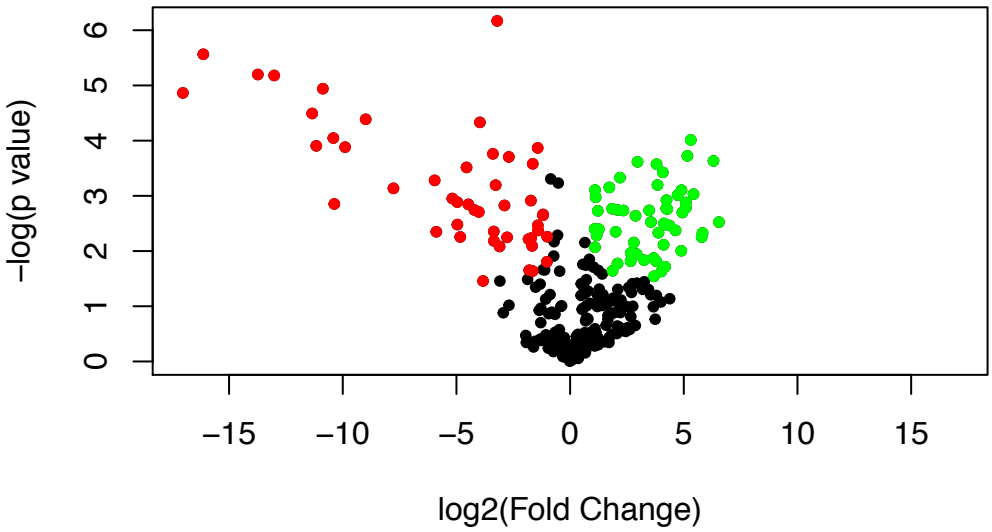

Figure 5.1. Volcano plot depicting differentially expressed secreted proteins between WT *P. aeruginosa* grown under phosphate stress and phosphate sufficient conditions. Significantly upregulated proteins when under phosphate stress are shown in red, and those that are significantly upregulated when phosphate is sufficient are in green (see Appendix 2 for full annotated list).

To investigate the role of membrane lipid remodelling in influencing the *P. aeruginosa* exoproteome, WT and glycolipid-deficient Δ*plcP* were grown under phosphate stress, and 15 mL of 0.22 µM pore size filtered supernatant was analysed using nanoLC-ESI-MS/MS instrumentation on a 1.5 hour run per sample. Overall, 7 proteins were more highly expressed in glycolipid-deficient Δ*plcP* and 32 were more highly expressed in WT *P. aeruginosa* compared to Δ*plcP* (Figure 5.2). Protein functions and locus tags are detailed in Table 5.1, and were considered significant when FDR < 0.05.

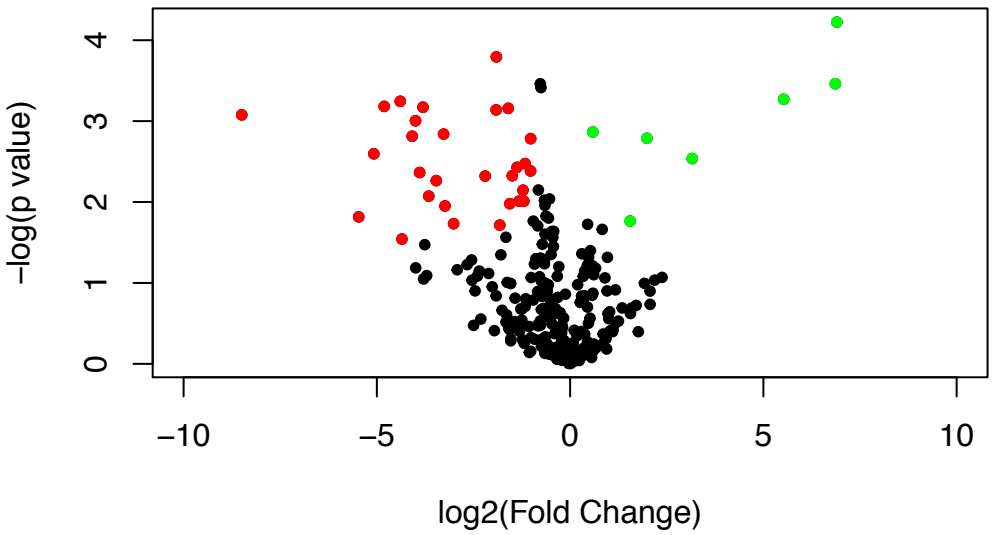

Figure 5.2. Volcano plot depicting differentially expressed secreted proteins between WT *P. aeruginosa* and glycolipid-deficient mutant Δ*plcP*, both cultured under phosphate stress. Significantly upregulated proteins in WT *P. aeruginosa* are shown in red, and those that are significantly upregulated in Δ*plcP* are in green.

Several proteins that were more highly expressed when *P. aeruginosa* is unable to produce glycolipids in response to phosphate stress (Δ*plcP*) had functions linked to host interaction. This included high upregulation of pilin proteins, where pili are used for adhesion to host surfaces (Bucior et al., 2012), higher expression of an outer membrane lipoprotein, OprI (PA2853), also linked to adherence to epithelial cells (Crouzet et al., 2017) and a probable QS signalling factor (PA3329) that has been linked to virulence in *P. aeruginosa* (Hwang et al., 2016). Interestingly, a contact dependent toxin (PA2462) was downregulated in Δ*plcP*, which also exhibited downregulation in the cellular proteome fraction (section 3.2.1), and is linked to cell-cell communication in biofilm formation (Melvin et al., 2017). Proteins that were highly upregulated in WT under phosphate stress compared to Δ*plcP* were often linked to iron acquisition. Ferripyoverdine receptor and PvdO, a protein involved in the process of siderophore maturation, were upregulated. Upregulated proteins PA2452 and PA2451 are thought to be similar to ferric enterobactin esterases (Purschke et al., 2012), involved in liberating iron from siderophores. TonB-dependent receptors are also upregulated, where the TonB family of proteins have critical roles in iron transport in *P. aeruginosa* (Shirley & Lamont, 2009). Overall, the Δ*plcP* mutant appears to downregulate a selection of iron-acquisition related proteins, which may be linked to the complex

interplay between QS systems and iron siderophores, as some QS related proteins are differentially expressed in Δ*plcP*.

Table 5.1. Glycolipid responsive exoproteome in WT *P. aeruginosa* PAO1. Locus tags from the *Pseudomonas* genome reference database are listed alongside known or predicted protein functions. Log2 transformation of fold change values show the differences between WT *P. aeruginosa* and glycolipid deficient Δ*plcP*, and are the mean of 3 replicates. Negative values indicate lower expression in Δ*plcP*.

Protein function	Locus tag	log2(Fold Change)
Uncharacterized protein	PA2452	-8.495341619
Probable TonB-dependent receptor	PA0192	-5.468896866
Uncharacterized protein	PA1053	-5.078798294
Uncharacterized protein	PA2451	-4.810215632
Uncharacterized protein	PA2462	-4.394367218
Probable bacteriophage protein	PA0620	-4.351142248
Ferripyoverdine receptor	PA2398	-4.085770289
Probable binding protein component of ABC iron transporter	PA5217	-3.999073664
Uncharacterized protein	PA1383	-3.89359347
Uncharacterized protein	PA3785	-3.808024089
Uncharacterized protein	PA1784	-3.657400131
Probable outer membrane protein	PA4837	-3.463530858
Probable hemagglutinin	PA0041	-3.273513794
Probable purine-binding chemotaxis protein	PA1464	-3.23715655
Probable TonB-dependent receptor	PA1922	-3.013306936
Uncharacterized protein	PA0981	-2.196970622
30S ribosomal protein S4	PA4239	-1.913990657
PvdO	PA2395	-1.907444
50S ribosomal protein L1	PA4273	-1.820249557
Uncharacterized protein	PA0689	-1.600654602
Ornithine carbamoyltransferase, catabolic (OTCase)	PA5172	-1.559135437
Insulin-cleaving metalloproteinase outer membrane protein	PA4370	-1.496131897
Dihydrolipoyl dehydrogenase	PA1587	-1.372701009
Isocitrate dehydrogenase	PA2623	-1.320631663
Succinate dehydrogenase flavoprotein subunit	PA1583	-1.218789419
Glutamine synthetase	PA5119	-1.197861354
Uncharacterized protein	PA4739	-1.164351781
60 kDa chaperonin (GroEL protein)	PA4385	-1.023035685
Aminopeptidase (PaAP)	PA2939	-1.020651499
Flagellar hook-associated protein 1 FlgK	PA1086	-0.820863724
Probable binding protein component of ABC transporter	PA0186	-0.771735509
ATP synthase subunit alpha	PA5556	-0.752683004

Uncharacterized protein	PA3250	0.587493261
Major outer membrane lipoprotein	PA2853	1.552043915
Glycerophosphoryl diester phosphodiesterase, periplasmic	PA0347	1.987220764
50S ribosomal protein L3	PA4263	3.159003576
Uncharacterized protein	PA3329	5.524848938
Fimbrial protein (Pilin)	PA4525	6.86285464
Type IV pilus biogenesis factor PilY1 (Pilus-associated adhesin PilY1)	PA4554	6.900447845

5.2.2 The role of *P. aeruginosa* glycolipids in interaction with *C. elegans*

In order to investigate the lethality of *P. aeruginosa* PAO1 WT in a *C. elegans* infection model when under phosphate stress, modified nematode growth medium (NGM) plates were used, as described previously (Zaborin et al., 2009; section 2.2.1). Briefly, potassium phosphate buffer used in NGM was removed ("NGM –P"), and the medium was adjusted to pH 6 and supplemented with $FeSO_4$ (0.5 µM). To ensure *P. aeruginosa* was starved of phosphate on modified NGM –P plates, the alkaline phosphatase substrate X-phosphate (also known as BCIP) was utilised as a chromogenic indicator of Pi stress. Streak plating indicated *P. aeruginosa* was Pi stressed only on NGM –P plates, as it exhibited a blue colour only under these conditions (Figure 5.3). As expected, due to siderophore production under Pi stress (section 3.2.4), *P. aeruginosa* under phosphate stress is coloured itself without the presence of X-phosphate. However, this did not interfere with the chromogenic indicator of Pi stress.

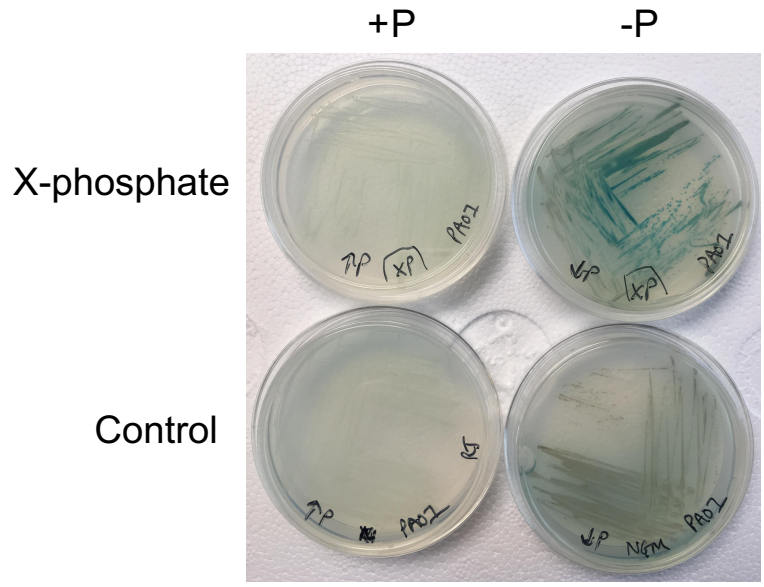

Figure 5.3. Modified nematode growth medium (NGM –P) induces phosphate stress in *P. aeruginosa* PAO1. X-phosphate is a substrate for alkaline phosphatases secreted by bacteria under phosphate stress, as indicated by blue colouring (top right panel).

Both standard NGM ("NGM +P") and NGM –P were able to facilitate the growth of *E. coli* OP50 and *P. aeruginosa* PAO1 lawns for feeding *C. elegans*. In order to establish if NGM –P conditions alone had any detrimental effect on the growth of *C. elegans*, long-term survival on *E. coli* OP50 was monitored. A total of 50 age synchronised L4 stage nematodes (10 worms per plate in 5 replicates; Figure 5.4B) were seeded onto NGM +P or NGM –P *E. coli* OP50 plates, and transferred to fresh plates every 48 hours to avoid interference from progeny. Nematodes were scored as alive, dead or censored. Nematodes were classed as censored when either missing or dried on the side of the petri dish. Over a two-week period, no difference was observed in the survival of *C. elegans* feeding on *E. coli* OP50 with a high concentration of phosphate or with no added phosphate (p = 0.898, log-rank test; Figure 5.2C). The median survival time was 9 days for NGM +P (95% CI: 8-12 days) and 10 days for NGM –P (95% CI: 9-12 days).

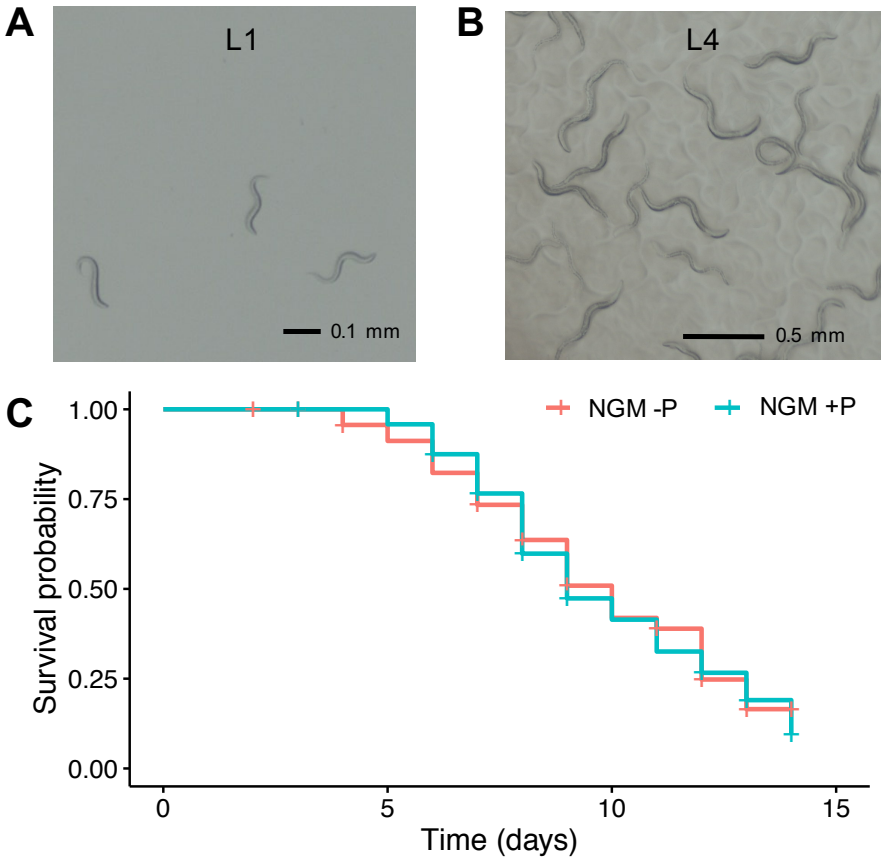

Figure 5.4. A) *C. elegans* arrested in L1 stage after bleach synchronisation. B) Age synchronised *C. elegans* grown to L4 stage for use in survival experiments. C) Kaplan-Meier survival curve of *C. elegans* seeded on standard NGM (NGM +P, blue) and NGM without phosphate based components (NGM –P, pink) with *E. coli* OP50 as the food source (n = 50 per condition, + denotes censored nematode).

It has been shown previously that *P. aeruginosa* strain PAO1 is attenuated for virulence in *C. elegans* when grown on standard NGM, unlike the very similar strain PA14 that can exhibit fast rates of killing (Lee et al., 2006). Intriguingly, NGM –P triggered a lethal phenotype in PAO1, with up to 70% mortality in *C. elegans* within 50 hrs, where no death was seen in NGM +P (Zaborin et al., 2009). To determine if the production of glycolipids under Pi stress in *P. aeruginosa* plays a role in this phenomenon, I first attempted to replicate the significant increase in virulence under Pi stress using WT *P. aeruginosa* PAO1. L4 nematodes were transferred from *E. coli* OP50 plates onto empty NGM +P plates, and starved for 24 hrs. 50 *C. elegans* (10 nematodes per plate in 5 replicates) were then transferred to pre-grown *P. aeruginosa* NGM +P or NGM –P plates, and placed at 20°C for 72 hrs. It was expected that significant death on NGM –P would occur within this time-frame. However, no deaths

were seen in either condition (p = 0.6, log-rank test; Figure 5.5A). Several modification attempts were made to no avail, including longer starvation periods, different volumes of bacterial inocula, covering the whole NGM plate with *P. aeruginosa* to mitigate any avoidance and altering incubation temperature. None of these factors were found to trigger a virulent phenotype in *P. aeruginosa* PAO1. Intriguingly, when extending bacterial growth surface area (Figure 5.5B), 40% of nematodes (20 out of 50) were censored under low phosphate conditions, suggesting an avoidance resulting in nematode disappearance.

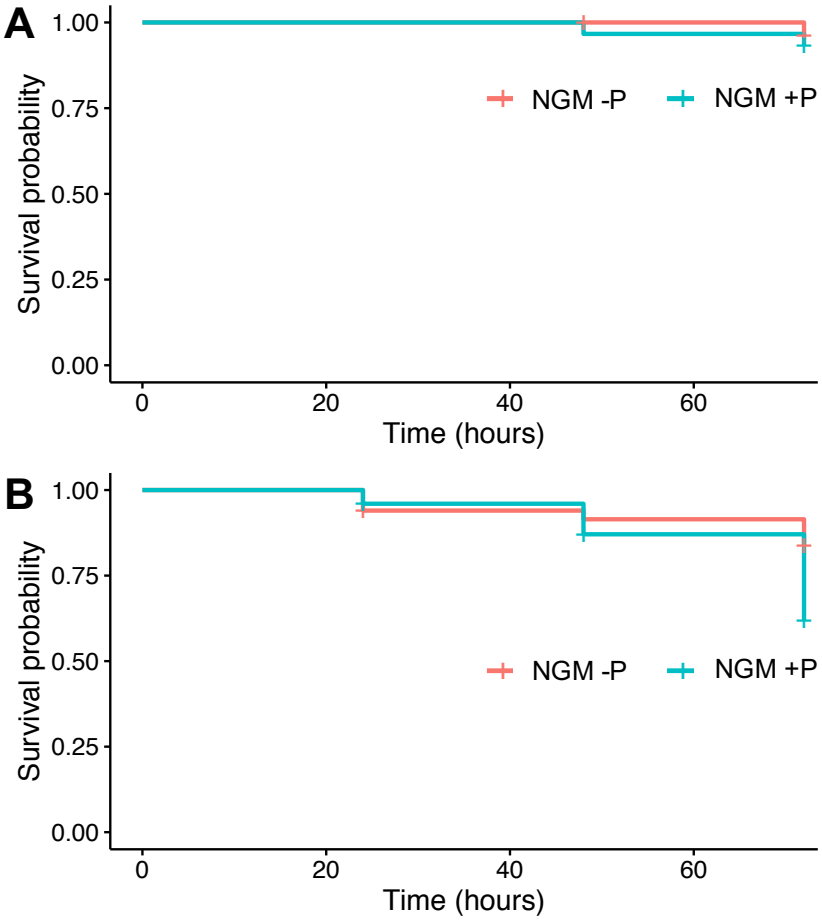

Figure 5.5. Kaplan-Meier survival curves of *C. elegans* feeding on *P. aeruginosa* PAO1 WT under phosphate rich (NGM +P, blue) or phosphate deplete (NGM –P, pink) conditions. A) Data generated using method described previously (Zaborin et al., 2009), n = 50 nematodes per condition. B) Data from extending the bacterial growth area to mitigate *C. elegans* avoidance of pathogenic bacteria (n = 50 nematodes per condition).

As the *C. elegans* had been passaged for a long time, and bleach synchronised numerous times, I tried the method again with a fresh batch of *C. elegans* N2 strain in attempt to mitigate any accrued mutations that may be contributing to their survival. In addition, *P. aeruginosa* NGM plates were aged for several days before use and *C. elegans* survival was monitored over a longer period of time, with nematodes transferred to fresh plates every 24 hrs. Under these conditions, some death did occur. However, the survival rate was independent of phosphate concentration (p = 0.41, log-rank test; Figure 5.6A). However, in this replicate I identified some redness in dead nematodes at 96 hrs feeding on NGM –P *P. aeruginosa*, consistent with the "red death" phenotype in previous findings (Figure 5.6B; Zaborin et al., 2009). In conclusion, I was unable to replicate the significant lethal phenotype linked to phosphate stress described previously in WT *P. aeruginosa* PAO1, and therefore was unable to investigate the role of lipid remodelling in this survival model.

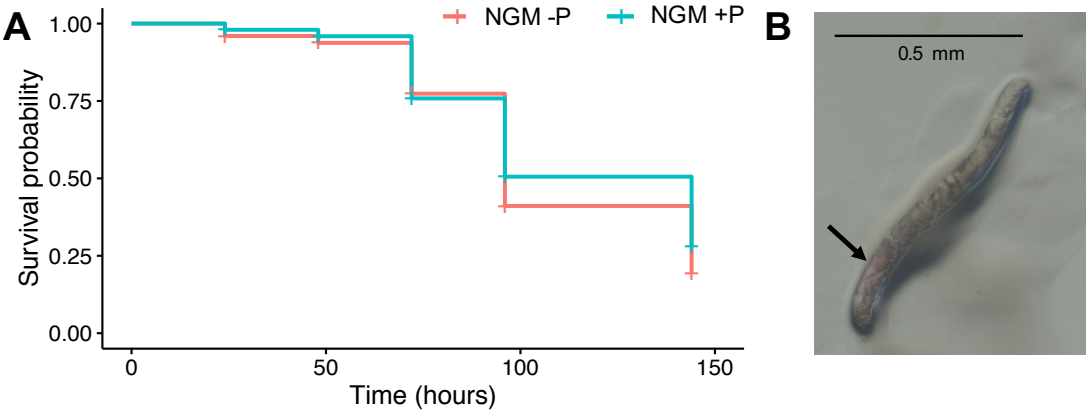

Figure 5.6. A) Kaplan-Meier survival curve of freshly sourced *C. elegans* feeding on *P. aeruginosa* PAO1 WT, after bacterial plates were aged for several days before use. *C. elegans* were transferred to fresh plates every 24 hrs (n = 50), + denotes censored nematode. B) Representative image of a dead nematode on NGM –P at 96 hrs, arrow indicates area of redness.

In a different approach to investigate the role of lipid remodelling in the *C. elegans* host-pathogen interaction model, a feeding preference assay was used to assess palatability of each *P. aeruginosa* mutant strain. The hypothesis was that *C. elegans* will preferentially avoid more pathogenic bacteria, as has been demonstrated previously (Lewenza et al., 2014). 5 µL aliquots of WT *P. aeruginosa* and lipid remodelling mutants were spotted equidistant apart on NGM –P plates, with 20 L4

stage *C. elegans* then placed in the middle (4 replicates, n = 80). The number of nematodes present in a particular spot at each time point was scored as an indicator of preference. WT was compared to Δ*plcP*, in which the production of glycolipids is essentially abolished. To further separate the roles of MGDG and GADG glycolipids, WT was compared to both Δ*agt1* and Δ*agt2*.

In all WT and lipid remodelling mutant comparisons, the general trend was a shift from *C. elegans* feeding on WT after 6 hrs to preferring mutant strains after 48 hrs (Figure 5.7). However, this difference was not always statistically significant. After 48 hrs, *C. elegans* preferred Δ*agt1* over WT *P. aeruginosa* ($p < 0.05$, *t*-test), followed by more nematodes feeding on Δ*agt2*, however Δ*agt2* was not significantly preferred over WT *P. aeruginosa* ($p = 0.127$, *t*-test). The result for Δ*agt1*, in which MGDG is not produced, was not corroborated by *C. elegans* choosing between WT and MGDG-negative Δ*plcP* (Figure 5.7C), in which there is was no significant difference at 48 hrs ($p = 0.58$, *t*-test), with Δ*plcP* exhibiting high variation (ranging between 5-15 nematodes).

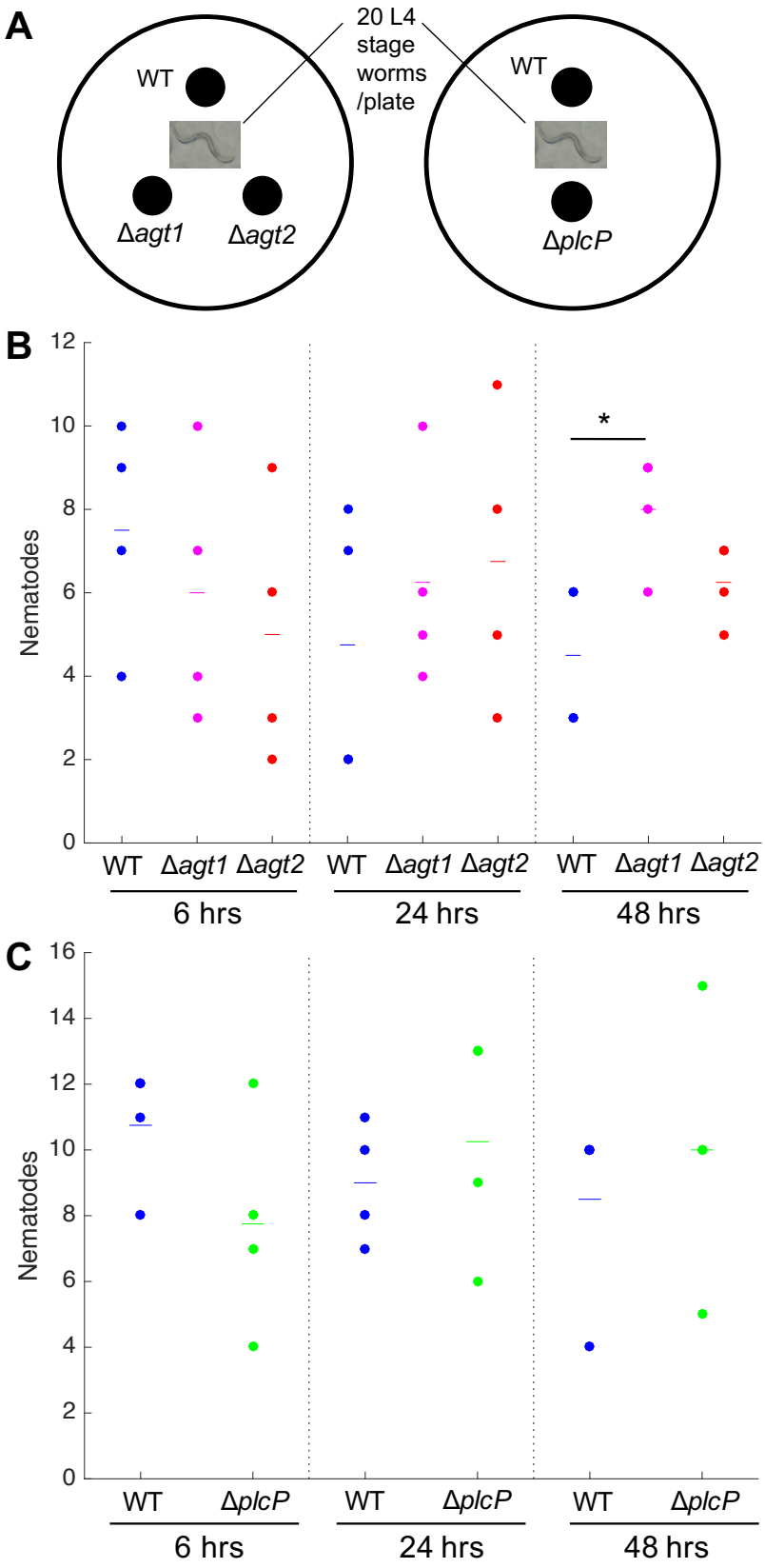

Figure 5.7. A) Feeding preference assay layout. B-C) Preference of *C. elegans* between *P. aeruginosa* PAO1 WT (blue) and glycolipid remodelling mutants Δ*agt1* (pink), Δ*agt2* (red) and Δ*plcP* (green) seeded on NGM –P plates. The mean of 4 independent experiments is shown (n = 20 per replicate, total = 80 nematodes, * $p < 0.05$).

5.2.3 The role of glycolipids in *P. aeruginosa* virulence in *Galleria mellonella*

To further investigate whether the production of glycolipids under Pi stress in *P. aeruginosa* affects the virulence capabilities of this bacterium, *G. mellonella* was used as a second model organism. In *G. mellonella*, a mutant *P. aeruginosa* strain with defective cell envelope stability was shown to have significantly impaired pathogenicity in this model (Lo Sciuto et al., 2018), suggesting lipid membrane alterations may result in a similar phenotype. In addition, preliminary data in *Burkholderia cenocepacia* (*B. cenocepacia*) showed a dramatic difference in survival of *G. mellonella* larvae when infected with WT compared to glycolipid-deficient Δ*plcP*, in that Δ*plcP* virulence was significantly impaired (H. Shropshire, personal communication). The method used for assessing *B. cenocepacia* virulence in *G. mellonella* does not introduce Pi stress before inoculation, suggesting phosphate limitation is a natural factor in this model. In this way, *P. aeruginosa* WT and Δ*plcP* were grown in LB medium until reaching mid-logarithmic phase (0.6 OD_{600}) before diluting in 10 mM $MgSO_4$ and injecting 10 µL of diluted culture containing an average of 2-3 bacterial cells per larvae.

Initially, a higher number of *P. aeruginosa* cells was used to infect larvae. However, this resulted in complete death in all larvae after only 16 hrs (Figure 5.8). Therefore, the method was adjusted to use very few *P. aeruginosa* cells, in line with previous reports of ~3 *P. aeruginosa* cells being the lethal dose 90% in *G. mellonella* (Lo Sciuto et al., 2014). This initial experiment, however, ruled out the possibility of glycolipid deficiency impacting pathogenicity to the extent seen in other mutant strains that required large fold-increases in bacterial cell number to reach LD_{90} (Fernandez-Pinar et al., 2015; Lo Sciuto et al., 2018). Further dilution allowed investigation of finer pathogenicity margins in comparing *G. mellonella* survival over 48 hrs with comparable CFU mL^{-1} for WT and Δ*plcP* (Table 5.2).

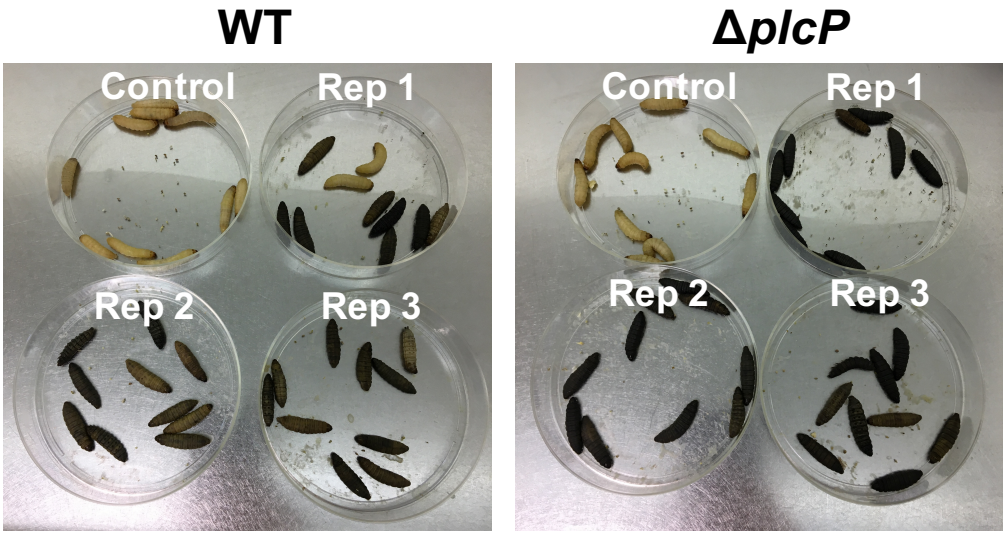

Figure 5.8. Significant death in *G. mellonella* larvae after 16 hr incubation at 37°C after injection with ~200 *P. aeruginosa* cells per larvae, using WT (left) or glycolipid-deficient strain Δ*plcP* (right). Melanisation was observed for both strains.

Table 5.2. Colony forming units (CFU) of each biological replicate for WT and Δ*plcP* strains of *P. aeruginosa* used for injection into *G. mellonella* larvae. Both raw data and average (± standard deviation) are reported (p = 0.085, t-test).

	WT (CFU mL^{-1})	**Δ*plcP* (CFU mL^{-1})**
Rep 1	235	296
Rep 2	251	281
Rep 3	132	300

	Average (±SD) infective dose
WT	2.06 (± 0.53)
Δ*plcP*	2.92 (± 0.09)

Monitoring *G. mellonella* survival at 24 and 48 hrs post-inoculation with WT or Δ*plcP* *P. aeruginosa* revealed no differences in pathogenicity (Figure 5.9), as survival rates were similar (p = 0.78 at 24 hrs, p = 0.35 at 48 hrs, t-tests). A health index score was calculated based on the degree of melanisation in dead larvae (Champion et al., 2018), in which black larvae scored 0, brown larvae scored 1, beige larvae with black spots scored 2 and beige larvae scored 3. At 24 hrs after WT inoculation, more larvae were noted to be brown, beige with spots or still beige, producing a health index score of 4.7. For Δ*plcP* at 24 hrs, the majority of larvae were already black, however the health score did not differ significantly from WT (p = 0.101, t-test). At 48 hrs, most dead larvae were black and decaying in both *P. aeruginosa* strains.

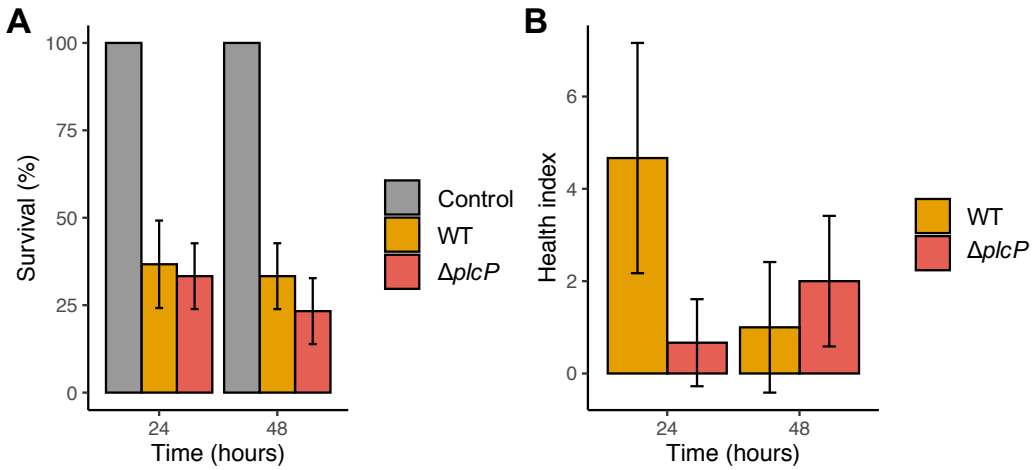

Figure 5.9. A) Percentage survival of *Galleria mellonella* larvae after inoculation with ~2 *P. aeruginosa* cells; WT (orange) and glycolipid-deficient Δ*plcP* (red) strains were compared. Error bars denote standard deviation (n = 3 replicates of 10 larvae). B) Health index score in dead larvae based on the degree of melanisation (Champion et al., 2018). Error bars denote standard deviation (n = 3 replicates of 10 larvae).

5.2.4 The effects of lipid remodelling on bacteriophage interaction

Given the importance of phosphorus limitation in enhancing the virulence and AMR of *P. aeruginosa* in clinical models, these changes may also extend to affecting the success of phage therapy. Receptor binding proteins used by phage for adsorption to bacterial cells are known to be highly diverse, including membrane surface proteins, polysaccharides and the O-antigen of the LPS layer, all of which are cell surface components (Chaturongakul & Ounjai, 2014). Membrane lipid remodelling potentially alters the abundance of membrane proteins and the presence of glycolipids in the outer membrane may perturb availability of the LPS layer, which is very commonly used as a receptor by *Pseudomonas* phage (Silva et al., 2016). To investigate the role of glycolipids in phage adsorption, firstly a novel lytic phage was isolated from sewage water, purified using several rounds of propagation and overlay agar methods and imaged using transmission electron microscopy (TEM).

The morphology and size of RJGB18 phage were assessed using TEM to identify the family affiliation of the novel phage (Figure 5.10). RJGB18 is approximately 200 nm in length and an icosahedral head of 72 nm diameter can be seen. The contractile tail has a length of 119 nm and a diameter of 16.5 nm, although tail fibres were not easily

visualised using TEM. Given the presence of a contractile tail and the overall size of the phage, RJGB18 belongs to the *Myoviridae* family of phage. This is a common phage type identified for *Pseudomonas* species, with 499 tailed phage being identified previously, of which 139 belong to the *Myoviridae* family (Ackermann, 2007).

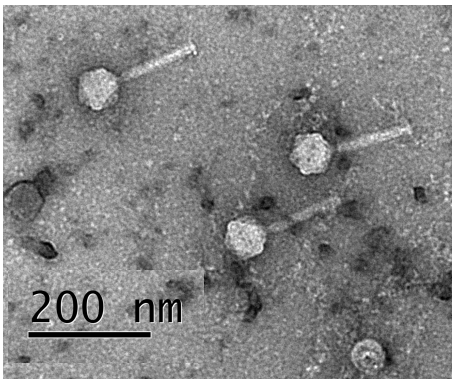

Figure 5.10. Image of RJGB18, a novel lytic *P. aeruginosa* phage, generated using negative stain transmission electron microscopy. Scale bar = 200 nm.

RJGB18 phage DNA was extracted using phenol-chloroform extraction and a sample was adjusted to 24 ng μL^{-1} (final volume 40 µL) before sending to MicrobesNG (Birmingham) for Illumina sequencing and genome assembly. The total length of the RJGB18 genome was 66,564 bp with 55.56% GC content. Using nucleotide BLAST, the whole genome sequence of RJGB18 was compared to other known *Pseudomonas* phages, with 63 sequenced phages producing significant alignments (e value: 0.0) ranging in nucleotide identity from 89.01% to 97.79%. These similar sequenced phages were aligned using MUSCLE software and used to construct an evolutionary relationship tree in MEGA7 (Figure 5.11).

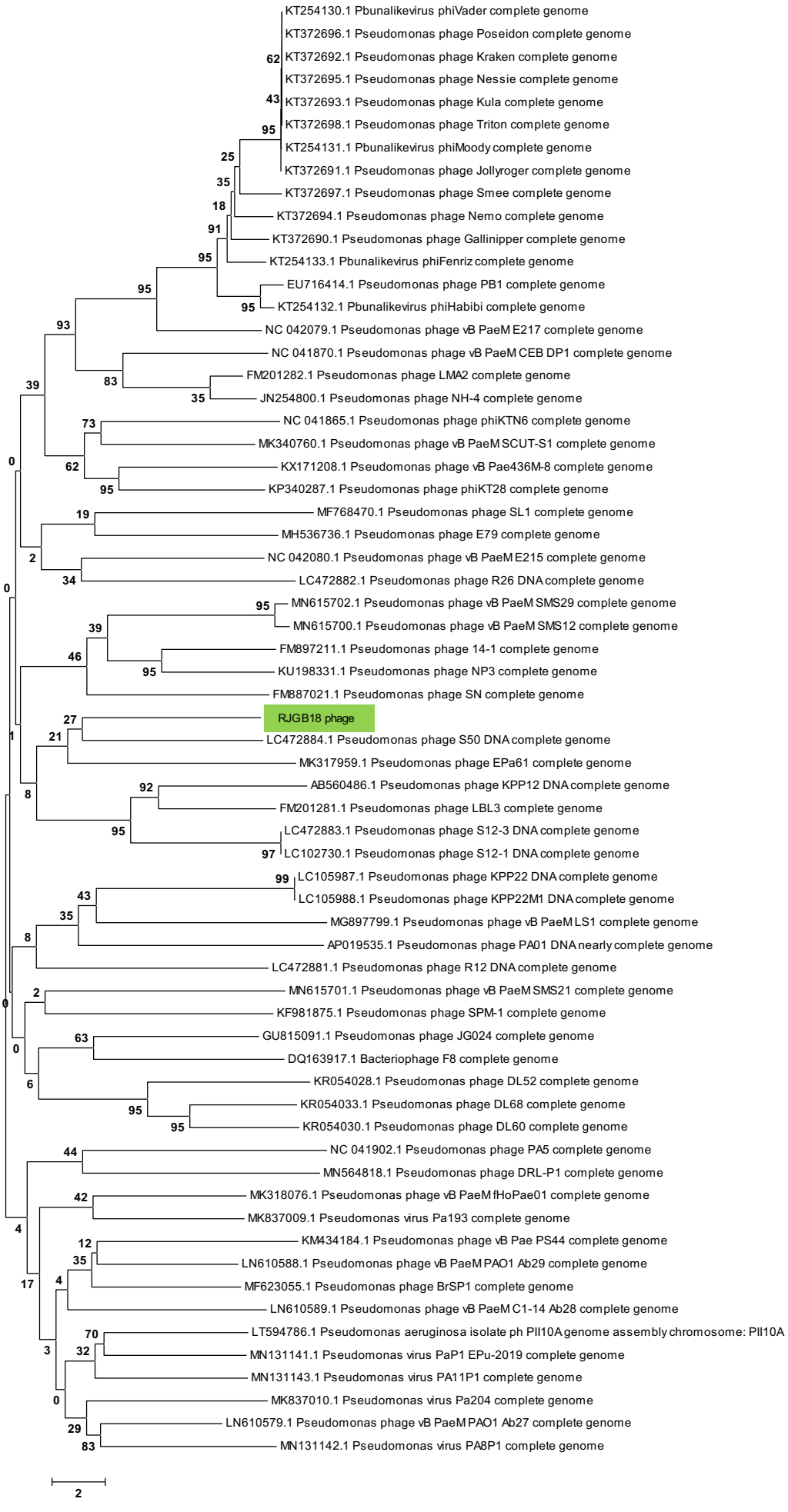
KT254130.1 Pbunalikevirus phiVader complete genome
KT372696.1 Pseudomonas phage Poseidon complete genome
KT372692.1 Pseudomonas phage Kraken complete genome
KT372695.1 Pseudomonas phage Nessie complete genome
KT372693.1 Pseudomonas phage Kula complete genome
KT372698.1 Pseudomonas phage Triton complete genome
KT254131.1 Pbunalikevirus phiMoody complete genome
KT372691.1 Pseudomonas phage Jollyroger complete genome
KT372697.1 Pseudomonas phage Smee complete genome
KT372694.1 Pseudomonas phage Nemo complete genome
KT372690.1 Pseudomonas phage Gallinipper complete genome
KT254133.1 Pbunalikevirus phiFenriz complete genome
EU716414.1 Pseudomonas phage PB1 complete genome
KT254132.1 Pbunalikevirus phiHabibi complete genome
NC 042079.1 Pseudomonas phage vB PaeM E217 complete genome
NC 041870.1 Pseudomonas phage vB PaeM CEB DP1 complete genome
FM201282.1 Pseudomonas phage LMA2 complete genome
JN254800.1 Pseudomonas phage NH-4 complete genome
NC 041865.1 Pseudomonas phage phiKTN6 complete genome
MK340760.1 Pseudomonas phage vB PaeM SCUT-S1 complete genome
KX171208.1 Pseudomonas phage vB Pae436M-8 complete genome
KP340287.1 Pseudomonas phage phiKT28 complete genome
MF768470.1 Pseudomonas phage SL1 complete genome
MH536736.1 Pseudomonas phage E79 complete genome
NC 042080.1 Pseudomonas phage vB PaeM E215 complete genome
LC472882.1 Pseudomonas phage R26 DNA complete genome
MN615702.1 Pseudomonas phage vB PaeM SMS29 complete genome
MN615700.1 Pseudomonas phage vB PaeM SMS12 complete genome
FM897211.1 Pseudomonas phage 14-1 complete genome
KU198331.1 Pseudomonas phage NP3 complete genome
FM887021.1 Pseudomonas phage SN complete genome
RJGB18 phage
LC472884.1 Pseudomonas phage S50 DNA complete genome
MK317959.1 Pseudomonas phage EPa61 complete genome
AB560486.1 Pseudomonas phage KPP12 DNA complete genome
FM201281.1 Pseudomonas phage LBL3 complete genome
LC472883.1 Pseudomonas phage S12-3 DNA complete genome
LC102730.1 Pseudomonas phage S12-1 DNA complete genome
LC105987.1 Pseudomonas phage KPP22 DNA complete genome
LC105988.1 Pseudomonas phage KPP22M1 DNA complete genome
MG897799.1 Pseudomonas phage vB PaeM LS1 complete genome
AP019535.1 Pseudomonas phage PA01 DNA nearly complete genome
LC472881.1 Pseudomonas phage R12 DNA complete genome
MN615701.1 Pseudomonas phage vB PaeM SMS21 complete genome
KF981875.1 Pseudomonas phage SPM-1 complete genome
GU815091.1 Pseudomonas phage JG024 complete genome
DQ163917.1 Bacteriophage F8 complete genome
KR054028.1 Pseudomonas phage DL52 complete genome
KR054033.1 Pseudomonas phage DL68 complete genome
KR054030.1 Pseudomonas phage DL60 complete genome
NC 041902.1 Pseudomonas phage PA5 complete genome
MN564818.1 Pseudomonas phage DRL-P1 complete genome
MK318076.1 Pseudomonas phage vB PaeM fHoPae01 complete genome
MK837009.1 Pseudomonas virus Pa193 complete genome
KM434184.1 Pseudomonas phage vB Pae PS44 complete genome
LN610588.1 Pseudomonas phage vB PaeM PAO1 Ab29 complete genome
MF623055.1 Pseudomonas phage BrSP1 complete genome
LN610589.1 Pseudomonas phage vB PaeM C1-14 Ab28 complete genome
LT594786.1 Pseudomonas aeruginosa isolate ph PII10A genome assembly chromosome: PII10A
MN131141.1 Pseudomonas virus PaP1 EPu-2019 complete genome
MN131143.1 Pseudomonas virus PA11P1 complete genome
MK837010.1 Pseudomonas virus Pa204 complete genome
LN610579.1 Pseudomonas phage vB PaeM PAO1 Ab27 complete genome
MN131142.1 Pseudomonas virus PA8P1 complete genome
2

Figure 5.11. Evolutionary relationships of novel *Pseudomonas* phage RJGB18 (green). The evolutionary history was inferred using the Neighbor-Joining method in the MEGA7 software (Kumar et al., 2016). The optimal tree with the sum of branch length = 364.5755 is shown. The percentage of replicate trees in which the associated taxa clustered together in the bootstrap test (100 replicates) are shown next to the branches (Felsenstein, 1985). The tree is drawn to scale, with branch lengths in the same units as those of the evolutionary distances used to infer the phylogenetic tree.

A total of 91 open reading frames were identified using PHAST and GeneMark.hmm (Besemer & Borodovsky, 1999; Zhou et al., 2011) (Figure 5.12). Of these, 40 had putative functions identified by protein BLAST with high degrees of protein sequence identity to other *Pseudomonas* phage proteins (Table 5.3), and the remaining 51 were hypothetical proteins with unknown functions. Replication enzymes that were identified included a putative DNA primase, terminase, a putative DNA ligase and a putative DNA helicase. Several putative structural proteins were identified including tail fibre proteins, baseplate proteins and a tail assembly protein. A putative endolysin was also identified, confirming RJGB18 to be a lytic phage. The presence of tRNA encoding genes was investigated using tRNAscan-SE v.2.0 (Lowe & Chan, 2016), with no tRNA encoding genes being identified by this software in RJGB18 phage.

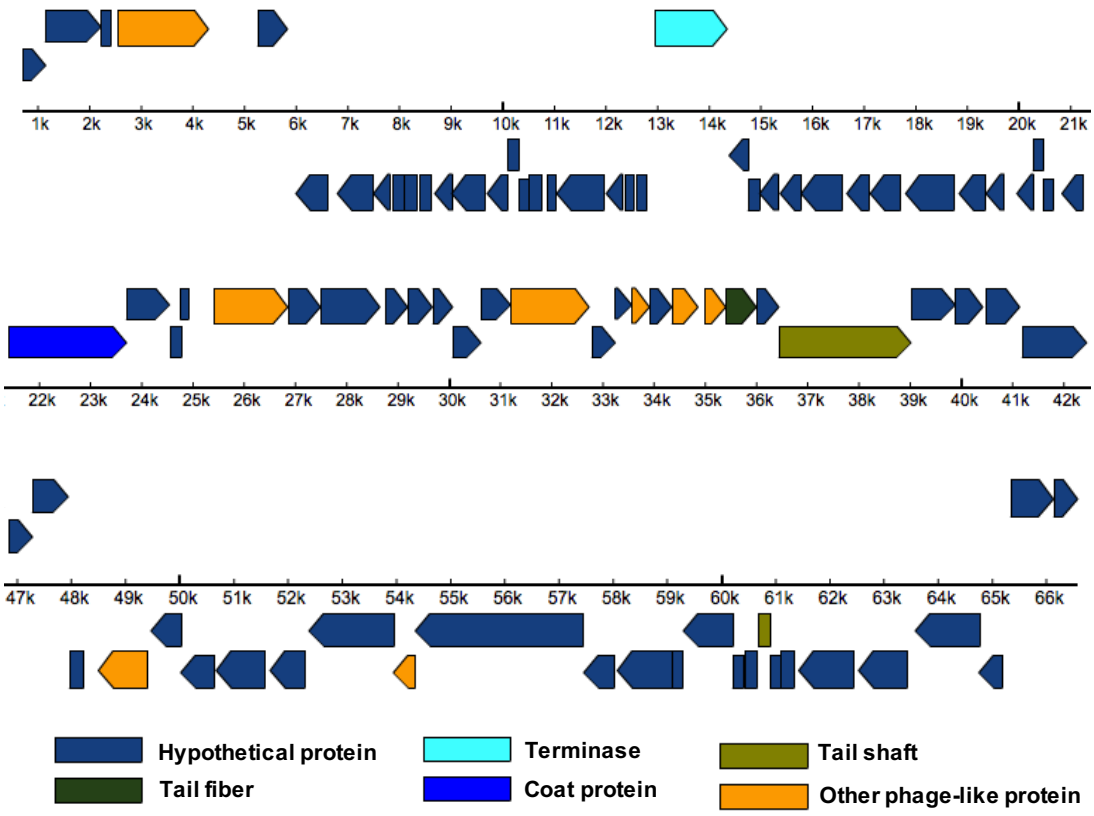

Figure 5.12. Schematic representation of RJGB18 *Pseudomonas* phage genome, with predicted gene functions indicated with different colours. Direction of arrows indicates direction of transcription.

Table 5.3. List of RJGB18 proteins that exhibit high protein identity to proteins with putative functions from other known *Pseudomonas* phage. Putative functions were identified using protein BLAST.

ORF	Putative function	*Pseudomonas* phage hit	% identity
3	DNA primase	PA8P1	99.44
5	DNA primase	vB_PaeM_fHoPae01	99.48
8	Minor head protein	vB_PaeM_SMS12	85.09
20	Tail length tape measure protein	E79	99.34
24	Terminase	JG024	99.78
33	Q-like anti-termination protein	vB_PaeM_SMS12	99.35
40	Minor head protein	PA8P1	99.87
41	Minor head protein	SN	98.92
44	Structural protein	KPP12	99.79
45	Structural protein	SN	100
46	Major structural protein	LMA2	99.74
48	Structural protein	LBL3	100

49	Structural protein	LBL3	99.24
52	Structural protein	vB_PaeM_fHoPae01	99.8
53	Structural protein	phiKT28	99.33
54	Structural protein	JG024	99.07
55	Structural protein	SL1	99.14
56	Structural protein	KPP12	98.6
57	Structural protein	KPP12	100
58	Structural protein	LMA2	100
59	Structural protein	KPP12	100
61	Lytic tail protein	LMA2	99.77
62	Structural protein	KPP12	100
64	Baseplate protein	KPP12	100
65	Baseplate protein	SN	99.76
66	Structural protein	PaP1_Epu-2019	99.6
67	Tail fiber protein	vB_PaeM_SCUT-S1	98.65
68	Tail fiber component	phiKTN6	100
69	Endolysin	LMA2	100
71	DNA ligase	LMA2	100
72	DNA-binding protein	vB_PaeM_LS1	99.46
76	DNA helicase	NH-4	100
77	DNA helicase	NH-4 and SN	100
78	DNA polymerase III alpha subunit	DL68	99.52
79	DNA polymerase III epsilon subunit	LMA2	98.37
80	Polynucleotide kinase	KPP12	99.41
82	Thymidylate synthase	NP3	99.02
85	Tail assembly protein	phiKTN6	97.22
89	Structural protein	JG024	98.98
90	ATP-dependent exonuclease	PA11P1	100

Next, *P. aeruginosa* lipid remodelling mutants were used to investigate the ability of RJGB18 to bind to different membrane lipid compositions, all conducted under phosphate stress. The number of free phage was quantified as a percentage of the phage titre added to each bacterial culture, thereby used to calculate the number of bound phage (phage adsorption). RJGB18 was added at a multiplicity of infection of 0.001 and adsorption was measured after three minutes (Figure 5.13). When *P.*

aeruginosa was unable to produce ornithine lipid in Δ*olsA*, the phage displayed increased adsorption compared to WT, increasing from 57.8% (± 4.6%) in WT to 76.5% (± 3.3%) in Δ*olsA* ($p < 0.01$, *t*-test). Additionally, when GADG glycolipid production is abolished (Δ*agt2*) or very significantly knocked down (Δ*plcP*), the ability of RJGB18 to bind also improved, with adsorption increasing from 57.8% (± 4.6%) in WT to 72.3% (± 4.9%, $p < 0.05$) for Δ*plcP* and 82.3% (± 5.7%, $p < 0.01$) for Δ*agt2*. However, when GADG is still produced to a large amount in Δ*agt1*, and only MGDG is ablated, there is no difference in RJGB18 adsorption; 57.8% (± 4.6%) for WT compared to 62.9% (± 5.1%) for Δ*agt1* ($p = 0.35$, *t*-test). Overall, the data suggest that lipid remodelling in WT under phosphate stress conditions does have a detrimental effect on phage adsorption, as RJGB18 displayed an increased ability to bind to mutant species unable to produce glycolipid GADG or amino acid lipid OL.

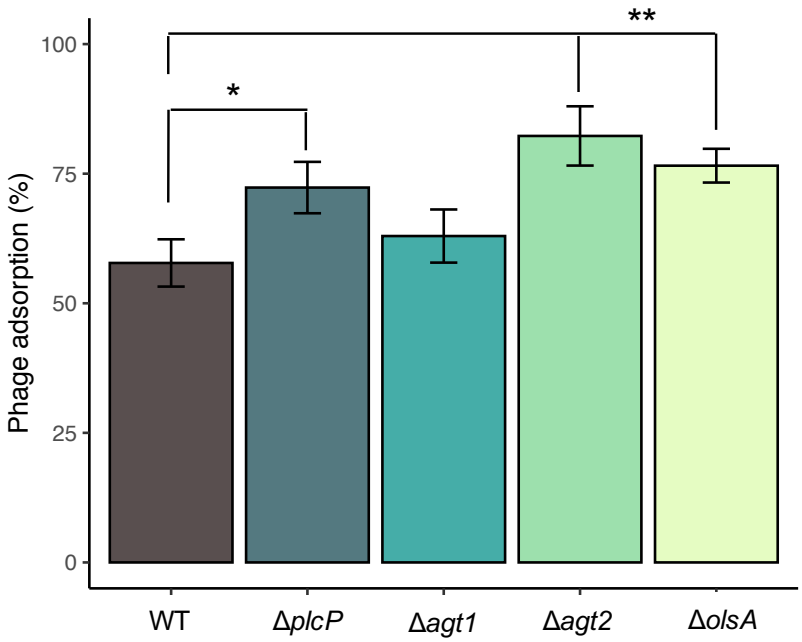

Figure 5.13. Phage adsorption assay using novel lytic *P. aeruginosa* phage RJGB18. RJGB18 phage was added to WT and lipid remodelling mutant cultures at an MOI of 0.001 and phage adsorption was measured after 3 minutes. Data are the average of 3 independent replicates (error bars ± standard deviation), * $p < 0.05$, ** $p < 0.01$.

5.3. Discussion

5.3.1 Host-pathogen interaction discussion

As for antimicrobial resistance, potential alterations to the *P. aeruginosa* membrane proteome due to lipid remodelling were hypothesised to influence host-pathogen interaction, perhaps through reduced adherence or virulence factor secretion. In the *G. mellonella* model that elicited a measureable result, and allowed comparison between WT and Δ*plcP*, there was no observed link between pathogenicity and the ability to produce glycolipids. An improved method to investigate *P. aeruginosa* pathogenicity in *G. mellonella* would be to use a wider range of infective doses to assess data such as lethal dose 90% (LD_{90}; the bacterial cell dose at which 90% of *G. mellonella* larvae die). Due to time constraints, only an initial screening comparing WT and Δ*plcP* at a low infective dose was able to be carried out. However, this proved sufficient as there was no significant difference between *P. aeruginosa* able to produce glycolipids and the glycolipid-deficient strain, whereas previous reports identify a 9-10,000-fold higher dose is required in a mutant where cell envelope stability is compromised (Lo Sciuto et al., 2018), indicating that glycolipids potentially do not alter cell envelope integrity. However, *P. aeruginosa* should be phosphate stressed before inoculation, as the concentration of available phosphate in the *G. mellonella* tract may not facilitate lipid remodelling, or death is caused too quickly for lipid remodelling to influence establishment of infection. This is an important further step as glycolipids may affect LPS availability, and a *P. aeruginosa* strain with a defective LPS layer, lacking the O-antigen and some core sugars, was shown to be over 10,000-fold less virulent in *G. mellonella* (Jarrell & Kropinski, 1982).

The exciting “red death” virulent phenotype induced by phosphate stress in *C. elegans* (Zaborin et al., 2009) could not be replicated using WT *P. aeruginosa*, and therefore comparing pathogenicity of glycolipid mutant strains was not possible. After contacting the original publication authors, it was suggested that bleach synchronisation of *C. elegans* can lead to resistance, which was the reason for re-trying with a fresh source of *C. elegans* (Figure 5.6). An alternative to bleaching was used for age synchronisation through allowing adult worms to lay eggs (3-4 hours) before

removing adult worms and allowing eggs to hatch and reach L4 stage at the same time. Unfortunately, although this did result in some *C. elegans* death, it was independent of phosphate concentration. A further suggestion was that their model was successful when using the *P. aeruginosa* P2 phenotype. This strain is actually genetically characterised as inclusive of mutations in *mexF* or *mexT*, where MexF forms part of the MexEF-OprN efflux pump, and MexT is a transcriptional regulator of this RND efflux pump (Köhler et al., 1999; Luong et al., 2014). Amongst changes to pyocyanin production, swarming ability and early induction of the *rhl*-dependent QS system, the P2 phenotype also displays a natural increase in virulence in *C. elegans* (Luong et al., 2014; Olivas et al., 2012). Given that the glycolipid mutant strains were not generated in a P2 background, it did not make sense to switch to use the P2 phenotype in attempt to replicate the "red death" phenotype.

Although the characterisation of virulence in *C. elegans* did not produce a result, the investigation of feeding preference provided intriguing results. Overall, after 48 hours *C. elegans* had migrated towards feeding on glycolipid remodelling mutant strains, favouring Δ*agt1*, Δ*agt2* and Δ*plcP* over WT *P. aeruginosa*, suggesting the mutants are less virulent. Of these, the statistically significant preference of Δ*agt1* implicates the production of MGDG glycolipid in the virulence of the WT strain. However, it is difficult to draw a definitive conclusion for the specific role of MGDG, as MGDG production is also ablated in Δ*plcP* in which the preference was not significantly different. However, for Δ*agt1* GADG represents ~32% of the lipidome compared to ~10% in the WT strain (section 3.2.3). It may be that the presence of this surrogate lipid to such a degree in Δ*agt1* influences the membrane proteome, for example in affecting virulence factor secretion. In addition, isolated LPS from *P. aeruginosa* is toxic to *C. elegans* in a concentration dependent manner (Vigneshkumar et al., 2012), and if a high proportion of GADG does alter LPS availability, *C. elegans* may recognise the decreased concentration as less virulent in Δ*agt1.* Overall, further investigation is required through membrane proteome and LPS analysis, and would be significantly aided by a successful host-pathogen killing assay.

5.3.2 Phage analysis discussion

The analysis of the RJGB18 genome revealed a lytic member of the *Myoviridae* phage family. The presence of putative DNA replication enzymes, including DNA helicase and DNA primase, DNA polymerase subunits, thymidylate synthase and a terminase, suggests that RJGB18 phage may not rely on host cell machinery for DNA replication. Phage terminases are DNA packaging enzymes (Garbe et al., 2011). The putative enzymes polynucleotide kinase and ATP-dependent exonuclease may also be involved in this process. A putative endolysin was also identified, that will cleave the *P. aeruginosa* cell wall during the lytic cycle of the phage. A number of structural proteins were identified, and it would be interesting to utilise this bioinformatic information to identify the potential receptor RJGB18 phage uses for binding to *P. aeruginosa*, and further whether this is influenced by lipid remodelling in the bacterium.

Several future directions are worthy of continuing the research into the impact of lipid remodelling on phage interaction, and subsequent potential impact on the success of phage therapy. Importantly, the binding data obtained after 3 minutes highlighted an improved ability for RJGB18 phage to bind when *P. aeruginosa* is unable to undergo lipid remodelling. Further assessment is required to analyse binding kinetics, rather than a single time-point snapshot, through reducing MOI and monitoring binding for a longer period of time, to ensure the differences in adsorption are consistent. In addition, it would be interesting to determine if lipid remodelling impacts overall bacterial cell size, thereby reducing the surface availability for phage binding, and therefore if a lack of lipid remodelling is the explanation for improved phage binding through returning bacterial cell size to normal. This research also needs expanding to include many more phage to assess whether the impact of lipid remodelling is consistent across *Pseudomonas* phage, and also across *P. aeruginosa* strains, for example in important clinical strains. Further control experiments could have been included, for example assessing phage binding ability under phosphate replete conditions. This could be important when comparing Pi-replete conditions to host environments that are phosphate scarce, particularly as my proteomic data revealed

LPS assembly proteins to be downregulated under phosphate stress in WT *P. aeruginosa*, as the LPS layer represents a key binding site for *Pseudomonas* phage.

5.3.3 Concluding summary

In summary, although a few proteins linked to host interaction were more highly expressed in the glycolipid-deficient mutant Δ*plcP*, the host-pathogen interaction models used did not suggest that glycolipid synthesis contributes to the phosphate stress virulence trigger in *P. aeruginosa*. That said, it would definitely be worth pre-starving *P. aeruginosa* for phosphate, hence triggering lipid remodelling, in future *G. mellonella* models to better determine the role of lipid remodelling in this model. Finally, as the differentially expressed proteins were linked to adherence to epithelia, an important further model to explore is human airway epithelial cells, to determine if the change in expression of these proteins does impact adherence in this model, with glycolipid synthesis genes previously shown to have increased expression in interaction with epithelial cells (Frisk et al., 2004).

Chapter 6 Summary and future perspectives

6.1 Lipid remodelling in opportunistic pathogen *P. aeruginosa*

The key definitive outcome of this work is the characterisation of glycolipid synthesis in *P. aeruginosa* as an adaptation to phosphorus stress. As such, three previously unknown genes in this important opportunistic pathogen have been annotated. *P. aeruginosa* is perhaps unusual in that it has two glycosyltransferases that both utilise the cleavage product generated by PlcP to synthesise glycolipids, yet *agt1* is located in an operon with *plcP* and *agt2* is in a distant location in the genome. In marine isolates, a *plcP/agt* operon is commonly observed, with a small proportion of isolates encoding the two genes in separate locations, and an even smaller minority encoding an additional putative *agt* locus (Sebastián et al., 2016). Glycosyltransferases from environmental organisms often have a bifunctional role, generating both MGDG and GADG (Sebastián et al., 2016; Semeniuk et al., 2014). The production of MGDG and GADG in *P. aeruginosa* has been confirmed through this work, as these known molecules were able to be identified by mass spectrometry. However, an additional unknown glycolipid (UGL) was also identified in *P. aeruginosa*. The UGL has a MS fragmentation pattern characteristic of a glycolipid. However, the unusual head group size did not allow for the identification of the glycolipid species. *P. aeruginosa* glycosyltransferases *agt1* and *agt2* do not appear to have a direct role in the synthesis of the UGL, as heterologous expression in *E. coli* did not elicit production of UGL. However, the presence of UGL in each glycolipid synthesis mutant is reduced, likely due to *P. aeruginosa* attempting to sustain viable membrane properties. In this way, the synthesis of UGL may well rely on the activity of PlcP to generate the diacylglycerol building block, warranting further investigation. Confirming the identity of the UGL through NMR and whether *P. aeruginosa* possesses another distinct pathway to synthesise UGL is an important next step, both for identifying an unknown glycolipid class, and to determine any additional role it may have in the impact of lipid remodelling on antimicrobial resistance in *P. aeruginosa*. The presence of an additional pathway is plausible, as *P. aeruginosa* encodes multiple phospholipase C enzymes, and as demonstrated these are located alongside glycosyltransferase genes. In addition, numerous uncharacterised probable glycosyltransferases in the *P.*

aeruginosa genome can be identified, with some degree of protein sequence similarity to Agt1 or Agt2.

6.2 *P. aeruginosa* lipid remodelling in antimicrobial resistance

Research into alternative lipid classes is under-represented in pathogenic bacteria, with reported membrane modifications focusing on the decoration of existing phospholipids in the membrane or lipid A modifications. The study characterising the production of an alternative non-phosphate lipid, ornithine lipid, in *P. aeruginosa* reported a 100-fold increase in resistance to polymyxin B under phosphate stress, and found that this was not ornithine lipid dependent (Lewenza et al., 2001). A further study over-expressing ornithine lipid, likely to above native levels produced by *P. aeruginosa* in response to phosphate stress, found this did contribute to resistance to antimicrobial peptides, including defensins and polymyxin B (Kim et al., 2018). It is likely that over-representation of zwitterionic OL in the membrane altered membrane charge resulting in the increase in resistance. The *P. aeruginosa* lipid membrane in its remodelled state in response to phosphate stress contains a higher proportion of glycolipids MGDG and GADG. MGDG is a neutral lipid and GADG is negatively charged. In all glycolipid synthesis mutants, sensitivity to polymyxin B was increased compared to WT under phosphate stress. Overall membrane composition analysis alludes to MGDG production being affected in all glycolipid synthesis mutants. This is likely due to the activity of PlcP removing negatively charged PG from the membrane (Wei et al., 2018), in combination with introducing neutral MGDG as a surrogate lipid, not representing a sustainable process for maintaining membrane integrity. The presiding hypothesis is that neutral MGDG provides some protection from polymyxin B by increasing the net membrane charge, thereby perturbing interaction with cationic molecules. Importantly, the well characterised mechanisms that modify lipid A with arabinose or phosphoethanolamine to result in polymyxin resistance were not found to be differentially expressed as a result of lipid remodelling. Overall, it appears that the production of glycolipids does contribute to the increased resistance to polymyxin B in *P. aeruginosa* when under phosphate stress, but the precise mechanism is unclear. The next step to assess the exact role glycolipids are playing in this

phenomenon is to measure membrane properties such as overall charge and permeability, and also to assess any changes to the LPS layer, for example novel modifications or overall availability, that may be contributing to the full increase in resistance.

The changes in carbapenem sensitivity as a result of membrane lipid remodelling in *P. aeruginosa* were more subtle, with each lipid remodelling mutant exhibiting a slight decrease in sensitivity to meropenem. Meropenem and imipenem are often characterised together in terms of their mode of entry, typically through membrane porin OprD, but also through hijacking the dipeptide transporter OpdP (Trias & Nikaido, 1990; Isabella et al., 2015). Proteomic analysis alluded to reduced expression of regulatory protein MexS when *P. aeruginosa* was unable to produce glycolipids, which in turn lead to a small, and not statistically significant, decrease in major carbapenem transporter OprD. Initially, the reduction in carbapenem transport as a result of decreased OprD expression was considered to be the pathway responsible for the slight reduction in sensitivity to meropenem in glycolipid-deficient *P. aeruginosa*. However, a lack of change in sensitivity to imipenem, for which OprD is considered a more major transporter, perhaps ruled out this pathway (Livermore, 2001). An additional carbapenem translocator, OpdP, was more highly expressed in WT *P. aeruginosa* compared to the glycolipid-deficient strain, and interestingly has been shown to have a higher affinity for meropenem (Soundararajan et al., 2017). Consequently, the lower expression of OpdP in glycolipid-deficient *P. aeruginosa* may confer the slight decrease in sensitivity to meropenem, and does not affect the sensitivity to imipenem. However, resistance to antibiotics in *P. aeruginosa* is a complex interplay between several systems, including efflux pumps, membrane porins and antibiotic-targeting enzymes. Overall, it is an unusual outcome for sensitivity to only one of meropenem or imipenem to be altered given the identical modes of entry. I would have expected that if lipid remodelling was destabilising the availability of carbapenem transporters in the membrane that sensitivity to both imipenem and meropenem would be altered.

6.3 *P. aeruginosa* lipid remodelling in host-pathogen interaction

Phosphate stress has been shown to trigger multiple virulence related systems in *P. aeruginosa* across several infection models. As glycolipid synthesis, and lipid remodelling in general, forms part of this blanket response to phosphate stress, and the membrane represents a critical part of adhesion in the infection process, it was hypothesised that membrane alterations could affect establishment of infection. In this study, no data was obtained from *C. elegans* or *G. mellonella* infection models that implicate lipid remodelling in altering infection dynamics. However, several improvements can be made to these models to investigate further (section 5.3.1), given that proteomic analysis revealed some virulence factors to be differentially regulated by lipid remodelling. This included downregulation of a contact dependent toxin (PA2462) in glycolipid-deficient Δ*plcP*, which has been shown to play a role in mediating competition during biofilm biogenesis in a CF bronchial cell model (Melvin et al., 2017). The production of glycolipids during WT *P. aeruginosa* lipid remodelling appears to aid expression of the contact-dependent toxin, and thus may be beneficial in inter-species competition in colonising lung environments. However, the proteomic datasets also suggest that the number of pili may be reduced as a result of lipid remodelling in WT *P. aeruginosa*, and this may interfere with establishment of infection in future epithelial cell models. Overall, no exciting results were obtained in the complex area of host-pathogen interaction as a result of this study.

6.4 Final conclusions

This work has demonstrated that critical priority pathogen *P. aeruginosa* is able to produce more alternative classes of membrane lipid than previously known, and that these can represent a significant proportion of overall membrane constituents. Further, the genes responsible for glycolipid synthesis in *P. aeruginosa* have been characterised, and thus further work can continue to determine phenotypic changes resulting from this adaptation to phosphorus stress. Excitingly, the production of glycolipids confers protection against the activity of cationic antimicrobial peptides, providing an insight into the dramatic decrease in sensitivity to polymyxin B as a result of phosphate stress conditions. The most important future direction is to elucidate

the mechanism by which glycolipids confer this protection against antimicrobial peptides.

References

Abbes, I., Rihouey, C., Hardouin, J., Jouenne, T., De, E., & Alexandre, S. (2018). Identification by mass spectrometry of glucosaminylphosphatidylglycerol, a phosphatidylglycerol derivative, produced by *Pseudomonas aeruginosa*. *Rapid Communications in Mass Spectrometry*, *32*(24), 2113–2121.

Ackermann, H. W. (2007). 5500 Phages examined in the electron microscope. *Archives of Virology*, *152*(2), 227–243.

Alekshun, M. N., & Levy, S. B. (2007). Molecular mechanisms of antibacterial multidrug resistance. *Cell*, *128*(6), 1037–1050.

Allen, H. K., Donato, J., Wang, H. H., Cloud-Hansen, K. A., Davies, J., & Handelsman, J. (2010). Call of the wild: Antibiotic resistance genes in natural environments. *Nature Reviews Microbiology*, *8*(4), 251–259.

Altincicek, B., Stötzel, S., Wygrecka, M., Preissner, K. T., & Vilcinskas, A. (2008). Host-derived extracellular nucleic acids enhance innate immune responses, induce coagulation, and prolong survival upon infection in insects. *The Journal of Immunology*, *181*(4), 2705–2712.

Altschul, S. F., Gish, W., Miller, W., Myers, E. W., & Lipman, D. J. (1990). Basic local alignment search tool. *Journal of Molecular Biology*, *215*(3), 403–410.

Alvarez-Ortega, C., Wiegand, I., Olivares, J., Hancock, R. E. W., & Martínez, J. L. (2011). The intrinsic resistome of *Pseudomonas aeruginosa* to β-lactams. *Virulence*, *2*(2).

Alvarez, M., & Mendoza, M. C. (1993). Molecular epidemiology of two genes encoding 3-N-aminoglycoside acetyltransferases AAC(3)I and AAC(3)II among gram-negative bacteria from a Spanish Hospital. *European Journal of Epidemiology*, *9*(6), 650–657.

Anba, J., Bidaud, M., Vasil, M. L., & Lazdunski, A. (1990). Nucleotide sequence of the *Pseudomonas aeruginosa* phoB gene, the regulatory gene for the phosphate regulon. *Journal of Bacteriology*, *172*(8), 4685–4689.

Arendt, W., Groenewold, M. K., Hebecker, S., Dickschat, J. S., & Moser, J. (2013). Identification and characterization of a periplasmic aminoacyl-phosphatidylglycerol hydrolase responsible for *Pseudomonas aeruginosa* lipid homeostasis. *Journal of Biological Chemistry*, *288*(34), 24717–24730.

Arendt, W., Hebecker, S., Jäger, S., Nimtz, M., & Moser, J. (2012). Resistance phenotypes mediated by aminoacyl-phosphatidylglycerol synthases. *Journal of Bacteriology*, *194*(6), 1401–1416.

Aubert, D., Naas, T., & Nordmann, P. (2012). Integrase-mediated recombination of the veb1 gene cassette encoding an extended-spectrum β-lactamase. *PLoS ONE*, *7*(12).

Bains, M., Fernández, L., & Hancock, R. E. W. (2012). Phosphate starvation promotes swarming motility and cytotoxicity of *Pseudomonas aeruginosa*. *Applied and Environmental Microbiology*, *78*(18), 6762–6768.

Barker, A. P., Vasil, A. I., Filloux, A., Ball, G., Wilderman, P. J., & Vasil, M. L. (2004). A novel extracellular phospholipase C of *Pseudomonas aeruginosa* is required for phospholipid chemotaxis. *Molecular Microbiology*, *53*(4), 1089–1098.

Barry, A. L., & Badal, R. E. (1982). Quality control limits for the agar overlay disk diffusion antimicrobial susceptibility test. *Journal of Clinical Microbiology*, *16*(6), 1145–1147.

Batrakov, S. G., Nikitin, D. I., Mosezhnyi, A. E., & Ruzhitsky, A. O. (1999). A glycine-containing phosphorus-free lipoaminoacid from the gram-negative marine bacterium *Cyclobacterium marinus* WH. *Chemistry and Physics of Lipids*, *99*(2), 139–143.

Benamara, H., Rihouey, C., Abbes, I., Ben Mlouka, M. A., Hardouin, J., Jouenne, T., & Alexandre, S. (2014). Characterization of membrane lipidome changes in *Pseudomonas aeruginosa* during biofilm growth on glass wool. *PLoS ONE*, *9*(9).

Benning, C., & Somerville, C. R. (1992). Identification of an operon involved in sulfolipid biosynthesis in Rhodobacter sphaeroides. *Journal of Bacteriology*, *174*(20), 6479–6487.

Bertozzi Silva, J., Storms, Z., & Sauvageau, D. (2016). Host receptors for bacteriophage adsorption. *FEMS Microbiology Letters*, *363*(4).

Besemer, J., & Borodovsky, M. (1999). Heuristic approach to deriving models for gene finding. *Nucleic Acids Research*, *27*(19), 3911–3920.

Bishop, R. E., Gibbons, H. S., Guina, T., Trent, M. S., Miller, S. I., & Raetz, C. R. H. (2000). Transfer of palmitate from phospholipids to lipid A in outer membranes of Gram-negative bacteria. *EMBO Journal*, *19*(19), 5071–5080.

Blanco, A. G., Sola, M., Gomis-Rüth, F. X., & Coll, M. (2002). Tandem DNA Recognition by PhoB, a two-component signal transduction transcriptional activator. *Structure*, *10*(5), 701–713.

Blus-Kadosh, I., Zilka, A., Yerushalmi, G., & Banin, E. (2013). The effect of PstS and PhoB on quorum sensing and swarming motility in *Pseudomonas aeruginosa*. *PLoS ONE*, *8*(9).

Bolard, A., Schniederjans, M., Haüssler, S., Triponney, P., Valot, B., Plésiat, P., & Jeannota, K. (2019). Production of norspermidine contributes to aminoglycoside resistance in pmrAB mutants of *Pseudomonas aeruginosa*. *Antimicrobial Agents and Chemotherapy*, *63*(10).

Bolon, M. K. (2009). The newer fluoroquinolones. *Infectious Disease Clinics of North America*, *23*(4), 1027–1051.

Botos, I., Majdalani, N., Mayclin, S. J., McCarthy, J. G., Lundquist, K., Wojtowicz, D., Barnard, T. J., Gumbart, J. C., & Buchanan, S. K. (2016). Structural and functional characterization of the LPS transporter lptDE from Gram-negative pathogens. *Structure*, *24*(6), 965–976.

Browne, N., Heelan, M., & Kavanagh, K. (2013). An analysis of the structural and functional similarities of insect hemocytes and mammalian phagocytes. *Virulence*, *4*(7), 597–603.

Bryan, L. E., & Van Den Elzen, H. M. (1977). Effects of membrane-energy mutations and cations on streptomycin and gentamicin accumulation by bacteria: a model for entry of

streptomycin and gentamicin in susceptible and resistant bacteria. *Antimicrobial Agents and Chemotherapy*, *12*(2), 163–177.

Bucior, I., Pielage, J. F., & Engel, J. N. (2012). *Pseudomonas aeruginosa* pili and flagella mediate distinct binding and signaling events at the apical and basolateral surface of airway epithelium. *PLoS Pathogens*, *8*(4).

Bush, K., & Bradford, P. A. (2016). β-lactams and β-lactamase inhibitors: An overview. *Cold Spring Harbor Perspectives in Medicine*, *6*(8).

Caiazza, N. C., Shanks, R. M. Q., & O'Toole, G. A. (2005). Rhamnolipids modulate swarming motility patterns of *Pseudomonas aeruginosa*. *Journal of Bacteriology*, *187*(21), 7351–7361.

Carman, G. M., & Han, G. S. (2009). Phosphatidic acid phosphatase, a key enzyme in the regulation of lipid synthesis. *Journal of Biological Chemistry*, *284*(5), 2593–2597.

Carmany, D. O., Hollingsworth, K., & McCleary, W. R. (2003). Genetic and biochemical studies of phosphatase activity of PhoR. *Journal of Bacteriology*, *185*(3), 1112–1115.

Cezairliyan, B., Vinayavekhin, N., Grenfell-Lee, D., Yuen, G. J., Saghatelian, A., & Ausubel, F. M. (2013). Identification of *Pseudomonas aeruginosa* phenazines that kill *Caenorhabditis elegans*. *PLoS Pathogens*, *9*(1).

CFF. (2018). *Cystic Fibrosis Foundation patient registry annual data report 2018*.

Champion, O. L., Titball, R. W., & Bates, S. (2018). Standardization of *G. mellonella* larvae to provide reliable and reproducible results in the study of fungal pathogens. *Journal of Fungi*, *4*(3).

Chan, F. Y., & Torriani, A. (1996). PstB protein of the phosphate-specific transport system of *Escherichia coli* is an ATPase. *Journal of Bacteriology*, *178*(13), 3974–3977.

Chaturongakul, S., & Ounjai, P. (2014). Phage-host interplay: Examples from tailed phages and Gram-negative bacterial pathogens. *Frontiers in Microbiology*, *5*(8).

Chevalier, S., Bouffartigues, E., Bodilis, J., Maillot, O., Lesouhaitier, O., Feuilloley, M. G. J., Orange, N., Dufour, A., & Cornelis, P. (2017). Structure, function and regulation of Pseudomonas aeruginosa porins. *FEMS Microbiology Reviews*, *41*(5), 698–722.

Chung, E. S., Lee, J. Y., Rhee, J. Y., & Ko, K. S. (2017). Colistin resistance in pseudomonas aeruginosa that is not linked to arnB. *Journal of Medical Microbiology*, *66*(6), 833–841.

Ciofu, O., & Bjarnsholt, T. (2010). Pseudomonas aeruginosa. In *Molecular Medical Microbiology, Three-Volume Set*. Elsevier Ltd.

Clifton, L. A., Skoda, M. W. A., Le Brun, A. P., Ciesielski, F., Kuzmenko, I., Holt, S. A., & Lakey, J. H. (2015). Effect of divalent cation removal on the structure of Gram-negative bacterial outer membrane models. *Langmuir*, *31*(1), 404–412.

Coakley, R. D., Grubb, B. R., Paradiso, A. M., Gatzy, J. T., Johnson, L. G., Kreda, S. M., O'Neal, W. K., & Boucher, R. C. (2003). Abnormal surface liquid pH regulation by cultured cystic fibrosis bronchial epithelium. *Proceedings of the National Academy of Sciences of the*

United States of America, *100*(26), 16083–16088.

Contreras, F. X., Ernst, A. M., Wieland, F., & Brügger, B. (2011). Specificity of intramembrane protein-lipid interactions. *Cold Spring Harbor Perspectives in Biology*, *3*(6), 1–18.

Corne, P., Godreuil, S., Jean-Pierre, H., Jonquet, O., Campos, J., Jumas-Bilak, E., Parer, S., & Marchandin, H. (2005). Unusual implication of biopsy forceps in outbreaks of *Pseudomonas aeruginosa* infections and pseudo-infections related to bronchoscopy. *Journal of Hospital Infection*, *61*(1), 20–26.

Cornelis, P., & Dingemans, J. (2013). *Pseudomonas aeruginosa* adapts its iron uptake strategies in function of the type of infections. *Frontiers in Cellular and Infection Microbiology*, *4*(11).

Correia, S., Poeta, P., Hébraud, M., Capelo, J. L., & Igrejas, G. (2017). Mechanisms of quinolone action and resistance: where do we stand? *Journal of Medical Microbiology*, *66*(5), 551–559.

Cronan, J. E. (2003). Bacterial membrane lipids: Where do we stand? *Annual Review of Microbiology*, *57*(1), 203–224.

Crouzet, M., Claverol, S., Lomenech, A. M., Le Sénéchal, C., Costaglioli, P., Barthe, C., Garbay, B., Bonneu, M., & Vilain, S. (2017). *Pseudomonas aeruginosa* cells attached to a surface display a typical proteome early as 20 minutes of incubation. *PLoS ONE*, *12*(7).

Cummins, J., Reen, F. J., Baysse, C., Mooij, M. J., & O'Gara, F. (2009). Subinhibitory concentrations of the cationic antimicrobial peptide colistin induce the pseudomonas quinolone signal in *Pseudomonas aeruginosa*. *Microbiology*, *155*(9), 2826–2837.

Davis, B. D. (1987). Mechanism of bactericidal action of aminoglycosides. *Microbiological Reviews*, *51*(3), 341–350.

de Almeida, L. G., Ortiz, J. H., Schneider, R. P., & Spira, B. (2015). PhoU inactivation in *Pseudomonas aeruginosa* enhances accumulation of ppGpp and polyphosphate. *Applied and Environmental Microbiology*, *81*(9), 3006–3015.

Dees, C., & Shively, J. M. (1982). Localization and quantitation of the ornithine lipid of *Thiobacillus thiooxidans*. *Journal of Bacteriology*, *149*(2), 798–799.

Delcour, A. H. (2009). Outer membrane permeability and antibiotic resistance. *Biochimica et Biophysica Acta - Proteins and Proteomics*, *1794*(5), 808–816.

Díaz-Pascual, F., Ortíz-Severín, J., Varas, M. A., Allende, M. L., & Chávez, F. P. (2017). In vivo host-pathogen interaction as revealed by global proteomic profiling of zebrafish larvae. *Frontiers in Cellular and Infection Microbiology*, *7*(JUL).

DiazGranados, C. A., Jones, M. Y., Kongphet-Tran, T., White, N., Shapiro, M., Wang, Y. F., Ray, S. M., & Blumberg, H. M. (2009). Outbreak of *Pseudomonas aeruginosa* infection associated with contamination of a flexible bronchoscope. *Infection Control & Hospital Epidemiology*, *30*(6), 550–555.

Diederich, A. K., Wobser, D., Spiess, M., Sava, I. G., Huebner, J., & Sakinç, T. (2014). Role of glycolipids in the pathogenesis of *Enterococcus faecalis* urinary tract infection. *PLoS*

ONE, *9*(5).

Diercks, H., Semeniuk, A., Gisch, N., Moll, H., Duda, K. A., & Hölzl, G. (2015). Accumulation of novel glycolipids and ornithine lipids in *Mesorhizobium loti* under phosphate deprivation. *Journal of Bacteriology*, *197*(3), 497–509.

Doi, Y., Ghilardi, A. C. R., Adams, J., De Oliveira Garcia, D., & Paterson, D. L. (2007). High prevalence of metallo-β-lactamase and 16S rRNA methylase coproduction among imipenem-resistant *Pseudomonas aeruginosa* isolates in Brazil. *Antimicrobial Agents and Chemotherapy*, *51*(9), 3388–3390.

Dowhan, W. (1997). Molecular basis for membrane phospholipid diversity: why are there so many lipids? *Annual Review of Biochemistry*, *66*(1), 199–232.

Drlica, K., Hiasa, H., Kerns, R., Malik, M., Mustaev, A., & Zhao, X. (2009). Quinolones: Action and resistance updated. *Current Topics in Medicinal Chemistry*, *9*(11), 981–998.

Edrington, T. C., Kintz, E., Goldberg, J. B., & Tamm, L. K. (2011). Structural basis for the interaction of lipopolysaccharide with outer membrane protein H (OprH) from *Pseudomonas aeruginosa*. *Journal of Biological Chemistry*, *286*(45), 39211–39223.

El'Garch, F., Jeannot, K., Hocquet, D., Llanes-Barakat, C., & Plésiat, P. (2007). Cumulative effects of several nonenzymatic mechanisms on the resistance of *Pseudomonas aeruginosa* to aminoglycosides. *Antimicrobial Agents and Chemotherapy*, *51*(3), 1016–1021.

Emerson, J., Rosenfeld, M., McNamara, S., Ramsey, B., & Gibson, R. L. (2002). *Pseudomonas aeruginosa* and other predictors of mortality and morbidity in young children with cystic fibrosis. *Pediatric Pulmonology*, *34*(2), 91–100.

Ernst, R. K., Adams, K. N., Moskowitz, S. M., Kraig, G. M., Kawasaki, K., Stead, C. M., Stephen Trent, M., & Miller, S. I. (2006). The *Pseudomonas aeruginosa* lipid A deacylase: Selection for expression and loss within the cystic fibrosis airway. *Journal of Bacteriology*, *188*(1), 191–201.

Ernst, R. K., Moskowitz, S. M., Emerson, J. C., Kraig, G. M., Adams, K. N., Harvey, M. D., Ramsey, B., Speert, D. P., Burns, J. L., & Miller, S. I. (2007). Unique Lipid A modifications in *Pseudomonas aeruginosa* isolated from the airways of patients with cystic fibrosis. *The Journal of Infectious Diseases*, *196*(7), 1088–1092.

EUCAST. (2016). Recommendations for MIC determination of colistin (polymyxin E) as recommended by the joint CLSI-EUCAST Polymyxin Breakpoints Working Group. *Http://Www.Eucast.Org*, *March*, *22*, 2016.

Falagas, M. E., Kasiakou, S. K., & Saravolatz, L. D. (2005). Colistin: The revival of polymyxins for the management of multidrug-resistant Gram-negative bacterial infections. *Clinical Infectious Diseases*, *40*(9), 1333–1341.

Falkiner, F. R., Jacoby, G. A., Keane, C. T., & McCann, S. R. (1982). Amikacin, gentamicin and tobramycin resistant *Pseudomonas aeruginosa* in a leukaemic ward. Epidemiology and genetic studies. *Journal of Hospital Infection*, *3*(3).

Faure, L. M., Llamas, M. A., Bastiaansen, K. C., Bentzmann, S. de, & Bigot, S. (2013).

Phosphate starvation relayed by PhoB activates the expression of the *Pseudomonas aeruginosa* σvreI ECF factor and its target genes. *Microbiology (United Kingdom)*, *159*(PART7), 1315–1327.

Felsenstein, J. (1985). Confidence limits on phylogenies: An approach using the bootstrap. *Evolution*, *39*(4), 783.

Feng, W., Huang, Q., Wang, Y., Yuan, Q., Li, X., Xia, P., & Sun, F. (2019). Changes in the resistance and epidemiological characteristics of *Pseudomonas aeruginosa* during a ten-year period. *Journal of Microbiology, Immunology and Infection*.

Fernandez-Pinar, R., Lo Sciuto, A., Rossi, A., Ranucci, S., Bragonzi, A., & Imperi, F. (2015). In vitro and in vivo screening for novel essential cell-envelope proteins in *Pseudomonas aeruginosa*. *Scientific Reports*, *5*.

Fernández, L., Álvarez-Ortega, C., Wiegand, I., Olivares, J., Kocíncová, D., Lam, J. S., Martínez, J. L., & Hancock, R. E. W. (2013). Characterization of the polymyxin B resistome of *Pseudomonas aeruginosa*. *Antimicrobial Agents and Chemotherapy*, *57*(1), 110–119.

Fernández, L., Gooderham, W. J., Bains, M., McPhee, J. B., Wiegand, I., & Hancock, R. E. W. (2010). Adaptive resistance to the "last hope" antibiotics polymyxin B and colistin in *Pseudomonas aeruginosa* is mediated by the novel two-component regulatory system ParR-ParS. *Antimicrobial Agents and Chemotherapy*, *54*(8), 3372–3382.

Fernández, L., & Hancock, R. E. W. (2012). Adaptive and mutational resistance: Role of porins and efflux pumps in drug resistance. *Clinical Microbiology Reviews*, *25*(4), 661–681.

Fernández, L., Jenssen, H., Bains, M., Wiegand, I., Gooderham, W. J., & Hancock, R. E. W. (2012). The two-component system CprRS senses cationic peptides and triggers adaptive resistance in *Pseudomonas aeruginosa* independently of ParRS. *Antimicrobial Agents and Chemotherapy*, *56*(12), 6212–6222.

Filloux, A., Bally, M., Soscia, C., Murgier, M., & Lazdunski, A. (1988). Phosphate regulation in *Pseudomonas aeruginosa*: Cloning of the alkaline phosphatase gene and identification of phoB- and phoR-like genes. *MGG Molecular & General Genetics*, *212*(3), 510–513.

Fischer, W., & Leopold, K. (1999). Polar lipids of four listeria species containing L-lysylcardiolipin, a novel lipid structure, and other unique phospholipids. *International Journal of Systematic Bacteriology*, *49*(2), 653–662.

Fol, M., Głłobińska, A., Stączek, P., Kowalewicz-Kulbat, M., Druszczyńska, M., Madiraju, M., & Rudnicka, W. (2013). The lack of L-PG production and the repercussions of it in regards to *M. tuberculosis* interactions with mononuclear phagocytes. *Acta Microbiologica et Immunologica Hungarica*, *60*(2), 127–144.

Folch, J., Lees, M., & Stanley, G. H. S. (1957). A simple method for the isolation and purification of total lipides from animal tissues. *Journal of Biological Chemistry*, *226*(1), 497–509.

Folkesson, A., Jelsbak, L., Yang, L., Johansen, H. K., Ciofu, O., Hoiby, N., & Molin, S. (2012). Adaptation of *Pseudomonas aeruginosa* to the cystic fibrosis airway: An evolutionary perspective. *Nature Reviews Microbiology*, *10*(12), 841–851.

Frisk, A., Schurr, J. R., Wang, G., Bertucci, D. C., Marrero, L., Hwang, S. H., Hassett, D. J., & Schurr, M. J. (2004). Transcriptome analysis of *Pseudomonas aeruginosa* after interaction with human airway epithelial cells. *Infection and Immunity*, *72*(9), 5433–5438.

Fuqua, C., Parsek, M. R., & Greenberg, E. P. (2001). Regulation of gene expression by cell-to-cell communication: acyl-homoserine lactone quorum sensing. *Annual Review of Genetics*, *35*(1), 439–468.

Gallagher, L. A., & Manoil, C. (2001). *Pseudomonas aeruginosa* PAO1 kills *Caenorhabditis elegans* by cyanide poisoning. *Journal of Bacteriology*, *183*(21), 6207–6214.

Gao, J. L., Weissenmayer, B., Taylor, A. M., Thomas-Oates, J., López-Lara, I. M., & Geiger, O. (2004). Identification of a gene required for the formation of lyso-ornithine lipid, an intermediate in the biosynthesis of ornithine-containing lipids. *Molecular Microbiology*, *53*(6), 1757–1770.

Garbe, J., Bunk, B., Rohde, M., & Schobert, M. (2011). Sequencing and characterization of *Pseudomonas aeruginosa* phage JG004. *BMC Microbiology*, *11*.

Gardner, S. G., Johns, K. D., Tanner, R., & McCleary, W. R. (2014). The PhoU protein from *Escherichia coli* interacts with PhoR, PstB, and metals to form a phosphate-signaling complex at the membrane. *Journal of Bacteriology*, *196*(9), 1741–1752.

Geiger, O., González-Silva, N., López-Lara, I. M., & Sohlenkamp, C. (2010). Amino acid-containing membrane lipids in bacteria. *Progress in Lipid Research*, *49*(1), 46–60.

Germovsek, E., Barker, C. I., & Sharland, M. (2017). What do i need to know about aminoglycoside antibiotics? *Archives of Disease in Childhood: Education and Practice Edition*, *102*(2), 89–93.

Griffith, L. J. (1966). Development of resistance to kanamycin. *Annals of the New York Academy of Sciences*, *132*(2), 796–799.

Gunn, J. S., Ryan, S. S., Van Velkinburgh, J. C., Ernst, R. K., & Miller, S. I. (2000). Genetic and functional analysis of a PmrA-PmrB-regulated locus necessary for lipopolysaccharide modification, antimicrobial peptide resistance, and oral virulence of *Salmonella enterica* serovar typhimurium. *Infection and Immunity*, *68*(11), 6139–6146.

Gutu, A. D., Sgambati, N., Strasbourger, P., Brannon, M. K., Jacobs, M. A., Haugen, E., Kaul, R. K., Johansen, H. K., Høiby, N., & Moskowitz, S. M. (2013). Polymyxin resistance of *Pseudomonas aeruginosa* phoQ mutants is dependent on additional two-component regulatory systems. *Antimicrobial Agents and Chemotherapy*, *57*(5), 2204–2215.

Haba, E., Pinazo, A., Jauregui, O., Espuny, M. J., Infante, M. R., & Manresa, A. (2003). Physicochemical characterization and antimicrobial properties of rhamnolipids produced by *Pseudomonas aeruginosa* 47T2 NCBIM 40044. *Biotechnology and Bioengineering*, *81*(3), 316–322.

Haddad, A., Jensen, V., Becker, T., & Häussler, S. (2009). The Pho regulon influences biofilm formation and type three secretion in *Pseudomonas aeruginosa*. *Environmental Microbiology Reports*, *1*(6), 488–494.

Haghi, F., Zeighami, H., Monazami, A., Toutouchi, F., Nazaralian, S., & Naderi, G. (2018). Diversity of virulence genes in multidrug resistant *Pseudomonas aeruginosa* isolated from burn wound infections. *Microbial Pathogenesis*, *115*, 251–256.

Han, M. L., Velkov, T., Zhu, Y., Roberts, K. D., Le Brun, A. P., Chow, S. H., Gutu, A. D., Moskowitz, S. M., Shen, H. H., & Li, J. (2018). Polymyxin-induced Lipid A deacylation in *Pseudomonas aeruginosa* perturbs polymyxin penetration and confers high-level resistance. *ACS Chemical Biology*, *13*(1), 121–130.

Han, M. L., Zhu, Y., Creek, D. J., Lin, Y. W., Anderson, D., Shen, H. H., Tsuji, B., Gutu, A. D., Moskowitz, S. M., Velkov, T., & Li, J. (2018). Alterations of metabolic and lipid profiles in polymyxin-resistant *Pseudomonas aeruginosa*. *Antimicrobial Agents and Chemotherapy*, *62*(6), 1–14.

Hancock, R. E. W., & Brinkman, F. S. L. (2002). Function of <i>Pseudomonas/i> porins in uptake and efflux. *Annual Review of Microbiology*, *56*(1), 17–38.

Hastie, A. T., Hingley, S. T., Higgins, M. L., Kueppers, F., & Shryock, T. (1986). Rhamnolipid from *Pseudomonas aeruginosa* inactivates mammalian tracheal ciliary axonemes. *Cell Motility and the Cytoskeleton*, *6*(5), 502–509.

Hayden, J. D., & Ades, S. E. (2008). The extracytoplasmic stress factor, σE, is required to maintain cell envelope integrity in *Escherichia coli*. *PLoS ONE*, *3*(2).

Heinzl, G. A., Huang, W., Robinson, E., Xue, F., Möenne-Loccoz, P., & Wilks, A. (2018). The Asp99–Arg188 salt bridge of the *Pseudomonas aeruginosa* HemO is critical in allowing conformational flexibility during catalysis. *Journal of Biological Inorganic Chemistry*, *23*(7), 1057–1070.

Henrichfreise, B., Wiegand, I., Pfister, W., & Wiedemann, B. (2007). Resistance mechanisms of multiresistant *Pseudomonas aeruginosa* strains from Germany and correlation with hypermutation. *Antimicrobial Agents and Chemotherapy*, *51*(11), 4062–4070.

Higgins, P. G., Fluit, A. C., Milatovic, D., Verhoef, J., & Schmitz, F. J. (2003). Mutations in GyrA, ParC, MexR and NfxB in clinical isolates of *Pseudomonas aeruginosa*. *International Journal of Antimicrobial Agents*, *21*(5), 409–413.

Hocquet, D., Muller, A., Blanc, K., Plésiat, P., Talon, D., Monnet, D. L., & Bertrand, X. (2008). Relationship between antibiotic use and incidence of mexXY-OprM overproducers among clinical isolates of *Pseudomonas aeruginosa*. *Antimicrobial Agents and Chemotherapy*, *52*(3), 1173–1175.

Hocquet, D., Plésiat, P., Dehecq, B., Mariotte, P., Talon, D., & Bertrand, X. (2010). Nationwide investigation of extended-spectrum β-lactamases, metallo-β-lactamases, and extended-spectrum oxacillinases produced by ceftazidime-resistant *Pseudomonas aeruginosa* strains in France. *Antimicrobial Agents and Chemotherapy*, *54*(8), 3512–3515.

Hoegy, F., Lee, X., Noel, S., Rognan, D., Mislin, G. L. A., Reimmann, C., & Schalk, I. J. (2009). Stereospecificity of the siderophore pyochelin outer membrane transporters in fluorescent peudomonads. *Journal of Biological Chemistry*, *284*(22), 14949–14957.

Hofmann, M., & Eichenberger, W. (1996). Biosynthesis of diacylglyceryl-N,N,N-

trimethylhomoserine in Rhodobacter sphaeroides and evidence for lipid-linked N methylation. *Journal of Bacteriology*, *178*(21), 6140–6144.

Hogardt, M., Schmoldt, S., Götzfried, M., Adler, K., & Heesemann, J. (2004). Pitfalls of polymyxin antimicrobial susceptibilty testing of *Pseudomonas aeruginosa* isolated from cystic fibrosis patients. *Journal of Antimicrobial Chemotherapy*, *54*(6), 1057–1061.

Hölzl, G., & Dörmann, P. (2007). Structure and function of glycoglycerolipids in plants and bacteria. In *Progress in Lipid Research* (Vol. 46, Issue 5, pp. 225–243).

Hoo, Z. H., Coates, E., Maguire, C., Cantrill, H., Shafi, N., Nash, E. F., McGowan, A., Bourke, S. J., Flight, W. G., Daniels, T. V., Nightingale, J. A., Allenby, M. I., Curley, R., & Wildman, M. J. (2018). Pragmatic criteria to define chronic *Pseudomonas aeruginosa* infection among adults with cystic fibrosis. *European Journal of Clinical Microbiology and Infectious Diseases*, *37*(11), 2219–2222.

Hwang, S., Kim, C. Y., Ji, S. G., Go, J., Kim, H., Yang, S., Kim, H. J., Cho, A., Yoon, S. S., & Lee, I. (2016). Network-assisted investigation of virulence and antibiotic-resistance systems in *Pseudomonas aeruginosa*. *Scientific Reports*, *6*.

Icho, T., Sparrow, C. P., & Raetz, C. R. (1985). Molecular cloning and sequencing of the gene for CDP-diglyceride synthetase of Escherichia coli. *The Journal of Biological Chemistry*, *260*(22), 12078–12083.

Ionescu, S. A., Lee, S., Housden, N. G., Kaminska, R., Kleanthous, C., & Bayley, H. (2017). Orientation of the OmpF porin in planar lipid bilayers. *ChemBioChem*, *18*(6), 554–562.

Isabella, V. M., Campbell, A. J., Manchester, J., Sylvester, M., Nayar, A. S., Ferguson, K. E., Tommasi, R., & Miller, A. A. (2015). Toward the rational design of carbapenem uptake in *Pseudomonas aeruginosa*. *Chemistry and Biology*, *22*(4), 535–547.

Islam, S., Jalal, S., & Wretlind, B. (2004). Expression of the MexXY efflux pump in amikacin-resistant isolates of *Pseudomonas aeruginosa*. *Clinical Microbiology and Infection*, *10*(10), 877–883.

Jackson, B. J., Bohin, J. P., & Kennedy, E. P. (1984). Biosynthesis of membrane-derived oligosaccharides: Characterization of MdoB mutants defective in phosphoglycerol transferase I activity. *Journal of Bacteriology*, *160*(3), 976–981.

Jacobs, M. A., Alwood, A., Thaipisuttikul, I., Spencer, D., Haugen, E., Ernst, S., Will, O., Kaul, R., Raymond, C., Levy, R., Chun-Rong, L., Guenthner, D., Bovee, D., Olson, M. V., & Manoil, C. (2003). Comprehensive transposon mutant library of *Pseudomonas aeruginosa*. *Proceedings of the National Academy of Sciences of the United States of America*, *100*(SUPPL. 2), 14339–14344.

Jacoby, G. A. (2009). AmpC β-Lactamases. *Clinical Microbiology Reviews*, *22*(1), 161–182.

Jacoby, G. A. (2017). Plasmid-mediated quinolone resistance. In *Antimicrobial Drug Resistance* (pp. 265–268).

Jana, S., & Deb, J. K. (2006). Molecular understanding of aminoglycoside action and resistance. *Applied Microbiology and Biotechnology*, *70*(2), 140–150.

Jander, G., Rahme, L. G., & Ausubel, F. M. (2000). Positive correlation between virulence of *Pseudomonas aeruginosa* mutants in mice and insects. *Journal of Bacteriology*, *182*(13), 3843–3845.

Jarrell, K. F., & Kropinski, A. M. (1982). The virulence of protease and cell surface mutants of *Pseudomonas aeruginosa* for the larvae of *Galleria mellonella*. *Journal of Invertebrate Pathology*, *39*(3), 395–400.

Jensen, V., Löns, D., Zaoui, C., Bredenbruch, F., Meissner, A., Dieterich, G., Münch, R., & Häussler, S. (2006). RhlR expression in *Pseudomonas aeruginosa* is modulated by the Pseudomonas quinolone signal via PhoB-dependent and -independent pathways. *Journal of Bacteriology*, *188*(24), 8601–8606.

Jin, Y., Yang, H., Qiao, M., & Jin, S. (2011). MexT regulates the type III secretion system through MexS and PtrC in *Pseudomonas aeruginosa*. *Journal of Bacteriology*, *193*(2), 399–410.

Johansen, H. K., & Hoiby, N. (1992). Seasonal onset of initial colonisation and chronic infection with *Pseudomonas aeruginosa* in patients with cystic fibrosis in Denmark. *Thorax*, *47*(2), 109–111.

Kaawai, Y., Yano, I., Kaneda, K., & Yabuuchi, E. (1988). Ornithine-containing lipids of some *Pseudomonas* species. *European Journal of Biochemistry*, *175*(3), 633–641.

Karaiskos, I., Lagou, S., Pontikis, K., Rapti, V., & Poulakou, G. (2019). The "Old" and the "New" antibiotics for MDR Gram-negative pathogens: For whom, when, and how. *Frontiers in Public Health*, *7*(6).

Karl, D. M., & Björkman, K. M. (2015). Dynamics of dissolved organic phosphorus. In *Biogeochemistry of Marine Dissolved Organic Matter: Second Edition* (pp. 233–334).

Karlowsky, J. A., Lob, S. H., Kazmierczak, K. M., Hawser, S. P., Magnet, S., Young, K., Motyl, M. R., & Sahm, D. F. (2018). In vitro activity of imipenem/relebactam against Gram-negative ESKAPE pathogens isolated in 17 European countries: 2015 SMART surveillance programme. *Journal of Antimicrobial Chemotherapy*, *73*(7), 1872–1879.

Kato, J., Ito, A., Nikata, T., & Ohtake, H. (1992). Phosphate taxis in *Pseudomonas aeruginosa*. *Journal of Bacteriology*, *174*(15), 5149–5151.

Kato, J., Sakai, Y., Nikata, T., & Ohtake, H. (1994). Cloning and characterization of a *Pseudomonas aeruginosa* gene involved in the negative regulation of phosphate taxis. *Journal of Bacteriology*, *176*(18), 5874–5877.

Kawalek, A., Modrzejewska, M., Zieniuk, B., Bartosik, A. A., & Jagura-Burdzy, G. (2019). Interaction of ArmZ with the DNA-binding domain of MexZ induces expression of mexXY multidrug efflux pump genes and antimicrobial resistance in Pseudomonas aeruginosa. *Antimicrobial Agents and Chemotherapy*, *63*(12).

Kawasaki, K., Ernst, R. K., & Miller, S. I. (2004). 3-O-deacylation of Lipid A by PagL, a PhoP/PhoQ-regulated deacylase of *Salmonella typhimurium*, modulates signaling through TLR4. *Journal of Biological Chemistry*, *279*(19), 20044–20048.

Kim, S. K., Park, S. J., Li, X. H., Choi, Y. S., Im, D. S., & Lee, J. H. (2018). Bacterial ornithine

lipid, a surrogate membrane lipid under phosphate-limiting conditions, plays important roles in bacterial persistence and interaction with host. *Environmental Microbiology*, *20*(11), 3992–4008.

Kizny Gordon, A. E., Mathers, A. J., Cheong, E. Y. L., Gottlieb, T., Kotay, S., Walker, A. S., Peto, T. E. A., Crook, D. W., & Stoesser, N. (2017). The hospital water environment as a reservoir for carbapenem-resistant organisms causing hospital-acquired infections - a systematic review of the literature. *Clinical Infectious Diseases*, *64*(10), 1436–1444.

Klein, S., Lorenzo, C., Hoffmann, S., Walther, J. M., Storbeck, S., Piekarski, T., Tindall, B. J., Wray, V., Nimtz, M., & Moser, J. (2009). Adaptation of *Pseudomonas aeruginosa* to various conditions includes tRNA-dependent formation of alanyl-phosphatidylglycerol. *Molecular Microbiology*, *71*(3), 551–565.

Koch, C. (2002). Early infection and progression of cystic fibrosis lung disease. *Pediatric Pulmonology*, *34*(3), 232–236.

Kohler, T., Curty, L. K., Barja, F., Van Delden, C., & Pechere, J. C. (2000). Swarming of *Pseudomonas aeruginosa* is dependent on cell-to-cell signaling and requires flagella and pili. *Journal of Bacteriology*, *182*(21), 5990–5996.

Köhler, T., Epp, S. F., Curty, L. K., & Pechère, J. C. (1999). Characterization of MexT, the regulator of the MexE-MexF-OprN multidrug efflux system of *Pseudomonas aeruginosa*. *Journal of Bacteriology*, *181*(20), 6300–6305.

Köhler, T., Michea-Hamzehpour, M., Epp, S. F., & Pechere, J. C. (1999). Carbapenem activities against *Pseudomonas aeruginosa*: Respective contributions of OprD and efflux systems. *Antimicrobial Agents and Chemotherapy*, *43*(2), 424–427.

Kondakova, T., D'Heygère, F., Feuilloley, M. J., Orange, N., Heipieper, H. J., & Duclairoir Poc, C. (2015). Glycerophospholipid synthesis and functions in Pseudomonas. *Chemistry and Physics of Lipids*, *190*, 27–42.

Kong, K. F., Jayawardena, S. R., Del Puerto, A., Wiehlmann, L., Laabs, U., Tümmler, B., & Mathee, K. (2005). Characterization of poxB, a chromosomal-encoded *Pseudomonas aeruginosa* oxacillinase. *Gene*, *358*(1–2), 82–92.

Kosorok, M. R., Zeng, L., West, S. E. H., Rock, M. J., Splaingard, M. L., Laxova, A., Green, C. G., Collins, J., & Farrell, P. M. (2001). Acceleration of lung disease in children with cystic fibrosis after *Pseudomonas aeruginosa* acquisition. *Pediatric Pulmonology*, *32*(4), 277–287.

Kownatzki, R., Tümmler, B., & Döring, G. (1987). Rhamnolipid of *Pseudomonas aeruginosa* in sputum of cystic fibrosis patients. *The Lancet*, *329*(8540), 1026–1027.

Kramer, A., Schwebke, I., & Kampf, G. (2006). How long do nosocomial pathogens persist on inanimate surfaces? A systematic review. *BMC Infectious Diseases*, *6*.

Kristian, S. A., Dürr, M., Van Strijp, J. A. G., Neumeister, B., & Peschel, A. (2003). MprF-mediated lysinylation of phospholipids in *Staphylococcus aureus* leads to protection against oxygen-independent neutrophil killing. *Infection and Immunity*, *71*(1), 546–549.

Kucharska, I., Liang, B., Ursini, N., & Tamm, L. K. (2016). Molecular interactions of

lipopolysaccharide with an outer membrane protein from *Pseudomonas aeruginosa* probed by solution NMR. *Biochemistry*, *55*(36), 5061–5072.

Kumar, S. S., Tandberg, J. I., Penesyan, A., Elbourne, L. D. H., Suarez-Bosche, N., Don, E., Skadberg, E., Fenaroli, F., Cole, N., Winther-Larsen, H. C., & Paulsen, I. T. (2018). Dual transcriptomics of host-pathogen interaction of cystic fibrosis isolate *Pseudomonas aeruginosa* PASS1 With zebrafish. *Frontiers in Cellular and Infection Microbiology*, *8*, 406.

Kumar, S., Stecher, G., & Tamura, K. (2016). MEGA7: Molecular Evolutionary Genetics Analysis version 7.0 for bigger datasets. *Molecular Biology and Evolution*, *33*(7), 1870–1874.

Laganowsky, A., Reading, E., Allison, T. M., Ulmschneider, M. B., Degiacomi, M. T., Baldwin, A. J., & Robinson, C. V. (2014). Membrane proteins bind lipids selectively to modulate their structure and function. *Nature*, *510*(7503), 172–175.

Lambert, M. L., Suetens, C., Savey, A., Palomar, M., Hiesmayr, M., Morales, I., Agodi, A., Frank, U., Mertens, K., Schumacher, M., & Wolkewitz, M. (2011). Clinical outcomes of health-care-associated infections and antimicrobial resistance in patients admitted to European intensive-care units: a cohort study. *The Lancet Infectious Diseases*, *11*(1), 30–38.

Landman, D., Georgescu, C., Martin, D. A., & Quale, J. (2008). Polymyxins revisited. *Clinical Microbiology Reviews*, *21*(3), 449–465.

Langton Hewer, S. C., & Smyth, A. R. (2017). Antibiotic strategies for eradicating *Pseudomonas aeruginosa* in people with cystic fibrosis. *Cochrane Database of Systematic Reviews*, *2017*(4).

Lavine, M. D., & Strand, M. R. (2002). Insect hemocytes and their role in immunity. *Insect Biochemistry and Molecular Biology*, *32*(10), 1295–1309.

Lee, D. G., Urbach, J. M., Wu, G., Liberati, N. T., Feinbaum, R. L., Miyata, S., Diggins, L. T., He, J., Saucier, M., Déziel, E., Friedman, L., Li, L., Grills, G., Montgomery, K., Kucherlapati, R., Rahme, L. G., & Ausubel, F. M. (2006). Genomic analysis reveals that *Pseudomonas aeruginosa* virulence is combinatorial. *Genome Biology*, *7*(10).

Lee, H., Han, S., Kwon, C. S., & Lee, D. (2016). Biogenesis and regulation of the let-7 miRNAs and their functional implications. *Protein and Cell*, *7*(2), 100–113.

Lee, J. K., Lee, Y. S., Park, Y. K., & Kim, B. S. (2005). Alterations in the GyrA and GyrB subunits of topoisomerase II and the ParC and ParE subunits of topoisomerase IV in ciprofloxacin-resistant clinical isolates of *Pseudomonas aeruginosa*. *International Journal of Antimicrobial Agents*, *25*(4), 290–295.

Lee, J., Wu, J., Deng, Y., Wang, J., Wang, C., Wang, J., Chang, C., Dong, Y., Williams, P., & Zhang, L. H. (2013). A cell-cell communication signal integrates quorum sensing and stress response. *Nature Chemical Biology*, *9*(5), 339–343.

Lee, J., & Zhang, L. (2014). The hierarchy quorum sensing network in *Pseudomonas aeruginosa*. *Protein and Cell*, *6*(1), 26–41.

Lee, M., & Sousa, M. C. (2014). Structural basis for substrate specificity in ArnB. A key enzyme in the polymyxin resistance pathway of Gram-negative bacteria. *Biochemistry*, *53*(4), 796–805.

Lewenza, S., Charron-Mazenod, L., Giroux, L., & Zamponi, A. D. (2014). Feeding behaviour of *Caenorhabditis elegans* is an indicator of *Pseudomonas aeruginosa* PAO1 virulence. *PeerJ*, *2014*(1).

Lewenza, S., Falsafi, R., Bains, M., Rohs, P., Stupak, J., Sprott, G. D., & Hancock, R. E. W. (2011). The olsA gene mediates the synthesis of an ornithine lipid in *Pseudomonas aeruginosa* during growth under phosphate-limiting conditions, but is not involved in antimicrobial peptide susceptibility. *FEMS Microbiology Letters*, *320*(2), 95–102.

Li, H., Luo, Y. F., Williams, B. J., Blackwell, T. S., & Xie, C. M. (2012). Structure and function of OprD protein in *Pseudomonas aeruginosa*: From antibiotic resistance to novel therapies. *International Journal of Medical Microbiology*, *302*(2), 63–68.

Lidbury, I. D. E. A., Murphy, A. R. J., Fraser, T. D., Bending, G. D., Jones, A. M. E., Moore, J. D., Goodall, A., Tibbett, M., Hammond, J. P., Scanlan, D. J., & Wellington, E. M. H. (2017). Identification of extracellular glycerophosphodiesterases in *Pseudomonas* and their role in soil organic phosphorus remineralisation. *Scientific Reports*, *7*(1).

Lidbury, I. D. E. A., Murphy, A. R. J., Scanlan, D. J., Bending, G. D., Jones, A. M. E., Moore, J. D., Goodall, A., Hammond, J. P., & Wellington, E. M. H. (2016). Comparative genomic, proteomic and exoproteomic analyses of three *Pseudomonas* strains reveals novel insights into the phosphorus scavenging capabilities of soil bacteria. *Environmental Microbiology*, *18*(10), 3535–3549.

Liko, I., Degiacomi, M. T., Lee, S., Newport, T. D., Gault, J., Reading, E., Hopper, J. T. S., Housden, N. G., White, P., Colledge, M., Sula, A., Wallace, B. A., Kleanthous, C., Stansfeld, P. J., Bayley, H., Benesch, J. L. P., Allison, T. M., & Robinson, C. V. (2018). Lipid binding attenuates channel closure of the outer membrane protein OmpF. *Proceedings of the National Academy of Sciences of the United States of America*, *115*(26), 6691–6696.

Liu, P. V. (1974). Extracellular toxins of *Pseudomonas aeruginosa*. *Journal of Infectious Diseases*, *130*, S94–S99.

Liu, Y. Y., Wang, Y., Walsh, T. R., Yi, L. X., Zhang, R., Spencer, J., Doi, Y., Tian, G., Dong, B., Huang, X., Yu, L. F., Gu, D., Ren, H., Chen, X., Lv, L., He, D., Zhou, H., Liang, Z., Liu, J. H., & Shen, J. (2016). Emergence of plasmid-mediated colistin resistance mechanism MCR-1 in animals and human beings in China: a microbiological and molecular biological study. *The Lancet Infectious Diseases*, *16*(2), 161–168.

Livermore, D. M. (2001). Of *Pseudomonas*, porins, pumps and carbapenems. *Journal of Antimicrobial Chemotherapy*, *47*(3), 247–250.

Llamas, M. A., Van Der Sar, A., Chu, B. C. H., Sparrius, M., Vogel, H. J., & Bitter, W. (2009). A novel extracytoplasmic function (ECF) sigma factor regulates virulence in *Pseudomonas aeruginosa*. *PLoS Pathogens*, *5*(9).

Llanes, C., Köhler, T., Patry, I., Dehecq, B., Van Delden, C., & Plésiat, P. (2011). Role of the MexEF-OprN efflux system in low-level resistance of *Pseudomonas aeruginosa* to

ciprofloxacin. *Antimicrobial Agents and Chemotherapy*, *55*(12), 5676–5684.

Lo Sciuto, A., Fernández-Piñar, R., Bertuccini, L., Iosi, F., Superti, F., & Imperi, F. (2014). The periplasmic protein TolB as a potential drug target in *Pseudomonas aeruginosa*. *PLoS ONE*, *9*(8).

Lo Sciuto, A., Martorana, A. M., Fernández-Piñar, R., Mancone, C., Polissi, A., & Imperi, F. (2018). *Pseudomonas aeruginosa* LptE is crucial for LptD assembly, cell envelope integrity, antibiotic resistance and virulence. *Virulence*, *9*(1), 1718–1733.

Lodge, J. M., Minchin, S. D., Piddock, L. J. V., & Busby, J. W. (1990). Cloning, sequencing and analysis of the structural gene and regulatory region of the *Pseudomonas aeruginosa* chromosomal ampC β-lactamase. *Biochemical Journal*, *272*(3), 627–631.

Long, J., Zaborina, O., Holbrook, C., Zaborin, A., & Alverdy, J. (2008). Depletion of intestinal phosphate after operative injury activates the virulence of *P. aeruginosa* causing lethal gut-derived sepsis. *Surgery*, *144*(2), 189–197.

López-Lara, I. M., & Geiger, O. (2017). Bacterial lipid diversity. *Biochimica et Biophysica Acta - Molecular and Cell Biology of Lipids*, *1862*(11), 1287–1299.

Loubens, I., Debarbieux, L., Bohin, A., Lacroix, J. -M, & Bohin, J. -P. (1993). Homology between a genetic locus (mdoA) involved in the osmoregulated biosynthesis of periplasmic glucans in *Escherichia coli* and a genetic locus (hrpM) controlling pathogenicity of *Pseudomonas syringae*. *Molecular Microbiology*, *10*(2), 329–340.

Lowe, T. M., & Chan, P. P. (2016). tRNAscan-SE On-line: integrating search and context for analysis of transfer RNA genes. *Nucleic Acids Research*, *44*(W1), W54–W57.

Luong, P. M., Shogan, B. D., Zaborin, A., Belogortseva, N., Shrout, J. D., Zaborina, O., & Alverdy, J. C. (2014). Emergence of the P2 phenotype in Pseudomonas aeruginosa PAO1 strains involves various mutations in MexT or MexF. *Journal of Bacteriology*, *196*(2), 504–513.

Macfarlene, E. L. A., Kwasnicka, A., & Hancock, R. E. W. (2000). Role of *Pseudomonas aeruginosa* Phop-PhoQ in resistance to antimicrobial cationic peptides and aminoglycosides. *Microbiology*, *146*(10), 2543–2554.

MacLeod, D. L., Nelson, L. E., Shawar, R. M., Lin, B. B., Lockwood, L. G., Dirk, J. E., Miller, G. H., Burns, J. L., & Garber, R. L. (2000). Aminoglycoside-resistance mechanisms for cystic fibrosis *Pseudomonas aeruginosa* isolates are unchanged by long-term, intermittent, inhaled tobramycin treatment. *The Journal of Infectious Diseases*, *181*(3), 1180–1184.

Mahajan-Miklos, S., Tan, M. W., Rahme, L. G., & Ausubel, F. M. (1999). Molecular mechanisms of bacterial virulence elucidated using a *Pseudomonas aeruginosa-Caenorhabditis elegans* pathogenesis model. *Cell*, *96*(1), 47–56.

Mahar, P., Padiglione, A. A., Cleland, H., Paul, E., Hinrichs, M., & Wasiak, J. (2010). *Pseudomonas aeruginosa* bacteraemia in burns patients: Risk factors and outcomes. *Burns*, *36*(8), 1228–1233.

Maloney, E., Stankowska, D., Zhang, J., Fol, M., Cheng, Q. J., Lun, S., Bishai, W. R., Rajagopalan, M., Chatterjee, D., & Madiraju, M. V. (2009). The two-domain LysX

protein of *Mycobacterium tuberculosis* is required for production of lysinylated phosphatidylglycerol and resistance to cationic antimicrobial peptides. *PLoS Pathogens*, *5*(7).

Marsh, E. K., & May, R. C. (2012). *Caenorhabditis elegans*, a model organism for investigating immunity. *Applied and Environmental Microbiology*, *78*(7), 2075–2081.

Masuda, N., Sakagawa, E., & Ohya, S. (1995). Outer membrane proteins responsible for multiple drug resistance in *Pseudomonas aeruginosa*. *Antimicrobial Agents and Chemotherapy*, *39*(3), 645–649.

Maurya, A. P., Talukdar, A. Das, Chanda, D. D., Chakravarty, A., & Bhattacharjee, A. (2014). Integron-borne transmission of VEB-1 extended-spectrum β-Lactamase in *Pseudomonas aeruginosa* in a tertiary care hospital in India. *Antimicrobial Agents and Chemotherapy*, *58*(11), 6966–6969.

McKnight, S. L., Iglewski, B. H., & Pesci, E. C. (2000). The Pseudomonas quinolone signal regulates rhl quorum sensing in *Pseudomonas aeruginosa*. *Journal of Bacteriology*, *182*(10), 2702–2708.

McPhee, J. B., Bains, M., Winsor, G., Lewenza, S., Kwasnicka, A., Brazas, M. D., Brinkman, F. S. L., & Hancock, R. E. W. (2006). Contribution of the PhoP-PhoQ and PmrA-PmrB two-component regulatory systems to Mg2+-induced gene regulation in *Pseudomonas aeruginosa*. *Journal of Bacteriology*, *188*(11), 3995–4006.

McPhee, J. B., Lewenza, S., & Hancock, R. E. W. (2003). Cationic antimicrobial peptides activate a two-component regulatory system, PmrA-PmrB, that regulates resistance to polymyxin B and cationic antimicrobial peptides in *Pseudomonas aeruginosa*. *Molecular Microbiology*, *50*(1), 205–217.

Mekalanos, J. J. (1992). Environmental signals controlling expression of virulence determinants in bacteria. *Journal of Bacteriology*, *174*(1), 1–7.

Melvin, J. A., Gaston, J. R., Phillips, S. N., Springer, M. J., Marshall, C. W., Shanks, R. M. Q., & Bomberger, J. M. (2017). *Pseudomonas aeruginosa* contact-dependent growth inhibition plays dual role in host-pathogen interactions. *MSphere*, *2*(6).

Minnikin, D. E., & Abdolrahimzadeh, H. (1974). The replacement of phosphatidylethanolamine and acidic phospholipids by an ornithine-amide lipid and a minor phosphorus-free lipid in *Pseudomonas flourescens* NCMB 129. *FEBS Letters*, *43*(3), 257–260.

Minnikin, D. E., Abdolrahimzadeh, H., & Baddiley, J. (1974). Replacement of acidic phospholipids by acidic glycolipids in *Pseudomonas diminuta*. *Nature*, *249*(5454), 268–269.

Mittal, R., Aggarwal, S., Sharma, S., Chhibber, S., & Harjai, K. (2009). Urinary tract infections caused by *Pseudomonas aeruginosa*: A minireview. *Journal of Infection and Public Health*, *2*(3), 101–111.

Molina, J., Cordero, E., & Pachón, J. (2009). New information about the polymyxin/colistin class of antibiotics. *Expert Opinion on Pharmacotherapy*, *10*(17), 2811–2828.

Monds, R. D., Newell, P. D., Gross, R. H., & O'Toole, G. A. (2007). Phosphate-dependent modulation of c-di-GMP levels regulates *Pseudomonas fluorescens* Pf0-1 biofilm formation by controlling secretion of the adhesin LapA. *Molecular Microbiology*, *63*(3), 656–679.

Monds, R. D., Silby, M. W., & Khris Mahanty, H. (2001). Expression of the Pho regulon negatively regulates biofilm formation by *Pseudomonas aureofaciens* PA147-2. *Molecular Microbiology*, *42*(2), 415–426.

Moore, E. K., Hopmans, E. C., Rijpstra, W. I. C., Villanueva, L., Dedysh, S. N., Kulichevskaya, I. S., Wienk, H., Schoutsen, F., & Sinninghe Damsté, J. S. (2013). Novel mono-, di-, and trimethylornithine membrane lipids in northern wetland Planctomycetes. *Applied and Environmental Microbiology*, *79*(22), 6874–6884.

Moore, E. K., Hopmans, E. C., Rijpstra, W. I. C., Villanueva, L., & Sinninghe Damsté, J. S. (2016). Elucidation and identification of amino acid containing membrane lipids using liquid chromatography/high-resolution mass spectrometry. *Rapid Communications in Mass Spectrometry*, *30*(6), 739–750.

Moradali, M. F., Ghods, S., & Rehm, B. H. A. (2017). Pseudomonas aeruginosa lifestyle: A paradigm for adaptation, survival, and persistence. *Frontiers in Cellular and Infection Microbiology*, *7*(2).

Moskowitz, S. M., Ernst, R. K., & Miller, S. I. (2004). PmrAB, a two-component regulatory system of *Pseudomonas aeruginosa* that modulates resistance to cationic antimicrobial peptides and addition of aminoarabinose to lipid A. *Journal of Bacteriology*, *186*(2), 575–579.

Mugnier, P., Dubrous, P., Casin, I., Arlet, G., & Collatz, E. (1996). A TEM-derived extended-spectrum β-lactamase in *Pseudomonas aeruginosa*. *Antimicrobial Agents and Chemotherapy*, *40*(11), 2488–2493.

Mulani, M. S., Kamble, E. E., Kumkar, S. N., Tawre, M. S., & Pardesi, K. R. (2019). Emerging strategies to combat ESKAPE pathogens in the era of antimicrobial resistance: A review. *Frontiers in Microbiology*, *10*(4).

Mulcahy, H., Charron-Mazenod, L., & Lewenza, S. (2010). *Pseudomonas aeruginosa* produces an extracellular deoxyribonuclease that is required for utilization of DNA as a nutrient source. *Environmental Microbiology*, *12*(6), 1621–1629.

Muraih, J. K., Pearson, A., Silverman, J., & Palmer, M. (2011). Oligomerization of daptomycin on membranes. *Biochimica et Biophysica Acta - Biomembranes*, *1808*(4), 1154–1160.

Muramatsu, H., Horii, T., Takeshita, A., Hashimoto, H., & Maekawa, M. (2005). Characterization of fluoroquinolone and carbapenem susceptibilities in clinical isolates of levofloxacin-resistant *Pseudomonas aeruginosa*. *Chemotherapy*, *51*(2–3), 70–75.

Murcia, N. R., Lee, X., Waridel, P., Maspoli, A., Imker, H. J., Chai, T., Walsh, C. T., & Reimmann, C. (2015). The Pseudomonas aeruginosa antimetabolite L -2-amino-4-methoxy-trans-3-butenoic acid (AMB) is made from glutamate and two alanine residues via a thiotemplate-linked tripeptide precursor. *Frontiers in Microbiology*, *6*(3).

Naenna, P., Noisumdaeng, P., Pongpech, P., & Tribuddharat, C. (2010). Detection of outer

membrane porin protein, an imipenem influx channel, in *Pseudomonas aeruginosa* clinical isolates. *Southeast Asian Journal of Tropical Medicine and Public Health*, *41*(3), 614–624.

Nakano, M., Deguchi, T., Kawamura, T., Yasuda, M., Kimura, M., Okano, Y., & Kawada, Y. (1997). Mutations in the gyrA and parC genes in fluoroquinolone-resistant clinical isolates of *Pseudomonas aeruginosa*. *Antimicrobial Agents and Chemotherapy*, *41*(10), 2289–2291.

Needham, B. D., & Trent, M. S. (2013). Fortifying the barrier: The impact of lipid A remodelling on bacterial pathogenesis. *Nature Reviews Microbiology*, *11*(7), 467–481.

Nesbitt, J. A., & Lennarz, W. J. (1968). Participation of aminoacyl transfer ribonucleic acid in aminoacyl phosphatidylglycerol synthesis. I. Specificity of lysyl phosphatidylglycerol synthetase. *Journal of Biological Chemistry*, *243*(11), 3088–3095.

Nichols, D., Chmiel, J., & Berger, M. (2008). Chronic inflammation in the cystic fibrosis lung: Alterations in inter- and intracellular signaling. *Clinical Reviews in Allergy and Immunology*, *34*(2), 146–162.

Nikata, T., Sakai, Y., Shibata, K., Kato, J., Kuroda, A., & Ohtake, H. (1996). Molecular analysis of the phosphate-specific transport (pst) operon of *Pseudomonas aeruginosa*. *Molecular and General Genetics*, *250*(6), 692–698.

Nishi, H., Komatsuzawa, H., Fujiwara, T., McCallum, N., & Sugai, M. (2004). Reduced content of lysyl-phosphatidylglycerol in the cytoplasmic membrane affects susceptibility to moenomycin, as well as vancomycin, gentamicin, and antimicrobial peptides, in *Staphylococcus aureus*. *Antimicrobial Agents and Chemotherapy*, *48*(12), 4800–4807.

Nowicki, E. M., O'Brien, J. P., Brodbelt, J. S., & Trent, M. S. (2015). Extracellular zinc induces phosphoethanolamine addition to Pseudomonas aeruginosa lipid A via the ColRS two-component system. *Molecular Microbiology*, *97*(1), 166–178.

Ogbolu, D. O., Daini, O. A., Ogunledun, A., Alli, A. O., & Webber, M. A. (2011). High levels of multidrug resistance in clinical isolates of Gram-negative pathogens from Nigeria. *International Journal of Antimicrobial Agents*, *37*(1), 62–66.

Olivas, A. D., Shogan, B. D., Valuckaite, V., Zaborin, A., Belogortseva, N., Musch, M., Meyer, F., L.Trimble, W., An, G., Gilbert, J., Zaborina, O., & Alverdy, J. C. (2012). Intestinal tissues induce an SNP mutation in *Pseudomonas aeruginosa* that enhances its virulence: possible role in anastomotic leak. *PLoS ONE*, *7*(8).

Ostroff, R. M., Wretlind, B., & Vasil, M. L. (1989). Mutations in the hemolytic-phospholipase C operon result in decreased virulence of *Pseudomonas aeruginosa* PAO1 grown under phosphate-limiting conditions. *Infection and Immunity*, *57*(5), 1369–1373.

Parsons, J. B., & Rock, C. O. (2013). Bacterial lipids: metabolism and membrane homeostasis. *Progress in Lipid Research*, *52*(3), 249–276.

Peschel, A., Jack, R. W., Otto, M., Collins, L. V., Staubitz, P., Nicholson, G., Kalbacher, H., Nieuwenhuizen, W. F., Jung, G., Tarkowski, A., Van Kessel, K. P. M., & Van Strijp, J. A. G. (2001). *Staphylococcus aureus* resistance to human defensins and evasion of neutrophil killing via the novel virulence factor MprF is based on modification of membrane lipids

with L-lysine. *Journal of Experimental Medicine*, *193*(9), 1067–1076.

Pesci, E. C., Milbank, J. B. J., Pearson, J. P., Mcknight, S., Kende, A. S., Greenberg, E. P., & Iglewski, B. H. (1999). Quinolone signaling in the cell-to-cell communication system of *Pseudomonas aeruginosa*. *Proceedings of the National Academy of Sciences of the United States of America*, *96*(20), 11229–11234.

Pesci, E. C., Pearson, J. P., Seed, P. C., & Iglewski, B. H. (1997). Regulation of las and rhl quorum sensing in *Pseudomonas aeruginosa*. *Journal of Bacteriology*, *179*(10), 3127–3132.

Petrushenko, Z. M., She, W., & Rybenkov, V. V. (2011). A new family of bacterial condensins. *Molecular Microbiology*, *81*(4), 881–896.

Pham, T. D. M., Ziora, Z. M., & Blaskovich, M. A. T. (2019). Quinolone antibiotics. *MedChemComm*, *10*(10), 1719–1739.

Phillips, I., King, A., & Shannon, K. (1986). Prevalence and mechanisms of aminoglycoside resistance: A ten-year study. *The American Journal of Medicine*, *80*(6), 48–55.

Pogliano, J., Pogliano, N., & Silverman, J. A. (2012). Daptomycin-mediated reorganization of membrane architecture causes mislocalization of essential cell division proteins. *Journal of Bacteriology*, *194*(17), 4494–4504.

Poirel, L., Lambert, T., Türkoglü, S., Ronco, E., Gaillard, J. L., & Nordmann, P. (2001). Characterization of class 1 integrons from *Pseudomonas aeruginosa* that contain the blaVIM-2 carbapenem-hydrolyzing β-lactamase gene and of two novel aminoglycoside resistance gene cassettes. *Antimicrobial Agents and Chemotherapy*, *45*(2), 546–552.

Poirel, L., & Nordmann, P. (2005). Acquired carbapenem-hydrolyzing β-lactamases and their genetic support. *Current Pharmaceutical Biotechnology*, *3*(2), 117–127.

Poirel, Laurent, Naas, T., Guibert, M., Chaibi, E. B., Labia, R., & Nordmann, P. (1999). Molecular and biochemical characterization of VEB-1, a novel class A extended-spectrum β-lactamase encoded by an *Escherichia coli* integron gene. *Antimicrobial Agents and Chemotherapy*, *43*(3), 573–581.

Poirel, Laurent, Naas, T., & Nordmann, P. (2010). Diversity, epidemiology, and genetics of class D β-lactamases. *Antimicrobial Agents and Chemotherapy*, *54*(1), 24–38.

Poole, K. (2004). Resistance to beta-lactam antibiotics. *Cellular and Molecular Life Sciences*, *61*, 2200–2223.

Poole, Keith. (2005). Aminoglycoside resistance in *Pseudomonas aeruginosa*. *Antimicrobial Agents and Chemotherapy*, *49*(2), 479–487.

Poole, Keith. (2011). Pseudomonas aeruginosa: Resistance to the max. *Frontiers in Microbiology*, *2*(4).

Pournaras, S., Maniati, M., Spanakis, N., Ikonomidis, A., Tassios, P. T., Tsakris, A., Legakis, N. J., & Maniatis, A. N. (2005). Spread of efflux pump-overexpressing, non-metallo-β-lactamase-producing, meropenem-resistant but ceftazidime-susceptible *Pseudomonas aeruginosa* in a region with blaVIM endemicity. *Journal of Antimicrobial Chemotherapy*,

56(4), 761–764.

Prayle, A., & Smyth, A. R. (2010). Aminoglycoside use in cystic fibrosis: Therapeutic strategies and toxicity. *Current Opinion in Pulmonary Medicine*, *16*(6), 604–610.

Price, M. N., & Arkin, A. P. (2017). PaperBLAST: Text mining papers for information about homologs. *MSystems*, *2*(4).

Purschke, F. G., Hiller, E., Trick, I., & Rupp, S. (2012). Flexible survival strategies of *Pseudomonas aeruginosa* in biofilms result in increased fitness compared with *Candida albicans*. *Molecular and Cellular Proteomics*, *11*(12), 1652–1669.

Quale, J., Bratu, S., Gupta, J., & Landman, D. (2006). Interplay of efflux system, ampC, and oprD expression in carbapenem resistance of *Pseudomonas aeruginosa* clinical isolates. *Antimicrobial Agents and Chemotherapy*, *50*(5), 1633–1641.

Quesada, J. M., Otero-Asman, J. R., Bastiaansen, K. C., Civantos, C., & Llamas, M. A. (2016). The activity of the *Pseudomonas aeruginosa* virulence regulator σVreI Is modulated by the anti-σ factor VreR and the transcription factor PhoB. *Frontiers in Microbiology*, *7*(AUG).

Raetz, C. R. H., & Whitfield, C. (2002). Lipopolysaccharide endotoxins. *Annual Review of Biochemistry*, *71*(1), 635–700.

Ramirez, M. S., & Tolmasky, M. E. (2010). Aminoglycoside modifying enzymes. *Drug Resistance Updates*, *13*(6), 151–171.

Rasmussen, L., & Toftlund, H. (1986). Phosphate compounds as iron chelators in animal cell cultures. *In Vitro*, *22*(4), 177–179.

Ratjen, F., Brockhaus, F., & Angyalosi, G. (2009). Aminoglycoside therapy against *Pseudomonas aeruginosa* in cystic fibrosis: A review. *Journal of Cystic Fibrosis*, *8*(6), 361–369.

Rechel, B., Jakubowski, E., & Nolte, E. (2018). The role of public health organizations in addressing public health problems in Europe – key policy lessons. *European Journal of Public Health*, *28*(suppl_4).

Réjiba, S., Aubry, A., Petitfrère, S., Jarlier, V., & Cambau, E. (2008). Contribution of ParE mutation and efflux to ciprofloxacin resistance in *Pseudomonas aeruginosa* clinical isolates. *Journal of Chemotherapy*, *20*(6), 749–752.

Rice, C. D., Pollard, J. E., Lewis, Z. T., & McCleary, W. R. (2009). Employment of a promoter-swapping technique shows that PhoU modulates the activity of the PstSCAB 2 ABC transporter in *Escherichia coli*. *Applied and Environmental Microbiology*, *75*(3), 573–582.

Rico-Jiménez, M., Reyes-Darias, J. A., Ortega, Á., Diez Pena, A. I., Morel, B., & Krell, T. (2016). Two different mechanisms mediate chemotaxis to inorganic phosphate in *Pseudomonas aeruginosa*. *Scientific Reports*, *6*.

Riekhof, W. R., Andre, C., & Benning, C. (2005). Two enzymes, BtaA and BtaB, are sufficient for betaine lipid biosynthesis in bacteria. *Archives of Biochemistry and Biophysics*,

441(1), 96–105.

Robertson, P., Smith, A., Mead, A., Smith, I., Khanna, N., Wright, P., Joannidis, P., Boyd, S., Anderson, M., Hamilton, A., Shaw, D., & Stewart, A. (2015). Risk-assessment-based approach to patients exposed to endoscopes contaminated with *Pseudomonas* spp. *Journal of Hospital Infection*, *90*(1), 66–69.

Rodríguez-Martínez, J. M., Poirel, L., & Nordmann, P. (2009). Molecular epidemiology and mechanisms of carbapenem resistance in *Pseudomonas aeruginosa*. *Antimicrobial Agents and Chemotherapy*, *53*(11), 4783–4788.

Rouhi, S., & Ramazanzadeh, R. (2018). Prevalence of blaoxacillinase-23- and blaoxacillinase-24/40-type carbapenemases in *Pseudomonas aeruginosa* species isolated from patients with nosocomial and non-nosocomial infections in the west of Iran. *Iranian Journal of Pathology*, *13*(3), 348–356.

Roy, H. (2009). Tuning the properties of the bacterial membrane with aminoacylated phosphatidylglycerol. *IUBMB Life*, *61*(10), 940–953.

Roy, H., Dare, K., & Ibba, M. (2009). Adaptation of the bacterial membrane to changing environments using aminoacylated phospholipids: MicroCommentary. *Molecular Microbiology*, *71*(3), 547–550.

Ruppé, É., Woerther, P. L., & Barbier, F. (2015). Mechanisms of antimicrobial resistance in Gram-negative bacilli. *Annals of Intensive Care*, *5*(1).

Rutten, L., Geurtsen, J., Lambert, W., Smolenaers, J. J. M., Bonvin, A. M., De Haan, A., Van Der Ley, P., Egmond, M. R., Gros, P., & Tommassen, J. (2006). Crystal structure and catalytic mechanism of the LPS 3-O-deacylase PagL from *Pseudomonas aeruginosa*. *Proceedings of the National Academy of Sciences of the United States of America*, *103*(18), 7071–7076.

Santos-Beneit, F. (2015). The Pho regulon: A huge regulatory network in bacteria. *Frontiers in Microbiology*, *6*(APR).

Schulman, H., & Kennedy, E. P. (1979). Localization of membrane-derived oligosaccharides in the outer envelope of *Escherichia coli* and their occurrence in other Gram-negative bacteria. *Journal of Bacteriology*, *137*(1), 686–688.

Schuster, M., Lostroh, C. P., Ogi, T., & Greenberg, E. P. (2003). Identification, timing, and signal specificity of *Pseudomonas aeruginosa* quorum-controlled genes: A transcriptome analysis. *Journal of Bacteriology*, *185*(7), 2066–2079.

Sebastián, M., Smith, A. F., González, J. M., Fredricks, H. F., Van Mooy, B., Koblížek, M., Brandsma, J., Koster, G., Mestre, M., Mostajir, B., Pitta, P., Postle, A. D., Sánchez, P., Gasol, J. M., Scanlan, D. J., & Chen, Y. (2016). Lipid remodelling is a widespread strategy in marine heterotrophic bacteria upon phosphorus deficiency. *ISME Journal*, *10*(4), 968–978.

Sedighi, M., Salehi-Abargouei, A., Oryan, G., & Faghri, J. (2014). Epidemiology of VIM-1-imipenem resistant *Pseudomonas aeruginosa* in Iran: A systematic review and meta-analysis. *Journal of Research in Medical Sciences*, *19*(9), 899–903.

Seemann, T. (2014). Prokka: Rapid prokaryotic genome annotation. *Bioinformatics*, *30*(14), 2068–2069.

Semeniuk, A., Sohlenkamp, C., Duda, K., & Hölzl, G. (2014). A bifunctional glycosyltransferase from agrobacterium tumefaciens synthesizes monoglucosyl and glucuronosyl diacylglycerol under phosphate deprivation. *Journal of Biological Chemistry*, *289*(14), 10104–10114.

Sharma, U., Pal, D., & Prasad, R. (2014). Alkaline phosphatase: An overview. *Indian Journal of Clinical Biochemistry*, *29*(3), 269–278.

Shiozaki, M., Deguchi, N., Ishikawa, T., Haruyama, H., Kawai, Y., & Nishijima, M. (1998). Revised structure of flavolipin and synthesis of its isomers. *Tetrahedron Letters*, *39*(25), 4497–4500.

Shirley, M., & Lamont, I. L. (2009). Role of TonB1 in pyoverdine-mediated signaling in *Pseudomonas aeruginosa*. *Journal of Bacteriology*, *191*(18), 5634–5640.

Shor, R., Halabe, A., Rishver, S., Tilis, Y., Matas, Z., Fux, A., Boaz, M., & Weinstein, J. (2006). Severe hypophosphatemia in sepsis as a mortality predictor. *Annals of Clinical and Laboratory Science*, *36*(1), 67–72.

Shoriridge, V. D., Lazdunski, A., & Vasil, M. L. (1992). Osmoprotectants and phosphate regulate expression of phospholipase C in *Pseudomonas aeruginosa*. *Molecular Microbiology*, *6*(7), 863–871.

Siehnel, R. J., Worobec, E. A., & Hancock, R. E. W. (1988). Regulation of components of the *Pseudomonas aeruginosa* phosphate-starvation-inducible regulon in *Escherichia coli*. *Molecular Microbiology*, *2*(3), 347–352.

Siehnel, Richard J., Egli, C., & Hancock, R. E. W. (1992). Polyphosphate-selective porin OprO of *Pseudomonas aeruginosa*: expression, purification and sequence. *Molecular Microbiology*, *6*(16), 2319–2326.

Slavetinsky, C. J., Peschel, A., & Ernst, C. M. (2012). Alanyl-phosphatidylglycerol and lysyl-phosphatidylglycerol are translocated by the same MprF flippases and have similar capacities to protect against the antibiotic daptomycin in *Staphylococcus aureus*. *Antimicrobial Agents and Chemotherapy*, *56*(7), 3492–3497.

Slavetinsky, C., Kuhn, S., & Peschel, A. (2017). Bacterial aminoacyl phospholipids – Biosynthesis and role in basic cellular processes and pathogenicity. *Biochimica et Biophysica Acta - Molecular and Cell Biology of Lipids*, *1862*(11), 1310–1318.

Smith, A. F., Rihtman, B., Stirrup, R., Silvano, E., Mausz, M. A., Scanlan, D. J., & Chen, Y. (2019). Elucidation of glutamine lipid biosynthesis in marine bacteria reveals its importance under phosphorus deplete growth in *Rhodobacteraceae*. *ISME Journal*, *13*(1), 39–49.

Smith, R. S., & Iglewski, B. H. (2003). *P. aeruginosa* quorum-sensing systems and virulence. *Current Opinion in Microbiology*, *6*(1), 56–60.

Smith, W. D., Bardin, E., Cameron, L., Edmondson, C. L., Farrant, K. V., Martin, I., Murphy, R. A., Soren, O., Turnbull, A. R., Wierre-Gore, N., Alton, E. W., Bundy, J. G., Bush, A.,

Connett, G. J., Faust, S. N., Filloux, A., Freemont, P. S., Jones, A. L., Takats, Z., … Davies, J. C. (2017). Current and future therapies for *Pseudomonas aeruginosa* infection in patients with cystic fibrosis. *FEMS Microbiology Letters*, *364*(14).

Sobel, M. L., Neshat, S., & Poole, K. (2005). Mutations in PA2491 (mexS) promote MexT-dependent mexEF-oprN expression and multidrug resistance in a clinical strain of *Pseudomonas aeruginosa*. *Journal of Bacteriology*, *187*(4), 1246–1253.

Soberón-Chávez, G., Lépine, F., & Déziel, E. (2005). Production of rhamnolipids by *Pseudomonas aeruginosa*. *Applied Microbiology and Biotechnology*, *68*(6), 718–725.

Sønderholm, M., Kragh, K. N., Koren, K., Jakobsen, T. H., Darch, S. E., Alhede, M., Jensen, P. Ø., Whiteley, M., Kühl, M., & Bjarnsholt, T. (2017). *Pseudomonas aeruginosa* aggregate formation in an alginate bead model system exhibits in vivo-like characteristics. *Applied and Environmental Microbiology*, *83*(9).

Soundararajan, G., Bhamidimarri, S. P., & Winterhalter, M. (2017). Understanding carbapenem translocation through OccD3 (OpdP) of *Pseudomonas aeruginosa*. *ACS Chemical Biology*, *12*(6), 1656–1664.

Staubitz, P., Neumann, H., Schneider, T., Wiedemann, I., & Peschel, A. (2004). MprF-mediated biosynthesis of lysylphosphatidylglycerol, an important determinant in staphylococcal defensin resistance. *FEMS Microbiology Letters*, *231*(1), 67–71.

Stover, C. K., Pham, X. Q., Erwin, A. L., Mizoguchi, S. D., Warrener, P., Hickey, M. J., Brinkman, F. S. L., Hufnagle, W. O., Kowallk, D. J., Lagrou, M., Garber, R. L., Goltry, L., Tolentino, E., Westbrock-Wadman, S., Yuan, Y., Brody, L. L., Coulter, S. N., Folger, K. R., Kas, A., … Olson, M. V. (2000). Complete genome sequence of *Pseudomonas aeruginosa* PAO1, an opportunistic pathogen. *Nature*, *406*(6799), 959–964.

Strateva, T., Ouzounova-Raykova, V., Markova, B., Todorova, A., Marteva-Proevska, Y., & Mitov, I. (2007). Widespread detection of VEB-1-type extended-spectrum beta-lactamases among nosocomial ceftazidime-resistant *Pseudomonas aeruginosa* isolates in Sofia, Bulgaria. *Journal of Chemotherapy*, *19*(2), 140–145.

Strateva, T., & Yordanov, D. (2009). *Pseudomonas aeruginosa* - A phenomenon of bacterial resistance. *Journal of Medical Microbiology*, *58*(9), 1133–1148.

Surin, B. P., Dixon, N. E., & Rosenberg, H. (1986). Purification of the phoU protein, a negative regulator of the pho regulon of *Escherichia coli* K-12. *Journal of Bacteriology*, *168*(2), 631–635.

Tabatabai, M. A., & Bremner, J. M. (1969). Use of p-nitrophenyl phosphate for assay of soil phosphatase activity. *Soil Biology and Biochemistry*, *1*(4), 301–307.

Tacconelli, E., Carrara, E., Savoldi, A., Harbarth, S., Mendelson, M., Monnet, D. L., Pulcini, C., Kahlmeter, G., Kluytmans, J., Carmeli, Y., Ouellette, M., Outterson, K., Patel, J., Cavaleri, M., Cox, E. M., Houchens, C. R., Grayson, M. L., Hansen, P., Singh, N., … Zorzet, A. (2018). Discovery, research, and development of new antibiotics: the WHO priority list of antibiotic-resistant bacteria and tuberculosis. *The Lancet Infectious Diseases*, *18*(3), 318–327.

Tagliaferri, T. L., Jansen, M., & Horz, H. P. (2019). Fighting pathogenic bacteria on two fronts:

phages and antibiotics as combined strategy. *Frontiers in Cellular and Infection Microbiology*, *9*, 22.

Tam, V. H., Schilling, A. N., LaRocco, M. T., Gentry, L. O., Lolans, K., Quinn, J. P., & Garey, K. W. (2007). Prevalence of AmpC over-expression in bloodstream isolates of *Pseudomonas aeruginosa*. *Clinical Microbiology and Infection*, *13*(4), 413–418.

Tan, B. K., Bogdanov, M., Zhao, J., Dowhan, W., Raetz, C. R. H., & Guan, Z. (2012). Discovery of a cardiolipin synthase utilizing phosphatidylethanolamine and phosphatidylglycerol as substrates. *Proceedings of the National Academy of Sciences*, *109*(41), 16504–16509.

Tan, M. W., Rahme, L. G., Sternberg, J. A., Tompkins, R. G., & Ausubel, F. M. (1999). *Pseudomonas aeruginosa* killing of *Caenorhabditis elegans* used to identify *P. aeruginosa* virulence factors. *Proceedings of the National Academy of Sciences of the United States of America*, *96*(5), 2408–2413.

Thaipisuttikul, I., Hittle, L. E., Chandra, R., Zangari, D., Dixon, C. L., Garrett, T. A., Rasko, D. A., Dasgupta, N., Moskowitz, S. M., Malmström, L., Goodlett, D. R., Miller, S. I., Bishop, R. E., & Ernst, R. K. (2014). A divergent *Pseudomonas aeruginosa* palmitoyltransferase essential for cystic fibrosis-specific lipid A. *Molecular Microbiology*, *91*(1), 158–174.

Thedieck, K., Hain, T., Mohamed, W., Tindall, B. J., Nimtz, M., Chakraborty, T., Wehland, J., & Jänsch, L. (2006). The MprF protein is required for lysinylation of phospholipids in listerial membranes and confers resistance to cationic antimicrobial peptides (CAMPs) on *Listeria monocytogenes*. *Molecular Microbiology*, *62*(5), 1325–1339.

Tian, Z., Cheng, S., Xia, B., Jin, Y., Bai, F., Cheng, Z., Jin, S., Liu, X., & Wu, W. (2019). *Pseudomonas aeruginosa* ExsA regulates a metalloprotease, ImpA, that inhibits phagocytosis of macrophages. *Infection and Immunity*, *87*(12).

Tran, J. H., Jacoby, G. A., & Hooper, D. C. (2005). Interaction of the plasmid-encoded quinolone resistance protein QnrA with *Escherichia coli* topoisomerase IV. *Antimicrobial Agents and Chemotherapy*, *49*(7), 3050–3052.

Trend, S., Fonceca, A. M., Ditcham, W. G., Kicic, A., & CF, A. (2017). The potential of phage therapy in cystic fibrosis: Essential human-bacterial-phage interactions and delivery considerations for use in *Pseudomonas aeruginosa*-infected airways. *Journal of Cystic Fibrosis*, *16*(6), 663–670.

Trias, J., & Nikaido, H. (1990). Outer membrane protein D2 catalyzes facilitated diffusion of carbapenems and penems through the outer membrane of *Pseudomonas aeruginosa*. *Antimicrobial Agents and Chemotherapy*, *34*(1), 52–57.

Tsakris, A., Poulou, A., Kristo, I., Pittaras, T., Spanakis, N., Pournaras, S., & Markou, F. (2009). Large dissemination of VIM-2-metallo-β-lactamase-producing *Pseudomonas aeruginosa* strains causing health care-associated community-onset infections. *Journal of Clinical Microbiology*, *47*(11), 3524–3529.

Turner, J. M., & Messenger, A. J. (1986). Occurrence, biochemistry and physiology of phenazine pigment production. *Advances in Microbial Physiology*, *27*(C), 211–275.

Tyanova, S., Temu, T., & Cox, J. (2016). The MaxQuant computational platform for mass spectrometry-based shotgun proteomics. *Nature Protocols*, *11*(12), 2301–2319.

Tyanova, S., Temu, T., Sinitcyn, P., Carlson, A., Hein, M. Y., Geiger, T., Mann, M., & Cox, J. (2016). The Perseus computational platform for comprehensive analysis of (prote)omics data. *Nature Methods*, *13*(9), 731–740.

Ulmschneider, M. B., & Sansom, M. S. P. (2001). Amino acid distributions in integral membrane protein structures. *Biochimica et Biophysica Acta - Biomembranes*, *1512*(1), 1–14.

Vaara, M. (1992). Agents that increase the permeability of the outer membrane. *Microbiological Reviews*, *56*(3), 395–411.

Van Caekenberghe, D. L., & Pattyn, S. R. (1984). In vitro activity of ciprofloxacin compared with those of other new fluorinated piperazinyl-substituted quinoline derivatives. *Antimicrobial Agents and Chemotherapy*, *25*(4), 518–521.

Van Mooy, B. A. S., Fredricks, H. F., Pedler, B. E., Dyhrman, S. T., Karl, D. M., Koblížek, M., Lomas, M. W., Mincer, T. J., Moore, L. R., Moutin, T., Rappé, M. S., & Webb, E. A. (2009). Phytoplankton in the ocean use non-phosphorus lipids in response to phosphorus scarcity. *Nature*, *458*(7234), 69–72.

Van Mooy, B. A. S., Rocap, G., Fredricks, H. F., Evans, C. T., & Devol, A. H. (2006). Sulfolipids dramatically decrease phosphorus demand by picocyanobacteria in oligotrophic marine environments. *Proceedings of the National Academy of Sciences of the United States of America*, *103*(23), 8607–8612.

Vasil, M. L., Stonehouse, M. J., Vasil, A. I., Wadsworth, S. J., Goldfine, H., Bolcome, R. E., & Chan, J. (2009). A complex extracellular sphingomyelinase of *Pseudomonas aeruginosa* inhibits angiogenesis by selective cytotoxicity to endothelial cells. *PLoS Pathogens*, *5*(5).

Vaziri, F., Peerayeh, S. N., Nejad, Q. B., & Farhadian, A. (2011). The prevalence of aminoglycoside-modifying enzyme genes (aac (6')-I, aac (6')-II, ant (2")-I, aph (3')-VI) in *Pseudomonas aeruginosa*. *Clinics*, *66*(9), 1519–1522.

Vences-Guzmán, M. Á., Geiger, O., & Sohlenkamp, C. (2012). Ornithine lipids and their structural modifications: From A to E and beyond. *FEMS Microbiology Letters*, *335*(1), 1–10.

Vences-Guzmán, M. Á., Guan, Z., Ormeño-Orrillo, E., González-Silva, N., López-Lara, I. M., Martínez-Romero, E., Geiger, O., & Sohlenkamp, C. (2011). Hydroxylated ornithine lipids increase stress tolerance in *Rhizobium tropici* CIAT899. *Molecular Microbiology*, *79*(6), 1496–1514.

Venkatachalam, V., Hendley, J. O., & Willson, D. F. (2011). The diagnostic dilemma of ventilator-associated pneumonia in critically ill children. *Pediatric Critical Care Medicine*, *12*(3), 286–296.

Viedma, E., Juan, C., Acosta, J., Zamorano, L., Otero, J. R., Sanz, F., Chaves, F., & Oliver, A. (2009). Nosocomial spread of colistin-only-sensitive sequence type 235 *Pseudomonas aeruginosa* isolates producing the extended-spectrum β-lactamases GES-1 and GES-5 in Spain. *Antimicrobial Agents and Chemotherapy*, *53*(11), 4930–4933.

Vigneshkumar, B., Pandian, S. K., & Balamurugan, K. (2012). Regulation of *Caenorhabditis elegans* and *Pseudomonas aeruginosa* machinery during interactions. *Archives of*

Microbiology, *194*(4), 229–242.

Villegas, M. V., Lolans, K., Correa, A., Kattan, J. N., Lopez, J. A., & Quinn, J. P. (2007). First identification of *Pseudomonas aeruginosa* isolates producing a KPC-type carbapenem-hydrolyzing β-lactamase. *Antimicrobial Agents and Chemotherapy*, *51*(4), 1553–1555.

Vitrac, H., Mallampalli, V. K. P. S., Bogdanov, M., & Dowhan, W. (2019). The lipid-dependent structure and function of LacY can be recapitulated and analyzed in phospholipid-containing detergent micelles. *Scientific Reports*, *9*(1).

Walsh, T. R. (2008). Clinically significant carbapenemases: An update. *Current Opinion in Infectious Diseases*, *21*(4), 367–371.

Walsh, T. R. (2010). Emerging carbapenemases: A global perspective. *International Journal of Antimicrobial Agents*, *36*(3).

Walsh, T. R., Toleman, M. A., Poirel, L., & Nordmann, P. (2005). Metallo-β-lactamases: The quiet before the storm? *Clinical Microbiology Reviews*, *18*(2), 306–325.

Wang, J., Zhou, J. ying, Qu, T. ting, Shen, P., Wei, Z. qing, Yu, Y. song, & Li, L. juan. (2010). Molecular epidemiology and mechanisms of carbapenem resistance in *Pseudomonas aeruginosa* isolates from Chinese hospitals. *International Journal of Antimicrobial Agents*, *35*(5), 486–491.

Wardell, S. J. T., Rehman, A., Martin, L. W., Winstanley, C., Patrick, W. M., & Lamont, I. L. (2019). A large-scale whole-genome comparison shows that experimental evolution in response to antibiotics predicts changes in naturally evolved clinical *Pseudomonas aeruginosa*. *Antimicrobial Agents and Chemotherapy*.

Wei, T., Quareshy, M., Zhang, Y. Z., Scanlan, D. J., & Chen, Y. (2018). Manganese is essential for PlcP metallophosphoesterase activity involved in lipid remodeling in abundant marine heterotrophic bacteria. *Applied and Environmental Microbiology*, *84*(15).

Weissenmayer, B., Gao, J. L., López-Lara, I. M., & Geiger, O. (2002). Identification of a gene required for the biosynthesis of ornithine-derived lipids. *Molecular Microbiology*, *45*(3), 721–733.

Whitfield, C., & Trent, M. S. (2014). Biosynthesis and export of bacterial lipopolysaccharides. *Annual Review of Biochemistry*, *83*(1), 99–128.

Wiegand, I., Hilpert, K., & Hancock, R. E. W. (2008). Agar and broth dilution methods to determine the minimal inhibitory concentration (MIC) of antimicrobial substances. *Nature Protocols*, *3*(2), 163–175.

Wieland, K., Chhatwal, P., & Vonberg, R. P. (2018). Nosocomial outbreaks caused by *Acinetobacter baumannii* and *Pseudomonas aeruginosa*: Results of a systematic review. *American Journal of Infection Control*, *46*(6), 643–648.

Wilkinson, S. G. (1969). Lipids of *Pseudomonas diminuta*. *Biochimica et Biophysica Acta (BBA)/Lipids and Lipid Metabolism*, *187*(4), 492–500.

Wilkinson, S. G. (1970). Cell walls of *Pseudomonas* species sensitive to ethylenediaminetetraacetic acid. *Journal of Bacteriology*, *104*(3), 1035–1044.

Wilton, M., Halverson, T. W. R., Charron-Mazenod, L., Parkins, M. D., & Lewenza, S. (2018). Secreted phosphatase and deoxyribonuclease are required by *Pseudomonas aeruginosa* to defend against neutrophil extracellular traps. *Infection and Immunity*, *86*(9).

Winsor, G. L., Van Rossum, T., Lo, R., Khaira, B., Whiteside, M. D., Hancock, R. E. W., & Brinkman, F. S. L. (2009). *Pseudomonas* Genome Database: Facilitating user-friendly, comprehensive comparisons of microbial genomes. *Nucleic Acids Research*, *37*(SUPPL. 1).

Wu, H., Kato, J., Kuroda, A., Ikeda, T., Takiguchi, N., & Ohtake, H. (2000). Identification and characterization of two chemotactic transducers for inorganic phosphate in *Pseudomonas aeruginosa*. *Journal of Bacteriology*, *182*(12), 3400–3404.

Xiao, X., Sankaranarayanan, K., & Khosla, C. (2017). Biosynthesis and structure–activity relationships of the lipid a family of glycolipids. *Current Opinion in Chemical Biology*, *40*, 127–137.

Yao, J., & Rock, C. O. (2013). Phosphatidic acid synthesis in bacteria. *Biochimica et Biophysica Acta*, *1831*(3), 495–502.

Yokoyama, K., Doi, Y., Yamane, K., Kurokawa, H., Shibata, N., Shibayama, K., Yagi, T., Kato, H., & Arakawa, Y. (2003). Acquisition of 16S rRNA methylase gene in *Pseudomonas aeruginosa*. *Lancet*, *362*(9399), 1888–1893.

Yuan, Z. C., Zaheer, R., Morton, R., & Finan, T. M. (2006). Genome prediction of PhoB regulated promoters in *Sinorhizobium meliloti* and twelve proteobacteria. *Nucleic Acids Research*, *34*(9), 2686–2697.

Zaborin, A., Romanowski, K., Gerdes, S., Holbrook, C., Lepine, F., Long, J., Poroyko, V., Diggle, S. P., Wilke, A., Righetti, K., Morozova, I., Babrowski, T., Liu, D. C., Zaborina, O., & Alverdy, J. C. (2009). Red death in *Caenorhabditis elegans* caused by *Pseudomonas aeruginosa* PAO1. *Proceedings of the National Academy of Sciences of the United States of America*, *106*(15), 6327–6332.

Zaborina, O., Holbrook, C., Chen, Y., Long, J., Zaborin, A., Morozova, I., Fernandez, H., Wang, Y., Turner, J. R., & Alverdy, J. C. (2008). Structure-function aspects of PstS in multi-drug-resistant *Pseudomonas aeruginosa*. *PLoS Pathogens*, *4*(2).

Zavaleta-Pastor, M., Sohlenkamp, C., Gao, J.-L., Guan, Z., Zaheer, R., Finan, T. M., Raetz, C. R. H., Lopez-Lara, I. M., & Geiger, O. (2010). Sinorhizobium meliloti phospholipase C required for lipid remodeling during phosphorus limitation. *Proceedings of the National Academy of Sciences*, *107*(1), 302–307.

Zhang, X., Ferguson-Miller, S. M., & Reid, G. E. (2009). Characterization of ornithine and glutamine lipids extracted from cell membranes of *Rhodobacter sphaeroides*. *Journal of the American Society for Mass Spectrometry*, *20*(2), 198–212.

Zhang, Y.-M., & Rock, C. O. (2008). Membrane lipid homeostasis in bacteria. *Nature Reviews Microbiology*, *6*(3), 222–233.

Zhao, W. H., Chen, G., Ito, R., & Hu, Z. Q. (2009). Relevance of resistance levels to carbapenems and integron-borne bla IMP-1, blaIMP-7, blaIMP-10 and bla VIM-2 in

clinical isolates of *Pseudomonas aeruginosa*. *Journal of Medical Microbiology*, *58*(8), 1080–1085.

Zhao, W. H., & Hu, Z. Q. (2010). β-Lactamases identified in clinical isolates of *Pseudomonas aeruginosa*. *Critical Reviews in Microbiology*, *36*(3), 245–258.

Zhou, Y., Liang, Y., Lynch, K. H., Dennis, J. J., & Wishart, D. S. (2011). PHAST: A Fast Phage Search Tool. *Nucleic Acids Research*, *39*.

Zulianello, L., Canard, C., Köhler, T., Caille, D., Lacroix, J. S., & Meda, P. (2006). Rhamnolipids are virulence factors that promote early infiltration of primary human airway epithelia by *Pseudomonas aeruginosa*. *Infection and Immunity*, *74*(6), 3134–3147.

Appendix 1

Pi-responsive cellular proteome in WT *P. aeruginosa* PAO1. Locus tags from the *Pseudomonas* genome reference database are listed alongside known or predicted protein functions. Log2 transformation of fold change values show the differences between high and low phosphate *P. aeruginosa* cultures, and are the mean of 3 replicates. All Pi-responsive proteins displayed have a log2(Fold Change) of ≥2 and all were considered significant with a false detection rate of <0.05 (FDR<0.05). Negative numbers indicate higher expression under phosphate stress.

Protein function	Locus Tag	log2(Fold Change)
Non-hemolytic phospholipase C (PlcN)	PA3319	-10.20673752
Extracellular DNA degradation protein (EddA)	PA3910	-9.755251567
Uncharacterized protein	PA2635	-9.698588053
Phenazine biosynthesis protein (PhzE)	PA4214	-8.654287974
Probable glutamine amidotransferase	PA3459	-8.394351323
Glycerophosphoryl diester phosphodiesterase (GlpQ)	PA0347	-8.350893021
Uncharacterized protein	PA5061	-8.117766062
Polyphosphate:ADP phosphotransferase	PA2428	-7.436549505
Rhamnosyltransferase chain B	PA3478	-7.369407018
Probable non-ribosomal peptide synthetase	PA4078	-7.135940552
Extracelullar DNA degradation protein (EddB)	PA3909	-7.1205616
Probable two-component response regulator	PA2881	-6.924730937
Uncharacterized protein	PA0690	-6.878400167
Probable carbamoyl transferase	PA2069	-6.420543671
Pyruvate dehydrogenase (cytochrome)	PA5297	-6.189308167
3-(3-hydroxydecanoyloxy)decanoate synthase	PA3479	-6.098758062
Probable bacterioferritin	PA4880	-6.079444885
Uncharacterized protein	PA0698	-5.714225133
Alkaline phosphatase H	PA3296	-5.619827906
Rhamnosyltransferase 2	PA1130	-5.496246974
Phenazine biosynthesis protein (PhzD2)	PA1902	-5.485527039
Uncharacterized protein	PA2171	-5.434581121
Probable acetyltransferase	PA3368	-5.278530757
Poly(3-hydroxyalkanoic acid) synthase 2	PA5058	-5.249589284
Anthranilate--CoA ligase	PA0996	-5.135194778
Phospho-2-dehydro-3-deoxyheptonate aldolase	PA4212	-5.017737071
Transport protein (ExbB2)	PA0693	-4.948032379
Uncharacterized protein	PA3374	-4.706494013
Uncharacterized protein	PA3219	-4.624661764
Probable type II secretion system protein	PA0685	-4.622166316
Poly(3-hydroxyalkanoic acid) depolymerase	PA5057	-4.482566198
Uncharacterized protein	PA1606	-4.477079391
UDP-glucose 6-dehydrogenase	PA2022	-4.273289998

Uncharacterized protein	PA2804	-4.227488836
Uncharacterized protein	PA0692	-4.22598203
Uncharacterized protein	PA1324	-4.198731105
Probable glycosyl transferase	PA0842	-4.078671137
Methyl-accepting chemotaxis protein (CtpH)	PA2561	-4.039987564
Uncharacterized protein	PA0695	-3.896328608
Phosphonates import ATP-binding protein (PhnC2)	PA3384	-3.790336609
Porin P	PA3279	-3.78040123
Membrane protein component of ABC phosphate transporter	PA5368	-3.768856684
Biotin synthase	PA0500	-3.715056101
Probable two-component sensor	PA2882	-3.714621862
Uncharacterized protein	PA2433	-3.680545171
Phosphate regulon transcriptional regulatory protein (PhoB)	PA5360	-3.665147781
Probable transcriptional regulator	PA0701	-3.653577805
Antimetabolite l-2-Amino-4-Methoxy-trans-3-Butenoic Acid (AMB) synthesis (AmbE)	PA2302	-3.63861084
Uncharacterized protein	PA2167	-3.637429555
Peptidylprolyl isomerase	PA0699	-3.605301539
Probable acetyltransferase	PA3460	-3.552387238
Probable short-chain dehydrogenase	PA2918	-3.534699122
Uncharacterized protein	PA0460	-3.524803162
Phenazine/pyocyanine biosynthesis protein (PhzF)	PA4215	-3.515024185
Acyl-homoserine-lactone synthase (LasI)	PA1432	-3.477566401
Anthranilate synthase component 1, pyocyanine specific (ASI)	PA1001	-3.471937815
Trans-aconitate 2-methyltransferase	PA2564	-3.468770981
Osmotically inducible protein (OsmC)	PA0059	-3.428434372
Uncharacterized protein	PA4738	-3.427829107
Phosphate transport system permease protein (PstA)	PA5367	-3.409196218
Lipotoxon F (LptF)	PA3692	-3.365186056
HxcT pseudopilin	PA0681	-3.364541372
Uncharacterized protein	PA4739	-3.36428388
Uncharacterized protein	PA3461	-3.343550364
(R)-3-hydroxydecanoyl-ACP:CoA transacylase (Quinolone sensitivity protein)	PA0730	-3.319576899
Uncharacterized protein	PA3819	-3.310759226
Probable Resistance-Nodulation-Cell Division (RND) efflux transporter	PA4207	-3.309268316
Uncharacterized protein	PA2915	-3.25749588
ECF sigma factor (VreI)	PA0675	-3.25052007
Probable transcriptional regulator	PA0275	-3.245417277
2-heptyl-4(1H)-quinolone synthase subunit (PqsC)	PA0998	-3.231575012
Uncharacterized protein	PA4139	-3.210337321
Uncharacterized protein	PA3691	-3.20965449
Uncharacterized protein	PA1216	-3.198550542
Periplasmic gluconolactonase (PpgL)	PA4204	-3.192895253
Phenazine biosynthesis protein PhzA1	PA4210	-3.161492666

Uncharacterized protein	PA4884	-3.11555926
Probable aldehyde dehydrogenase	PA2378	-3.089309692
Probable trehalose synthase	PA2152	-3.038731257
Uncharacterized protein	PA0696	-3.033399582
Uncharacterized protein	PA2803	-3.010194143
Putative quercetin 2,3-dioxygenase (Putative quercetinase)	PA3240	-3.00465711
Methyl-accepting chemotaxis protein (CtpL)	PA4844	-3.001227697
Binding protein component of ABC phosphonate transporter	PA3383	-2.984984716
Uncharacterized protein	PA5299	-2.971493403
Phosphate import ATP-binding protein (PstB)	PA5366	-2.940657298
Uncharacterized protein	PA3844	-2.935982386
Phenazine-1-carboxylate N-methyltransferase	PA4209	-2.930987676
Uncharacterized protein	PA1323	-2.913213094
Probable transcriptional regulator	PA3381	-2.907595317
Antimetabolite l-2-Amino-4-Methoxy-trans-3-Butenoic Acid (AMB) synthesis (AmbB)	PA2305	-2.888827642
Antimetabolite l-2-Amino-4-Methoxy-trans-3-Butenoic Acid (AMB) synthesis (AmbD)	PA2303	-2.874830246
Uncharacterized protein	PA3572	-2.827032725
Antimetabolite l-2-Amino-4-Methoxy-trans-3-Butenoic Acid (AMB) synthesis (AmbC)	PA2304	-2.79532814
Phospholipase C (PlcB)	PA0026	-2.792703629
Uncharacterized protein	PA2771	-2.775707881
Uncharacterized protein	PA3734	-2.775616328
Probable glycosyl hydrolase	PA2160	-2.72849528
5-methyltetrahydropteroyltriglutamate--homocysteine methyltransferase	PA1927	-2.690607707
Chitinase	PA2300	-2.678885142
Catalase HPII	PA2147	-2.6479702
Uncharacterized protein	PA3846	-2.640010198
Putative zinc metalloprotease	PA3649	-2.612800598
Porin O	PA3280	-2.550654093
Sigma factor regulator (VreR)	PA0676	-2.514614105
Serine protease	PA1327	-2.498445511
Uncharacterized protein	PA3705	-2.488183975
Osmotically inducible lipoprotein (OsmE)	PA4876	-2.47485288
Uncharacterized protein	PA0697	-2.450276693
Protease (PfpI)	PA0355	-2.429958979
Alpha-1,4-glucan:maltose-1-phosphate maltosyltransferase	PA2151	-2.419034958
Uncharacterized protein	PA5446	-2.347930272
Adenosylhomocysteinase	PA0432	-2.347044627
Phosphate-binding protein (PstS)	PA5369	-2.344860077
Probable hydrolase	PA2067	-2.336758296
Aconitate hydratase A (ACN)	PA1562	-2.323865255
Uncharacterized protein	PA4993	-2.306030273
Uncharacterized protein	PA4205	-2.290850957
Phosphate-specific transport system accessory protein PhoU homolog	PA5365	-2.276836395

Probable metal-transporting P-type ATPase	PA3690	-2.253185908
Probable pyridoxamine 5'-phosphate oxidase	PA4216	-2.240835826
GTP 3',8-cyclase 2	PA1505	-2.193239848
Protease (LasA)	PA1871	-2.185289383
Phosphate regulon sensor protein (PhoR)	PA5361	-2.128717422
2,4-dienoyl-CoA reductase (FadH1)	PA3092	-2.091956457
Uncharacterized protein	PA0557	-2.083759308
Probable type II secretion system protein	PA0687	-2.080123266
Chloroperoxidase	PA2717	-2.076198578
Probable lipid kinase YegS-like	PA3023	-2.0685908
Probable Resistance-Nodulation-Cell Division (RND) efflux membrane fusion protein	PA4206	-2.033835729
Uncharacterized protein	PA2927	-2.013376236
Catalase	PA4236	-2.008307139
Putative imidazole glycerol phosphate synthase subunit (hisF2)	PA3151	1.974990209
Uncharacterized protein	PA1513	2.102914174
Ferric enterobactin receptor (PirA)	PA0931	2.332770665
Probable antioxidant protein	PA3450	2.342319489
Probable ATP-binding component of ABC transporter	PA2408	2.393850327
Uncharacterized protein	PA5137	2.402357101
Probable hydrolase	PA0562	2.449858348
Probable binding protein component of ABC transporter	PA0602	2.498491923
Probable MFS dicarboxylate transporter	PA5530	2.516822179
Negative regulator of type III secretion (ExsD)	PA1714	2.575972239
Regulator of liu genes	PA2016	2.58658282
Uncharacterized protein	PA1746	2.639357885
Probable amino acid binding protein	PA3865	2.641301473
Uncharacterized protein	PA1043	2.665437698
Uncharacterized protein	PA4132	2.67109553
Probable binding protein component of ABC transporter	PA2204	2.726812363
High-affinity branched-chain amino acid transport system permease protein (BraE)	PA1072	2.792919159
Probable transcriptional regulator	PA0942	2.803567886
Heme oxygenase	PA0672	2.809711456
Alkyl hydroperoxide reductase (AhpD)	PA2331	2.81463623
Transcriptional regulator (Dnr)	PA0527	2.814872106
Uncharacterized protein	PA1665	2.881585439
Alkanesulfonate monooxygenase	PA3444	2.959523519
Uncharacterized protein	PA2033	3.003330866
Probable chemotaxis transducer	PA1646	3.181678136
Probable periplasmic taurine-binding protein	PA3938	3.245528539
Uncharacterized protein	PA4129	3.273066839
Uncharacterized protein	PA2453	3.4348526
Aspartate 1-decarboxylase	PA4731	3.467517853
Second ferric pyoverdine receptor (FpvB)	PA4168	3.497207006

Uncharacterized protein	PA5346	3.578495026
Uncharacterized protein	PA1888	3.58943367
Probable nitroreductase	PA5190	3.604694366
Fumarate hydratase class II	PA4470	3.621372223
Uncharacterized protein	PA1657	3.901093801
Cytochrome c oxidase subunit (Cbb3-type)	PA4133	3.952099482
Uncharacterized protein	PA3445	4.076587041
Polyphosphate:ADP/GDP phosphotransferase	PA0141	4.09273084
Probable hemin degrading factor	PA4709	4.898995717
Probable ClpA/B-type protease	PA1662	5.367067973
Superoxide dismutase [Mn]	PA4468	5.989256541
Major exported protein (Secreted protein hcp)	PA5267	6.057260513
Uncharacterized protein	PA1658	6.723980586

Appendix 2

Pi-responsive exoproteome in WT *P. aeruginosa* PAO1. Locus tags from the *Pseudomonas* genome reference database are listed alongside known or predicted protein functions. Log2 transformation of fold change values show the differences between high and low phosphate *P. aeruginosa* cultures, and are the mean of 3 replicates. Negative numbers indicate higher expression under phosphate stress.

Protein function	Locus tag	log2(Fold Change)
Extracelullar DNA degradation protein, EddB	PA3909	-17.03111013
Alkaline phosphatase L	PA0688	-16.13372739
Uncharacterized protein	PA0981	-13.73392423
Hemolytic phospholipase C PlcH	PA0844	-13.01614062
Non-hemolytic phospholipase C PlcN	PA3319	-11.34411939
Phosphate depletion regulated TPS partner A, PdtA	PA0690	-11.16284116
Uncharacterized protein	PA2635	-10.87584941
Alkaline phosphatase H	PA3296	-10.41443825
Phosphate-binding protein PstS	PA5369	-10.37128321
Porin O (OprO)	PA3280	-9.896238963
Uncharacterized protein	PA0689	-8.991081238
Glycerophosphoryl diester phosphodiesterase, GlpQ	PA0347	-7.769381841
Phospholipase C PlcB	PA0026	-5.957550049
Uncharacterized protein	PA4739	-5.884564718
Uncharacterized protein	PA3250	-5.179430644
Probable binding protein component of ABC transporter	PA1810	-4.962363561
Extracelullar DNA degradation protein, EddA	PA3910	-4.958661397
Probable glycerophosphoryl diester phosphodiesterase	PA2352	-4.832132339
Uncharacterized protein	PA2913	-4.555594126
Adenosylhomocysteinase	PA0432	-4.475900014
Protease LasA	PA1871	-4.208909353
Glutamyl-tRNA(Gln) amidotransferase subunit A	PA4483	-4.017015457
Uncharacterized protein	PA1112	-3.967375437
Probable binding protein component of ABC transporter	PA4195	-3.830432892
Elastase, Pseudolysin	PA3724	-3.394061406
Uncharacterized protein	PA3922	-3.358172099
Catalase LasB	PA4236	-3.350656509
5-methylphenazine-1-carboxylate 1-monooxygenase	PA4217	-3.274669647
Aminopeptidase	PA2939	-3.208181381
Binding protein component of ABC phosphonate transporter	PA3383	-3.103005091
Probable binding protein component of ABC dipeptide transporter	PA5317	-2.886916478
Type IV pilus biogenesis factor PilY1	PA4554	-2.770886103
Gluconate dehydrogenase	PA2265	-2.694224675
Alkyl hydroperoxide reductase subunit C	PA0139	-1.827186584

S-adenosylmethionine synthase	PA0546	-1.797954559
Exotoxin A	PA1148	-1.7254378
Uncharacterized protein	PA0371	-1.71386083
Probable bacteriophage protein	PA0622	-1.671819687
Elongation factor Ts (EF-Ts)	PA3655	-1.643960953
Uncharacterized protein	PA2328	-1.64356041
UPF0312 protein	PA0423	-1.425890605
Uncharacterized protein	PA2218	-1.420120239
Uncharacterized protein	PA1689	-1.405044556
Superoxide dismutase	PA4366	-1.191827774
Immunomodulating metalloprotease	PA0572	-1.19090271
Peptidyl-prolyl cis-trans isomerase A	PA3227	-1.02249972
60 kDa chaperonin (GroEL protein)	PA4385	-1.005175908
ATP synthase subunit alpha	PA5556	-0.853571574
Flagellar hook protein FlgE	PA1080	-0.704167048
Uncharacterized protein	PA1053	-0.521537781
Succinate dehydrogenase flavoprotein subunit	PA1583	1.079560598
Isocitrate dehydrogenase	PA2624	1.09360377
Probable outer membrane protein	PA4974	1.09561348
Porin D	PA0958	1.122681936
Ferredoxin--NADP+ reductase	PA3397	1.167729696
Uncharacterized protein	PA0781	1.219767253
Outer membrane porin F	PA1777	1.262638728
Uncharacterized protein	PA3785	1.724728266
Probable outer membrane protein	PA2760	1.848415375
Chaperone protein DnaK	PA4761	1.86507225
Uncharacterized protein	PA0434	2.002360662
LPS-assembly protein LptD	PA0595	2.084973017
50S ribosomal protein L2	PA4260	2.099852244
Flagellar hook-associated protein type 3 FlgL	PA1087	2.193519592
Probable outer membrane protein	PA4837	2.342248281
30S ribosomal protein S1	PA3162	2.662420909
Oligopeptidase A	PA0067	2.67080307
Glutamine--tRNA ligase	PA1794	2.8019104
Tol-Pal system protein TolB	PA0972	2.877503077
Esterase EstA	PA5112	2.923124949
Ferripyoverdine receptor	PA2398	2.966099421
Probable TonB-dependent receptor	PA4675	3.253964106
50S ribosomal protein L1	PA4273	3.476421992
Probable carboxyl-terminal protease	PA5134	3.556570053
Uncharacterized protein	PA0616	3.670638402
Probable outer membrane receptor for iron transport	PA4514	3.689865748

Phosphoenolpyruvate synthase	PA1770	3.781647364
Glycine cleavage system protein T2	PA2442	3.804490407
Succinylornithine transaminase/acetylornithine aminotransferase	PA0895	3.843825022
Uncharacterized protein	PA2831	3.884831111
Uncharacterized protein	PA0194	4.010964712
50S ribosomal protein L4	PA4262	4.07584699
3-hydroxyacyl-[acyl-carrier-protein] dehydratase FabA	PA1610	4.1108977
Probable outer membrane protein	PA1288	4.126063029
Phosphoglycerate kinase	PA0552	4.180334727
Probable molybdopterin-binding protein	PA3441	4.194664637
Uncharacterized protein	PA1597	4.23174413
Branched-chain-amino-acid aminotransferase (BCAT)	PA5013	4.239657084
LPS-assembly lipoprotein LptE	PA3988	4.270786921
30S ribosomal protein S3	PA4257	4.36377271
Electron transfer flavoprotein subunit beta	PA2952	4.635903676
Cysteine synthase	PA2709	4.728702545
Putative copper transport outer membrane porin OprC	PA3790	4.89086469
50S ribosomal protein L3	PA4263	4.897993088
Uncharacterized protein	PA4423	4.93740654
Outer membrane protein OprG	PA4067	5.092091242
Uncharacterized protein	PA0070	5.094888051
Fimbrial protein (Pilin)	PA4525	5.160231272
Endolytic peptidoglycan transglycosylase RlpA	PA4000	5.308782578
Uncharacterized protein	PA4639	5.428572337
Cell division coordinator CpoB	PA0974	5.786687851
Uncharacterized protein	PA3931	5.824700673
Uncharacterized protein	PA4163	6.305969874
Electron transfer flavoprotein subunit alpha	PA2951	6.545958837